ADVANCED TECHNOLOGY LABORATORIES

DESIGN CRITERIA FOR ZERO LEAKAGE CONNECTORS FOR LAUNCH VEHICLES

STATISTICAL INTERFACE-LEAKAGE ANALYSIS AND FEASIBILITY OF SUPERFINISHED SURFACES FOR SEALING

L.G. GITZENDANNER

F.O. RATHBUN, JR.

GENERAL ⊛ ELECTRIC

FINAL REPORT FOR THIRD CONTRACT PERIOD

(January 1964 through March 1965)

DESIGN CRITERIA

FOR ZERO LEAKAGE CONNECTORS

FOR LAUNCH VEHICLES

Contract NAS 8-4012

STATISTICAL INTERFACE-LEAKAGE ANALYSIS

AND FEASIBILITY OF SUPERFINISHED

SURFACES FOR SEALING

L. G. Gitzendanner

F. O. Rathbun, Jr.

May 1, 1965

PREPARED FOR: Propulsion and Vehicle Engineering Division
George C. Marshall Space Flight Center
National Aeronautics and Space Administration
Huntsville, Alabama

PREPARED BY: Advanced Technology Laboratories
General Electric Company
Schenectady, New York

SPONSORED BY: Missile and Space Division
General Electric Company
Philadelphia, Pennsylvania
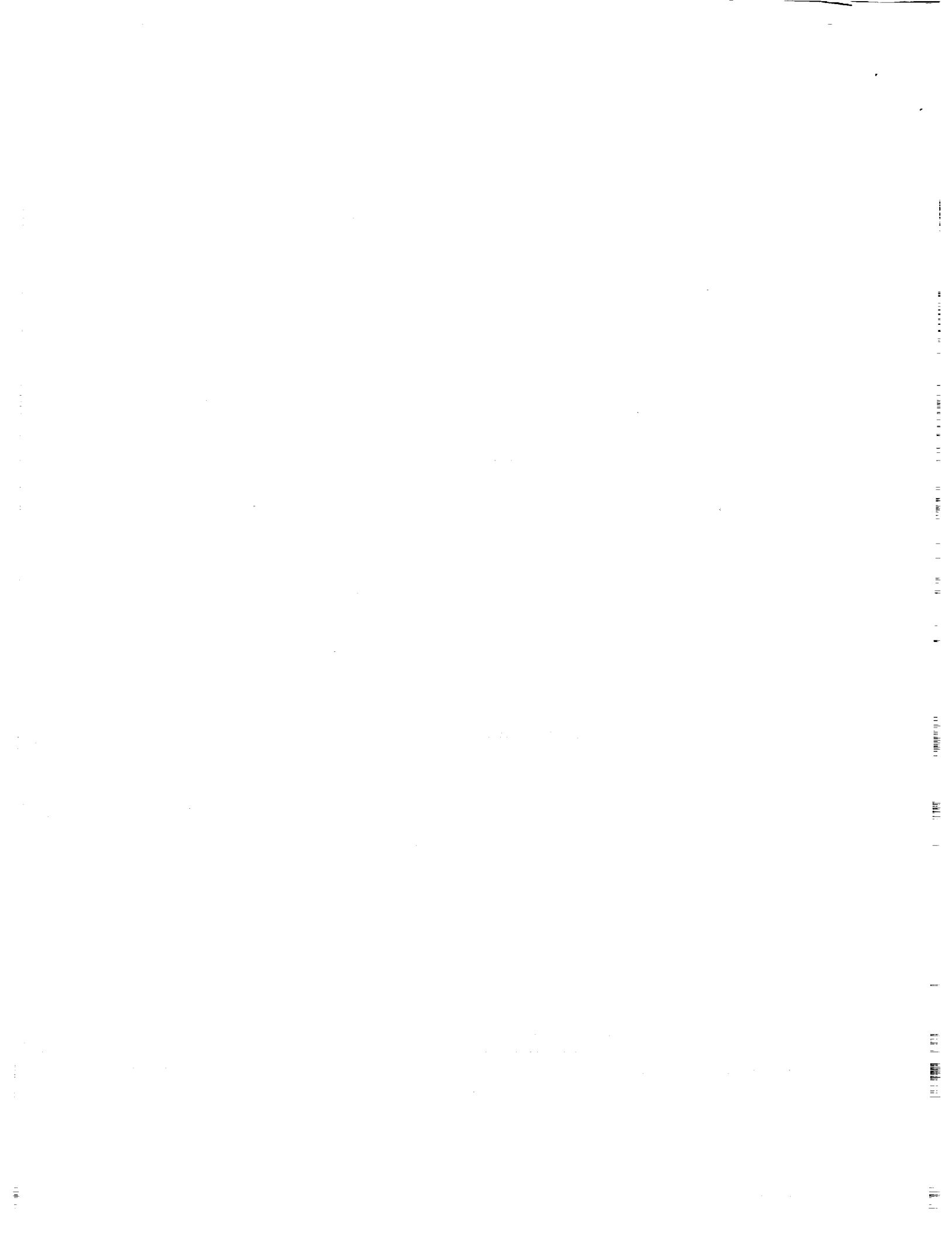
NASA TECHNICAL MANAGER: C. C. Wood (M-P&VE-PT)

TABLE OF CONTENTS

1.0 Project Scope

1.1 Introduction

The goals of this investigation have been to evaluate the feasibility of utilizing extremely fine finished surfaces as mating components for sealing in fluid connectors under stresses less than the yield strengths of the materials, and to perform a statistical analysis of the interface leakage phenomenon, thus working toward an ultimate ability to predict leakage through a given seal as a function of the seal and loading parameters. This work constitutes the third phase of an investigation begun in March 1962 under NAS8-4012. Also published during this phase of the investigation is a Separable Connector Design Handbook, which outlines procedures for the design of flanged connectors, threaded connectors, and cantilever-type pressure energized seals.

The first phase of this contract had as its goal "the establishment of fundamental design criteria that will provide for zero leakage in separable connectors used in launch vehicles." In the first investigation, the approach was taken to regard the separable connector as an interface between two surfaces, backed up by a supporting structure, designed to withstand a variety of environmental conditions.

The principle results from that investigation were:

1. Substantial plastic flow of at least one of the materials at the seal interface is necessary for zero leakage.

2. The plastic flow required for zero leakage can never be achieved in a conventional flared fitting with metal-to-metal contact, because the fitting will fail by hoop compression before the plastic stress range is reached at the seal interface.

3. To reduce the effect of flange rolling in the larger sizes of bolted flanged connectors, efficient lightweight designs can often be obtained by having the flanges in contact outside the bolt circle.

4. The many interacting factors in connector design can best be evaluated by building and testing connectors for specific applications.

The results of the first investigation have been published in six volumes, dated March 15, 1963:

Volume I   "Summary Conclusions and Design Examples," edited by T.P. Goodman, N63-18390, NASA-CR-50557.

Volume II   "Leakage Flow," edited by T.P. Goodman, N63-18493, NASA-CR-50558.

Volume III "Sealing Action at the Seal Interface," edited by F.O. Rathbun, Jr., N63-18159, NASA-CR-50559.

Volume IV   "Design of Connectors," edited by S. Levy, N-63-18494, NASA-CR-50560.

Volume V   "Pressure Energized Seals," edited by B.T. Fang, N-63-18391, NASA-CR-50561.

Volume VI   "Environmental Effects," edited by S. Levy, N-63-18323, NASA-CR-50562.

The second phase of the contract had as its goal an increase in the understanding of the effect of gasket material properties and geometry on leakage flow and the "proof testing" of the validity of the principles of connector design gained under the first phase of the contract. The principal conclusions from the second phase of the overall investigation were:

1. The cold-flow of plastic gaskets can be reduced to a negligible rate by the reduction of the gasket height to width ratio to the point where the sealing surface asperities effectively contain the plastic.

2. A solid soft metal O-ring, compressed between two sealing surfaces having semi-circular grooves provides an excellent low-load gasket system.

3. The analytic design procedure established for large flanged connectors was verified by test.

4. A tube connector which utilized knife edges and a soft metal replaceable gasket was tested and shown to be adequate at -300°F, 70°F, and 500°F (with an internal pressure of 1500 psi).

5. The use of soft metal crush washers with stainless steel MC fittings reduces the leakage rate considerably; however, their use with aluminum MC fittings does not appreciably affect the leakage rate.

The results of the second phase investigation have been published in a single volume, dated June 1, 1964:

"Fundamental Seal Interface Studies and Design and Testing of Tube and Duct Separable Connectors," edited by F.O. Rathbun, Jr., N-64-27305, NASA-CR-56571.

The present investigation, reported upon in detail in sections 2 and 3 of this report has been divided into two separate tasks.

1. Having determined previously that when surfaces with measurable asperities are mated together under normal stress to effect sealing, the required stresses to reduce the leakage to 10^{-6} atm cc/sec exceeds the yield strength of one or both materials in contact, an experimental program has been accomplished in which metal sealing surfaces being extremely smooth and flat were mated together in order to determine whether leakage can be quelled by the imposition of normal stresses less than yield strength. Altogether, sixty-one separate tests, involving nine different combinations of sealing surfaces have been conducted. Internal pressures up to 2000 psi have been considered. The four primary questions concerning the feasibility of superfinished surfaces for sealing have been:

    a. Determination of the required maximum magnitude of asperities,

    b. Determination of the required flatness characteristics,

    c. Assessment of the problem of surface protection, and

    d. Evaluation of the candidate techniques of surface finishing, to include costs.

A requirement of the seals effected by mating such surfaces together is one of reusability, hence, a measure of the degradation of surfaces under repeated assemblies is necessary.

2. Having previously approached the sealing interface problem experimentally with seals of various shapes, finishes, materials, and widths from an experimental point of view, a mathematical model has been developed to predict the probability of leakage through a given seal system. Several methods of approach were tried, one of which appears to be quite successful. The problem has been divided into a number of parts and involves, in one step, the development of sets of numbers which mathematically describe the surface characteristics of a set of sample surfaces such as may be drawn at random from a large population of surfaces of the type considered. A digital computer program has been developed for generating sets of numbers for surfaces which have only random irregularities. Such a program can be extended to include various periodic functions representing tool marks, but this has yet to be done. The surface thus generated can be mated with other surfaces mathematically such that, as the surfaces are brought together incrementally, the change in gap height (which determines the probability of leakage) can be assessed.

1.2 Conclusions

The principal conclusions from the present investigation are:

1. Seals which reduce leakage rates to below 10^{-6} atm cc/sec at internal pressures up to 2000 psi are possible by pressing together parallel superfinished metal surfaces. The stress required to produce such a seal is less than the yield strength of the metals used; up to ten successful assemblies of the same components are possible.

2. Finishing techniques which yield surfaces capable of producing such seals are:

    a. The "Monomolecule" finishing process, by UP-HI Ltd., Tokyo, Japan, and

    b. Polishing technique by the A.D. Jones Optical Works, Burlington, Mass.

    Both techniques, when applied to 347 stainless steel, produce surfaces capable of several reassemblies. The Jones technique is also successful when applied to KANIGEN plated aluminum. A Jones finished 347 stainless steel specimen, when mated with a Jones finished silver plated specimen, is effective as a seal for ten assemblies.

3. The surface finish required for a superfinished 1/8-inch wide flat seal can be specified as follows:

    a. No low relief asperities deeper than 1/2 microinch

    b. Flatness to within one helium light band (11.6 microinches).

    A means of protecting the surfaces during handling and assembling through use of retaining walls appears to offer no major problems to further connector developments.

4. Present cost for a single component surface finishing, on an experimental basis, is $100 per surface. For quantities as low as ten, this cost can be reduced to approximately $70 per surface. These costs are valid for developmental surfaces only and do not represent realistic costs for large quantity lots.

5. The present computer program used to generate surfaces appeared successful when utilized for a lapped surface having random directionality of asperities.

6. The use of such a generated surface, when mated with a perfectly smooth surface (mathematically), appeared successful in yielding a realistic gap distribution between surfaces as a function of decreasing distance between surfaces.

7. The use of a maze threader in the computer program to determine the point at which a barrier to fluid flow has been set up by a continuous area of contact about the seal periphery appears useful.

8. Ultimate use of the computer program and the statistics involved must await further work which will incorporate:

   a. Larger digital arrays for representing surfaces

   b. A larger number of asperity height allocations

   c. Incorporation of periodic functions into the surface of asperity distribution

   d. Incorporation of leakage probability into the program

   e. Verification by adequate experimentation of the techniques

   f. Incorporation of reliable load-displacement relationship into the program.

1.3 Plans for Fourth Contract Period

During the fourth contract period (April 8, 1965 - May 15, 1966), the following tasks will be undertaken:

Task A - Design procedures for separable connectors

Task A-1 - Establishment of flanged connector check designs.

Four flanged connectors will be designed utilizing techniques previously developed under NAS8-4012 and published in the Separable Connector Design Handbook. The sizes, service requirements, and environments under which the connectors will be designed will be identical to four requirements which have already resulted in NASA connectors designed under conventional procedures. The four designs will be optimized within the framework of the design procedures; where applicable, computer programs presently in existence will be used to minimize the manual mathematical manipulations.

The resulting computer configurations will be compared with the configurations determined previously by already existing procedures. Where qualitative and quantitative information as to the performance of the previously designed connectors is available, an appraisal will be made of the differences in designs.

Task A-2 - Computer programs for design procedures of flanged and threaded
          connectors.

Transformation of the logic in arithmetic manipulations of the design procedures for flanged and threaded connectors presently listed in Separable Connector Design Handbook into computer language, thereby allowing the designer to establish inputs for design and to accomplish the laborious portion of the design task on a digital computer, will be performed. The result of this task will be a deck of computer cards to be used by NASA and a procedure for use of those cards. The computer program will incorporate not only arithmetic manipulations and the human logic presently accomplished by the designer, but also the iterative steps necessary to optimize the design within the framework of the design procedures.

Task A-3 - Subject to the successful completion of the computer programs,
          standard designs for often-used design requirements will be
          established.

Task B - Mathematical model of interface sealing phenomena

Continuation of the study reported herein on the statistical interface leakage problem will include: a) determination of the flow through a given interface gap geometry, b) establishing relationships between applied normal force and resultant interface gap geometry, c) incorporation of periodic functions into the computer program for establishing mathematical surfaces d) the modification and refinement of the existing computer program where necessary to ensure realistic surface reproduction. Such a mathematical model is intended to make it feasible to predict the probability that leakage will be less than a stated amount for a given seal.

Task C - The experimental leakage investigations previously conducted under this contract will be extended to include the effect of temperature on the interface sealing problem. The pressure capacity of the experimental apparatus will be increased to 6000 psi; the temperature extremes will be -321°F and +700°F. Many of the sealing systems already appraised at room temperature plus several others will be tested in the new apparatus.

Task D - A separable connector design suitable for production based on utilization of the fine finished sealing principle outlined in this present report will be developed for one set of operating requirements. The specifications of the design will be:

Size	Operating pressure	Temperature range
3/4-inch	6,000 psi	LOX to +700°F

The design will be reduced to hardware and tested under pressure, temperature, and vibration environments. Several prototypes will be constructed for limited reliability testing.

1.4 Separable Connector Design Handbook

A Separable Connector Design Handbook has been published during this reporting period. Included in the Handbook are seven chapters all dealing with the general problem of separable connector design.

Chapter 1, FUNDAMENTAL CONSIDERATIONS OF SEPARABLE CONNECTOR DESIGN, deals with the various modes of leakage possible in a separable connector; it cites information pertinent to the surface deformation of material at the interface, some causes of leakage in a connector, and gives a discussion of the general problems associated with connector design. The intent of the chapter is to be educational in nature and to put the various aspects of the design problem in perspective.

Chapter 2, FLANGED CONNECTOR DESIGN, outlines in detail procedures for the establishment of flanged connectors for aero-space applications. Included are four combinations of flanged configurations, those with contact outside the bolt circle, those having no contact outside the bolt circle, those having two integral flanges and those possessing one integral and one loose flange. Simplified procedures for establishing initial designs, procedures for sophisticated analysis of the designs, and rules for altering the designs are included. Sample problems are shown in detail to guide the design engineer in use of the chapter.

THREADED CONNECTOR DESIGN, the subject of Chapter 3, performs the same service with regard to threaded tube connectors as Chapter 2 does for flange connectors. Again, a design example is present to guide a designer in use of the procedure.

Chapter 4, PRESSURE ENERGIZED CANTILEVER SEALS AND HOLLOW METALLIC O-RINGS, gives detailed design procedures for the establishment of cantilever-type pressure energized seals. Included in detail are cantilever-type seals having horizontal straight legs, horizontal tapered legs, and angled legs. Where applicable, nomographs have been included to reduce mathematical manipulations.

Chapter 5, LEAKAGE MEASUREMENT TECHNIQUES, deals with recommended practices for measurement of leakage during development of separable connectors. Various equipment and details of apparatus setup are cited.

Chapter 6, MATERIAL PROPERTIES AND COMPATIBILITY, lists candidate structural and sealing materials along with their mechanical properties and information pertinent to compatibility with possible fluids. References are cited wherein further material information can be gained.

The last chapter, CATALOG OF SEALS, presents a set of seal configurations (and their characteristics) which have proven successful under limited testing. The chapter is intended for modification and addition of new seals when such information becomes available.

2.0 Superfinished Surfaces for Sealing

2.1 Introduction

2.1.1 Problem Statement

In all experimental interface leakage studies reported in earlier reports under NAS8-4012 (References 1,2,3) the stress required to effect a seal on a flat annular system has exceeded the yield strength of one of the mated materials. The original surface finish of the softer of the two materials in contact deformed plastically in order to close the gaps existing between the surfaces. The amount of plastic deformation and the level of stress necessary to cause that deformation proved highly sensitive to the original surface finish of the stronger material. The conclusion has been that, in order to insure that a system will seal, independent of the surface finishes, the applied stress must equal 2.75 times the yield strength of the weaker material.

In that the above results dictate that plastic deformation takes place in the system, the most likely approach to the sealing problem has been to utilize a separate removable gasket which can be thrown away after its use and replaced by another identical gasket. If such is not done, and merely the surfaces on the structural parts are mated, then the necessary plastic deformation during the first assembly will cause the response of the connector during succeeding assemblies to differ from that for which it was designed. The latter approach is, of course, unsatisfactory from a reliability standpoint when reusability is required. The former approach, that of using a removable gasket, is less than satisfactory due to the added complexity in the assembly procedure.

A possible answer to this undesirable situation is to design a connector which will seal adequately under stresses which are less than the yield strength of the materials concerned, thus resulting in elastic deformation of the mating materials (which would be integral connector components such as flange and union in a threaded connector). A connector designed encompassing elastic sealing is by no means a simple task to accomplish. Since it is known from previous experimental investigations that, for surfaces having asperities as small as those resulting from diamond burnishing, plastic deformation is necessary to effect a seal, it becomes obvious that a necessary criterion for elastic sealing is that the surfaces are even smoother than those gained from a diamond burnishing technique.

Aside from the smoothness requirement, the requirement of extreme flatness is also present. Even though, locally a surface may be extremely free of irregularities, in order for the entire seal to mate against its opposing part, essentially all deviations from flatness must be removed about the periphery of the seal.

Another problem immediately evident is that when one deals with surfaces which are extremely smooth and one requires that a system in which these surfaces are mated be used up to ten to fifteen times, extremely careful handling is necessary in order to preclude surface damage. Damage to the surfaces may occur during the assembly of the connector, either by rough handling or by sliding of one surface upon the other during torquing of a threaded connector, or by foreign particles existing in the system and being compressed between the mated surfaces during tightening of the connector.

A fourth problem which arises when one considers the elastic sealing phenomenon is that of a means of manufacturing surfaces which are proved adequate in sealing tests. Given that a particular set of surfaces are smooth enough and flat enough to effect a proper seal, the added requirement remains that such a surface can be manufactured easily, in large quantities, and without excessive cost. It is well known that the cost of surface finishing increases drastically with decreasing roughness. Hence, should the feasibility of an elastic seal be shown, it is also necessary to show the feasibility of manufacturing such parts.

Thus, four separate problems arise in the potential use of an elastic seal for a separable connector:

a. Extreme surface smoothness (freedom from asperities) on the mated parts,

b. Extreme flatness of the mated parts,

c. A handling and assembly procedure which precludes surface damage to the parts,

d. A manufacturing procedure for the proper surfaces which is not cost prohibitive.

2.1.2 Earlier Efforts

During Phases 1 and 2 of NAS Contract 8-4012 (References 1,2) conventional lapped surfaces and diamond burnishing surfaces were used in leakage experiments. Both 347 stainless steal and 2024 aluminum components were used in these tests. Where diamond burnishing was attempted, the resultant surface finish was approximately 4 microinches, rms. The surface finishing technique was applied to the tops of flat annular rings which were allowed to remain in high relief on the sealing specimens. Talysurf traces in a radial direction showed that not only were asperities present but the diamond burnishing technique also caused roll-off at the inner and outer edges of the seal, resulting in a sealing surface which was severely rolled down at the edges, leaving only about one half of the surface actually flat. When two such surfaces were subjected to a leakage test under 1100 psi, the normal stress required for sealing ranged from 0.7 times the yield stress of the material up to approximately 1.3 times the yield stresses of the material. In both cases, since the specimens were not flat, that stress resulted in plastic deformation of the components. Post leakage test Talysurf traces and photomicrographs showed a different characteristic to the surfaces than that existing prior to the tests.

Where conventional lapping was the means of applying a surface finish, the results were even less satisfactory. A lapped surface had the characteristic of not only round-off at the edges of the specimens but also low relief randomly directed scratches. Since both surfaces were of the same type, when they were pressed together a reasonably large area of contact was effected, but the low relief scratches on each component allowed leakage. Even though the stress was increased well above the yield stress, the low relief scratches were not filled and leakage continued. Photomicrographs taken of the surfaces after the leakage tests showed that plastic deformation had taken place on both surfaces and the surface characteristics were different from the virgin condition.

Succeeding leakage tests on both diamond burnish finished surface finishes and conventionally lapped specimens showed that the leakage-pressure-stress

response of those components differed from the response during the first test. No pattern in succeeding responses nor trends were seen. However, in that in each case the leakage varied with the stress from the previous case (along with the surface finish being altered each time), such a system could not reliably be used in a system where a given stress level was utilized.

2.1.3 Experimental Program

In order to determine the feasibility of using superfinished surfaces for sealing, an experimental program has been carried out in which several different finishing techniques have been used. Flat annular sealing specimens, having been surface finished by a given technique, were subjected to leakage tests under varying stresses and internal pressures. Different numbers of tests were run on each combination of specimens, depending on the relative success gained with the initial experimentation.

Basically, two materials were used for sealing surfaces, 347 stainless steel and 2024 T4 aluminum, although in the case of the aluminum, plating was used in some experiments.

Altogether, 61 separate leakage tests were accomplished, with nine different sets of sealing surface finishes being tested.

Table 2.1 lists all of the experiments run, citing the surface finish used, the material, the number of repetitions with each combination of specimens, and the height of the sealing surface existing above the substructure. In that the original specimens had high relief annular rings present on which the surface finishes to be investigated were affixed, it was possible to cut away material repetitively during the successive experimentation, thus allowing the annular height to be a variable in the tests. Details of the finishing techniques and resultant finishes are described in Section 2.3.

2.1.4 Experimental Apparatus

Except for experiment 37, the sealing systems investigated were identical in configuration (except for height). Each sealing surface was nominally flat on an annular rise having an inside diameter of 0.9375 inches and an outside diameter of 1.1875 inches. The actual components to be mated together were as shown in Figure 2.1.
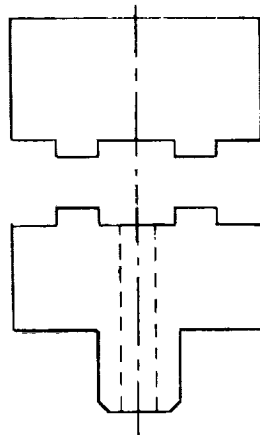

Figure 2.1 Leakage Experiment Specimens

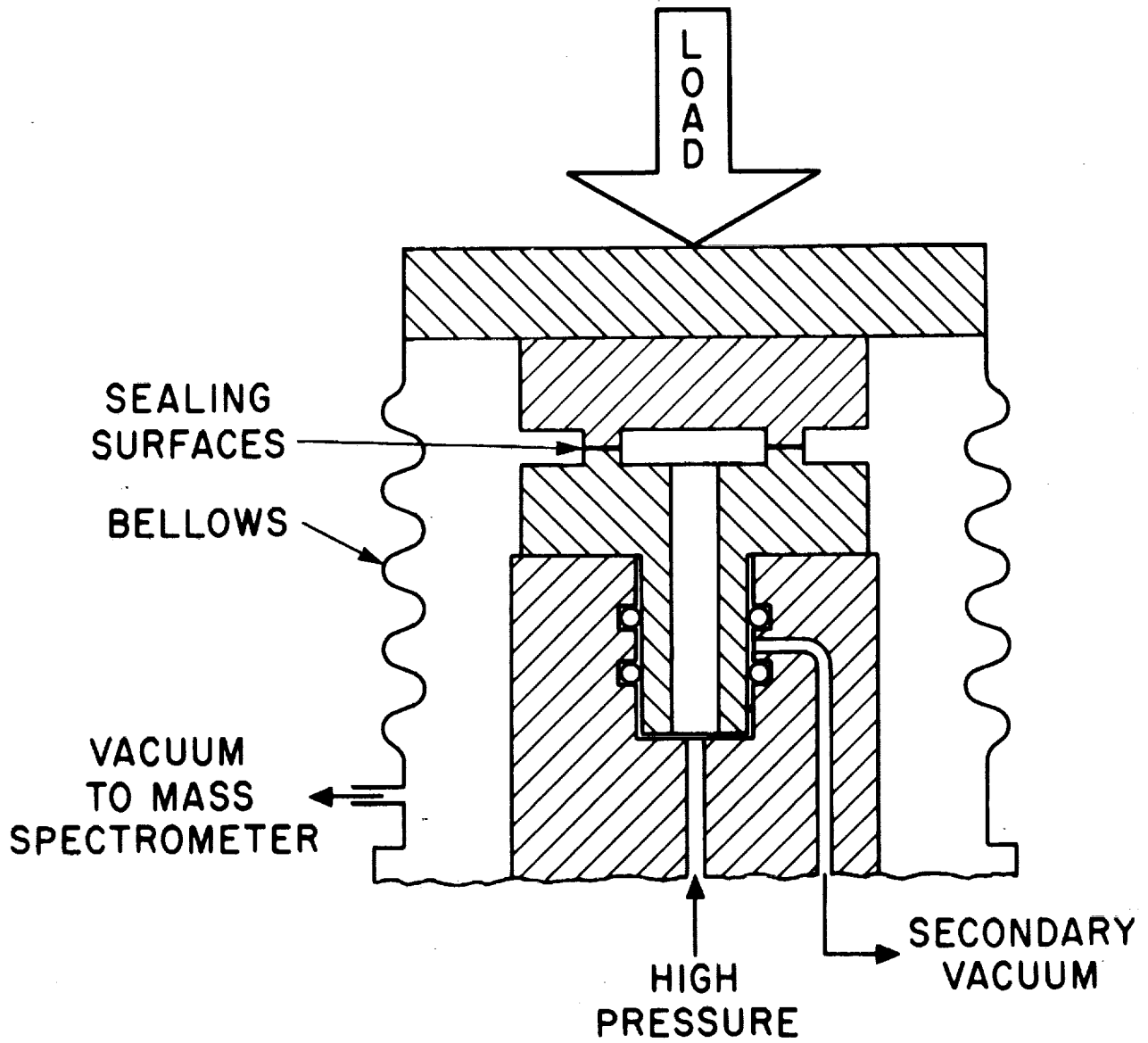The two sealing specimens fit into the system shown schematically in Figure 2.2.

FIGURE 2.2 Schematic of Experimental Apparatus for Sealing
Investigations.

Basically the experimental apparatus encompasses a high pressure helium system, a vacuum system, a mass spectrometer, and a loading mechanism. The details of this apparatus have been described in Reference 1.

Several specimens as shown in Figure 2.1 were used, an equal number being constructed of 2024 aluminum and of 347 stainless steel. Each sealing specimen was initially constructed so that the annular rises were 0.030 inches in height.

In that the surface to be investigated was established on the tops of the flat annular rises, the substructure both inside and outside of the rises could be machined off after the surface finishes had been prepared and during the repetitive testing operations. The material to be removed in order to leave a more flexible sealing system is as shown in Figure 2.3.
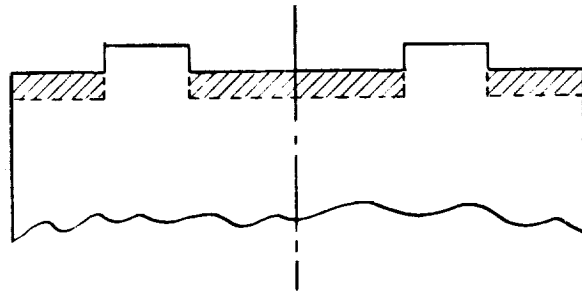

Figure 2.3 Raised Annular Sealing Surfaces

The amount of material removed by machining varied from test to test and is described in both Table 2.1 and Section 2.4.

Because the requirement of flatness exists on the actual surfaces to be mated, during the actual surface finishing, soft metal rings were placed inside the inside and outside of the annular sealing surfaces such that a much broader surface was surface finished. In this manner, edge roll-off was precluded. Surfaces finished in this manner were much flatter near the edges than surfaces previously finished without such rings.

2.1.5 Experimental Procedure

All tests conducted utilized essentially the same experimental procedure. A maximum allowable normal stress was calculated for each material. The specimens were mated together carefully and a one atmosphere pressure differential was impressed across the system. The leakage rate was recorded incrementally with increases in normal stress, (Phase I). The normal stress was increased until either

   a)   the leakage rate dropped well below 10^{-6} atm cc/sec or

   b)   a predetermined allowable stress level had been reached.

At this time, the internal pressure was increased incrementally and the load

applied to the seal was adjusted incrementally such that the calculated normal stress remained constant, (Phase II). The leakage was recorded with the increases in internal pressure. The maximum internal pressure used varied from 2000 to 2200 psi, depending on the pressure available at the time of the test. With the maximum internal pressure applied to the system, the stress was again incrementally increased and further decreases in leakage were recorded until either the yield stress was reached or extremely low leakage rates were again found, (Phase III). Finally, the stress was incrementally decreased, and the resulted increases in leakage were recorded, (Phase IV). The resultant data, shown in this report, are that of the leakage rate plotted as a function of normally applied stress for all four phases of the experiments and, in some cases, the leakage plotted as a function of the internal pressure during Phase II of the experiment. It is to be noted that on the leakage-stress graph, (leakage being measured by log scale), Phase II of the experiment is shown as a vertical line. When leakage is plotted against internal pressure, the log-log scale is used.

The four phases of the experimental procedures are shown schematically in Figure 2.4. In one series of tests, described in Section 2.4.8, the selection of the terminal points of Phases I and III were chosen slightly differently from those levels described above.

2.2   Theoretical Considerations

In References 1 and 3, application is made of an analysis citing leakage through an annular passage of constant gap height as a function of internal pressure and path dimensions. The analysis included both the viscous flow terms and the molecular flow terms, and accounted for the transition region between them. In Reference 1, experimental results of real sealing systems were compared with the leakage predicted by analysis. In many cases, it was found that the concept of an average gap height representing the conglomeration of real leak paths existing in a seal was not adequate to describe the phenomenon. In some cases (Reference 1) where extremely small surfaces had been used, as in the case of diamond burnished finishes, the concept of an average gap height faired better.

Herein, where extremely small surfaces have been mated together, and the leakage paths would typically be more like those described in the constant gap height analysis, it was expected that experimental results would agree better with the analysis. Herein, where leakage can be conceived of occurring due to very wide slits existing between the annular sealing surfaces and low stress levels, the agreement between the real system and the model is as close as is possible in reasonably conceived experiments. In Section 2.5 of this report the degree of agreement found is discussed. The test for agreement between theory (analysis) and experimental results would come, of course, during Phase II of the experiment.

In that Phase II of the experiment encompassed an increase in internal pressure while the stress was maintained constant on the sealing system, it was suspected that rather pure relationships between leakage and pressure could be drawn, regardless of the shape of the leak paths. In other words, when plotted on a log-log graph, the relationship between leakage and internal pressure should vary from the condition of linearity (at extremely low leakage levels, indicating molecular flow) to one of the leakage being proportional to the square of the pressure (at higher leakage levels, indicating viscous flow). Between those two

regimes, the relationship between leakage and pressure should allow a transition region. Neither molecular flow nor viscous flow need exist individually in any one experiment; however, one or the other or both should exist in every experiment. Plots of the actual relationship between measured leakage and recorded internal pressure are shown in Section 2.5.

In that extremely smooth surfaces had been manufactured for investigation, it was assumed initially that where the asperity free condition was maintained, the leakage should result from waviness of surface rather than scratches. In other words, about the periphery of the seal, one, two or even three periods of sinusoidal rise heights could be expected, with the amplitude of the waviness being extremely small, due to the polishing techniques used. Because of this, and because of the elasticity of the annular rises, it was expected that the effects of waviness could be overcome by adjusting the height of the annular rise upward, thus allowing increased flexibility of the elastic system. Approximately, in an elastic system such as the one used, the displacement of the annular rise in the vertical direction is equal to the applied stress times the rise height divided by the elastic modulus of the material. As the height is increased, the displacement possible is also increased in direct proportion. Hence, should waviness affect the sealing (permit leakage,) an increase of the height of the annular rise would allow a greater depression of those parts of the annular rise in contact and under a stress, hence bringing all portions of the sealing surfaces not in contact in closer proximity. This phenomenon would continue until all points about the periphery were brought in contact. The degree to which this concept was realized was minimal, due to conflicting circumstances (gradual degradation of the surface finishes) during the repetitive sealing. Further comments on this phenomenon are made in Section 2.4.

In most experiments, the stress levels which terminated Phase I and Phase IV were those stress levels which caused leakage rates to diminish to less than 10^{-6} atm cc/sec at the internal pressure at hand. Hence, as the surface finish damage accumulated, during Phase I, when a one atmosphere pressure differential existed across the seal, an increase in the stress level terminating Phase I could be expected. Similarly, during Phase III, when a 2000 to 2200 psi pressure differential existed across the seal, and surface damage accumulated, an increase in the stress level to leakage during this phase could also be expected. The only criterion on stress level during Phase III was that it never exceeded the yield strength of the material based on the nominal area of contact. An alternate approach to this procedure would have been to maintain a given stress level terminating Phase I and Phase III during each repetition. The latter technique would be more closely allied to the occurrences the seal would see in a real fluid connector. A given stress level would be applied upon each reassembly. During one set of tests, that of stainless steel mated with silver plated stainless steel, such a procedure was used. In all others the earlier mentioned procedure was used, mainly for the accumulation of meaningful data with regard to the effect of surface degradation.

2.3 Surface Finishing Techniques

As shown in Table 2.1, nine different combinations of material and surface finishing techniques were investigated. Within this framework, five finishing techniques were used on the two already stated materials, (347 stainless steel 2024 aluminum). a KANIGEN plated aluminum surface, and a silver plated stainless

TABLE 2.1

SUPERFINISHED SEALING SURFACE EXPERIMENTS

Test No.	Surface Finishing Technique	Specimen Material	Height of Annulus	No. of Tests of Specimens
1	Yatabe Fine Finish Sample #1	347 Stainless Steel	0.030"	1
2	" " "	" " "	0.030"	2
3	" " "	" " "	0.030"	3
4	" " "	" " "	0.060"	4
5	" " "	" " "	0.060"	5
6	" " "	" " "	0.090"	6
7	" " "	" " "	0.090"	7
8	" " "	" " "	0.090"	8
9	" " "	" " "	0.090"	9
10	" " "	" " "	0.090"	10
11	" " "	" " "	0.090"	11
12	Yatabe Fine Finish Sample #2	" " "	0.030"	1
13	" " "	" " "	0.030"	2
14	" " "	" " "	0.030"	3
15	" " "	" " "	0.030"	4
16	" " "	" " "	0.030"	5
17	" " "	" " "	0.060"	6
18	" " "	" " "	0.060"	7
19	" " "	" " "	0.090"	8
20	" " "	" " "	0.090"	9
21	" " "	" " "	0.120"	10
22	" " "	" " "	0.120"	11
23	Jones Optical Polished Surfaces	" " "	0.030"	1
24	" " "	" " "	0.030"	2
25	" " "	" " "	0.030"	3
26	" " "	" " "	0.030"	4
27	" " "	" " "	0.030"	5
28	" " "	" " "	0.060"	6
29	" " "	" " "	0.060"	7
30	" " "	" " "	0.090"	8
31	" " "	" " "	0.090"	9
32	" " "	" " "	0.090"	10
33	" " "	" " "	0.090"	11
34	" " "	" " "	0.120"	12
35	" " "	" " "	0.120"	13
36	Jones Optical Lapped Surfaces	" " "	0.030"	1
37	Parker Finish	A286 Stainless Steel	N/A	1
38	ATL Lead Lap	347 Stainless Steel	0.030"	1
39	" " "	" " "	0.030"	2

TABLE 2.1 CONT.

Test No.	Surface Finishing Technique	Specimen Material	Height of Annulus	No. of Tests of Specimens
40	Yatabe Fine Finish Sample #1	2024 Aluminum	0.030"	1
41	" " "	" "	0.030"	2
42	Jones Optical Polished Surfaces	2024 Aluminum KANIGEN Plated	0.030" "	1
43	" " "	" "	"	2
44	" " "	" "	"	3
45	" " "	" "	"	4
46	" " "	" "	"	5
47	" " "	" "	"	6
48	" " "	" "	"	7
49	" " "	" "	"	8
50	" " "	" "	"	9
51	" " "	" "	"	10
52	Jones Optical Polished Surfaces	347 Stainless Steel (one surface silver plated)	0.090"	1
53	" " "	" " "	"	2
54	" " "	" " "	"	3
55	" " "	" " "	"	4
56	" " "	" " "	"	5
57	" " "	" " "	"	6
58	" " "	" " "	"	7
59	" " "	" " "	"	8
60	" " "	" " "	"	9
61	" " "	" " "	"	10

steel surface. Superfinishing techniques used (except test 37) were the "Monomolecule Surface Finish" produced by the UP-HI Corporation of Tokyo, Japan, a Jones Optical Company (Boston, Massachusetts), polishing technique, a lapping technique by the Jones Company, and a lead lapping technique produced by the Advanced Technology Laboratories of the General Electric Company. One other surface was tried, that of a polishing technique on A286 steel produced by the Parker Aircraft Company of Inglewood, California (test 37). The latter specimens were of a different geometry and size than all of the other tests. Each of the resulting surface finish characteristics is described below.

2.3.1 Yatabe "Monomolecule Surface" Finish

Two sets of 347 stainless steel specimens and two sets of 2024 aluminum specimens were forwarded to the UP-HI Company, Ltd. of Tokyo, Japan for surface finishing by the Yatabe "Monomolecule Surface" finishing process (Reference 4). The Monomolecule Surface finishing process, United States patent No. 3,092,476, held by Yoshio Yatabe (Reference 5), is a high finish grinding or honing technique characterized by a) the grinder or hone having fine cushiony surfaces of polymeric materials distributed around the bonded abrasives and b) the use of such a grinding material. Coupled with the grinding abrasives being suspended in a resilient matrix, the removal of shocks, vibrations, and impulses from the grinding process succeeds in yielding an extremely flat asperity free surface. The resiliency of the matrix in which the abrasives lie acts as a cushiony absorber to the invitable vibration and shock during grinding. This occurs on an individual polymer particle scale. Brochures describing the technique claim asperity amplitudes not greater than 0.08 microinches. The technique can be used on cylindrical, spherical, or flat specimens. For purposes of this investigation only flat surface finishing was utilized. Literature describing the process lists as suitable material for finishing under this technique steel, stainless steel, Hastelloy, Stellite, tungsten carbide, chromium plated surfaces, and others.

Surface finish photomicrographs were received from the UP-HI Company with the specimens. It was obvious from initial observations of the surfaces that the stainless steel specimens were much better in quality than the aluminum specimens. The interference photographs of each surface, both stainless steel and aluminum, are shown in Figures 2.5 and 2.6. Unfortunately, the scale of the photographs and the interference techniques used are not known. However, assuming that the same techniques were used on each photograph, the relative quality between the stainless steel and the aluminum can be easily seen.

To more exactly appraise the surface finishes, both aluminum and stainless steel specimens were subjected to interference photography by ATL. Figures 2.7 and 2.8 show the character of the surface finishes. Both photographs were made at the same scale and with the same interference techniques. As can be seen, no surface roughness is evident at all under this magnification on the 347 stainless steel surface. Interference lines such as shown will illustrate surface roughness down to approximately 1 microinch. Inspection of the aluminum finish shows that the scratches are approximately five to 12 microinches in depth.

In order to learn more about the character of the surface on the stainless steel specimen, the surfaces were subjected to Nomarski microscope techniques (Reference 6). In this technique, the vertical variations in surface finish can

be discerned down to approximately 75 angstroms. At the same time, a large area can be inspected, the lateral magnification being kept rather small. Figures 2.9 and 2.10 show two different locations on the same surface. The obvious scratches are due to improper handling. The notable feature to the surfaces, if the obvious scratches are dismissed, is the pebbly nature. No scratches of any length are noted. Rather, the characteristic is one of random small hills and pits. Such a surface would be thought intuitively to be much better for sealing than one having directional scratches. The asperities are local in nature, discontinuous, and apparently independent of direction. No such photographs were made of the aluminum surfaces in that the Zeiss interference photos showed them to be vastly inferior to the stainless steel. Each set of aluminum samples and stainless steel samples evidenced the same characteristics.

It is to be further noted in the photos of the aluminum surfaces that, in that the overall surfaces are annular in shape, and the scratches are uni-directional, about a certain part of the periphery the scratches are tangential while in another section of periphery they are radial. In the latter case, they are natural leak paths. Hence, it would be expected that the aluminum surfaces would not possess characteristics well suited for sealing.

While the Nomarski and interference photographs readily illustrate the smoothness of the surface, little information is gained with regard to the flatness or freedom from waviness of the surface. A measure of the flatness may be gained by placing an optical flat over the surface to be evaluated and observing light band readings through the flat using a monochromatic light source. In this case, a helium filled tube source was used which produced interference bands 11.6 microinches apart. Should a curvature in the light and dark bands be noted such that, across the length to be evaluated, a tangent drawn between the end points reached the next light band, then between ends of the light bands, the surface would be high or low by an amount of 11.6 microinches. This technique is very applicable to immediate visual observation, but does not lend itself necessarily well to photography. Figure 2.11 shows the technique used on the 347 stainless steel. The Lap-master device was utilized (Reference 7). As can be noted, within the limitations of the photograph the surface is flat.

2.3.2   Jones Optical Works Polishing Techniques

Several test specimens were sent to the A.D. Jones Optical Works, Cambridge, Massachusetts for high quality optical polishing. The specifications which had been requested were:

a)   Flatness, within one helium light band (11.6 microinches).

b)   Roughness, no low relief scratches deeper than one half microinch.

The Jones Optical Works, which specializes in smooth surface finishes for many optical applications, was able, by successive polishing operations, to produce surface finishes to approximately this specification on the 347 stainless steel specimens. In order to accomplish this degree of flatness, the rings mentioned previously had to be placed inside and outside of the annular rises in order to prevent round-off. Figures 2.12 and 2.13 show high magnification photographs of the resultant stainless steel surfaces. Figure 2.12 is an interference photograph while 2.13 is a Nomarski photograph. As can be noted from the interference photograph, no scratches are present which are sufficient to

displace the interference bands to a noticeable extent. The Nomarski photograph shows only a few isolated pits and a few scratches which are randomly oriented but of obvious shallow depth. Two obvious scratches running from upper right to lower left were placed on the surface by improper handling and were not of sufficient length to cause a sealing problem. Lap-master inspection of the surfaces showed essentially no edge round-off.

In discussions with personnel from the Jones Optical Works, and after having extremely good results with their polished stainless steel specimens, another technique was offered by the Jones Company to effect a satisfactory surface finish. Two 347 stainless steel samples were lapped by the Jones Optical Works techniques, with the surface shown in Figure 2.14 resulting. As can be noted, the surface resembles in texture that of a sandblasted surface. Again, from observation, it was felt that these surfaces would not perform satisfactorily in a leak test. However, a single test on the specimens was run.

No aluminum specimens were finished to the Jones Polishing technique in that it was recognized by their personnel at the outset that the difficult-to-polish characteristic of aluminum would not allow results equal to the stainless steel samples. However, it was suggested that perhaps aluminum might still be used as a structural material if the surface to be finished is first plated with some metal more prone to surface polishing. The plating suggested was the KANIGEN nickel plate (Reference 8). The Jones Company plated the aluminum and surface finished the specimens. The KANIGEN process is one of plating aluminum or its alloys with nickel in an aqueous solution of a nickel salt and a hypophosphite. The resultant plate is not purely nickel and has a certain phosphorous content. No studies have been made as to the compatibility of the resultant plating with either fuels or oxidizers. The KANIGEN process was utilized merely in an effort to judge whether aluminum base metals can be, in some manner, affixed with a satisfactory surface finish. The resultant surface finishes are shown in Figures 2.15 and 2.16. Figure 2.15, an interference photograph, shows straight characteristics to the interference lines, but obvious scratches lying perpendicular to the light bands. The Nomarski photo, Figure 2.16, clearly shows very shallow scratches which are directional. While the surfaces shown are not as smooth or as asperity free as the Jones Optical technique applied to the 347 stainless steel nor the Yatabe stainless steel specimens, they are much better than those produced by the Yatabe technique aluminum specimens. Hence while it was doubted that the test specimens would perform as adequately as the stainless steel samples, it was thought that they might be satisfactory within the requirements set.

One further specimen was surface finished by the Jones techniques, that of a silver plated stainless steel sample. The purpose of such a surface would be for mating with a stainless steel superfinished surface. Such a combination was put into the program since it was surmised that, should surface damage be done to the system because of specks of particulate material or fluids trapped in the interface, virtually all of the damage would be done to the softer material. Upon reassembly, if the particulate material had been removed from that location, the application of the stress slightly less than the yield strength of the harder material would result in any previously produced asperities in the silver being rubbed out. It was conceded that the surface finishing technique would not produce results on the soft silver anywhere near the quality experienced on the stainless steel.

While that turned out to be the case, the silver plated specimens were quite flat and possessed very shallow asperities. Figures 2.17 and 2.18 show the resultant finish. It can be noted from Figure 2.18 that the edge roll-off which evidenced itself was within two hundredths of an inch of the edge and did not constitute a serious problem. It can also be noted that while the scratches are of some length, they are randomly oriented. In that surface finish on the silver was not a critical parameter in the proposed experiment, the lack of quality in comparison with the other superfinished surfaces by the Jones Company was not disappointing. The thickness of silver plate was 0.003 ± 0.0003 inches.

2.3.3 Diamond Lead Lapping Technique

A process which had been found successful in several applications requiring smooth surfaces at the Advanced Technology Laboratories was used on two sets of stainless steel samples. The lead lapping technique is one in which successively smaller diamond particles, backed by a soft lead matrix, are used as a polishing abrasive. Two means of accomplishing this polish were tried. The first was done by hand, resulting in randomly oriented scratches. Figures 2.19 and 2.20 show the surface characteristics. The surface has a speckled appearance as can be noted from both photos. The speckled effect is more pronounced near the center of the annulus than near the edges. It appears that a lead deposit has formed. As can be noted, some deep scratches exist on the surface. The second technique of lead lapping was to accomplish the process by rotating the specimens at high speed and bringing the diamond filled lead into contact with the specimen, thus trying to give tangential directionality to the asperities. It is recognized that wherever diamond is used, long scratches will result. The results of this endeavor are shown in Figures 2.21 and 2.22. As can be noted, the surfaces are not particularly good and defy the description "Superfinish". No leakage tests were even attempted on these latter specimens, although tests were run on the surfaces shown in Figure 2.19 and 2.20.

2.3.4 Parker Aircraft A286 Steel Fine Finish

A single leak test experiment was accomplished on a set of samples received from the Parker Aircraft Company. In general discussions with Parker personnel on the sealing phenomenon, Parker submitted, free of charge, to the Advanced Technology Laboratories, a set of surfaces to be mated which were machined on A286 steel, having a yield strength of approximately 90,000 psi. One specimen was annular in shape, having inside diameter of approximately 0.3 inches, an outside diameter of approximately 0.42 inches; the second specimen was much smaller in sealing area, having an inside diameter of 0.343 inches and outside diameter of 0.3835 inches. Hence, when mated together, the larger sealing area represented a semi-infinite medium while the second surface represented the true sealing area. Photomicrographs of the surface are shown in Figures 2.23 and 2.24. The surfaces are extremely flat, but were pebble grained in texture. In that the surfaces were much smaller than the pebbly structure of the Jones Optical Company lapped finish previously described, it was felt that the response in a leak test would be slightly better than that of the Jones technique but probably not adequate.

2.4 Leakage Test Results

Three methods have been used for presentation of the leakage data. The first, and the most important, since it yields data relating the required

stresses and the leakage rates obtainable, is that of plotting the leakage rate for all four phases of the experiment as a function of the normally applied stress. The leakage rate, plotted on the ordinate of the graph utilizes a logarithmic scale. The range of leakages measurable on the scale is from 10^{-2} atm cc/sec to 10^{-8} atm cc/sec, with the mass spectrometer used having the ability to measure to approximately 4×10^{-8} cc/sec. The normal stress, plotted on the abscissa, is plotted linearly, with the maximum stress on the scale being somewhat larger than the yield strength of the stronger surface material in contact for that experiment. Depending on the relative positions of the various data points, one, two, or three different tests are pictured on one graph. Arrows accompanying each portion of the curve indicate the chronological order of occurrences in the test procedure. Generally four segments are shown in each curve, signifying each phase of the four phase experimental procedure. In each, a vertical line (increasing leakage while normally applied stresses are held constant) is that of Phase II, wherein the internal pressure was increased incrementally. In reviewing the curves presented, significant points to be considered are: the stress level necessary to reduce the leakage rate to below 10^{-6} atm cc/sec while a one atmosphere pressure differential exists across the seal (Phase I); the amount of increase in leakage due to the increase in internal pressure from 14.7 psi to approximately 2000 psi; the increment of applied stress necessary to reduce the leakage to below 10^{-6} atm cc/sec while 2000 psi internal pressure is present (if indeed possible in some cases); and the extent of the increase in leakage as a function of decreasing stress level at the high internal pressure. Data presented in this section are presented in the manner described above.

A second way of presenting elements of data is that of plotting the increase in leakage during Phase II of the experiment as a function of the increase in pressure. Data presented in this manner are not overly important with regard to proof of feasibility of the elastic sealing technique, but do add greatly to the knowledge of the leakage phenomenon in a real sealing system. Data plotted in this manner are shown on log-log paper, wherein a purely molecular leak should ideally follow a slope of one and a purely viscous laminar leak should follow a slope of two. Selected plots of Phase II data are shown in Section 2.5.

Another method of presenting the information gained from Phase II of the experiment is to plot the experiment data gained on a graph of a family of leakage rates which, in turn, have been plotted logarithmically as a function of internal pressure and gap height between sealing surfaces. The model system for such an analysis is an annular shaped passage of perfectly smooth surfaces separated by a known gap height. The analysis considers both laminar viscous flow, molecular flow, and the transition region between. The dimensions of the annular system are compatible with the experimental dimensions used. As in the previous plot of Phase II information data plotted in this manner do not aid in showing feasibility of the technique, but rather help in gaining an understanding of the phenomenon. Information plotted thusly is shown in Section 2.5.

2.4.1 Yatabe Monomolecule Finish, 347 Stainless Steel Specimens

Both sets of stainless steel specimens received from the UP-HI Company of Tokyo were subjected to leakage tests. Eleven assemblies were made on each set.

2-14

The only changes in the systems from test to test were those of alteration of the height of the annuli. As shown in Table 2.1, the first set of samples were tested three times at a 0.030 inch annular height, twice at a 0.060 inch annular rise, and six times at the ultimate height of 0.090 inches. The second set was tested five times at the 0.030 inch height, twice at the 0.060 inch height, twice at the 0.090 inch height, and finally twice at a height of 0.012 inches. The purpose in altering the heights was that of assessing the effects on sealing of the increase flexibility of the annular rises. In that a certain amount of waviness certainly does exist on the sealing surfaces, at least microscopic variations in height, and since the stress levels are quite low, it was felt that the higher the rise, the more apt the low stress would be in bringing together any surfaces spaced due to waviness on the surfaces. Unfortunately, because the increases in annulus height had to be accomplished on a given set of specimens, and hence was changed from test to test, the increases accompanied any degradation which occurred to the surfaces. Any improvements due to the increased flexibility were at least potentially counteracted by the reductions on surface finish quality. Any trends in results toward ease in sealing could not have been solely accredited to the changes in rise height because of this associated problem.

The yield strength of the stainless steel being 39,000 psi, the maximum stress utilized on either set of samples was 37,000, and that stress was used only once. The leakage level which was adjudged to be satisfactory and sufficient to terminate further increases in stress was below 10^{-6} atm cc/sec. In some cases, however, this leakage was allowed to go below 10^{-7}. The actual data from the twenty-two separate tests done on the two sets of samples are shown in Figures 2.25 through 2.29 for the first set and 2.30 through 2.34 for the second set.

Review of the data from Figures 2.25 through 2.29 shows that, out of the eleven tests run, it was possible to seal to less than 10^{-6} atm cc/sec except in tests number 2, 10, and 11. In test number 2, the stress level was allowed to reach only slightly higher than 20,000 psi. The data from test number 3 show a curve shape similar to that in test number 2, and would indicate that, had the stress been allowed to increase in test number 2, 10^{-6} atm cc/sec could have easily been reached at a higher stress level. As it was, the leakage level did reach approximately 3×10^{-6}. However, in tests 10 and 11, leakage levels only slightly less than 10^{-5} atm cc/sec were possible, even though the stress levels reached 37,000 psi for test number 10 and 31,000 psi for test number 11. The shape of the decreasing leakage as a function of increasing stress are such in both cases that it would not have been possible to reach 10^{-6} atm cc/sec even with further increases in stress to the yield strength of the stainless steel. From these data it can be concluded that nine successful tests were possible, even with the degradation of surface finish that was noticed after several reassemblies.

Photomicrographs taken of the sealing surfaces after the first leakage test showed that some change did take place in the surface finish. Figures 2.35, 2.36 and 2.37 show the types of damage caused. Figure 2.35 shows, in general, the same surface characteristics as the unused specimen, thus indicating the actual mating to be elastic. However, imposed on this are series of indentations which could have only resulted from foreign particles resting between the two surfaces. This could have been caused either by liquid droplets or by solid

particles passing through the seal during the early stages of the test and then becoming entrapped in the system. Figure 2.36 shows the same general background characteristics as the unused specimens plus a rather large defect which appears to be the result of a globule of oil or other particle impressed between the elastic surfaces. Neither of the defects shown in the two photographs would affect the sealing characteristics significantly. However, Figure 2.37 shows a series of scratches which extended approximately one third across the seal width. The scratches appear on both surfaces and were mere images of each other. It would appear from the photographs that relative motion had occurred between the surfaces during the test. However, due to the manner in which the test specimens were placed together and secured, relative motion was impossible. An alternate cause of the scratches might be the motion of a particle or particles moving in the interface area. However, no positive cause for the scratches is known. Defects of this type could well be expected to decrease the sealing ability of the system. No further photographs were made of the first set of Yatabe specimens, although visual inspection of the surfaces after the eleventh assembly showed no significant increase in surface damage over that displayed after the first assembly. Hence, it must be conceded that the handling technique during the first assembly was not as carefully accomplished as it should have been.

While surface damage was apparent as a result of the first assembly, and it can be assumed that an accumulation of surface damage was caused as a result of further matings, the data as shown in Figures 2.25 and 2.29, do not particularly show a trend towards diminishing sealability, except for the last two tests. Tests 3, 4, 5, 6, 7, and 9 all required approximately 30,000 psi stress level in order to seal at the 2000 psi internal pressure. In order to seal at the one atmosphere internal pressure, the first and the eighth test required less than 8,000 psi, while the second, third, and sixth, required approximately 15,000 psi. The seventh, and ninth tests required approximately 10,000 psi stress. In tests number four and five, stress was allowed to be increased beyond the necessary level in order to reduce the leakage down to approximately 4×10^{-8} atm cc/sec. Because of this, the stress level required was approximately 25,000 psi. Review of the data shows that, in order to reduce the leakage to approximately 5×10^{-6}, which had been the level attained in previous tests, 15,000 psi would have been required. Thus, while no monotonic trends for degradation and sealability were seen, it does become apparent that the limit of sealability was, for the first set of specimens, nine assemblies.

Where the first set of Yatabe specimens (stainless steel) were encouraging, the results on the second set, which were an exact duplication as far a surface finishing is concerned, were even more encouraging. Only in one test, that of number 8 assembly, was 10^{-6} atm cc/sec leakage level unattainable. That test, shown in Figure 2.33, required 36,000 psi to reach 10^{-5} atm cc/sec. No explanation is readily available for this, since, in tests number 9, 10, and 11, 10^{-6} leakage rates and below were easily attainable. In general, lower stress levels were required than in the previous set of specimens. For the first seven tests, stress levels as low as 5500 psi down to 3000 psi were satisfactory in reducing the leakage level to below 10^{-6} atm cc/sec with a one atmosphere pressure differential existing across the seal. For tests 8, 10, and 11, stress levels of between 7000 and 8000 psi were satisfactory to accomplish the same leakage level. Only for test number 8, which was the unsatisfactory test, was a stress level of approximately 11000 psi required. In this series of tests, however, the slow decrease in surface quality was somewhat evident. While the degradation

was not monotonic in its leakage results, it could be generally noticed. The final tests, numbers 10 and 11, required up to 35000 psi in order to seal, where earlier tests, numbers one through six, required at the most 21000 psi. The significant difference between the second set of samples and first was that of the low stress required for sealing at the one atmosphere pressure differential and the successful sealing during the 10th and 11th tests. The resultant damage due to the eleven assemblies is shown in Figures 2.38 through 2.40. All three photomicrographs show areas away from the edges of the annular sealing rises. Figure 2.38 shows that even the more severe scratches are not deeper than five microinches. Figure 2.39, an extremely high magnification photograph, shows that the original surface characteristics are still present, however, now being superimposed by indentations obviously due to foreign matter being compressed between the two surfaces during the mating experiments. Figure 2.40, a relatively low magnification photo, shows a large number of scratches in one section of the sealing area. However, while the scratches present are obviously much deeper than the original surface scratch distribution, none of the scratches are as deep as those from normal machining processes.

From the data gained from the second set of samples, it can be concluded that the Yatabe Monomolecule surface finishing technique would indeed be satisfactory for repeated sealing at stress levels less than yield strength for 347 stainless steel connectors reused up to at least seven times. Unfortunately, no positive conclusions can be drawn from the technique of increasing the flexibility by cutting back on the material adjacent to the annular rises.

2.4.2 Yatabe Monomolecular Surface Finishing Technique-2024 Aluminum Specimens

Only two tests were run on the 2024 T4 aluminum samples received from the UP-HI Company in Tokyo. Because of the rather poor results gained in the two experiments, no photomicrographs were made of the surfaces to show the degradation in surface finish. It is apparent that the original surface finishes were not sufficient to allow sealing even in their virgin conditions. While the yield strength of the aluminum samples was approximately 51,000 psi, only 42,000 psi was applied to the seals. It was apparent, even at this stress level, because of the large leak that existed at this time, that further application of stress could not possibly decrease the leak to less than even 10^{-3} atm cc/sec. Figure 2.41 shows the results from the two tests run. As opposed to the stress level of around 10,000 to 20,000 psi required to seal at an internal pressure of one atmosphere for the stainless steel samples, 42,000 psi was required to decrease the leakage to approximately 2 x 10^{-5} atm cc/sec. When the internal pressure was increased to 2000 psi, the leakage level increased to almost the limits of the mass spectrometer, around 10^{-2} atm cc/sec. This being so poor in comparison with the previously tested stainless steel samples, no further attempts were made with either these aluminum samples or surface finishing aluminum without plating. As was pointed out in Section 2.3.1, the surface finishes on the aluminum in the as-received condition were highly directional and poor results were expected.

2.4.3 Jones Optical Works Polished Surfaces - 347 Stainless Steel

Thirteen assemblies were accomplished on the stainless steel samples received from the Jones Optical Works. Because of the high quality of the surface finishes noticed, good results in leak tests were expected. Again, as in the

Yatabe tests, the prospect of gaining information about the effects of increase in flexibility by increasing the annular rise heights was tried. In this case, five tests were accomplished at the 0.030 inch height, two tests at the 0.060 inch height, four tests at the 0.090 inch height, and the final two tests, at 0.120 inches.

The results of the leakage as a function of applied stress are shown in Figures 2.42 through 2.47. In these figures, the effects of surface degradation is quite apparent. During the first two assemblies and the fourth and fifth assemblies, extremely low stress levels were necessary to seal even at 2000 psi internal pressure. Commencing with test three, and for tests six and above, much higher stresses were necessary. However, up through test number nine sealing to less than 10^{-6} atm cc/sec was still possible at stress levels well less than the yield strength, the largest stress required being 31,000 psi. Test number ten, however, proved disappointing, with 31,000 psi applied stress reducing the leakage to only 10^{-5} atm cc/sec with the slope of the curve being very shallow, indicating little chance of reducing the stress to below 10^{-6} atm cc/sec with an increase in stress level to the yield stress. Test number 11 again proved satisfactory, yielding 10^{-6} atm cc/sec with a stress level of 36,000 psi. However, tests 12 and 13 proved quite unsatisfactory with only approximately 10^{-4} atm cc/sec being attainable in test number 12 and 10^{-5} atm cc/sec being attainable in test number 13. However, even with the negative results of the latter tests, the surface finish can be considered satisfactory for repeated use up to nine assemblies, which is even better than the Yatabe surface finishes. Of course, in this case, only one set of samples was used.

One odd set of data, that of test number 4 is to be noted. When the internal pressure was increased from one atmosphere to 2000 psi during Phase II of the experiment, essentially, no increase in leakage was noted.

The amount of damage done to the surfaces by the repetitive assemblies can be seen in Figures 2.48 through 2.50. Figure 2.48, a high magnification Nomarski photo, shows that the surface retained its original texture, however, now being superimposed with much more severe pits. Figure 2.49, a low magnification interference photograph, shows that the pits, in some cases are several wavelengths in depth, although the general flat characteristic of the surface still exists. Figure 2.50, showing a particularly badly damaged area, illustrates that while the original surface finishes were still apparent, a great number of scratches have been superimposed on the surface. It appears obvious that some of these scratches were sufficient to reduce the sealing capabilities of the Jones Optical finish. It is not known during which assembly the bulk of the surface damage was accumulated, or whether the accumulation was roughly linear with the number of assemblies.

2.4.4 Jones Optical Company Lapped 347 Stainless Steel Specimens

The lapped stainless steel specimens, supplied by the Jones Optical Works, described and shown in Section 2.3.1, were not expected to yield satisfactory sealing results. However, in that they were available, and constituted a separate method of surface finishing, one test was accomplished. The results are shown in Figure 2.51. Inspection shows that, the technique is obviously not amenable to elastic sealing. No further attempts at lapping by this means were tried.

2-18

2.4.5 ATL Lead Lapping Technique - 347 Stainless Steel

Only the first set of specimens finished by the lead lapping technique were leak tested due to the obvious poor surface quality of the second set. The leakage results attained with the first set were certainly unsatisfactory, as is shown in Figure 2.52. Stress levels equal to the yield strength of the stainless steel succeeded in reducing the leakage level to approximately 3×10^{-4} atm cc/sec in one case and 2×10^{-5} atm cc/sec in the second case. No further experimentation was done with the lead lapping technique.

2.4.6 Parker Aircraft A286 Steel Finishing Technique

One leakage experiment was accomplished on the specimens received from the Parker Aircraft Company. The results of this test are not amenable to simple comparison with all other tests done due to the difference in yield strength of the material used and the different configuration, along with the difference in sealing geometry. However, it can be seen that, for the particular samples considered, the application of stresses approaching the yield strength, above 80,000 psi, did not cause sealing at 2000 psi internal pressure. Based on previously gained slopes of the decrease in leakage as a function of increasing stress when a 2000 psi internal pressure had been used, little hope was seen for reducing the leak significantly below 2×10^{-4} atm cc/sec. This test must be considered only as a side venture and not relevant in the determination of the overall feasibility of superfinishing as a sealing technique. Figure 2.53 shows a plot of the leakage as a function of stress for this particular case.

2.4.7 Jones Optical Works KANIGEN Process Superfinished Surfaces - 2024 Aluminum

Ten assemblies were made on the KANIGEN plated 2024 aluminum surfaces received from the Jones Optical Works. In these tests, the relationship between leakage rate and applied stress as a function of the yield stress of the material is not as clear cut as in all previous cases mentioned. Herein, the yield strength of the aluminum was used as the determining factor for setting the allowable stresses. The yield strength of the aluminum being approximately 51,000 psi, the allowable stress was set at 42,000 psi. The yield strength of the plate, which is not a pure nickel, is certainly less than 40,000. (The yield strength of "A" nickel is approximately 14,000 psi). Also, the thickness of the plate was not known exactly, although it did not exceed a few mils. Because of previous poor results in assessing the merits of increasing the flexibility of the annular rises by cutting back on the material adjacent to the rises, such was not tried in this case. The concept of superfinishing, in this case, is not quite as pure as in previous cases because of the recognition that surface plastic deformation of the nickel would occur. Because of the thinness of the nickel plate, particularly after the superfinishing process, it was expected that rigid backup material under the plating would keep surface deformation to a minimum. The results of the tests are shown in Figures 2.54 through 2.60. One test, the second assembly, was not completed due to an error in the test procedure. The stress was allowed to be removed from the specimens prematurely. Review of all other test data shows a reproducibility of results not apparent in previous tests. While 10^{-6} atm cc/sec was not reached in all cases, levels below 2×10^{-6} were reached. Tests 6 through 10 showed almost identical results. Extremely low stresses were required for quelling the leakage during a one atmosphere internal pressure application, while the predetermined

stress level 42,000 psi was required to reduce the leakage to its ultimate level. However, the slope of the leakage stress curve is very shallow in all cases, with the improvement in leakage level being rather insensitive to the increase in stress. For instance, were 4×10^{-6} atm cc/sec be adjudged allowable, then only 20,000 psi would be required to reach the successful leakage rate. The three significant features of this particular combination of surfaces are then, a) extremely low stress levels required for initial sealing, b) a pronounced insensitivity of leakage to increase in stress level and c) nearly perfect reproducibility of results from one assembly to the other.

Because of the reproducibility, and the near attainment of 10^{-6} stress level, it must be judged that the KANIGEN process is successful as far as sealing with stresses is less than the yield of the substructure, 2024 T4 aluminum.

2.4.8 Jones Optical Works Superfinished Surfaces - 347 Stainless Steel vs Silver Plated Specimens

The specimens subjected to leakage experiments described below were not, in the exact sense, a test of purely elastic sealing. In that a great deal of surface degradation had been noted on both of the stainless steel surfaces in both the Yatabe finished specimens and the KANIGEN finished specimens, it was felt that, by plating one of the surfaces with a soft material, any damage which would result from mating the surfaces together would tend to be accumulated on the softer surface only. In that the surfaces were cleaned prior to each assembly, and any particulate matter removed from the system when the following mating was accomplished, the previously accumulated damage on the softer surface would be "rubbed out" in that the allowable stress would be set slightly less than the yield strength of the truly superfinished stronger surface. Hence, the softer plated surface would be loaded to well above its yield strength. Thus, the combination of surfaces and materials would be somewhat akin to the experiments reported in References 1 and 2 except for the superfinished characteristic of the stronger material in contact.

A modification to the testing procedure was made in this series of tests; rather than place whatever stress was necessary during each test to attain a leakage level less than 10^{-6} atm cc/sec, thus having different stress levels placed on the system each time, it was decided that whatever stress levels were used the first time would be used throughout, regardless of the leakage levels attained. It is easily noted that this procedure, which yields somewhat different information than previous tests, is more closely related to the true chronological loading a seal would see in an operational connector, that of a planned stress level on each reassembly.

The test results for the series of ten experiments are shown in Figures 2.61 through 2.65. During the first experiment, the leakage was reduced to below 10^{-6} atm cc/sec almost immediately after the start of the test. Hence, it was allowed to reduce to approximately 10^{-7} atm cc/sec, which was associated with a stress level of 8200 psi. Thus, 8200 psi remained the stress level ending Phase I of the experiments in all of the succeeding tests. Upon subjecting the system to 2000 psi internal pressure during test 1, the leakage rose to approximately 10^{-5} atm cc/sec. Addition of applied stress to the system brought the leakage gradually down to below 10^{-7} atm cc/sec at a stress level of 33,500 psi. A stress level of only 24,000 psi brought the leakage to less than 10^{-6} atm cc/sec.

As it turned out all succeeding tests, except number five, performed better with regard to required stress levels than test number one. During test number two, even with the 8200 psi applied stress the leakage never rose above 10^{-6} atm cc/sec. During test number three, the leakage rate was totally insensitive to the increase in pressure. During test number four, the leakage rate was reduced to less than 10^{-6} atm cc/sec at a stress level of approximately 12,000 psi. Test six required approximately 14,000 psi; test seven required approximately 17,000 psi; test eight required approximately 14,000 psi; test nine required 18,000 psi, and test ten required approximately 11,000 psi. Only test number five required a higher stress, that of approximately 27,000 psi. In all cases, the 8200 psi was sufficient to reduce leakage to less than 10^{-6} atm cc/sec; in most cases it was reduced well below that level.

If Figures 2.61 through 2.65 are compared with all previous data as plotted for superfinished mated surfaces, one striking discrepancy can be noted. In all previous tests, the traces signifying Phases III and IV, those portions of the experiment where the stress was raised and lowered at the same internal pressure, the lines lay very close together, denoting a very small hysteresis loop. In other words, since the mating (and hence sealing) was completely elastic, the response of the system was nearly reversible. Review of the data for the silver plated specimens shows that not to be the case. Herein, even though only three mils of silver thickness was available for compression, the system seems to be somewhat more insensitive to stress reduction than any system previously tested in this program. This phenomenon can be noted quite distinctly in tests one, five, seven, and nine. The phenomenon exists to a lesser extent in all other tests.

The results shown above are most encouraging. It is recognized that certain limitations to such a system exist, notably those of temperature limitations for such soft plated materials. However, because of the added characteristic of reduced sensitivity to stress removal, this combination of surfaces must be considered successful and warranting further tests should a prototype connector be built incorporating the elastic sealing principle.

The primary reason for accomplishing the tests described above was that of causing most of the damage to be done to the softer material, hence protecting the stronger material and increasing the reusability of the system. In this case, the technique proved notably successful. After ten experiments, the stainless steel surface remained extremely free of the type of pits and scratches evident on the Yatabe stainless steel specimens or the previously used Jones stainless steel specimens. However, the silver plated specimen had very poor surface quality. Hence, it is obvious that most of the damage was done to the silver plated surface; but little damage "rubbed out" by the reassemblies. Also, the stainless steel surface was noted to be tarnished after the several experiments and several weeks in normal atmosphere. Neither the degradation in surface finish nor the tarnish seem to affect the sealing. It appears that, while the surface becomes rougher and rougher, the harder material being extremely smooth, "rubs out" sufficient asperities on the silver to allow adequate sealing.

2.5 Leakage Flow Characteristics

In that sixty-one separate experiments were done involving very similar systems, a great deal of data became available for assessment and comparison with regard to the flow characteristics of the existing leaks. While, during

Phases I, III, and IV, few theoretical comments can be made concerning the flow because of the variation with time of the passage configuration, Phase II of the experiments offers some opportunity for theoretical considerations. During Phase II, the internal pressure is increased incrementally, while the applied load is adjusted such that the stress remains constant on the seal. The adjustment of load is based on the assumption that the pressure acts only to the inside radius of the seal, and not completely across the seal face. Of course, since a leak exists, the assumption is not completely valid. However, it is suspected that the gradient of pressure across the seal is very steep near the inside and quite shallow as the outside edge is reached. Thus, while the assumption is not perfect, it is probably reasonably sound.

If such be the case, then the leak path remains very nearly constant in configuration during Phase II of the experiment. That being so, then a rather pure relationship between leakage and pressure should exist. Such would be true no matter what the asperity characteristics of the surfaces in contact. However, in that in all cases, the surfaces were extremely smooth, opportunity is gained for comparison with analytically predicted flows as outlined in Reference 3.

Thus, two comparisons are available:

a. Evaluation of the molecular and viscous flow regimes of the leakage rate as a function of pressure, and

b. comparison of the leakage rate with flow rates predicted analytically on the assumption of constant passage height.

Analytically, should the flow be molecular in nature, the leakage rate should vary linearly with the internal pressure (since the external pressure is essentially zero). For viscous laminar flow, the leakage rate should vary with the square of the internal pressure (again since the external pressure is essentially zero). Moreover, a smooth transition between molecular flow and viscous flow should exist, molecular flow being in evidence for the lower flow rates at lower pressures and viscous flow at the higher flow rates at higher pressures. Should the leakage be plotted as a function of pressure on log-log paper, then molecular flow should show up as a straight line with a slope of one and viscous flow as a straight line with a slope of two, with the curve being faired in smoothly between the two straight line segments. For each test which yielded a valid Phase II, such plotting was done. Typical curves are shown in Figures 2.66 through 2.78. The large majority of curves followed the expected theoretical patterns very closely. Both Yatabe stainless steel sets of specimens yielded the results in each case perfectly compatible with the initial slopes of one and the final slopes of two. Figures 2.66 and 2.67 show three sample curves for the first Yatabe stainless steel specimens; Figures 2.68 and 2.69 show similar curves for three tests on the second Yatabe stainless steel samples. In each of the six curves shown, it can be noticed that the transition region, the part of the curve between the slopes of one and two, is extremely short. In Figures 2.67 and 2.68, the transition region is almost nonexistent, with an extremely sharp break in the curve between molecular and viscous flow.

Figures 2.70 and 2.71 show three leakage-pressure curves for the Jones Optical stainless steel polished finished samples. Two of the curves shown,

from data gained during the latter tests in the series, follow the expected
theoretical configuration; however, the results of test number five, shown in
Figure 2.70, yield a slope less than one for a low pressure and a slope greater
than two at higher pressures. In this series of thirteen separate tests, two
tests yielded results as shown in Figure 2.70.

The results from the KANIGEN plated specimens deviated furthest from the
expected theoretical results. Figures 2.72 and 2.73 showed two traces from that
series, the first showing the deviation from theory and the second one showing
nearly complete agreement with theory except for the final three data points at
the high pressure. However, during this series nearly all of the traces deviated
from a slope of two at the high internal pressures. Only one test, that of test
number one, shown in Figure 2.72, deviated at low pressures, showing a slope at
less than one.

Of the ten tests done with the stainless steel surface mated with the silver
plated surface, nine leakage-pressure curves are shown. (Test number three
yielded leakage results independent of pressure, signifying either a liquid in
the interface, or some other form of passage blockage). The nine curves are
shown in Figures 2.74 through 2.78. Of the traces shown, those concerning tests
4, 5, 7, and 8 agree almost perfectly with theory, while tests 1, 2, 6, 9, and
10 show a distinct deviation from theory in that slope of the curve at low
pressure is much less than one. Small deviations in the same manner can be seen
in the other traces. At the high pressures however, all of the slopes mate quite
closely with two.

With deviations such as are shown in the data presented, a search was made
for some explanation. For the slopes greater than two at the high internal
pressures, it is possible that a cleaning action is taking place in the leak
path as has been noted and reported upon in Reference 2. Such occurs when par-
ticles locked in the flow passages are blown out by the increasing pressure
differential. Generally, discrete rises in the leakage-pressure trace are noted
when a flow path is cleaned. If this did occur in the cases cited herein, it
is not completely obvious. Another possibility for the phenomenon is that the
correction in applied load is insufficient at the higher pressures to counter-
act the pressure acting across a certain portion of the seal. Should this be
the case, then the true stress acting on the seal is decreasing, and a larger
leak path exists at the high pressures.

The explanations for the slopes less than one at the extremely low pressures
and leakage rates is less apt to relate to the true flow phenomenon and leak
path geometry then it is to the flow rate measurements. Immediately prior to the
start of Phase II, the high initial leakage rate has been reduced by the imposition
of stress on the system. However, the possibility of system saturation exists
wherein helium is being received into the mass spectrometer from the components
rather than by the direct leak to be measured. Should this be the case, and a
roughly constant rate were to be measured, then, when the true leak rate is
added to it, the result would be a fairing in of the curve as is shown on the
graphs. The rate measured due to the possible saturation would be the deviation
from the theoretical curve at the first point of measurement. By the time the
theoretical and experimental curves coincide, nearly a decade of leakage rate
has been traversed, and the possible saturation rate would be negligible com-
pared to the actual leak rate.

An interesting pattern to the location of the transition flow regime exists in the accumulated data. Should the location of a transition "point" be arbitrarily chosen as the intersection between two straight line segments of slopes one and two coinciding with the experimental curves during the viscous and molecular flow regimes, and a histogram of the leakage rate existing at that point of intersection drawn, then Figure 2.79 results.

A distinction has been made in plotting of the data between the results of the stainless steel-silver plated specimens and all the rest of the data. The transition region for the stainless steel-silver tests lies predominantly at the $(1 - 3) \times 10^{-6}$ range. Should this data be omitted from a histogram, then a rather symmetric distribution with a mean value between 1×10^{-5} and 2×10^{-5} atm cc/sec exists for the transition region. Figure 2.79, a bell shaped Gaussian type continuous distribution has been shown in a dotted line. Thus, for the pure elastic type sealing phenomenon (between superfinished surfaces), it appears that the transition region between molecular and viscous flow exists about at the 10^{-5} atm cc/sec leak level. In tests previously accomplished and reported in References 1 and 2, concerning sealing systems which required plastic deformation at the interface, a great deal more scatter than is shown in the data herein has been noted. Generally, in the literature, the transition region is said to exist between 10^{-6} and 10^{-4} atm cc/sec, varying slightly with the type system employed.

A possible explanation for the difference in the location of the transition "point" in the silver tests as opposed to the other tests concerns the probable shape of the leakage paths. For the purely elastic test, since few low relief asperities exist on the sealing surface, then the leakage paths are very probably wide slits of extremely low height caused primarily due to the waviness of the surfaces and any deviation from uniform stress about the periphery. Should this be the case, then, since the flow regime is a function of passage height, the entire leakage path would approach the molecular flow regime rather uniformly; i.e., the few paths existing would reduce in height, changing the flow from viscous to molecular uniformly. In the case of the stainless steel-silver plated specimens, however, because the silver plate deforms plastically, as has been shown by its rough nature after assembly as compared with the stainless steel surface, the total leak probably results from many leak paths, some of which are due to low relief scratches. Should this be the case, then the leak paths will be closed off by the increasing stress by blocking at some point along each path at a different level of stress. Since the low relief scratches possess critical dimensions larger than the height of the narrow slits existing in the true superfinished specimens, then, until each of the individual paths is closed off, viscous flow can exist. Thus, the decrease in total leak is accomplished by successive closing off of each of many leaks, reducing the total leak flow, while viscous leakage exists in the individual leak paths for a longer period of time during the test.

The theoretical analysis relating the leakage flow from an annular shaped passage with the internal pressure of the system and a uniform gap height of the passage has been carried out for the seal dimensions of the present tests. A family of four leakage rates have been plotted on log-log paper with internal pressure as the ordinate and gap height (in microinches) as the abscissa. Provision has been made in the analysis for viscous flow and the molecular correction factor. A test of the proximity of the superfinished sealing phenomenon to the

model used for the analysis is to plot the leakage results of Phase II of the experiment on such a graph. Should the leakage path approximate an annular flow passage of constant height, then the data should plot as a straight vertical line. Should variations in the passage geometry occur during Phase II, or should the total leak become comprised of the sum of several small leaks each having the potential of being molecular or viscous at any given time, then a deviation from the vertical should result. Each of the Phase II sets of data has been so plotted. As might be expected, when a large amount of data is compared with theory, some of it agrees very well with the model, and some does not.

Should a straight line be fitted to the data for each case, (even though a straight line may not be the best curve for the data points), then, in all cases, all of the straight lines would lie within 20° from the vertical, with nearly all of them within 10° of the vertical. In all cases save one, the line, if deviating from the vertical, would lean toward the right at the higher pressures and leakage rates. Such would indicate that, as the pressure was increased, the gap height was increasing. This assessment of the phenomenon would be in accord with the previous observation of the increase in the leakage as a function of pressure greater than pressure squared.

To buttress this argument further, if, rather than a straight line be fitted through the data, a curve passing through each data point were to be plotted, then the deviation from the vertical becomes greater at the higher pressures and leakage rates.

Sample traces of the Phase II data from tests selected at random are shown in Figures 2.80 through 2.86.

While the information presented in this section does not add to or detract from the conclusions of the feasibility study, it does show that the leakage through pure superfinished seals obeys rather closely the theoretical leakage as gained from an analysis of a model hypothesizing the uniform gap height. Also, a closer approximation than had been thought possible has been gained of the location of the transition regime. The importance of this knowledge is that, since above the transition region the leakage varies as the pressure squared, should it be possible to utilize seals for in a connector for a given pressure range while maintaining molecular flow, then the increases in leakage due to increase in pressure can be determined and known to be less severe than had the flow been initially above the transition region. Such knowledge buttresses the logic for specifying leakage rates of 10^{-6} atm cc/sec in a system rather than allowing a leakage rate of 10^{-4} atm cc/sec, even though the rate may be satisfactory from an operational point of view.

2.6 Conclusions

From the tests performed under the program described herein, it can be concluded that it is possible to seal repetitively a system made up of super-finished metal surfaces pressed together at stress levels less than their yield strength. It has been shown experimentally that for both 347 stainless steel and for KANIGEN nickel plated aluminum, satisfactory surface finishes can be attained. It has been shown that, for the Japanese Yatabe surface finish technique, up to seven reassemblies are possible under the framework of an allowable

leakage rate of 10^{-6} atm cc/sec and an internal pressure of 2000 psi and that the Jones Optical Polishing technique yields surfaces capable of sustaining nine assemblies. It has also been shown that the use of a thin soft plating on one of the superfinished surfaces produces even better results as far as the number of assemblies and the reduction in sensitivity of the seal to stress removal.

As far as present costs are concerned, the Yatabe surface finish can be attained for approximately $200.00. The cost for a single Jones Optical Surface finish is approximately $100.00. In that the Jones technique has proven satisfactory, and that such a surface finishing technique exists in this country, the Jones technique or its equivalent represents the better choice for the development of a prototype connector. It is not known the extent to which the cost can be reduced for such surface finishes, although in that the surfaces used for the present study were special single endeavors, it is highly likely that, for a mass produced undertaking, the cost would be reduced greatly.

The specifications for surface finish and flatness which were used as standards for the Jones Optical Works process appear to be adequate for satisfactory sealing results. They are:

a) flatness to within one helium light band, 11.6 microinches, and

b) roughness, no low relief scratches deeper than 1/2 microinch.

The remaining problem stated in Section 2.1.1, that of protection of the surfaces during handling and assembly, requires two separate considerations. First, no sliding can be allowed to exist between the mated parts. Secondly, in that the surfaces must be polished on high relief lands, a means of physical protection must be assured. A possibility for such protection is shown in Figure 2.87. In the proposed design, sheet metal rings would be attached to the connector components immediately after surface finishing and clean. Throughout the life of the connector, they would remain in place. Their dimensions and position in the connector would be such that no interference in connector assembly would be realized. In order to insure that no sliding exists between superfinished surfaces, a tongue and groove type interlock can be used to prevent rotational sliding during the torquing operation; a shallow concentric male-female fit can be used to prevent lateral sliding.

The limitations to the concept of elastic sealing appear to be concerned with the size of the connector. In that flatness as well as surface smoothness are important, it appears that the technique will be valid only in fluid connectors having a rather small radius. It is recommended that only tube fittings, those up to one inch, be considered for application of this principle. As larger diameters are considered, the problem of maintaining flatness becomes more and more acute and the radial rotations of the sealing surfaces under bolt loads becomes more and more significant.

2.7 References

1) "Sealing Action at the Seal Interface", edited by F.O. Rathbun, Jr., N63-18159, NASA-CR-50559, (Technical Information Series Report 63GL43), March 15, 1963.

2) "Fundamental Seal Interface Studies and Design and Testing of Tube and Duct Separable Connectors", edited by F.O. Rathbun, Jr., N64-27305, NASA-CR-56571, (Technical Information Series Report 64GL97), June 1, 1964.

3) "Leakage Flow", edited by T.P. Goodman, N63-18493, NASA-CR-50558, (Technical Information Series Report 63GL42), March 15, 1963.

4) Brochure, "Monomolecule Surface Finish", UP-HI Company, Ltd, Tokyo, Japan.

5) United States Patent 3,092,476, June 4, 1963, "Method of Manufacturing a Grinder or Hone Having Fine Cushiony Surfaces", Yoshio Yatabe.

6) Brochure, "Interference Contrast Equipment", after NOMARSKI, Reichert Optische Werk AG, Austria.

7) Brochure, "Measuring Flatness with Lap-master Monochromatic Light and Optical Flats", Crane Packing Company.

8) "The Patent Situation", by Gregoire Gutzeit, Symposium on Electroless Nickel Plating, ASTM Special Technical Publication No. 265, November 1959.
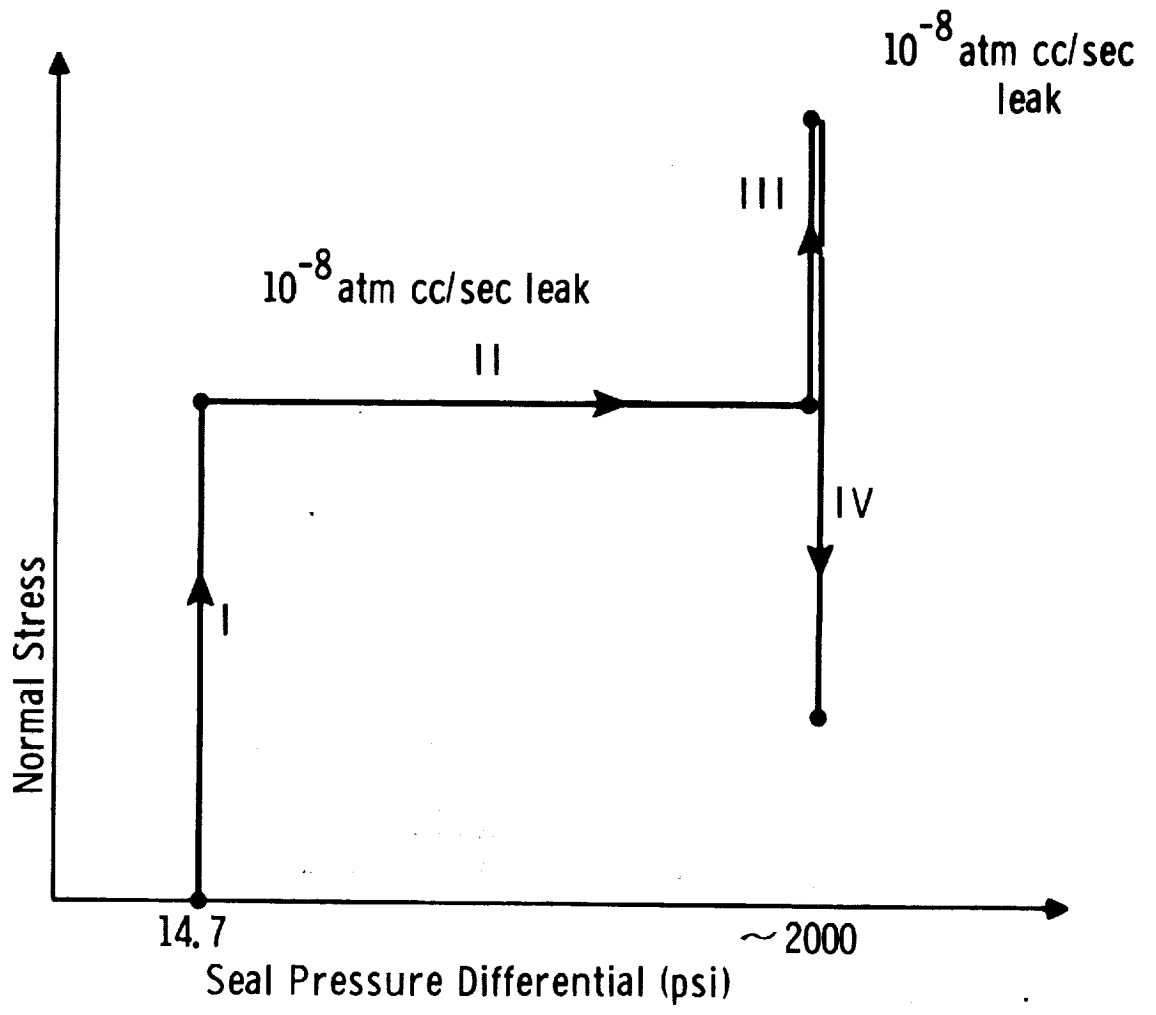
FIGURE 2.4 Experimental Procedure for Accumulation of Data

2-28
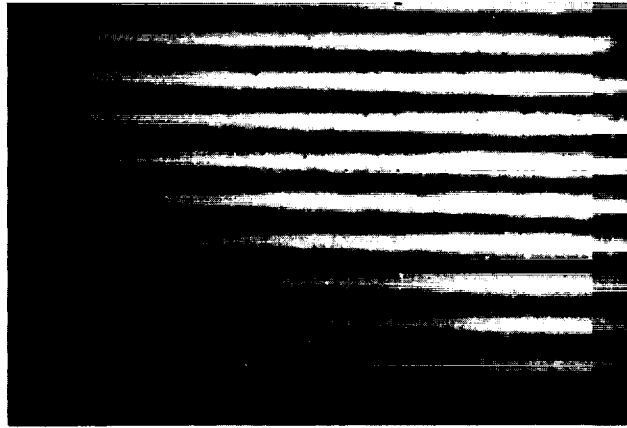
FIGURE 2.5 Japanese Interference Photograph of
347 Stainless Steel Specimen (Scale not known)
"Monomolecular Finish".
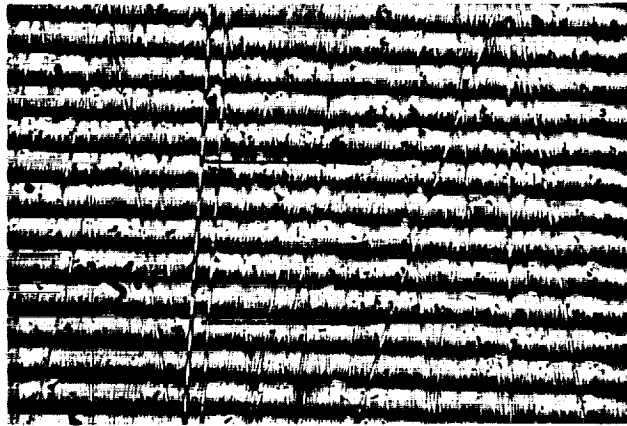
FIGURE 2.6 Japanese Interference Photograph
of 2024 Aluminum Specimen (Scale not known,
but same as in Figure 2.5) "Monomolecular
Finish".
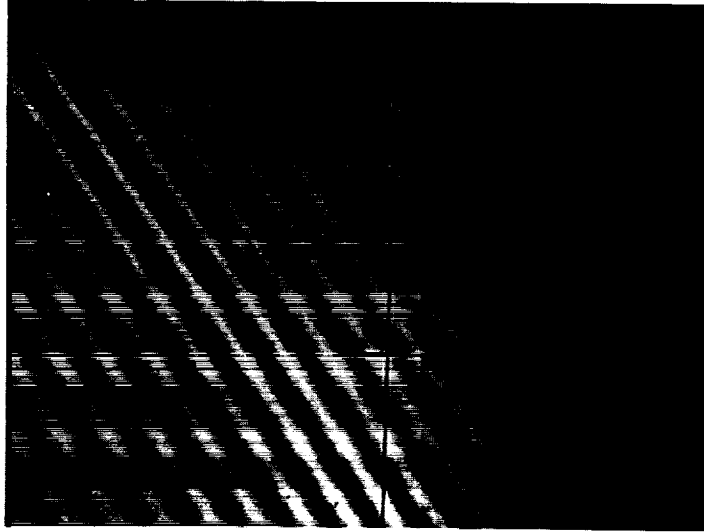
FIGURE 2.7 Interference Photo of
Monomolecular Finish on 347 Stainless
Steel - Scale: 0.00194 inches between
Scale Marks; 11.8 microinches between
interference lines.
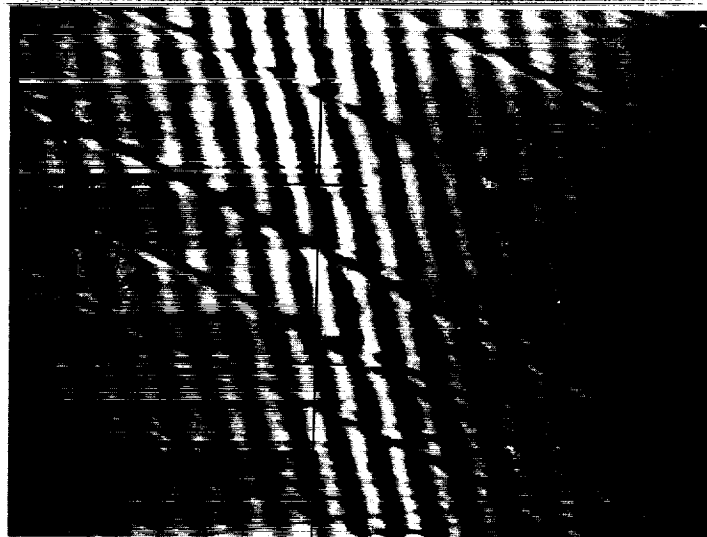
FIGURE 2.8 Interference Photo of Monomolecular
Finish on 2024 Aluminum. Scale: 0.00194 inches
between scale marks; 11.8 microinches between
interference lines.
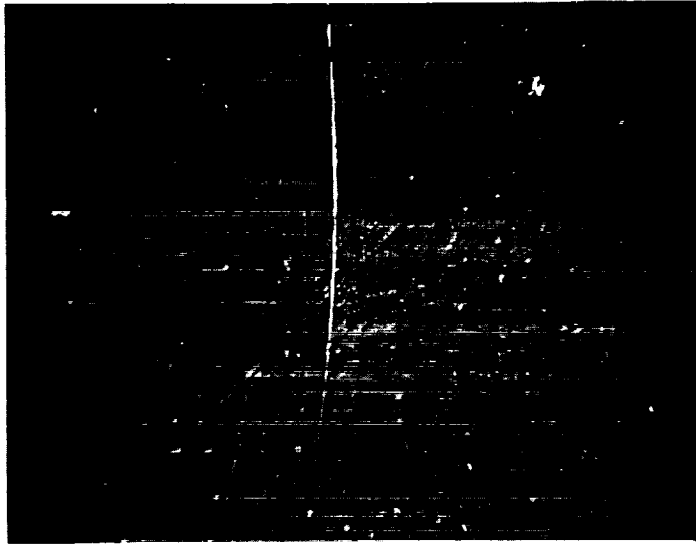
FIGURE 2.9 Nomarski Photo of Monomolecular
Finish on 347 Stainless Steel - Magnification =
168.
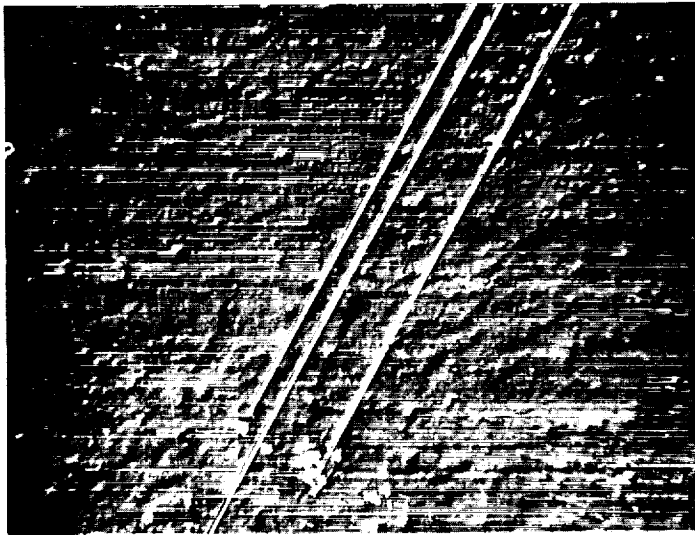
FIGURE 2.10 Nomarski Photo of Monomolecular
Finish on 347 Stainless Steel - Magnification = 168.
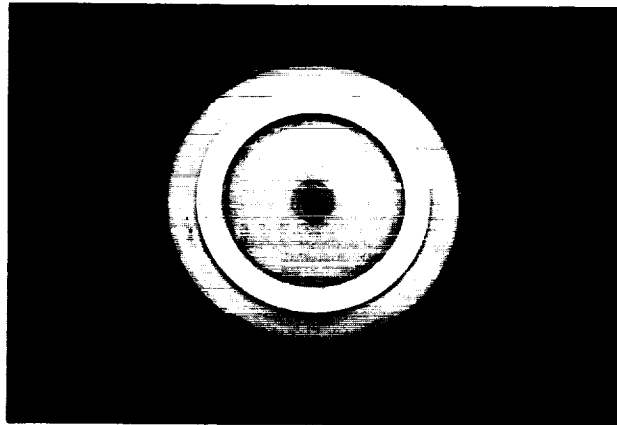
FIGURE 2.11 Lapmaster Glass Photo of 347 Stain-
less Steel "Monomolecular Finish".
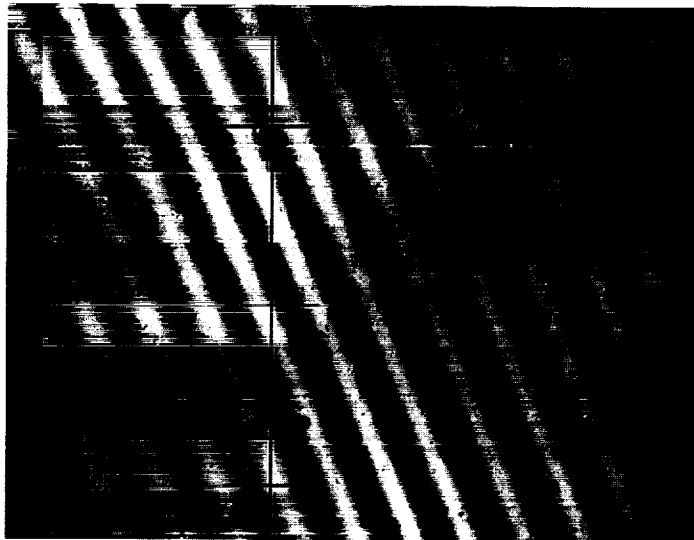
FIGURE 2.12

Interference Photo of New Jones Optical Co. Polished
347 Stainless Steel Specimen - 11.8 microinches between
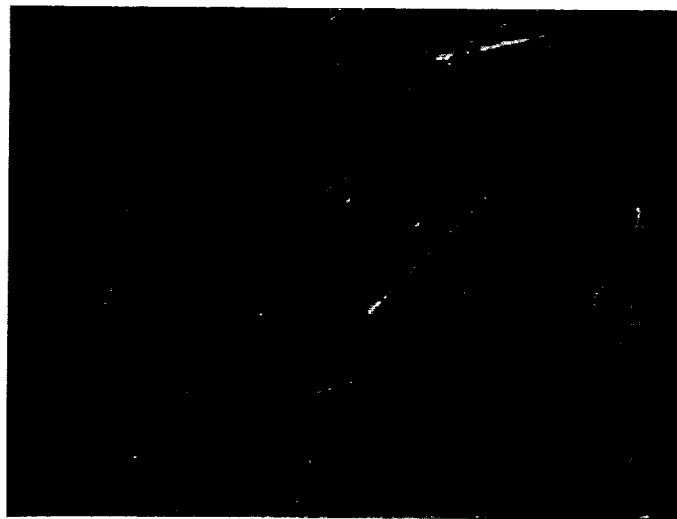interference lines. Scale: 0.00482 inches between
scribe marks.

FIGURE 2.13

Nomarski Photo of New Jones Optical Co. Polished 347
Stainless Steel Specimen - 11.8 microinches between
interference lines. Magnification: X900.
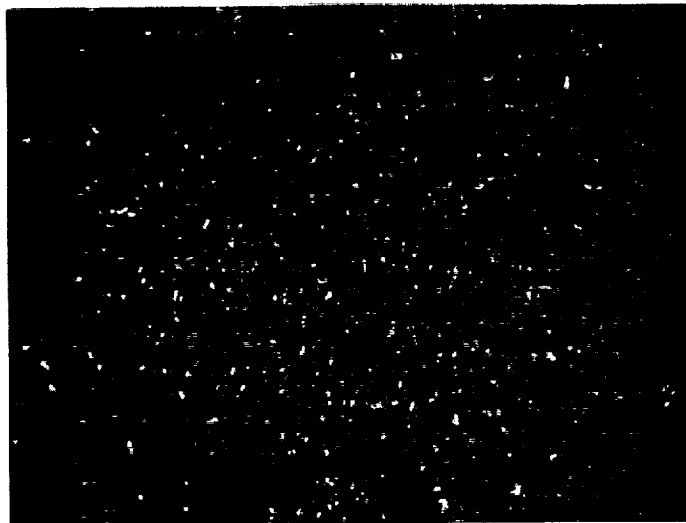
FIGURE 2.14

Photo of Jones Optical Co. Lapped
347 Stainless Steel Specimen.
Magnification: X510

2-33
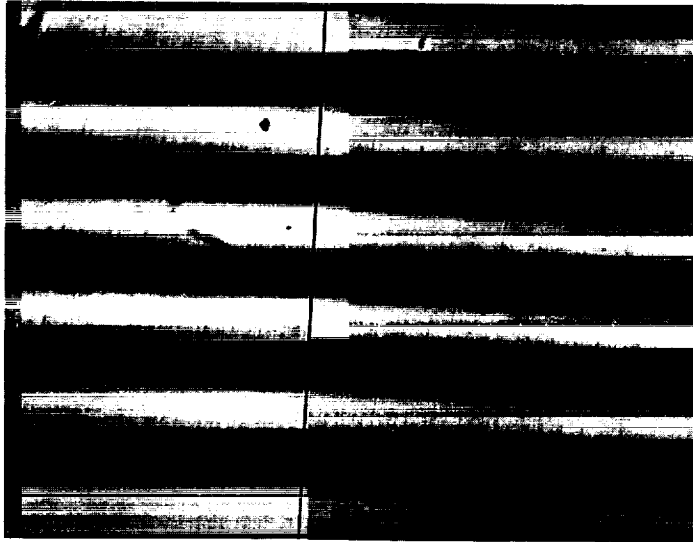
FIGURE 2.15

Interference Photo of Jones Optical Co. Polished KANIGEN
plated 2024 aluminum specimen. - 11.8 microinches between
interference lines. Scale: 0.00192 inches between scribe
marks.
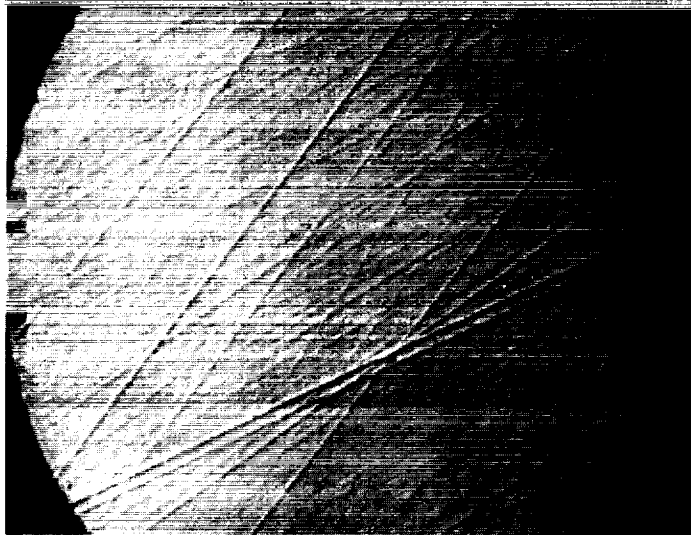
FIGURE 2.16

High Magnification Photo of KANIGEN Plated
Aluminum Specimen Superfinished by the Jones
Optical Company - Magnification: X900
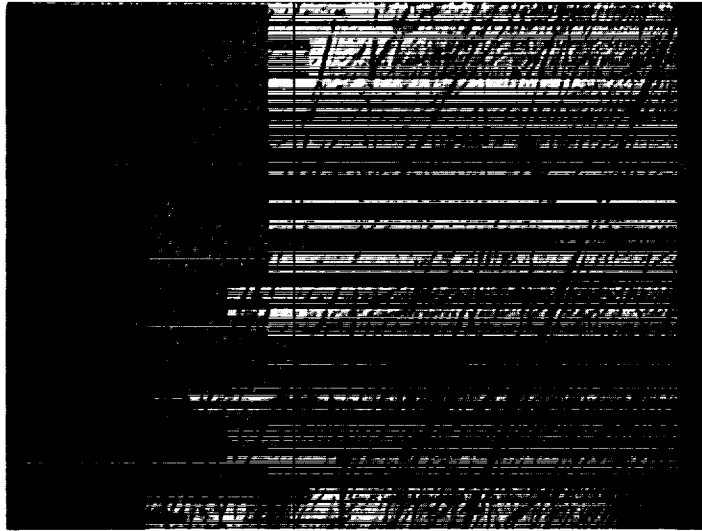
FIGURE 2.17

High Magnification Photo of Silver Plated 347 Stainless
Steel Specimen Superfinished by the Jones Optical
Company. Scale: 0.00194 Inches between Scale Marks.

FIGURE 2.18

Interference Photo of Silver Plated 347 Stainless
Steel Specimen Superfinished by the Jones Optical
Company. - 11.8 Microinches between Interference
Lines. Scale: 0.0125 Inches between Scale Marks.
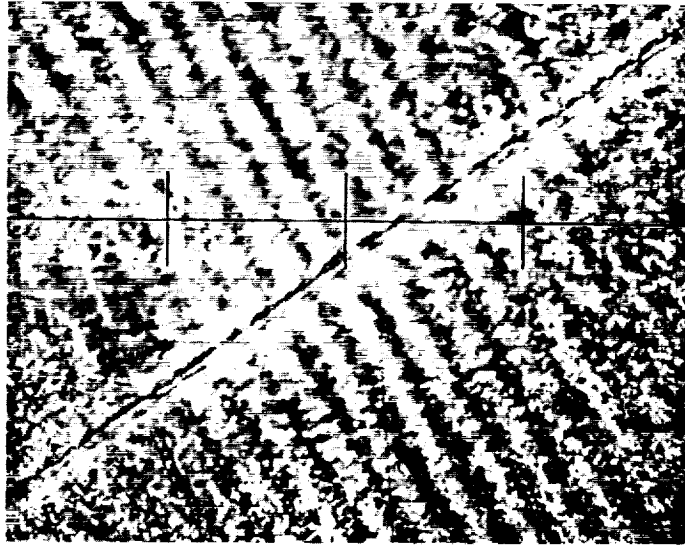
FIGURE 2.19 Diamond-lead Lapped Finish - Inter-
ference Photo. Scale: 0.00194 inches between
Scale Marks. 11.8 microinches between interference
lines.
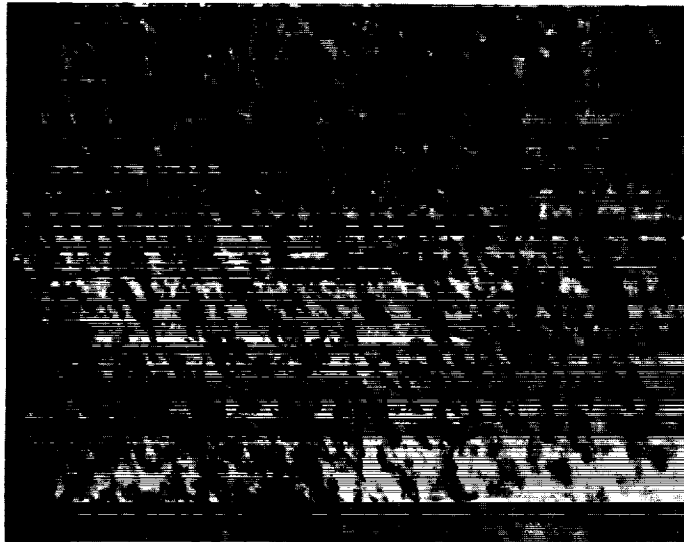
FIGURE 2.20 Diamond-lead Lapped Surface - Nomarski
Photo; Magnification 900X.
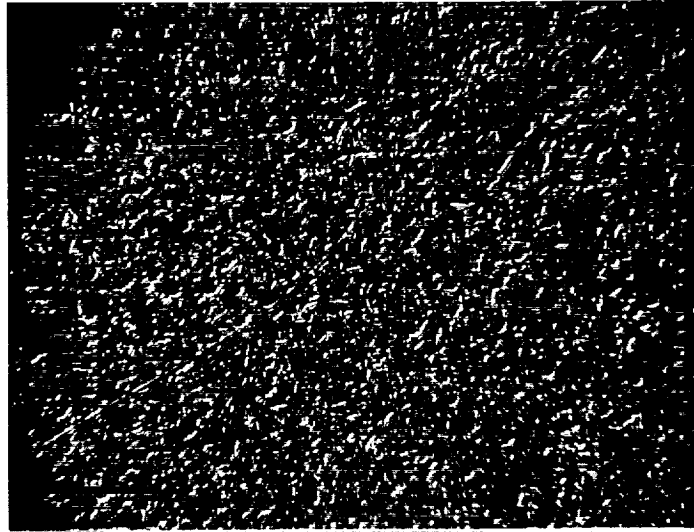
FIGURE 2.21

Nomarski Photo of Second General Electric Lead
Lapped 347 Stainless Steel Specimen.
Magnification: X168
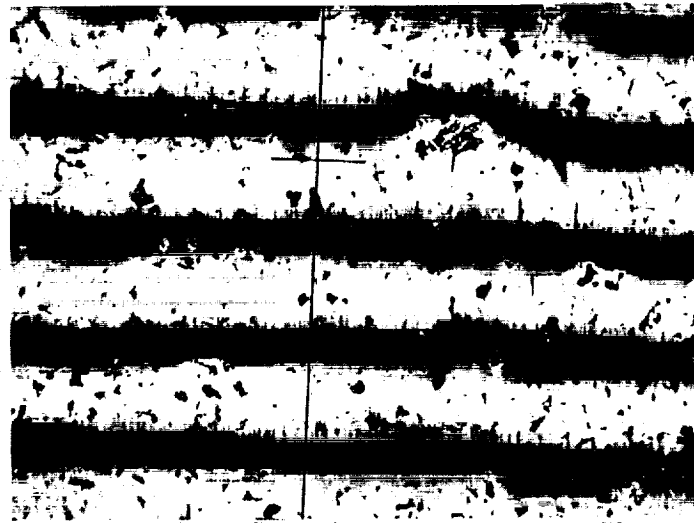
FIGURE 2.22

Interference Photo of Second General Electric
Leak Lapped 347 Stainless Steel Specimen.
Scale: 0.00194 inches between scribe marks.

FIGURE 2.23

Interference Photo of Parker Aircraft Polished A286 Steel
Specimen - 11.8 microinches between interference lines.
Scale: 0.00482 inches between scribe marks.

FIGURE 2.24

Nomarski Photo of Parker Aircraft Polished A286 Steel
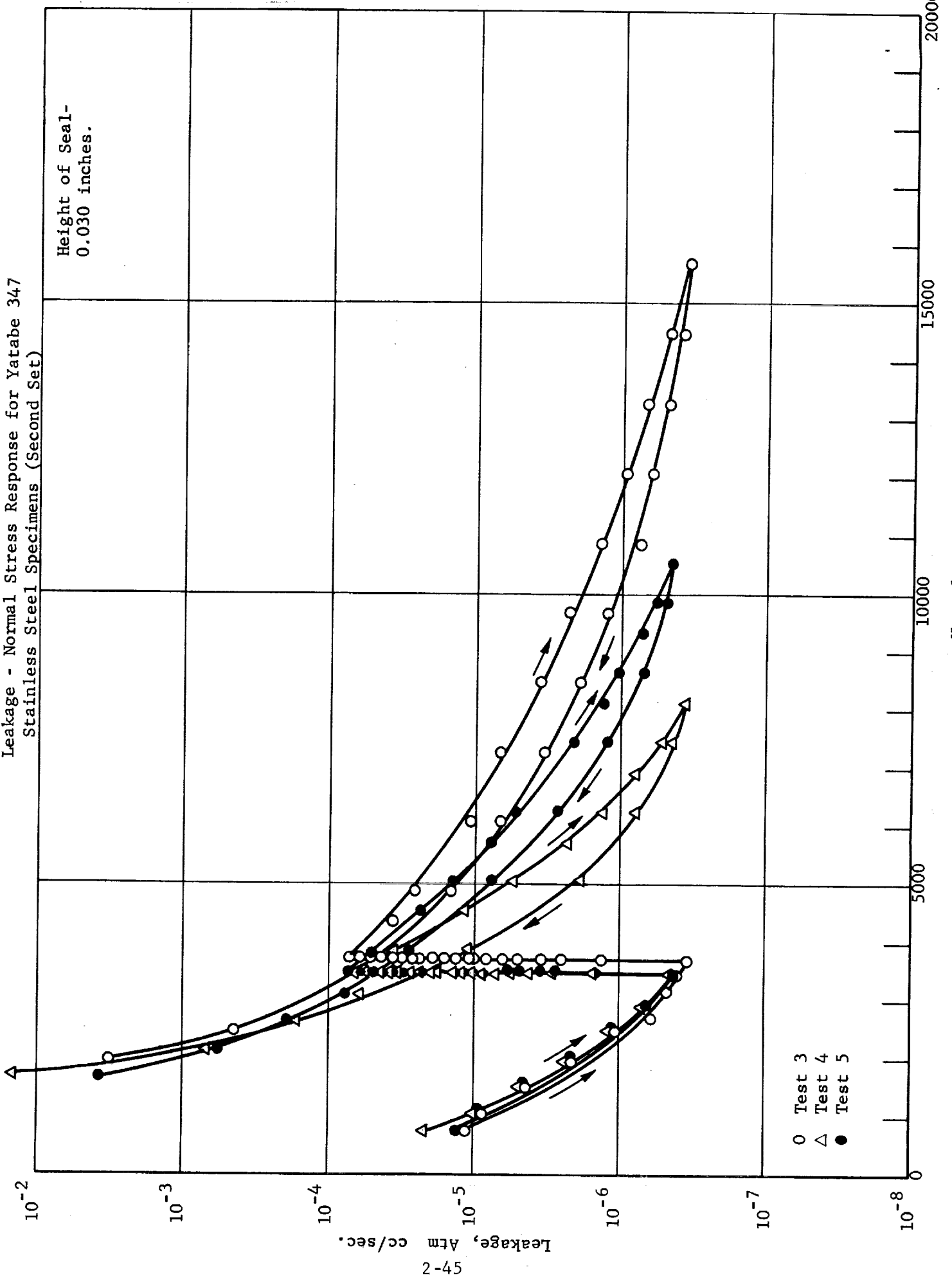Specimen - 11.8 microinches between interference lines.
Magnification: X900.

FIGURE 2.25

Leakage - Normal Stress Response for Yatabe 347
Stainless Steel Specimens (First Set)
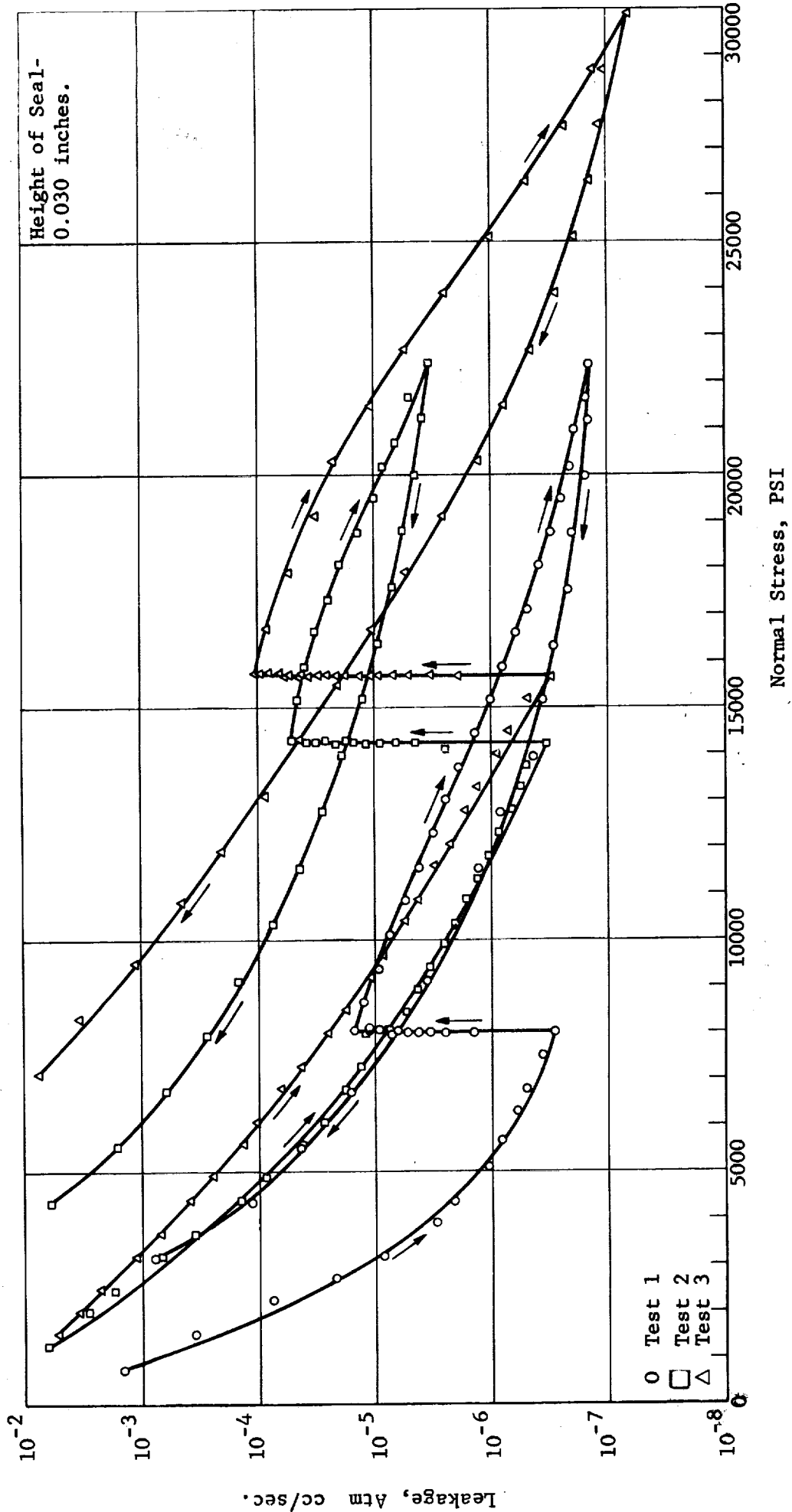
FIGURE 2.26

Leakage – Normal Stress Response for Yatabe 347
Stainless Steel Specimens (First Set)
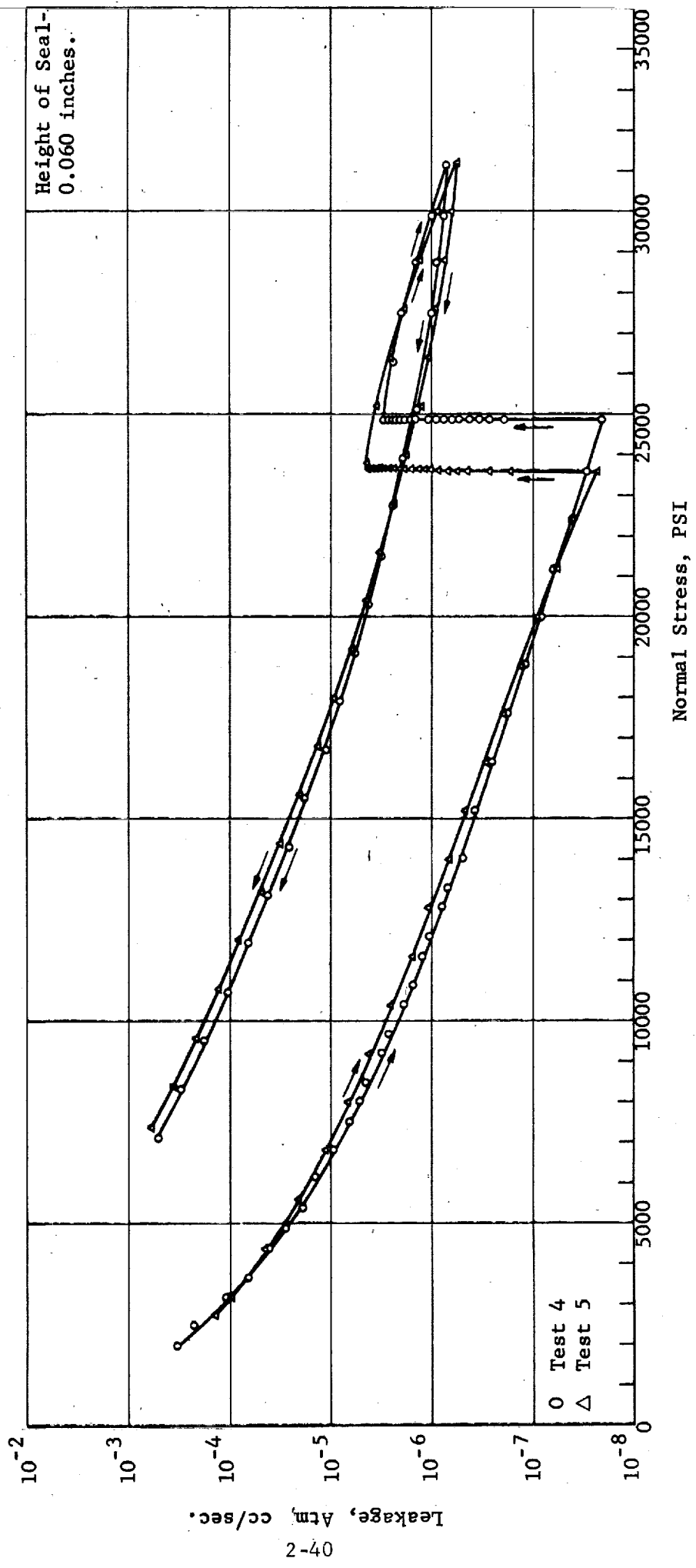
FIGURE 2.27

Leakage - Normal Stress Response for Yatabe 347
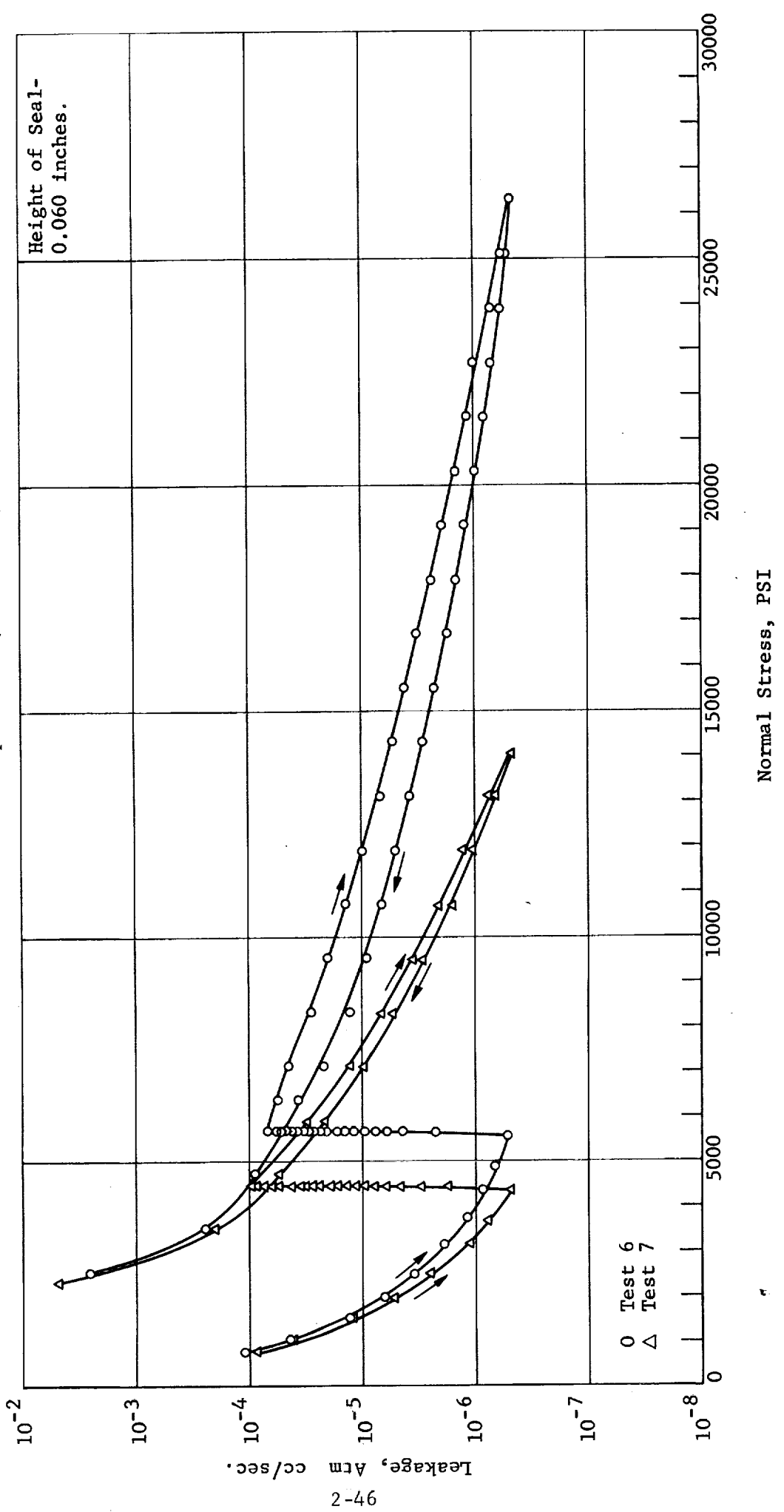Stainless Steel Specimens (First Set)
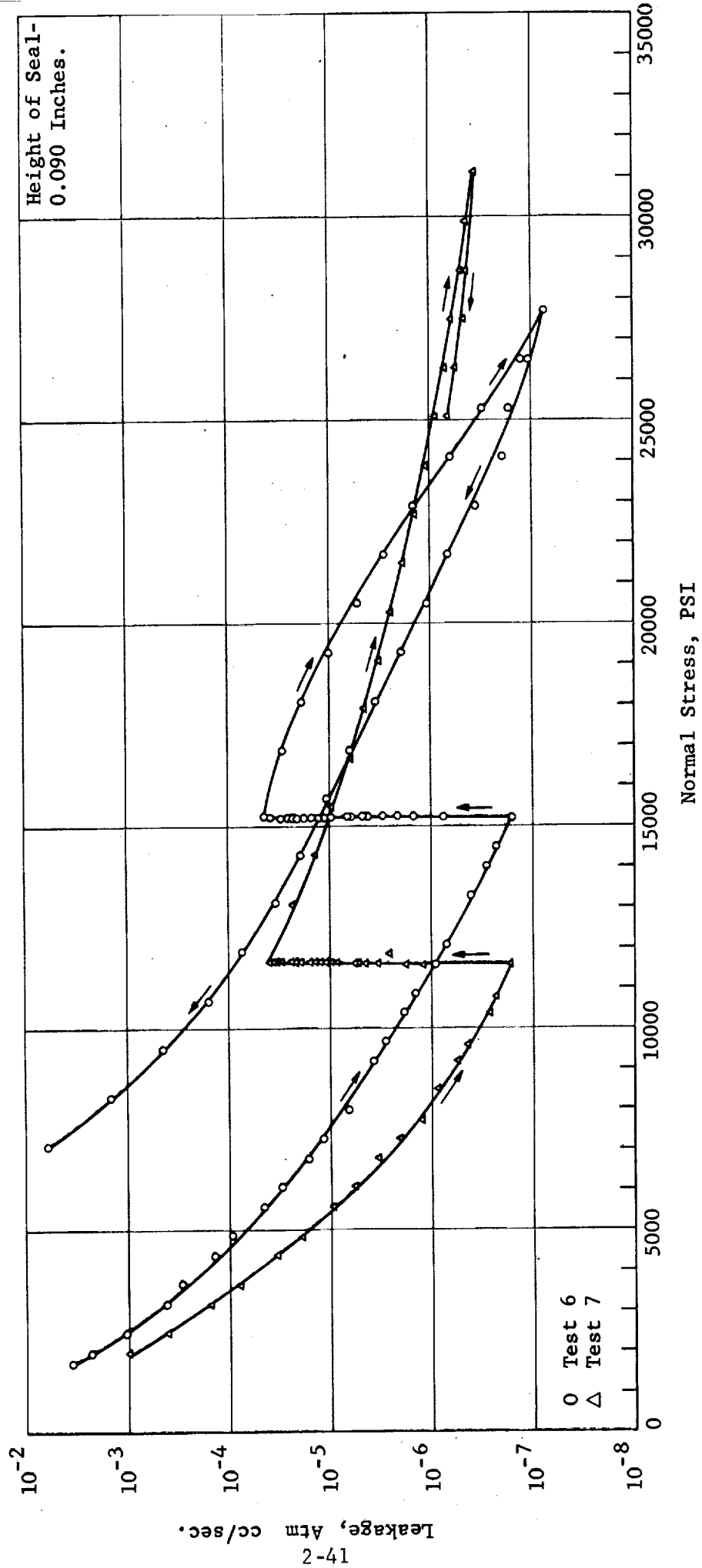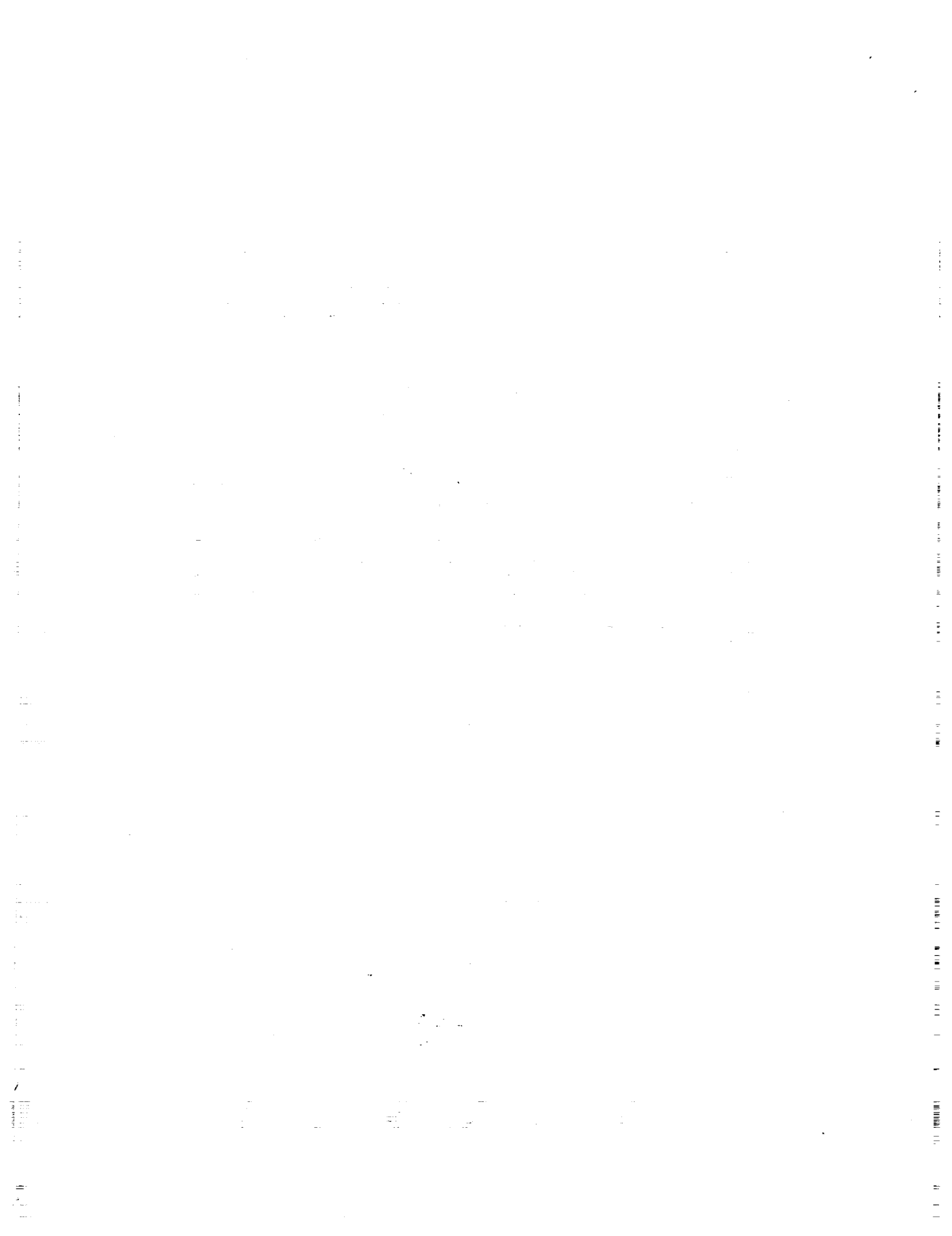
Test 10
Test 11

URE 2.29

s Response for Yatabe 347
ecimens (First Set)

Height of Seal-
0.090 inches.

20000   25000   30000   35000   40000
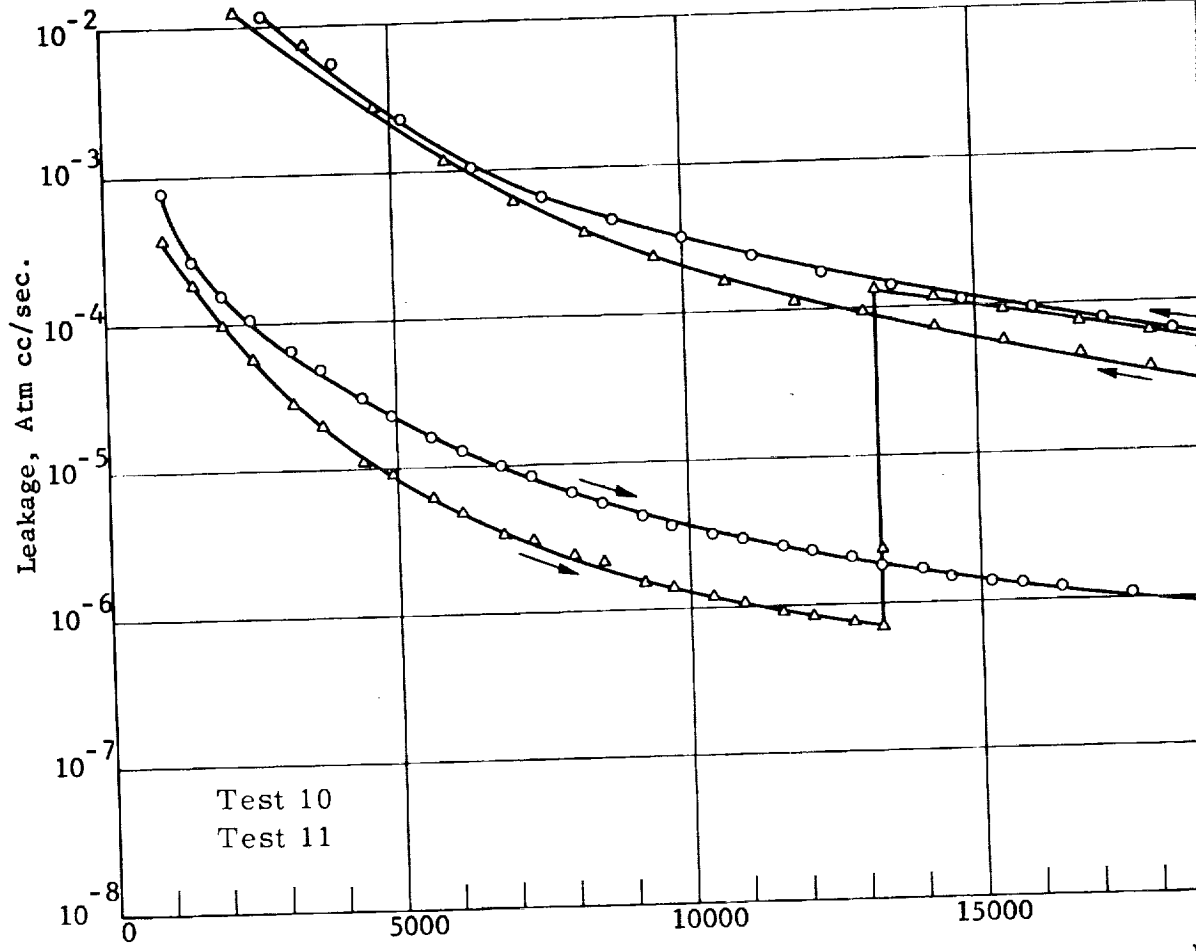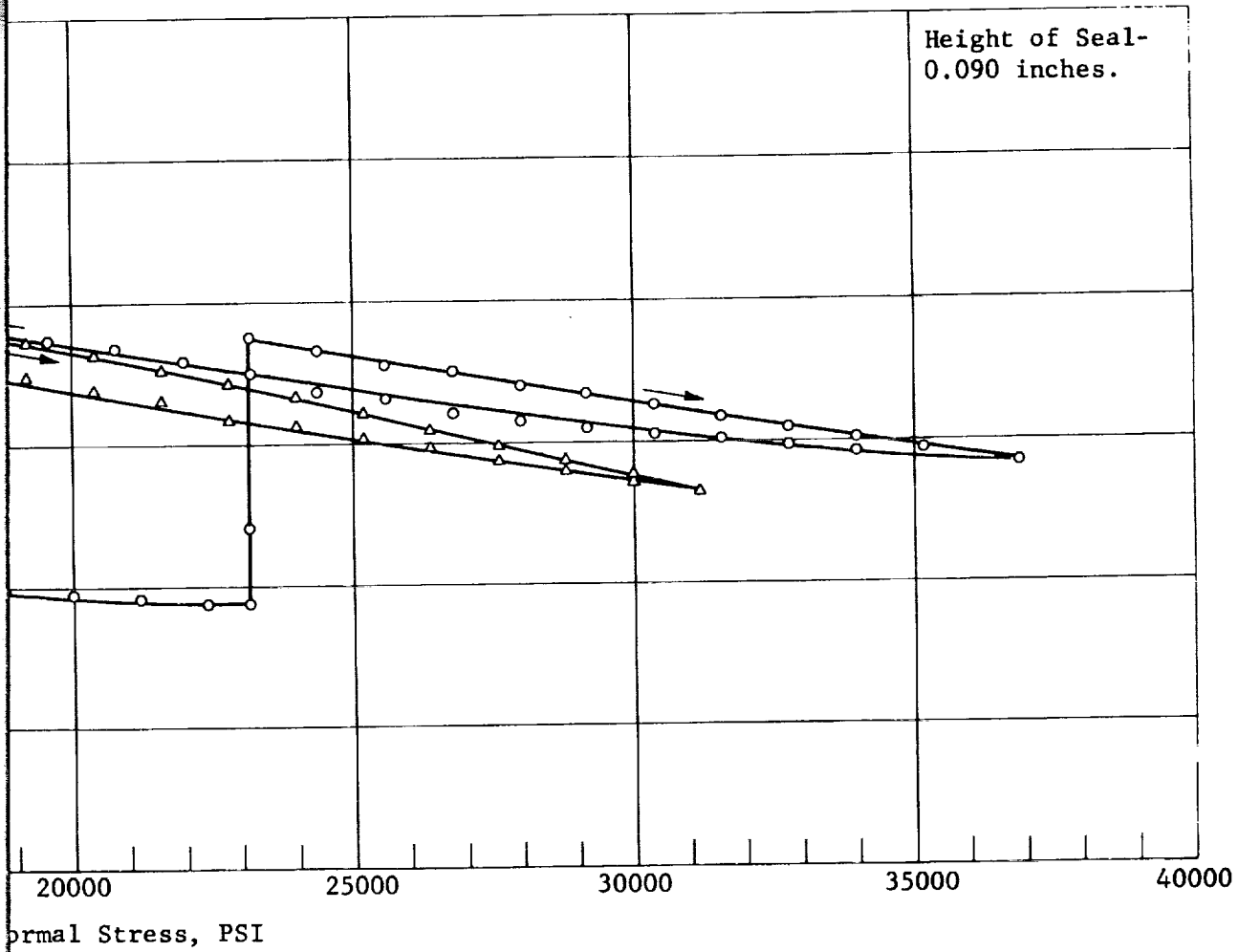
rmal Stress, PSI

FOLDOUT FRAME 2

FIGURE 2.30

Leakage - Normal Stress Response for Yatabe 347
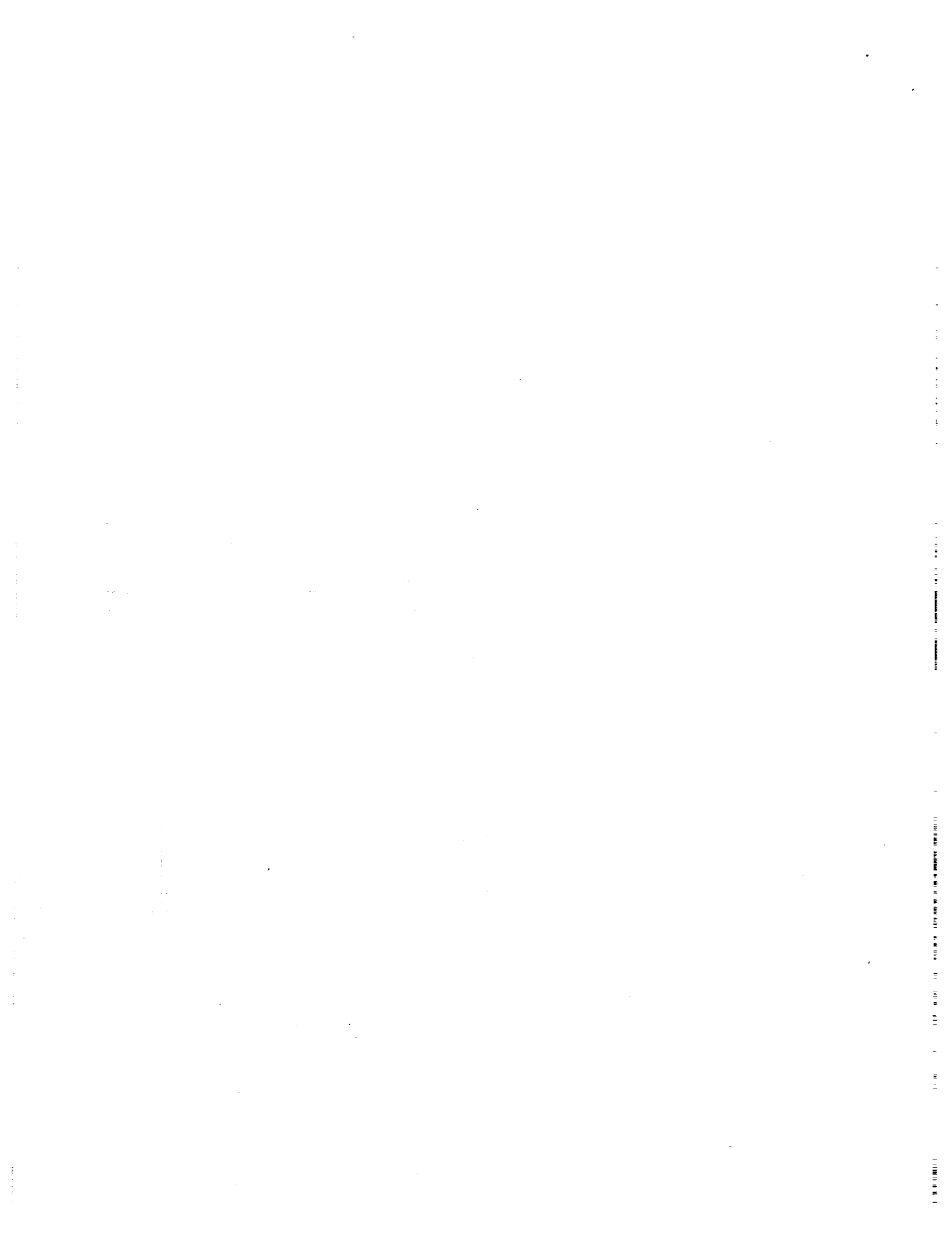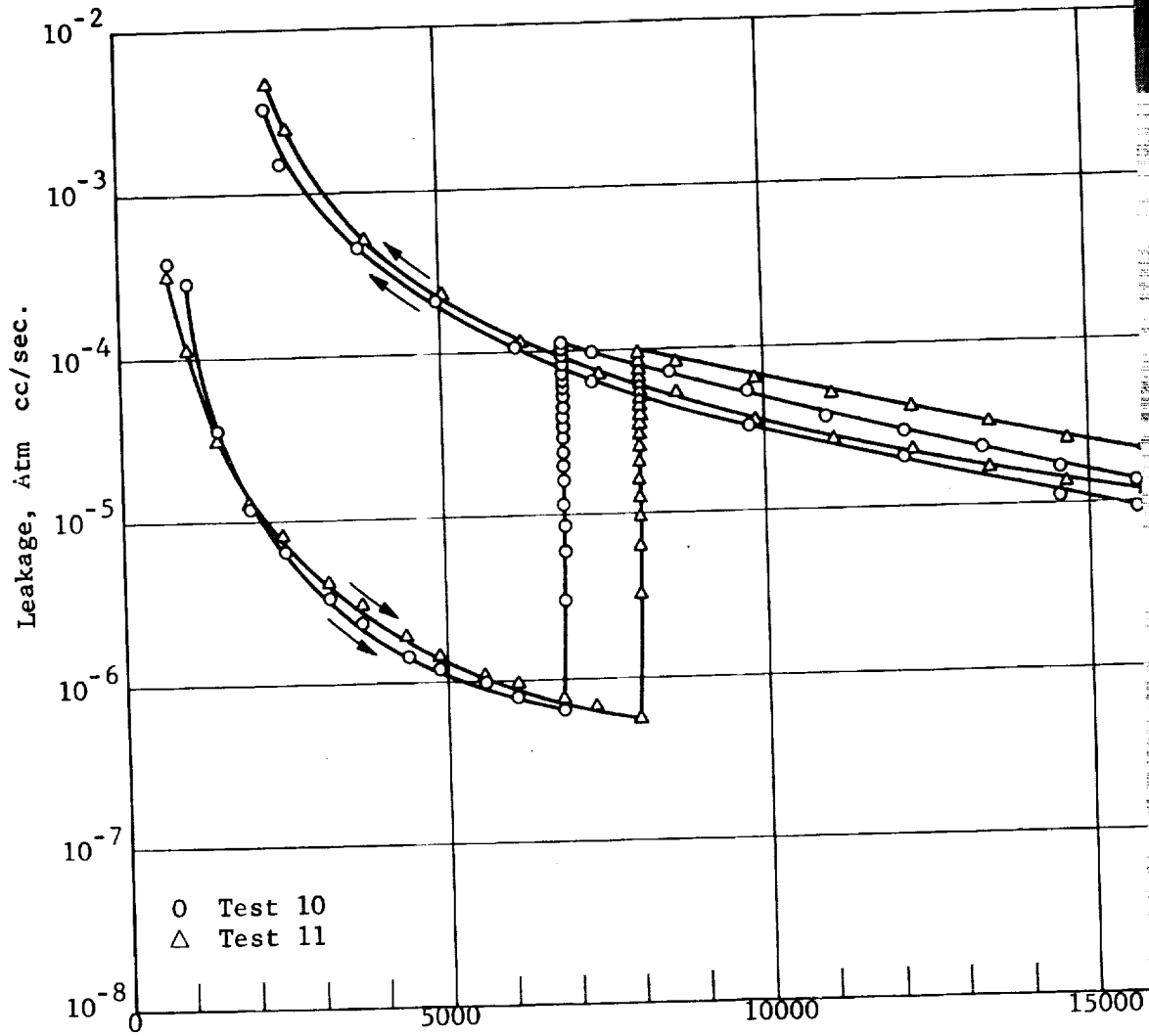Stainless Steel Specimens (Second Set)

Height of Seal-
0.030 inches.

O Test 1
▲ Test 2

Normal Stress, PSI

Leakage, Atm cc/sec.

2-44
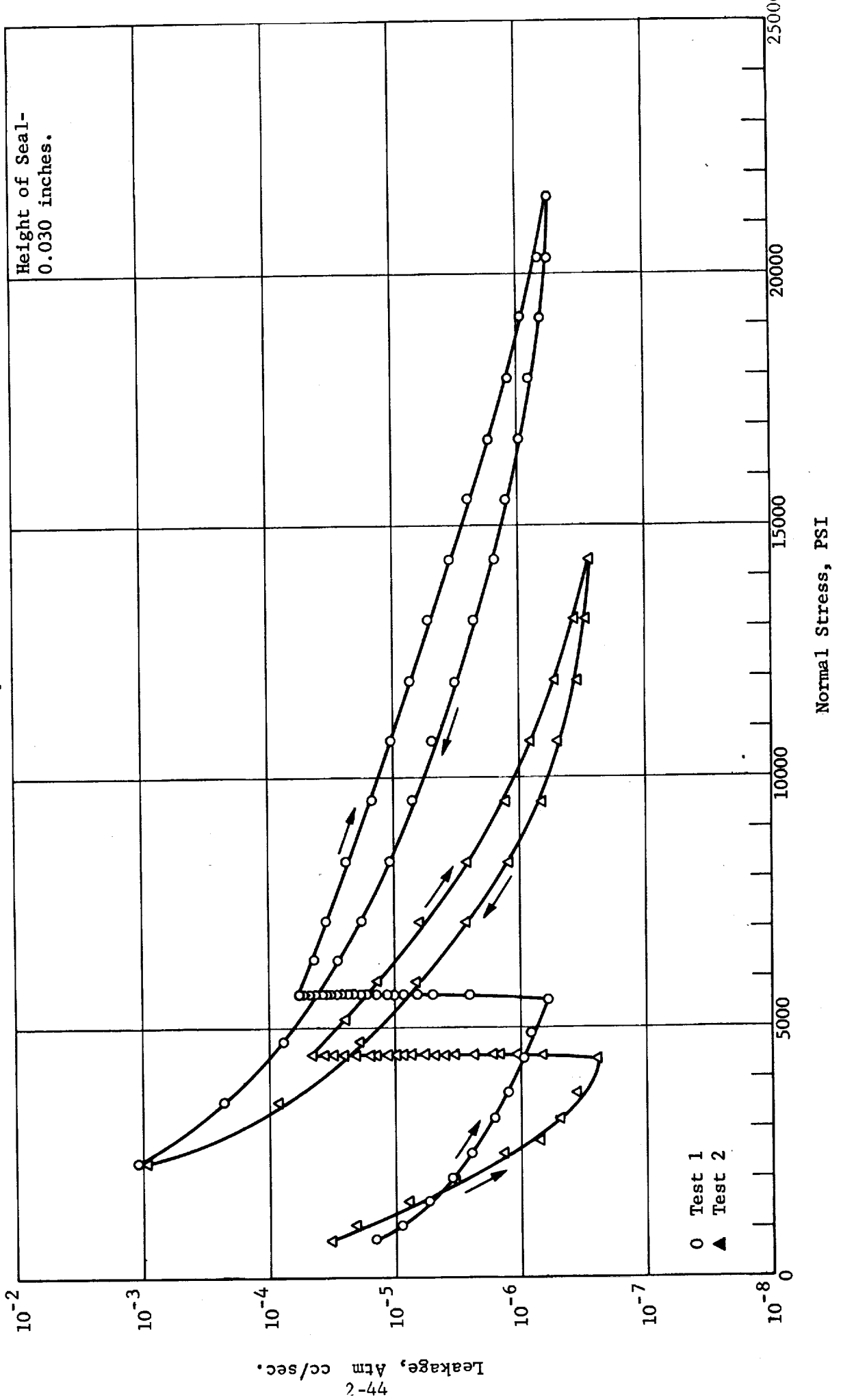
FIGURE 2.31

Leakage - Normal Stress Response for Yatabe 347
Stainless Steel Specimens (Second Set)

Height of Seal-
0.030 inches.

O Test 3
△ Test 4
● Test 5

Leakage, Atm cc/sec.

Normal Stress, PSI

2-45

FIGURE 2. 32

Leakage - Normal Stress Response for Yatabe 347
Stainless Steel Specimens (Second Set)

Height of Seal-
0.060 inches.

Normal Stress, PSI

Leakage, Atm cc/sec.

O Test 6
△ Test 7

Leakage, Atm cc/sec.

10^{-2}

10^{-3}

10^{-4}

10^{-5}

10^{-6}

10^{-7}

O Test 10
△ Test 11

10^{-8}

0   5000   10000   15000

No

FOLDOUT FRAME

FIGURE 2.34

l Stress Response for Yatabe 347
teel Specimens (Second Set)

Height of Seal-
0.120 inches.

20000   25000   30000   35000

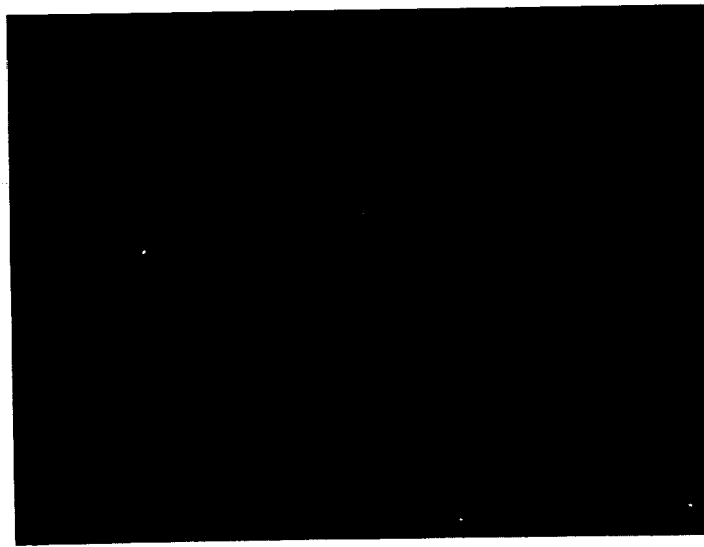rmal Stress, PSI
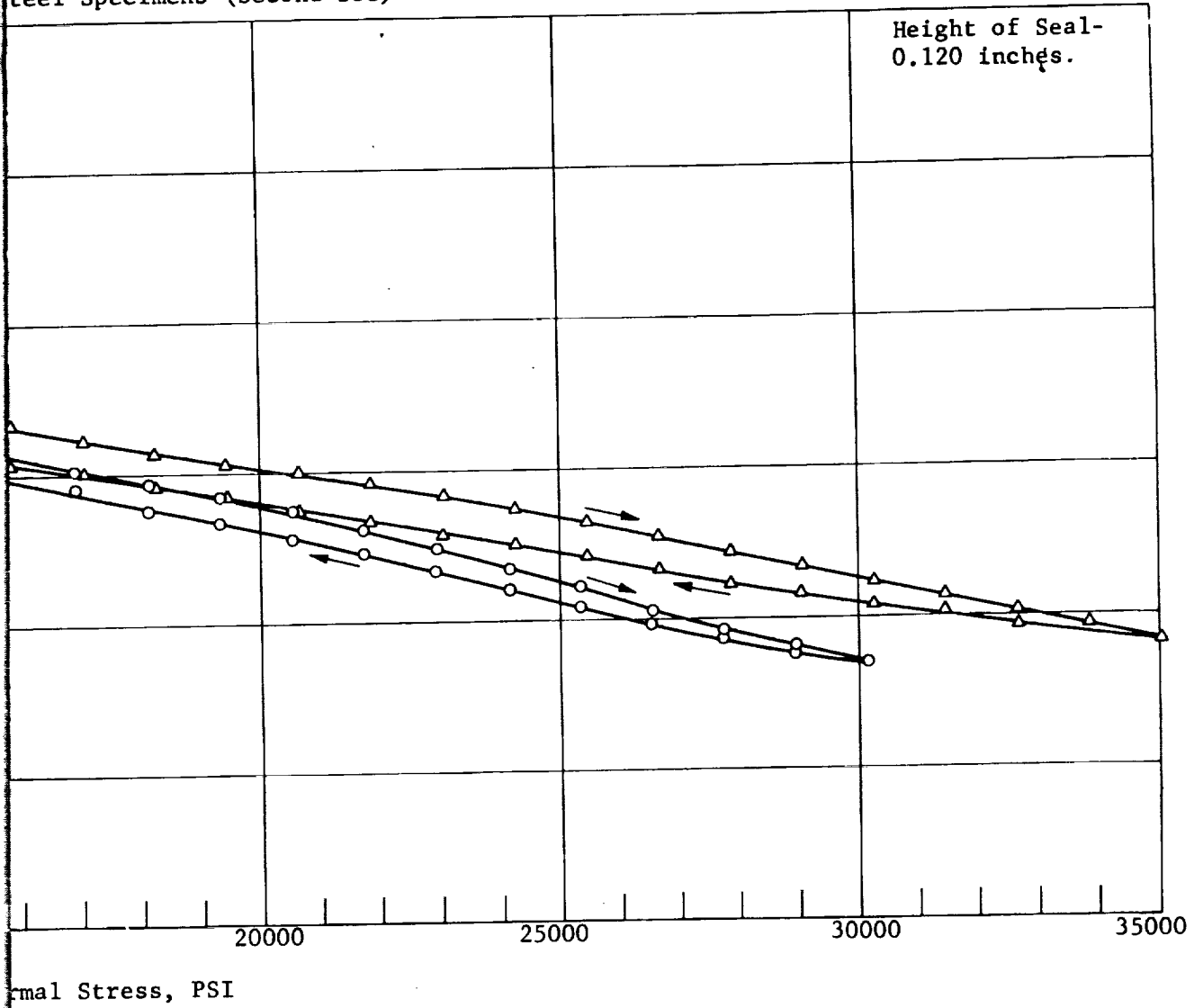
FOLDOUT FRAME 2
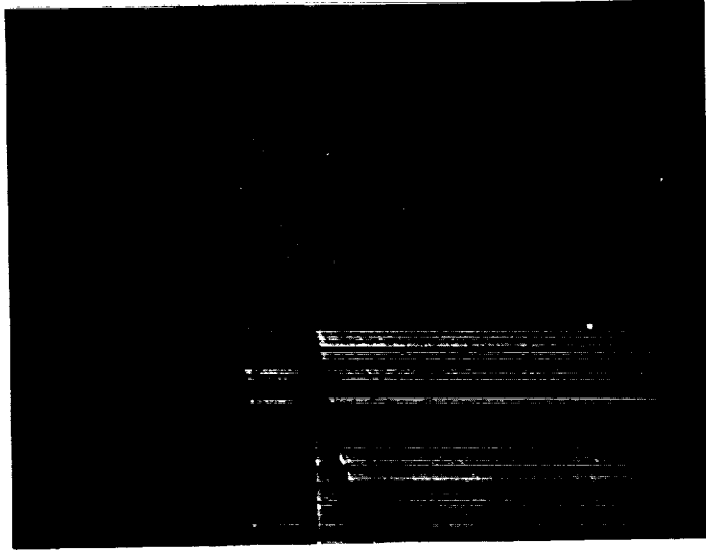
FIGURE 2.35 Photo of Yatabe Stainless Steel
Finish - After First Assembly Magnification: 510X.

FIGURE 2.36 Photo of Yatabe Stainless Steel
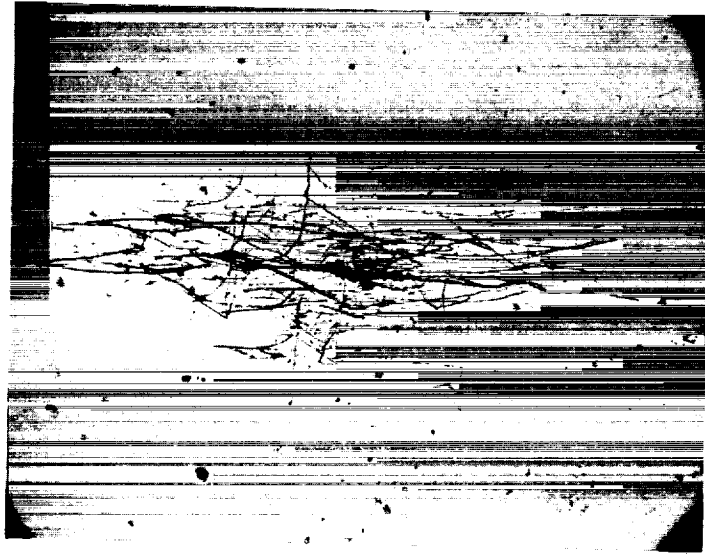Finish - After First Assembly Magnification: 510X.

FIGURE 2.37 Photo of Yatabe Stainless Steel
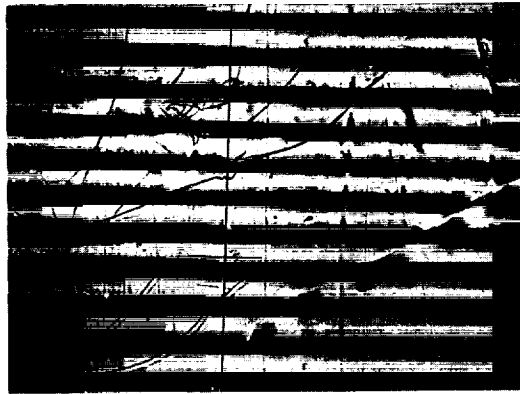Finish - After First Assembly Magnification: 47X.

FIGURE 2.38

Interference Photo of Surface Damage After 11th
Test - Yatabe, Stainless Steel Specimens (Second
Set) - 11.8 microinches between interference lines.
Scale: 0.00194 inches between scribe marks.

FIGURE 2.39

Nomarski Photo of Surface Damage After 11th
Test - Yatabe, Stainless Steel Specimens (Second
Set) - 11.8 microinches between interference lines.
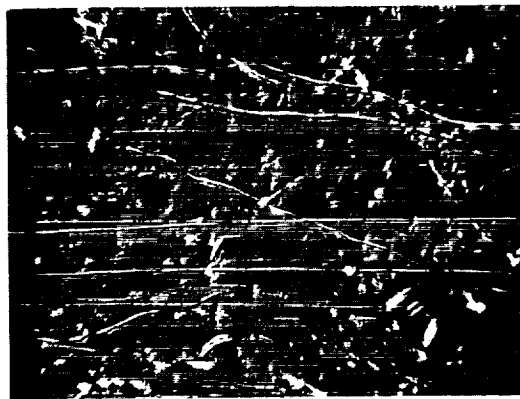Magnification: X900.

FIGURE 2.40

Nomarski Photo of Surface Damage After 11th Test -
Yatabe, Stainless Steel Specimens (Second Set) -
11.8 microinches between interference lines.
Magnification: X168.

2-51

FIGURE 2.41

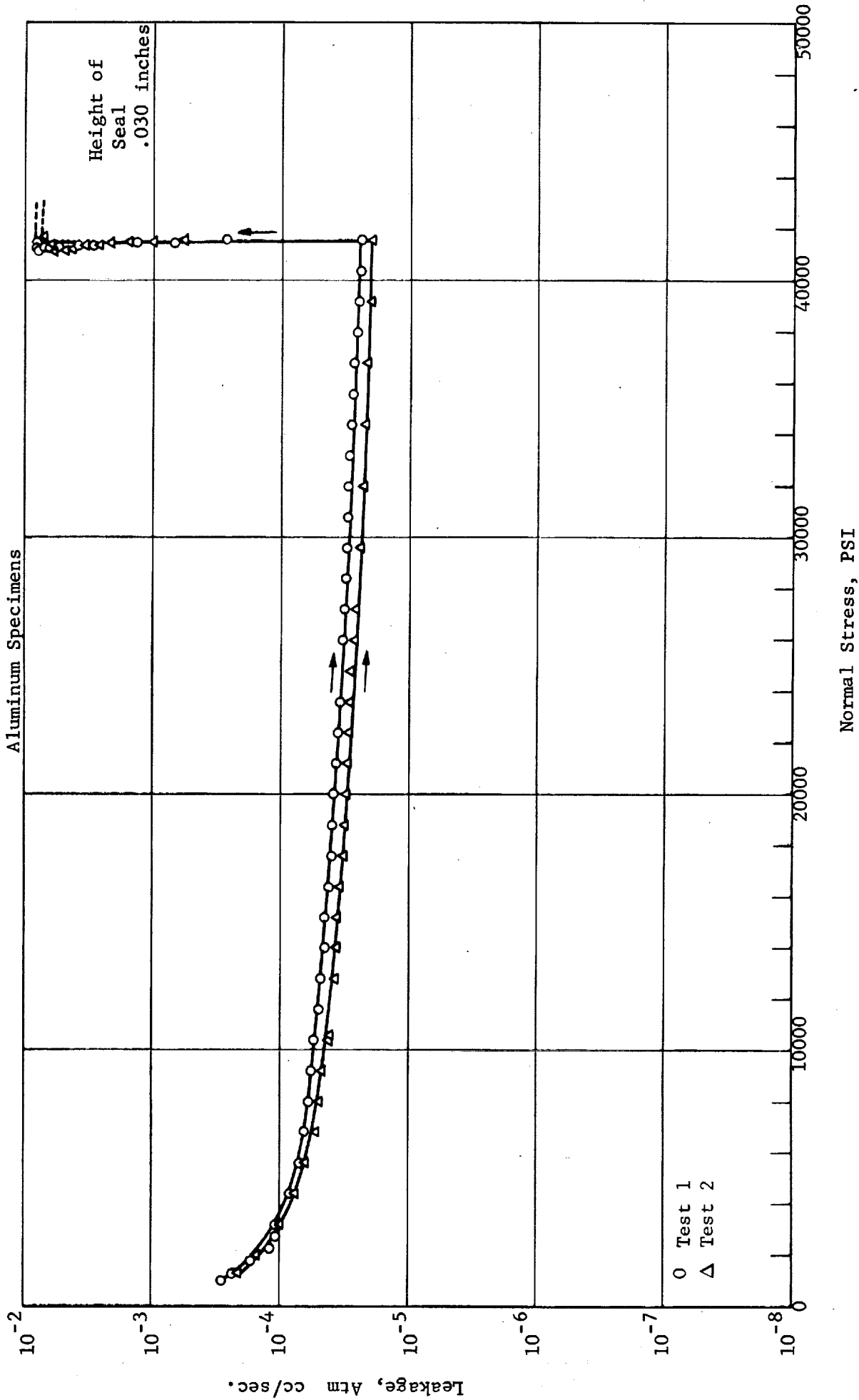Leakage - Normal Stress Response for Yatabe 2024 T4
Aluminum Specimens

FIGURE 2.42

Leakage - Normal Stress Response for Jones Optical
Co. Polished 347 Stainless Steel Specimens

FIGURE 2.43

Leakage - Normal Stress Response for Jones Optical
Co. Polished 347 Stainless Steel Specimens

Leakage, Atm cc/sec.
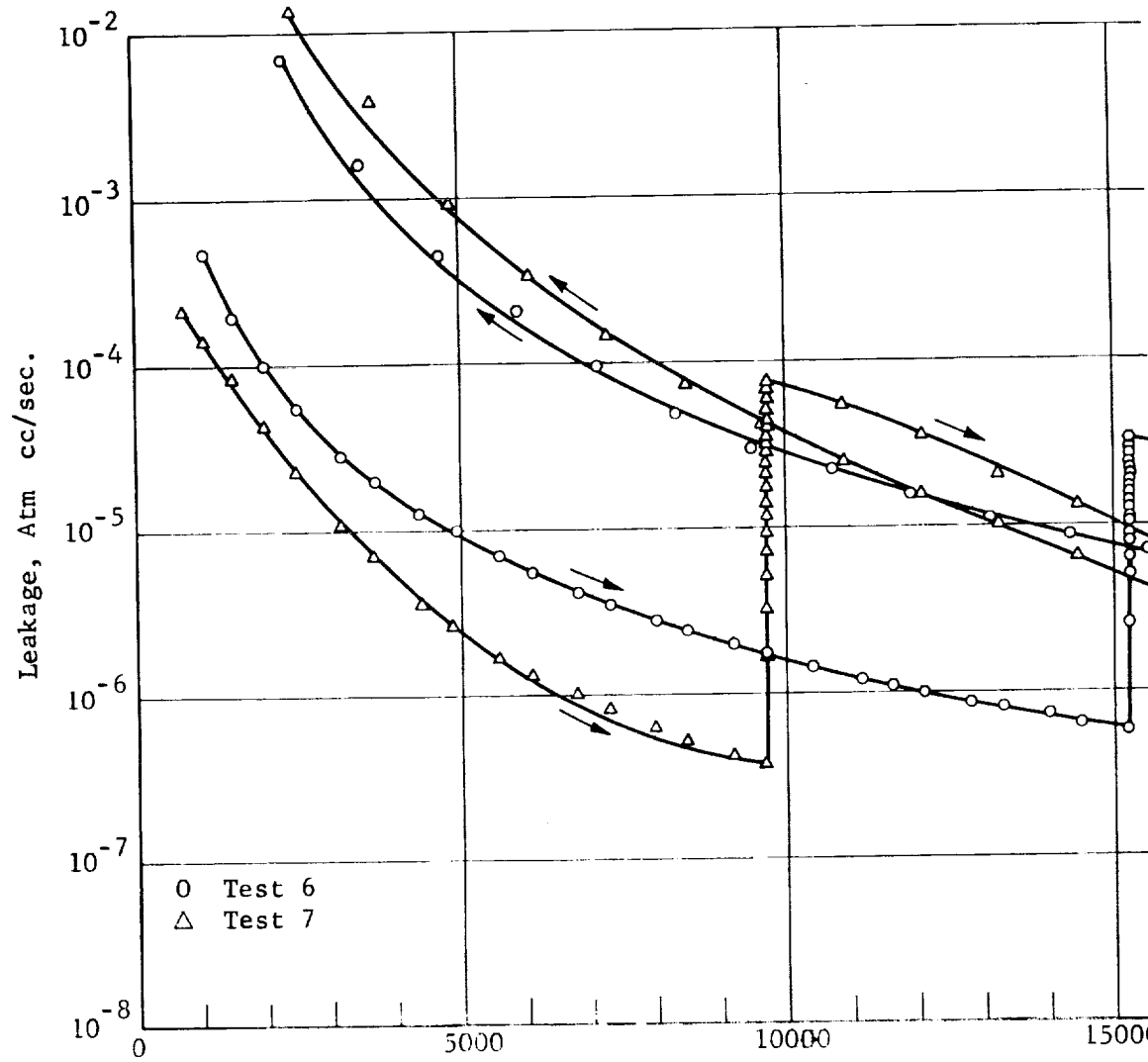
10^{-2}

10^{-3}

10^{-4}

10^{-5}

10^{-6}

10^{-7}

10^{-8}

0   5000   10000   15000

O   Test 6
△   Test 7

FOLDOUT FRAME

FIGURE 2.44

rmal Stress Response for Jones Optical
shed 347 Stainless Steel Specimens

Height of Seal-
0.060 inches.

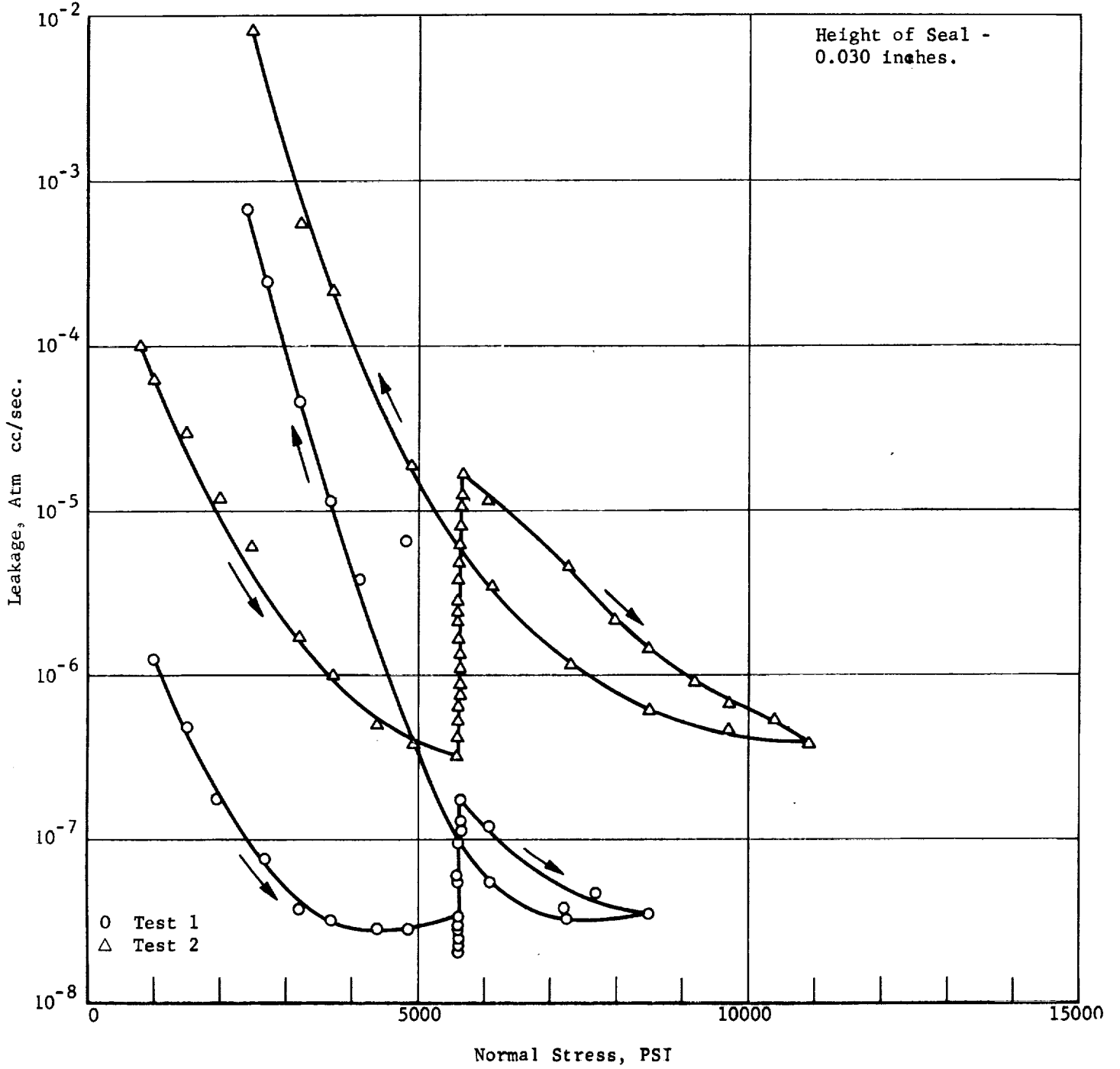20000   25000   30000   35000
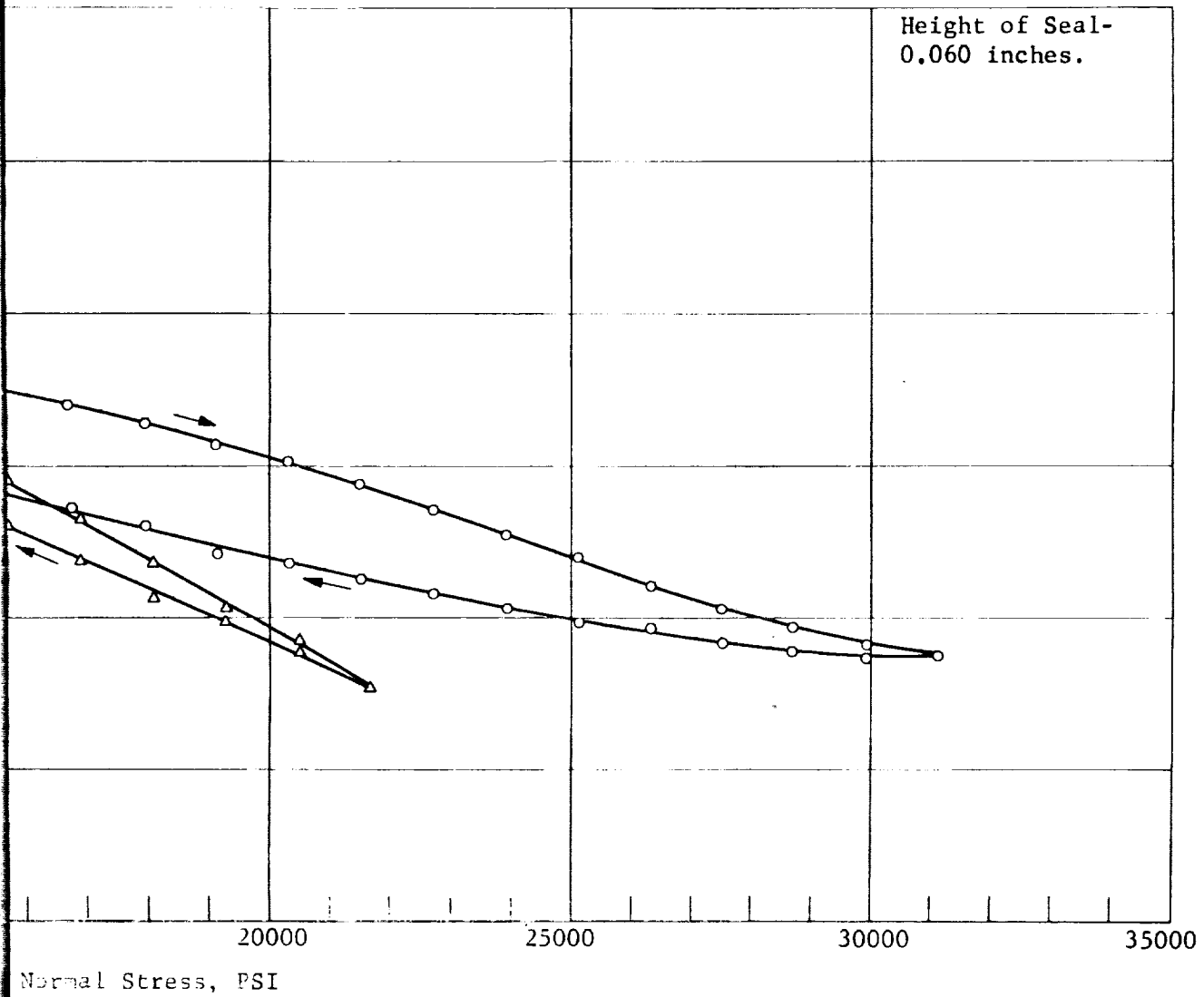
Normal Stress, PSI

FIGURE 2.45

Leakage - Normal Stress Response for Jones Optical
Co. Polished 347 Stainless Steel Specimens

Height of Seal-
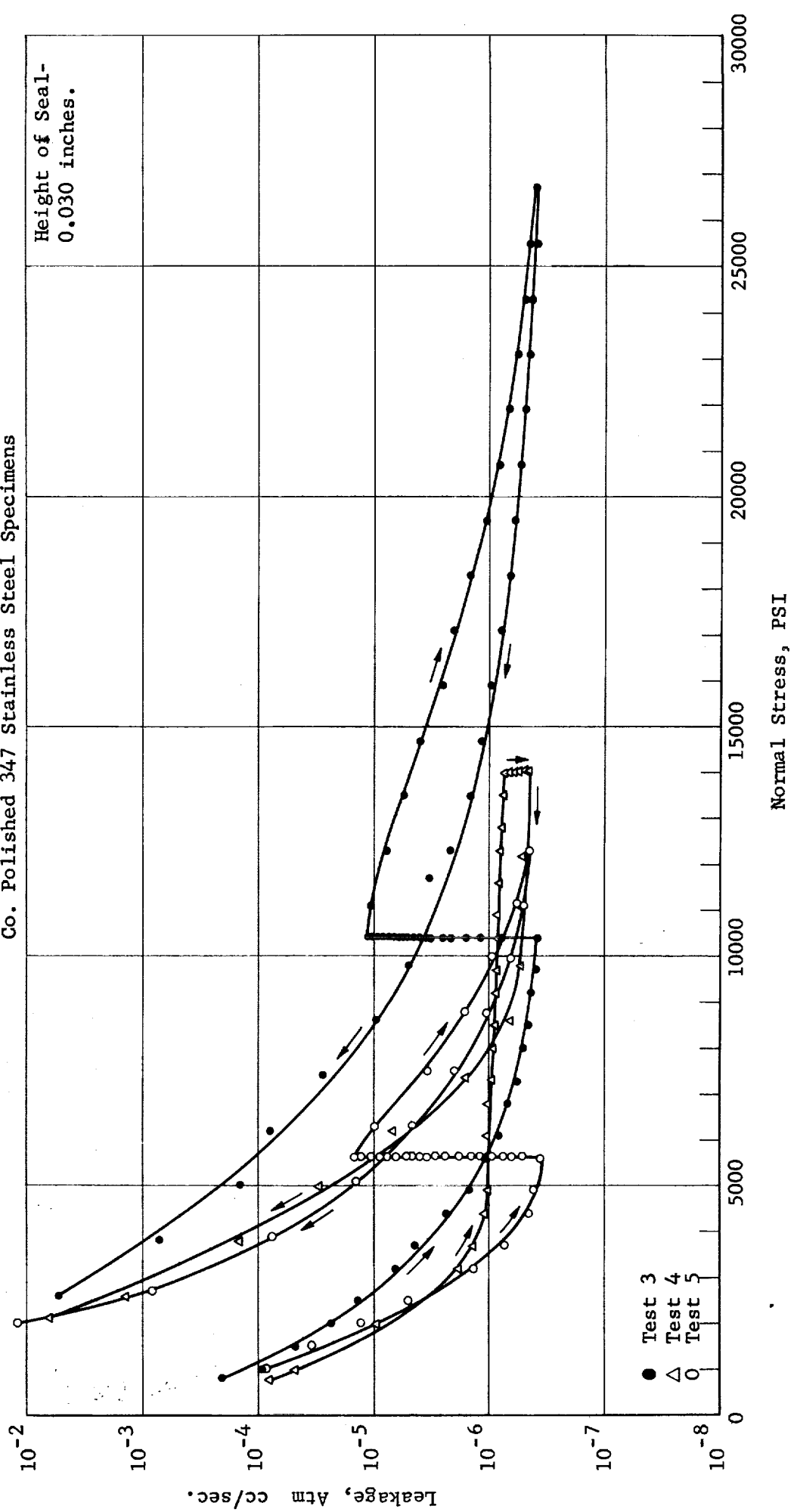0.090 inches.

Normal Stress, PSI

Leakage, Atm cc/sec.

△ Test 8
O Test 9

Response for Jones Optical
ainless Steel Specimens.
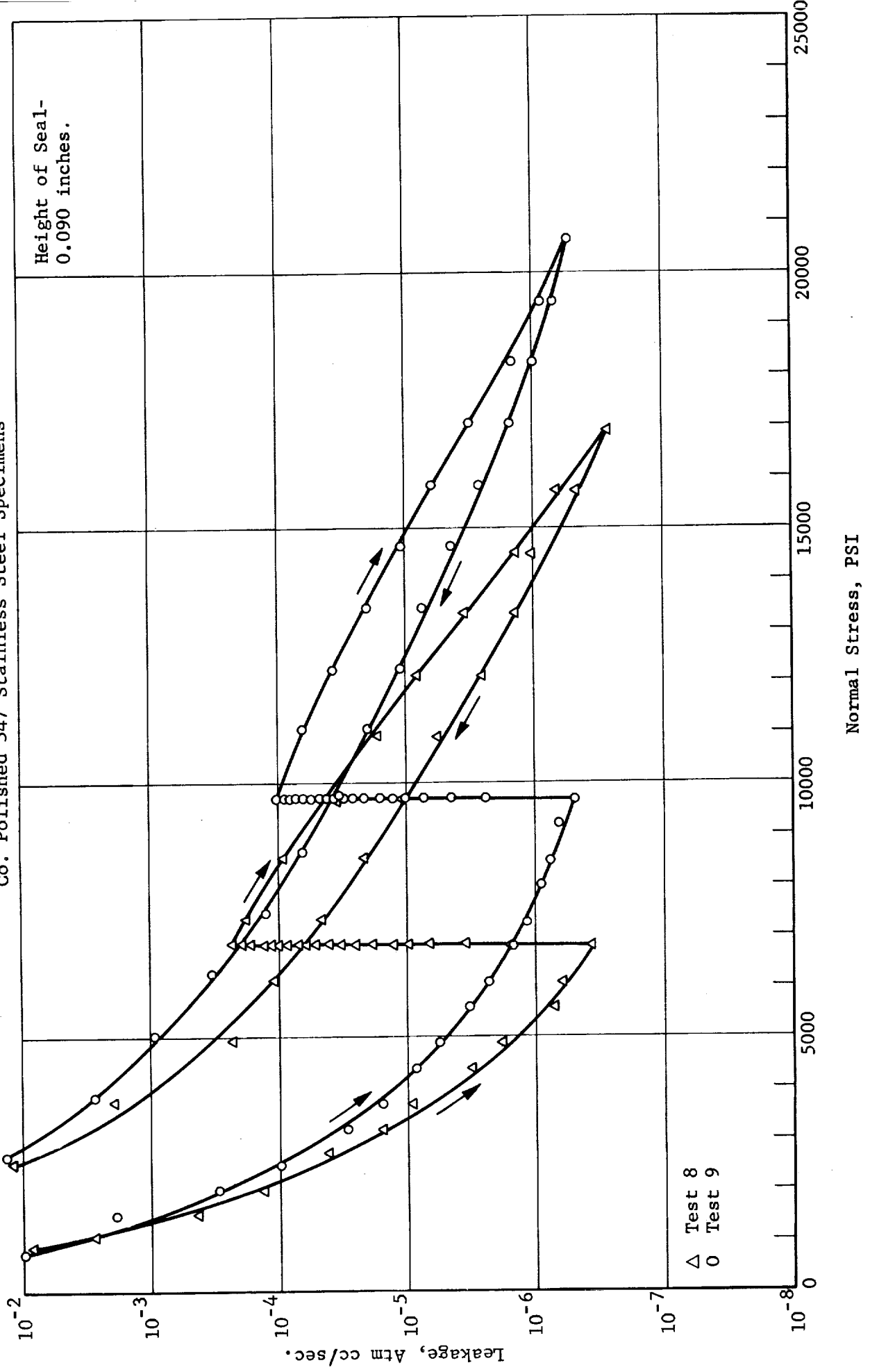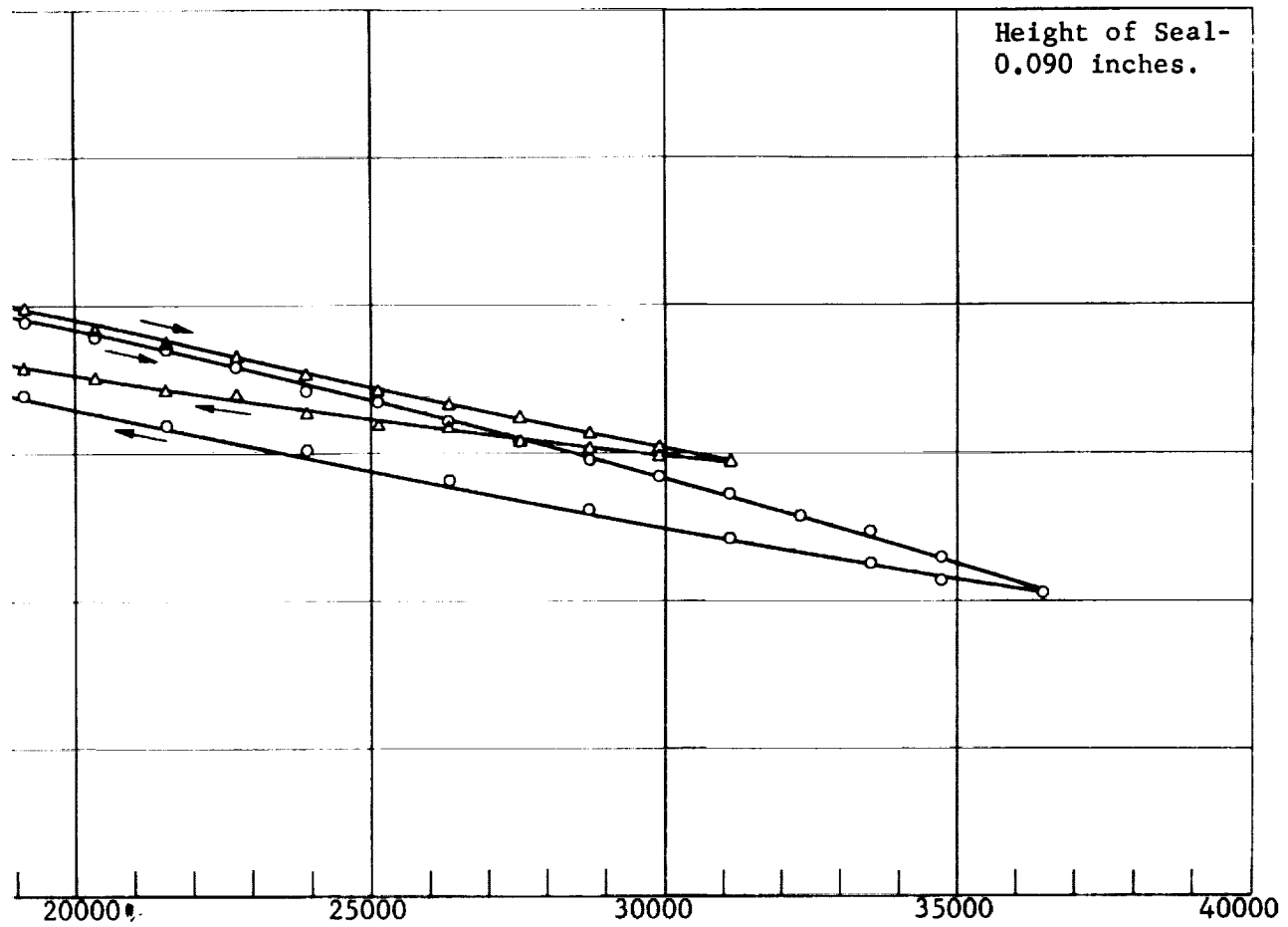
mal Stress, PSI

Leakage - Normal
Co. Polished

esponse for Jones Optical
nless Steel Specimens

Height of Seal-
0.120 inches.

20000   25000   30000   35000   40000

mal Stress, PSI
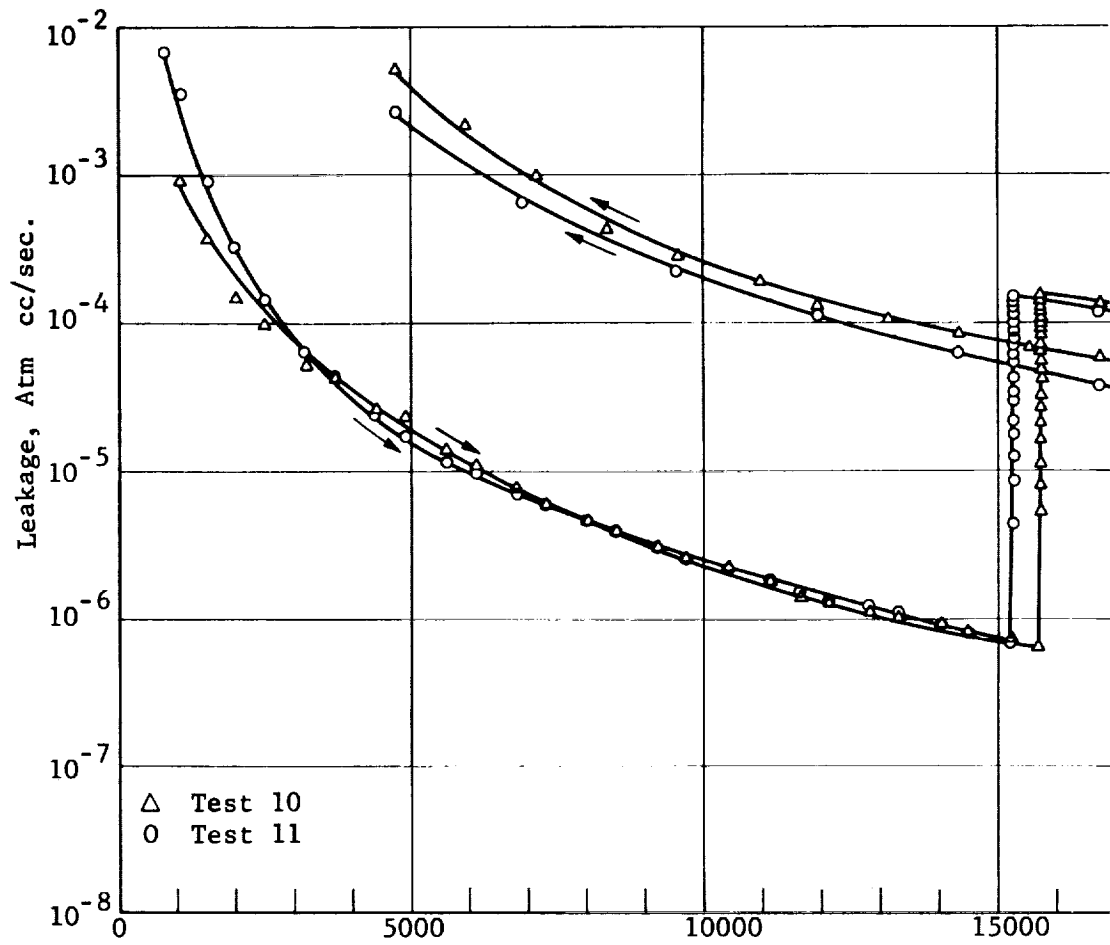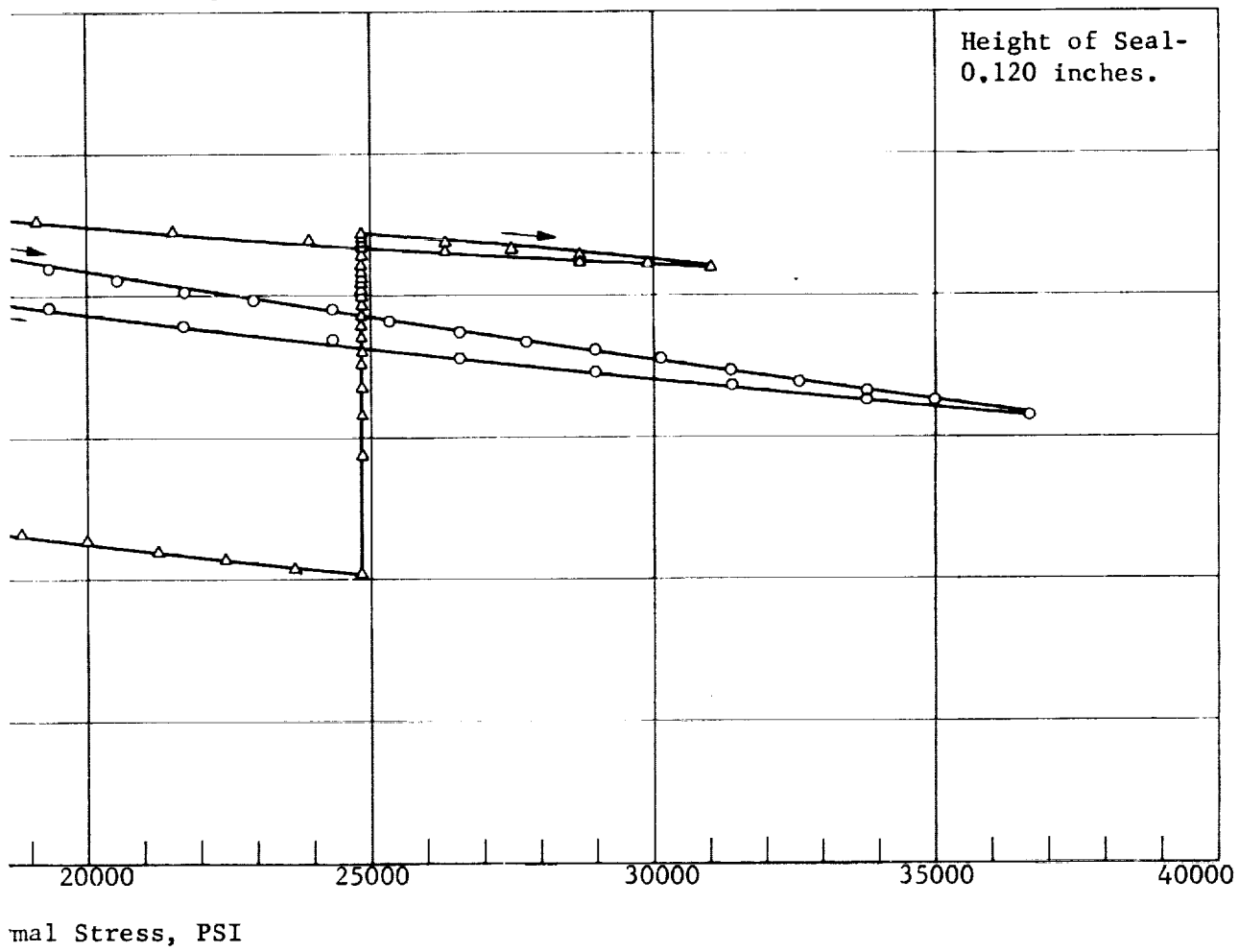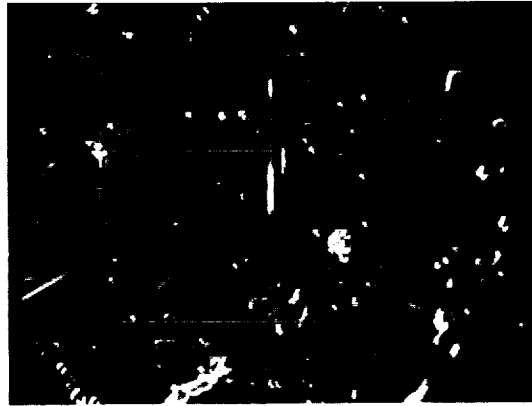
FIGURE 2.48

Nomarski Photo of Jones Optical Co. Polished 347
Stainless Steel Specimen after thirteen assemblies.
Magnification: X900.
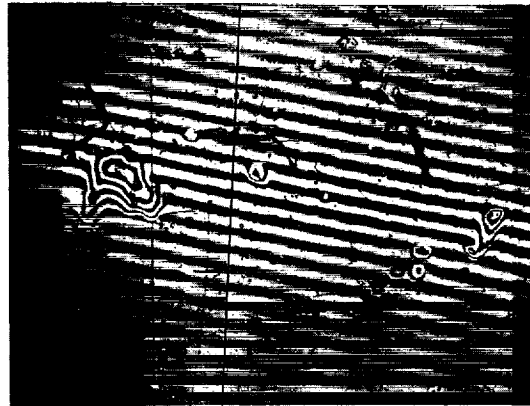
FIGURE 2.49

Interference Photo of Jones Optical Co. Polished 347
Stainless Steel Specimen after thirteen assemblies.
- 11.8 microinches between interference lines.
Scale: 0.0125 inches between scribe marks.
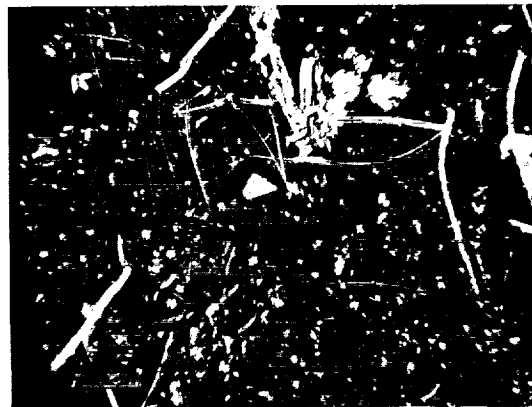
FIGURE 2.50

Nomarski Photo of Jones Optical Co. Polished 347
Stainless Steel Specimen after thirteen assemblies.
Magnification: X168.

Leakage, Atm cc/sec.

FIGURE 2.51

ess Response for Jones Optical Co.
tainless Steel Specimens

Height of Seal-
.030 inches.

20000   25000   30000   35000   40000

ormal Stress, PSI

FOLDOUT FRAME

FIGURE 2.52

Leakage - Normal Stress Response for ATL Lead
Lapped 347 Stainless Steel Specimens

Height of Seal-
.030 inches.
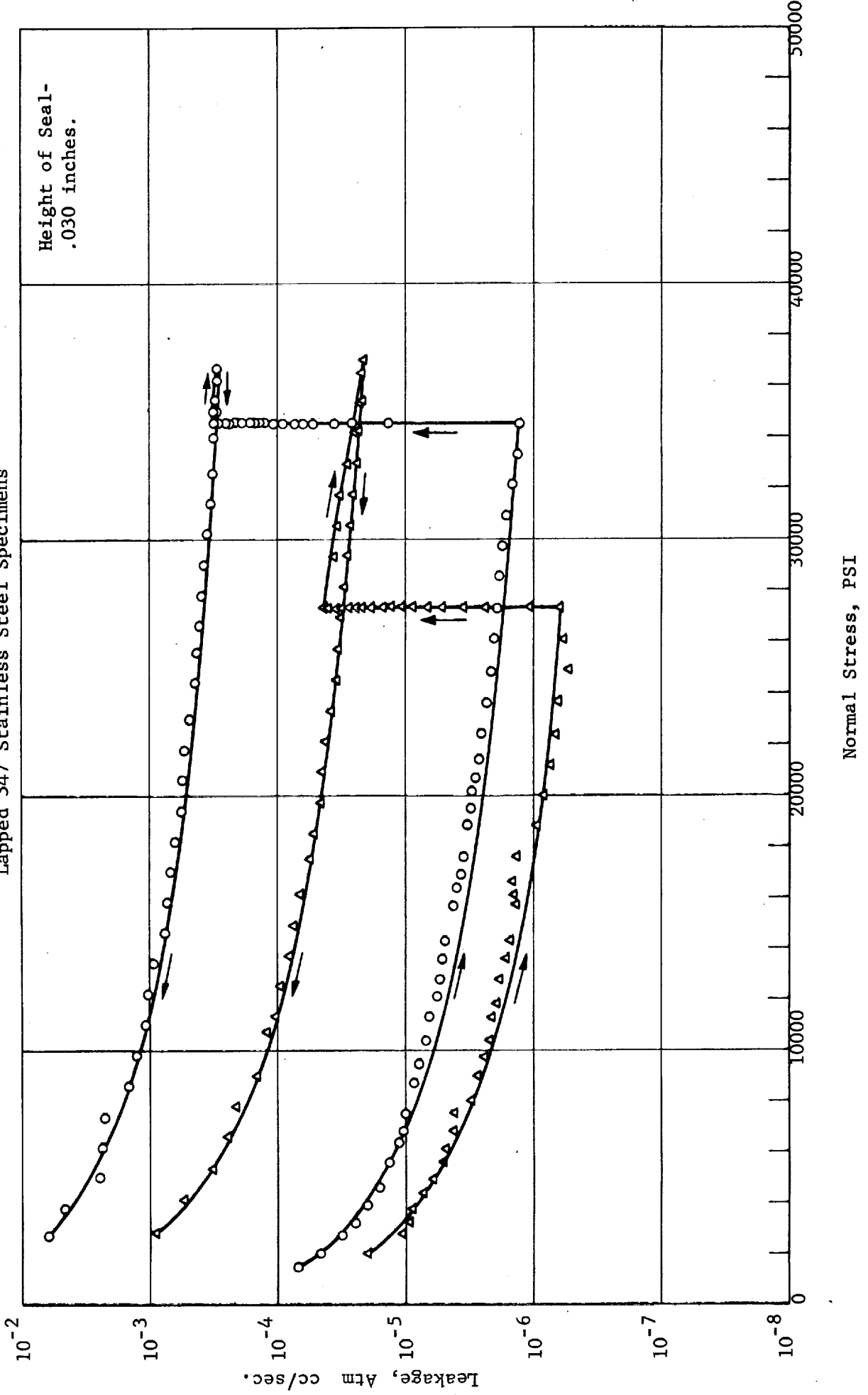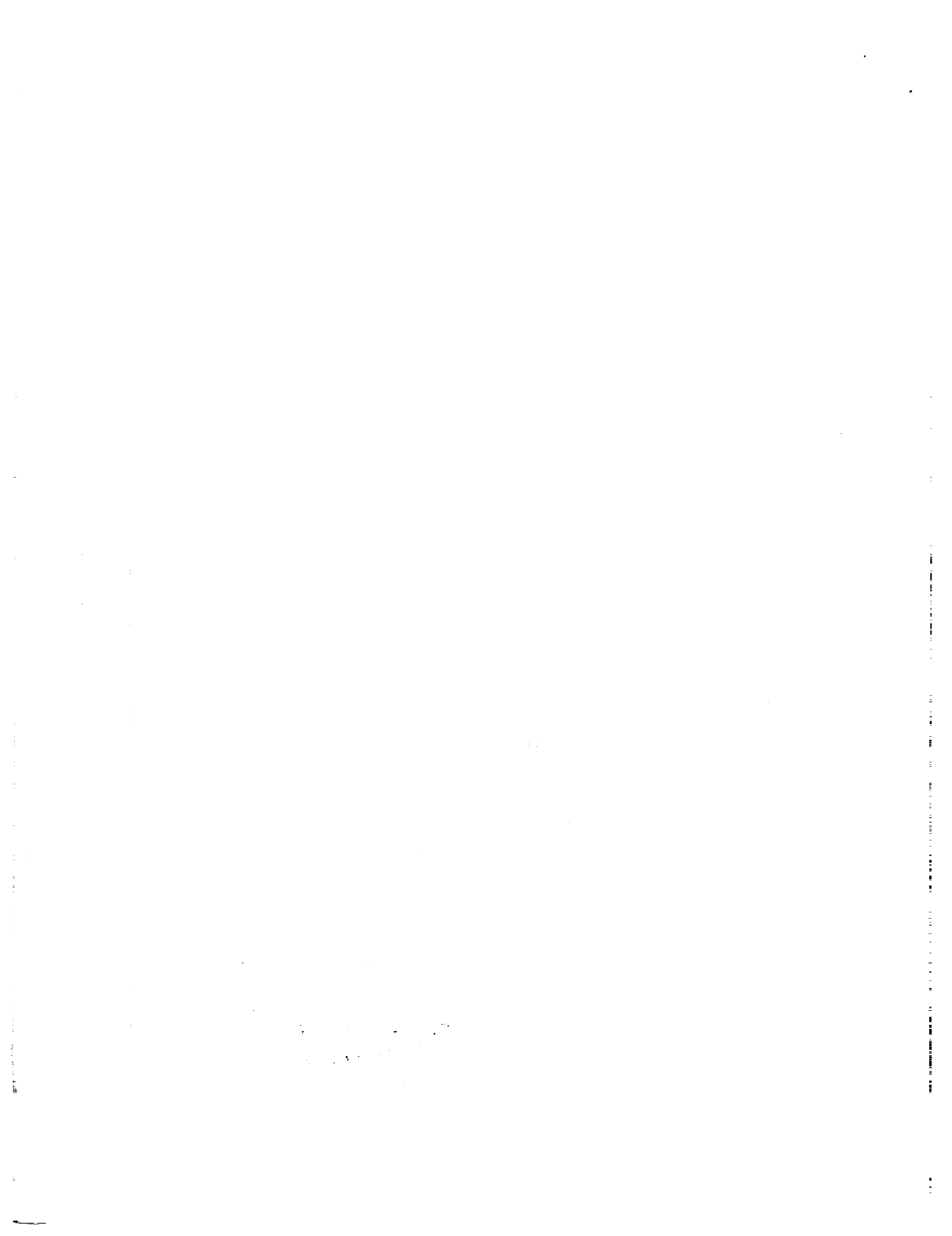
Leakage - Normal Stress Res
A286 Stee
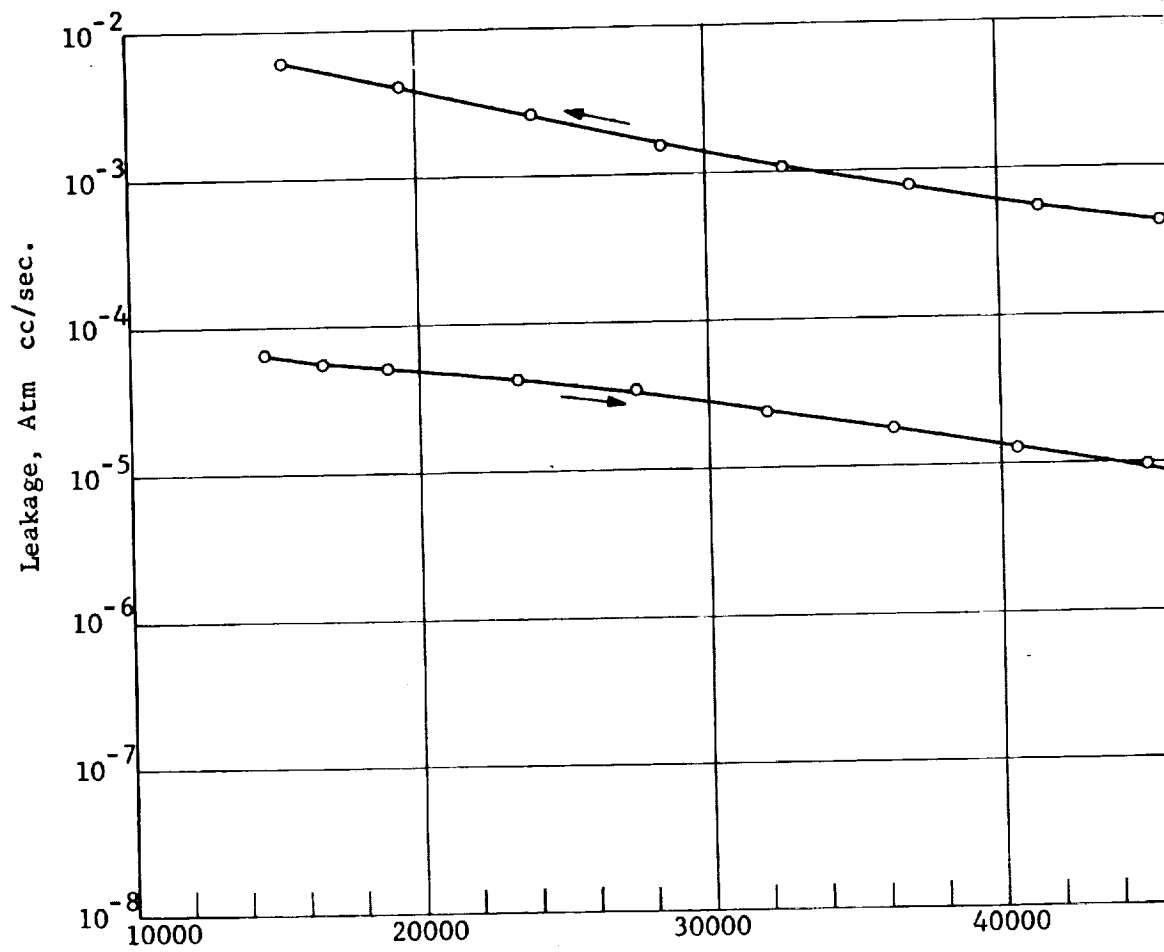
ponse for Parker Aircraft Polished
l Specimens

50000   60000   70000   80000   90000

rmal Stress, PSI
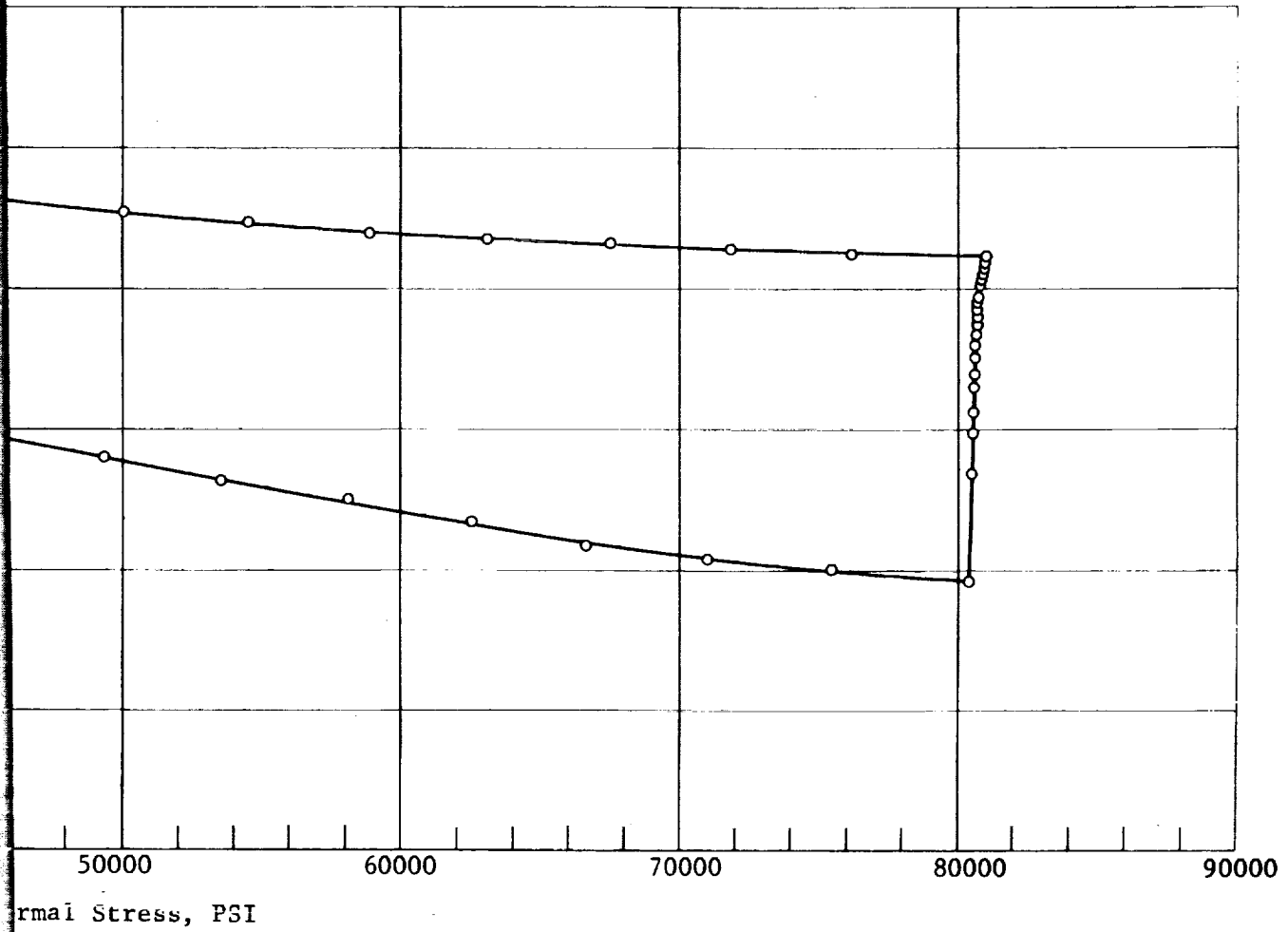
FOLDOUT FRAME $\mathcal{V}$

Figure 2.54

Leakage Applied Stress Response for 2024 Aluminum
Specimens with Jones Optical Co. KANIGEN Nickel
Plated Superfinished Surfaces

O   First Assembly
Δ   Second Assembly

APPLIED STRESS, psi

LEAKAGE atm cc/sec
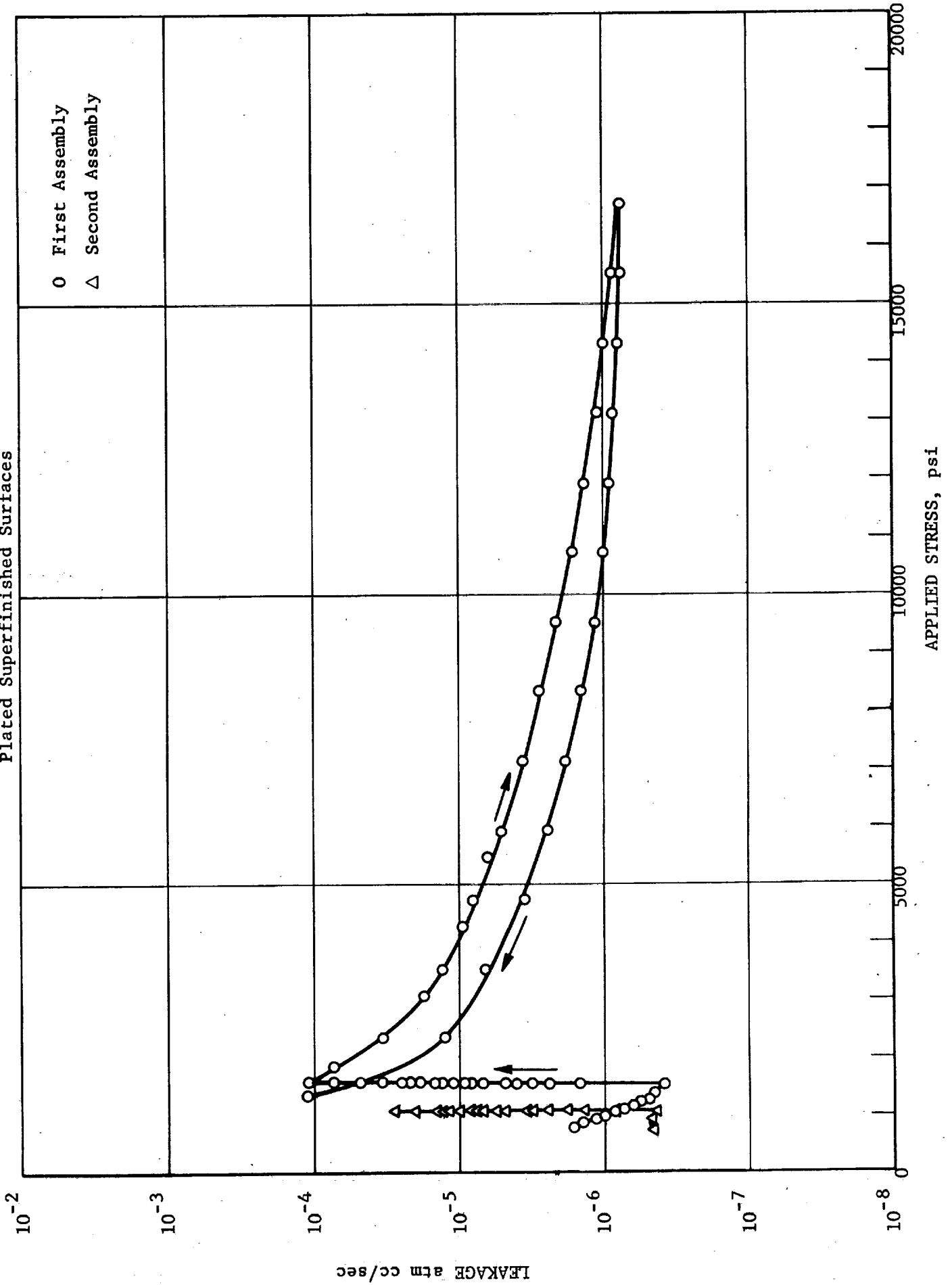
Figure 2.55

Leakage Applied Stress Response for 2024 Aluminum
Specimens with Jones Optical Co. KANIGEN Nickel
Plated Superfinished Surfaces
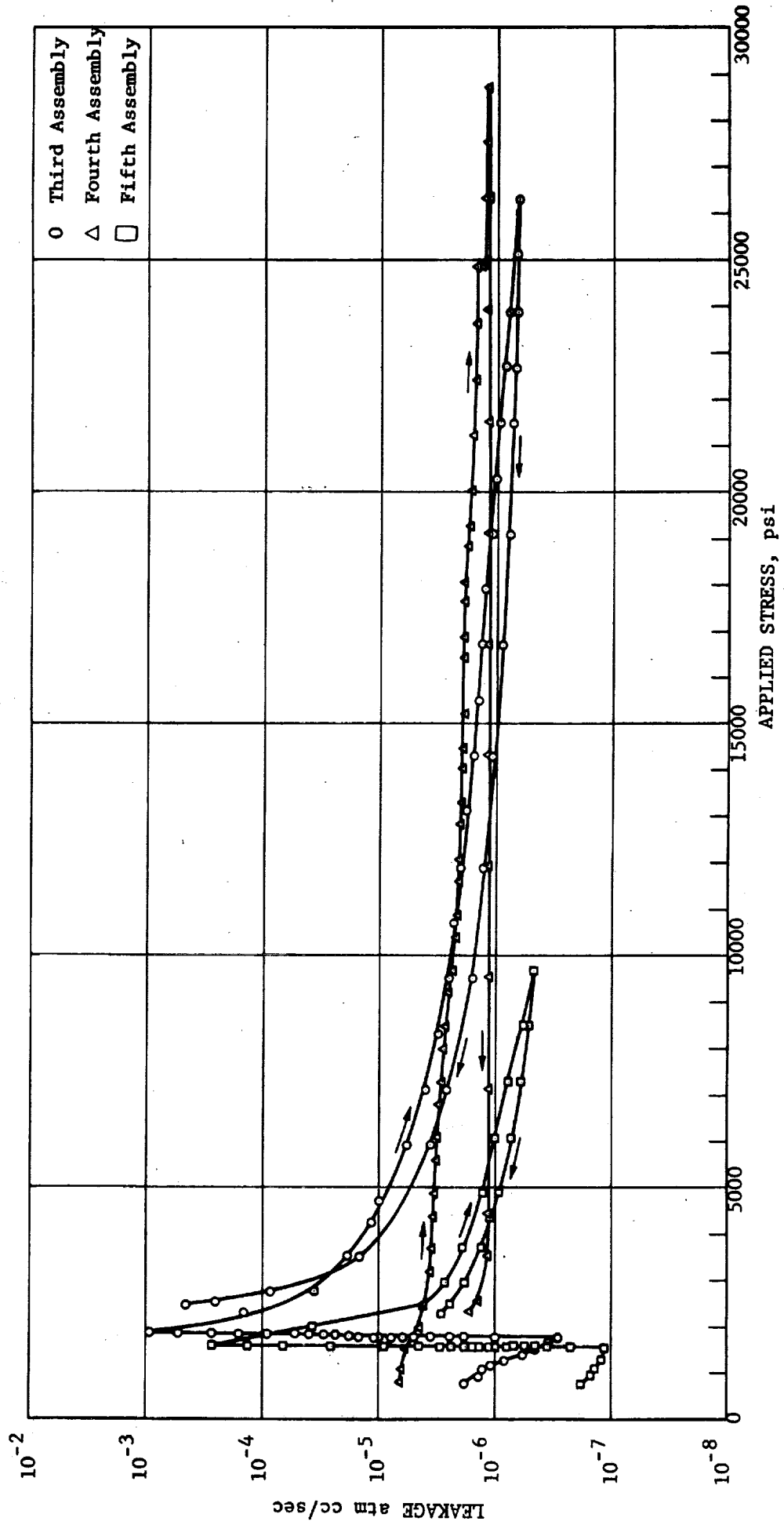
Figure 2.56

Leakage Applied Stress Response for 2024 Aluminum
Specimens with Jones Optical Co. KANIGEN Nickel
Plated Superfinished Surfaces - Sixth Assembly
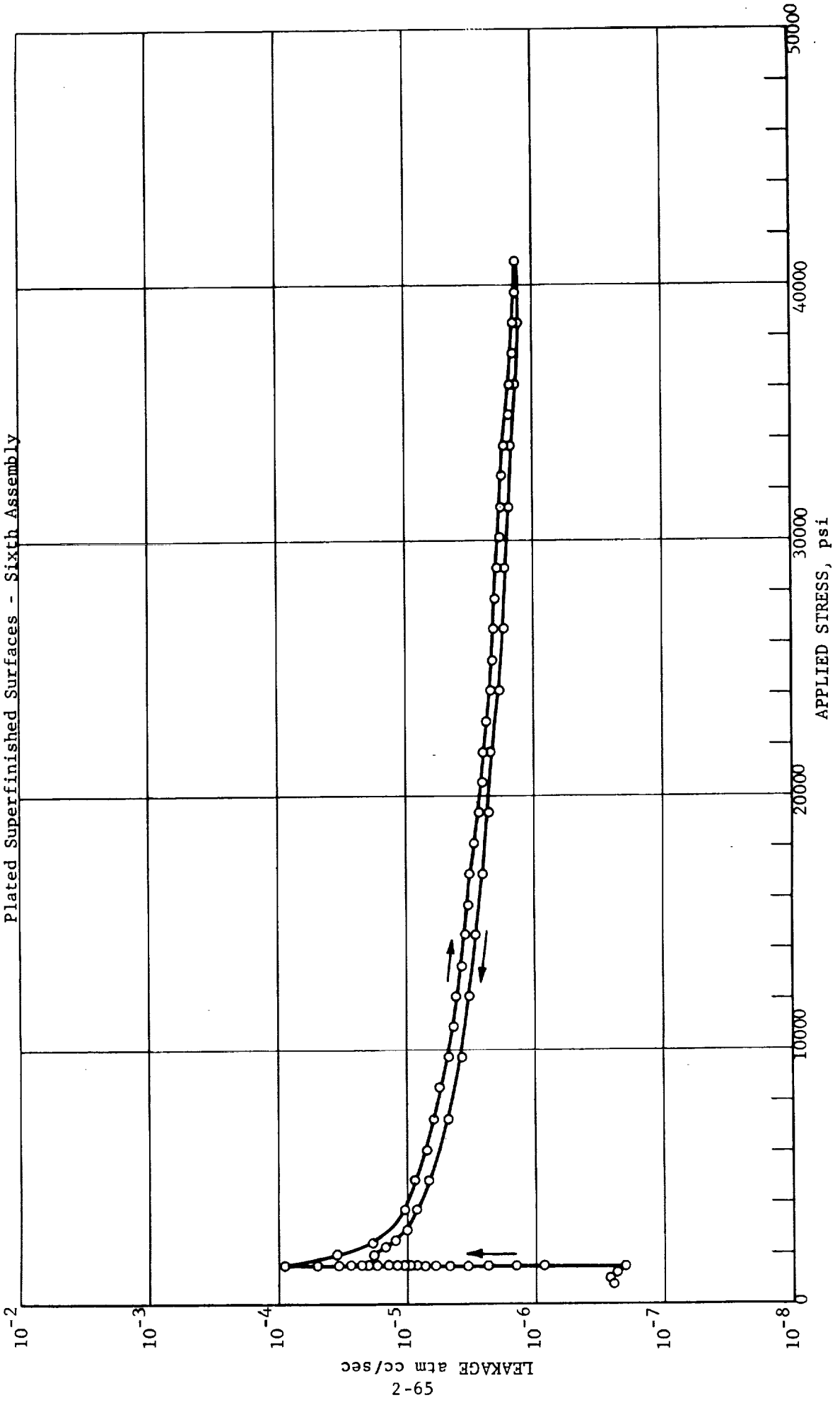
Figure 2.57

Leakage Applied Stress Response for 2024 Aluminum
Specimens with Jones Optical Co. KANIGEN Nickel
Plated Superfinished Surfaces - Seventh Assembly

2-66
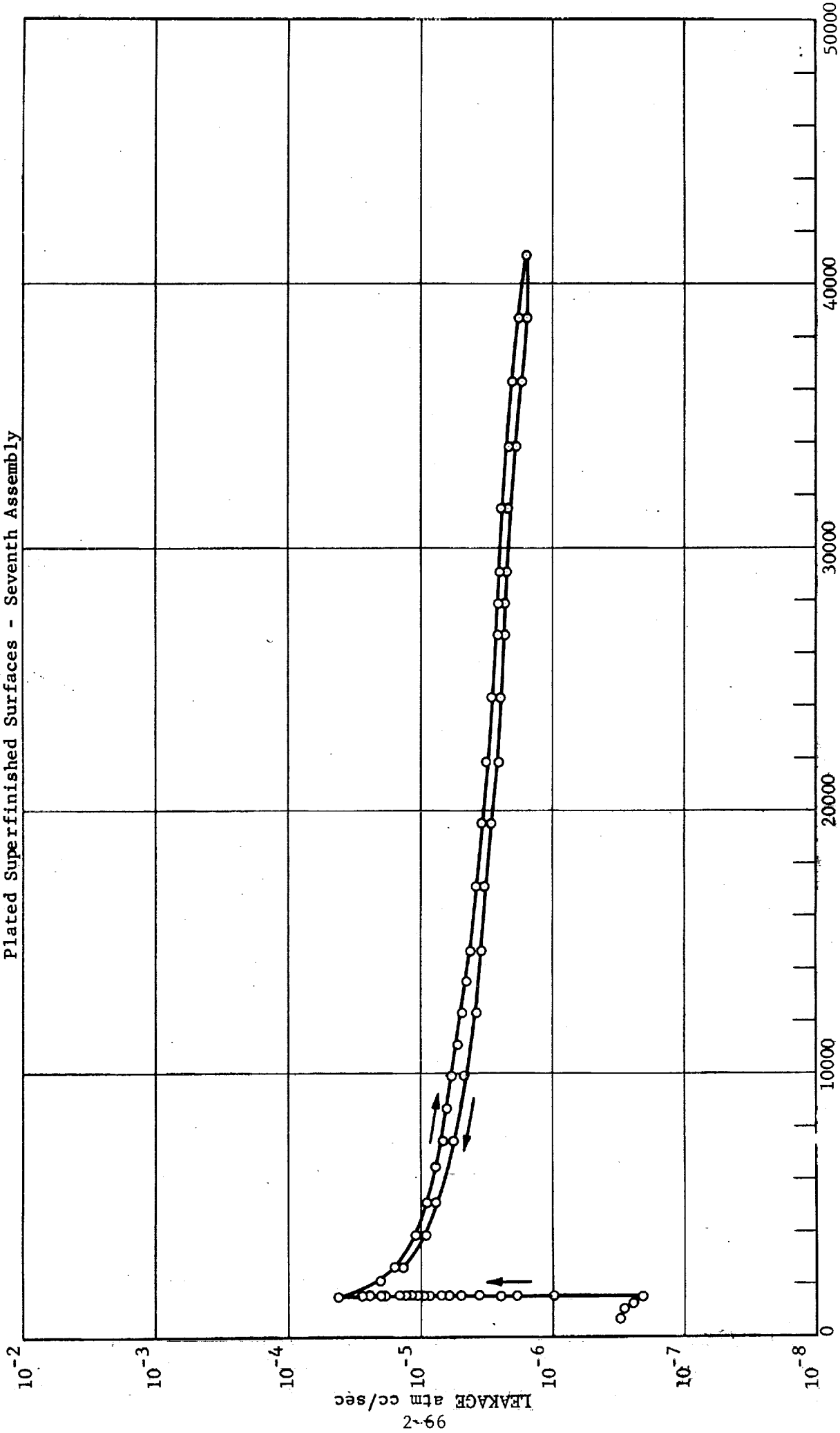
Figure 2.58

Leakage Applied Stress Response for 2024 Aluminum
Specimens with Jones Optical Co. KANIGEN Nickel
Plated Superfinished Surfaces - Eight Assembly
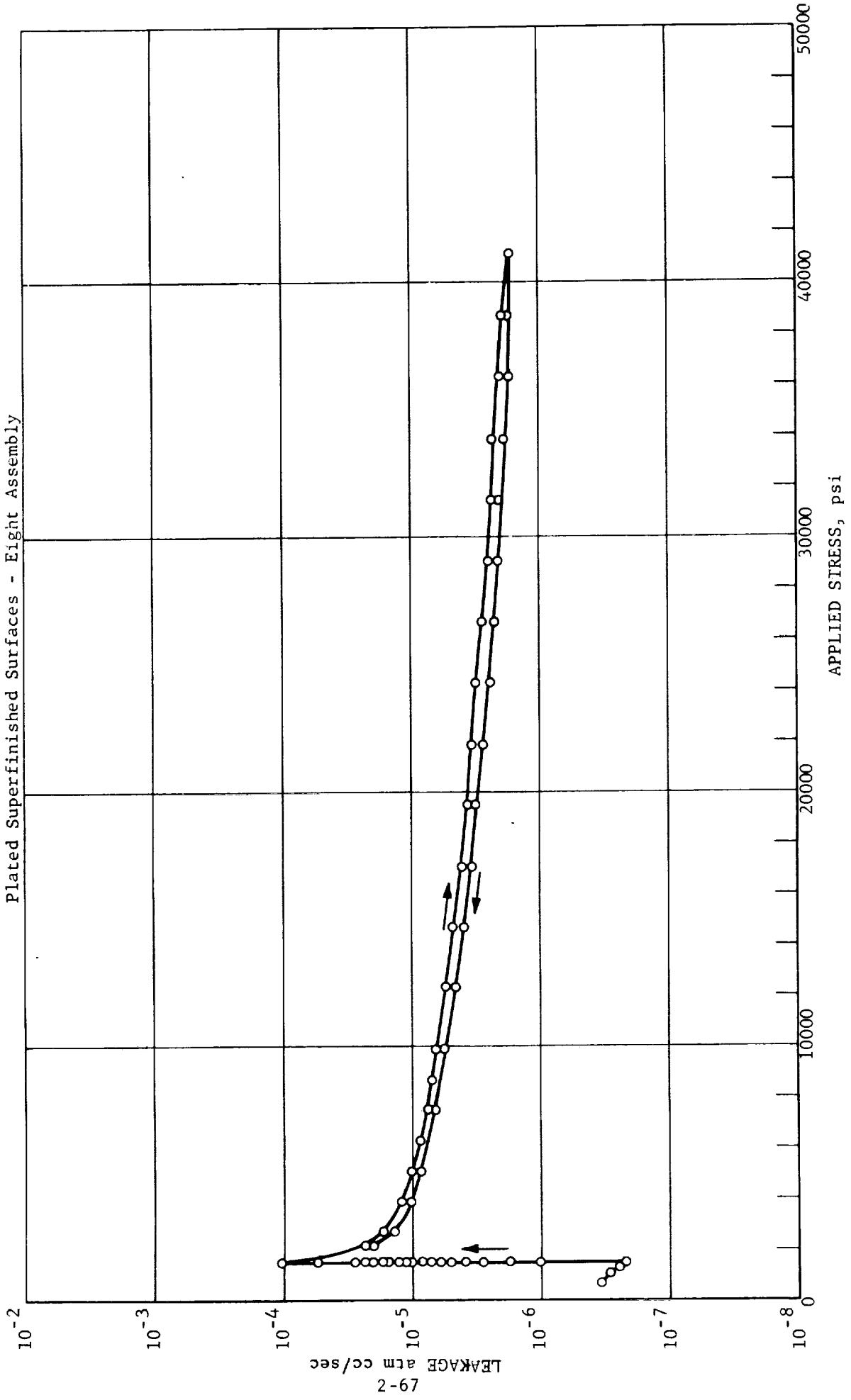
Figure 2.59

Leakage Applied Stress Response for 2024 Aluminum
Specimens with Jones Optical Co. KANIGEN Nickel
Plated Superfinished Surfaces - Ninth Assembly
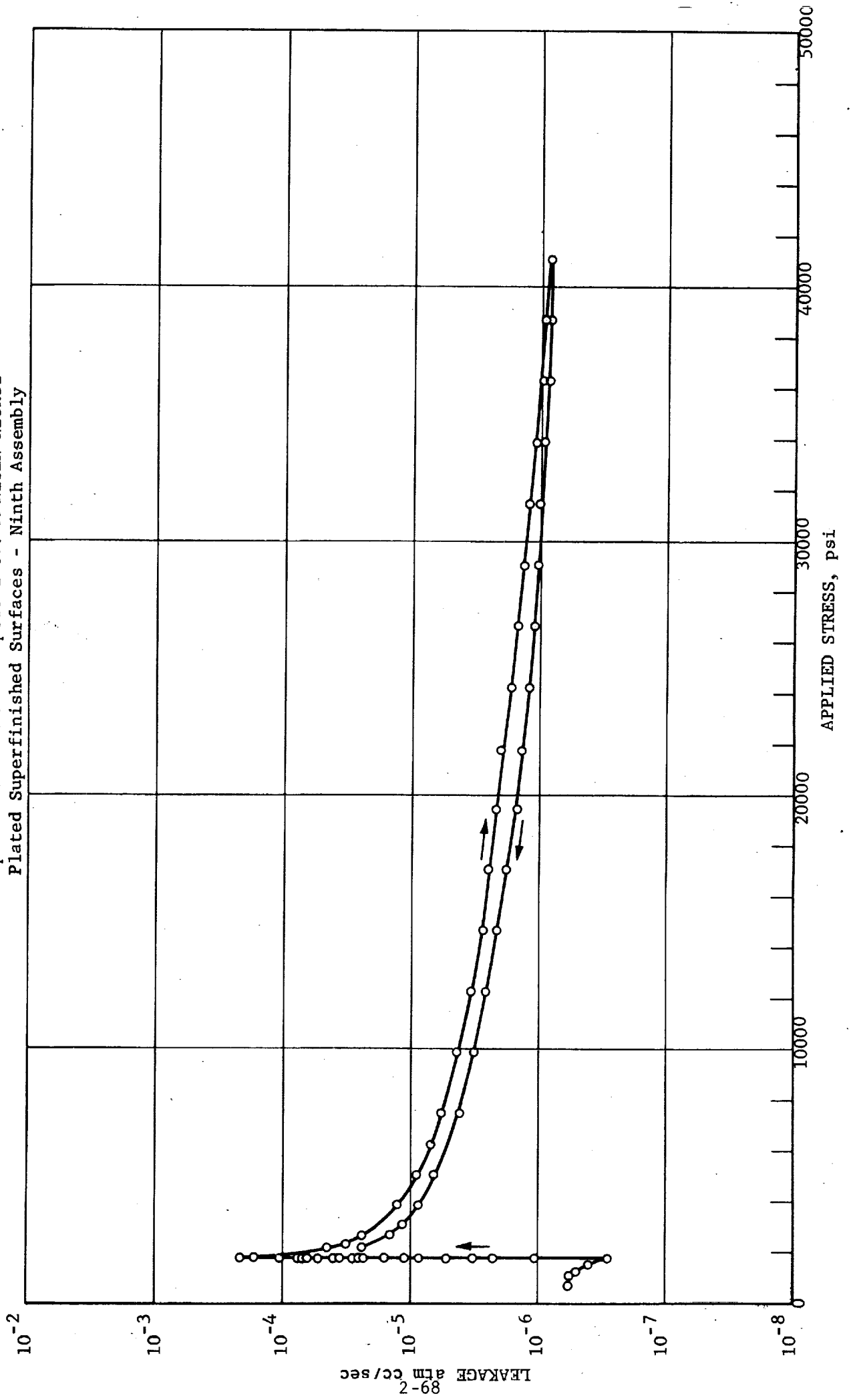
Figure 2.60

Leakage Applied Stress Response for 2024 Aluminum
Specimens with Jones Optical Co. KANIGEN Nickel
Plated Superfinished Surfaces - Tenth Assembly
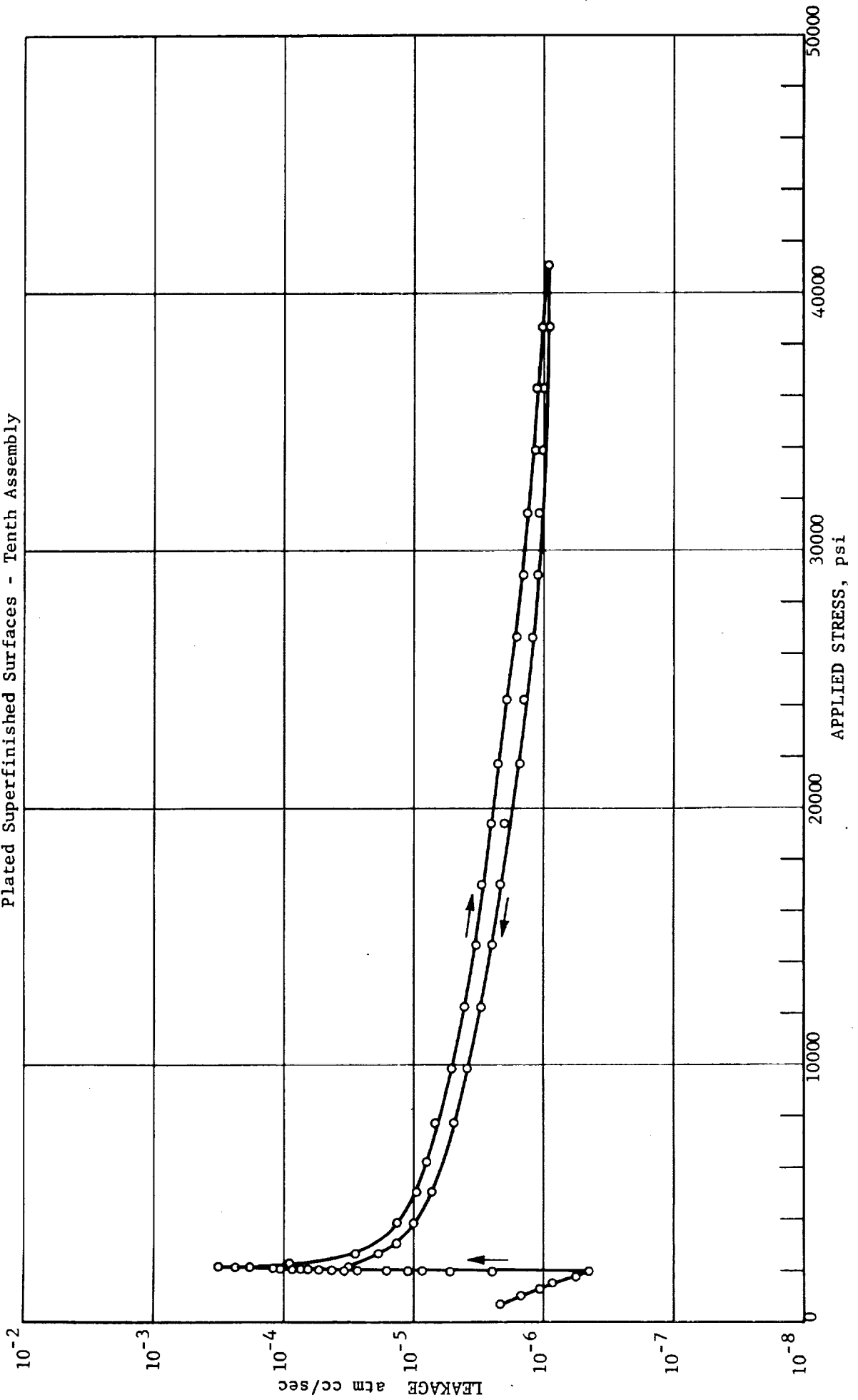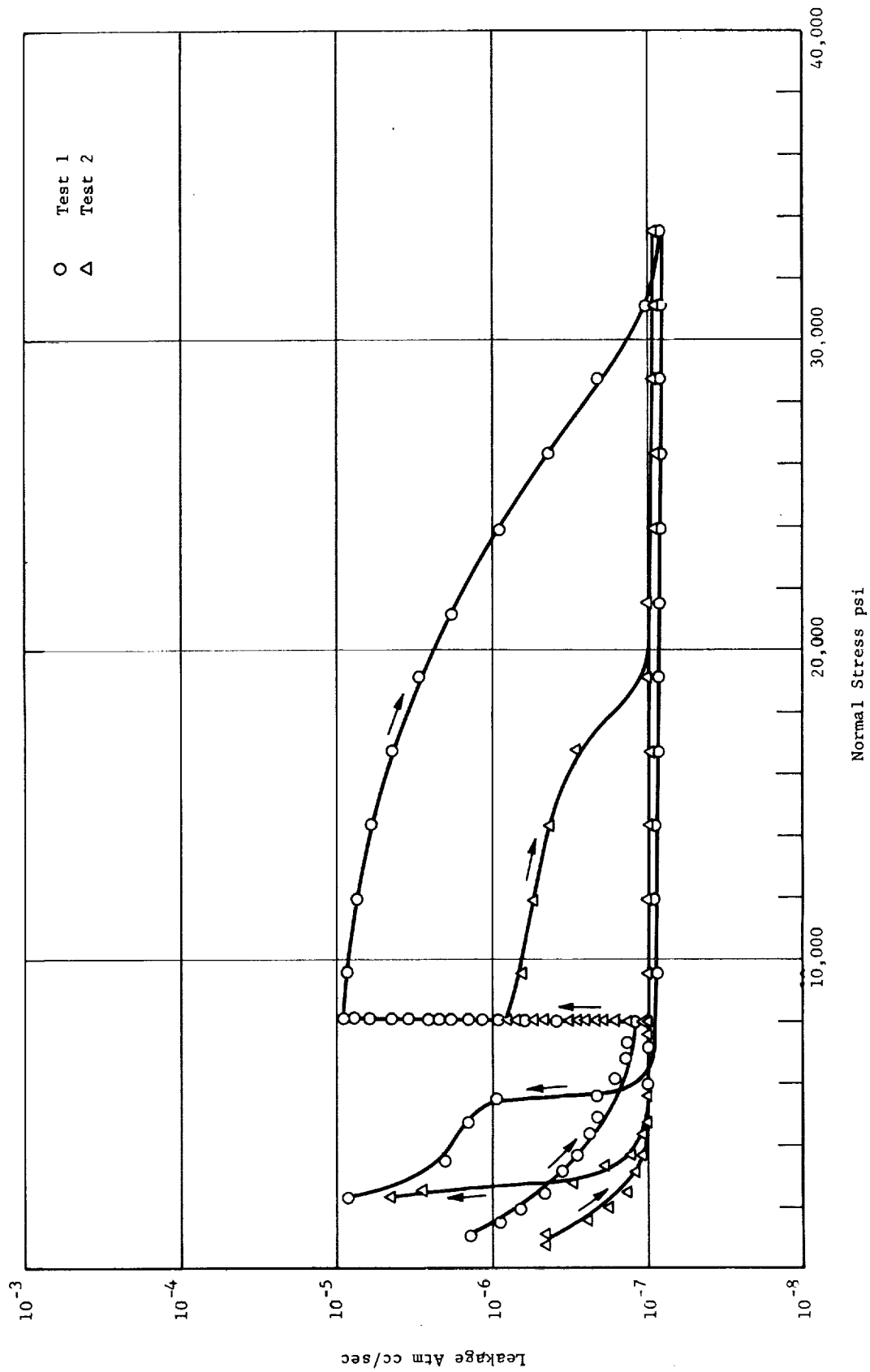
Figure 2. 61. Leakage–Normal Stress Response for 347 Stainless Steel-Silver Plated Combination
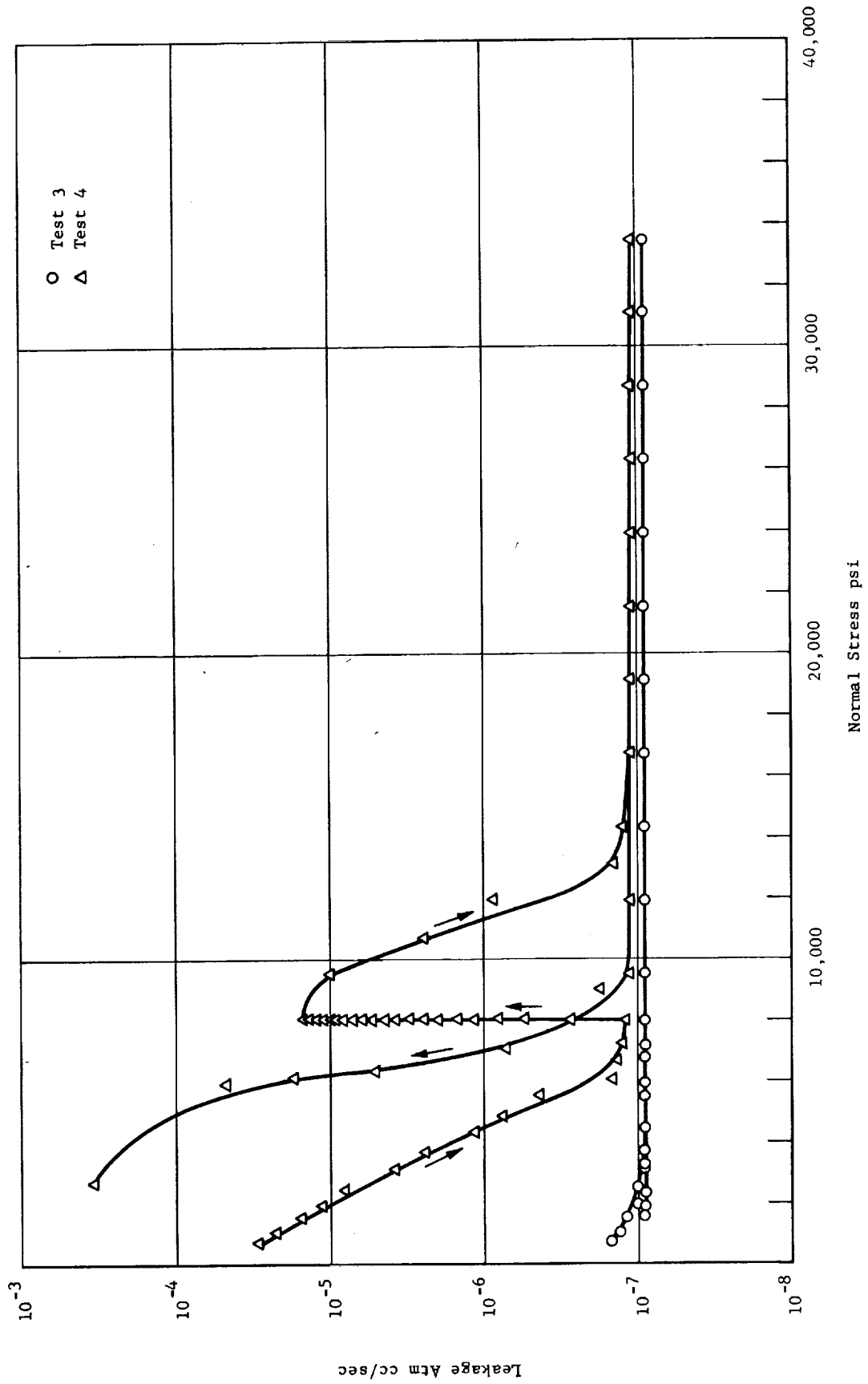
Figure 2.62. Leakage-Normal Stress Response for 347 Stainless Steel-Silver Plated Combination
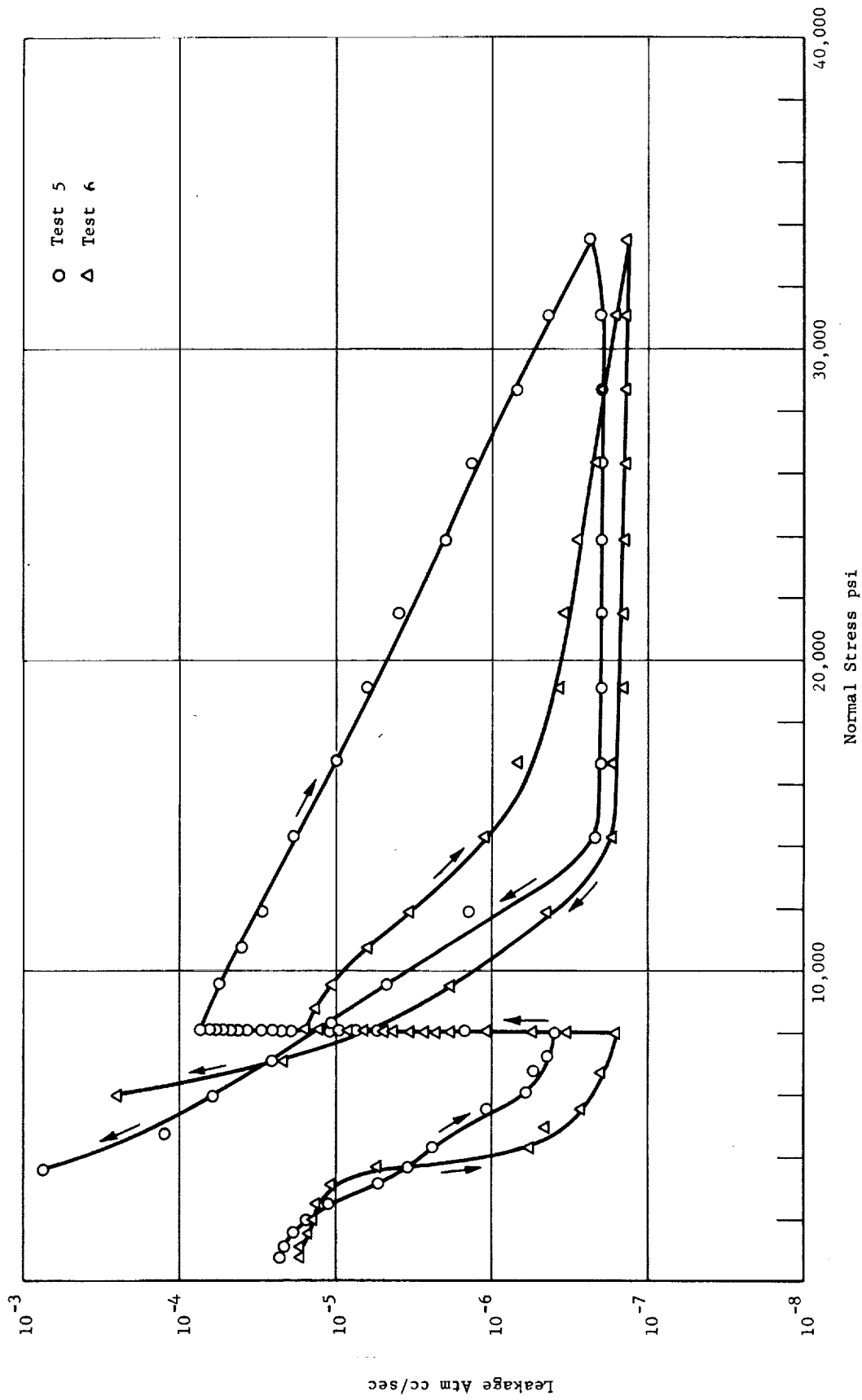
Figure 2.63. Leakage-Normal Stress Response for 347 Stainless Steel-Silver Plated Combination
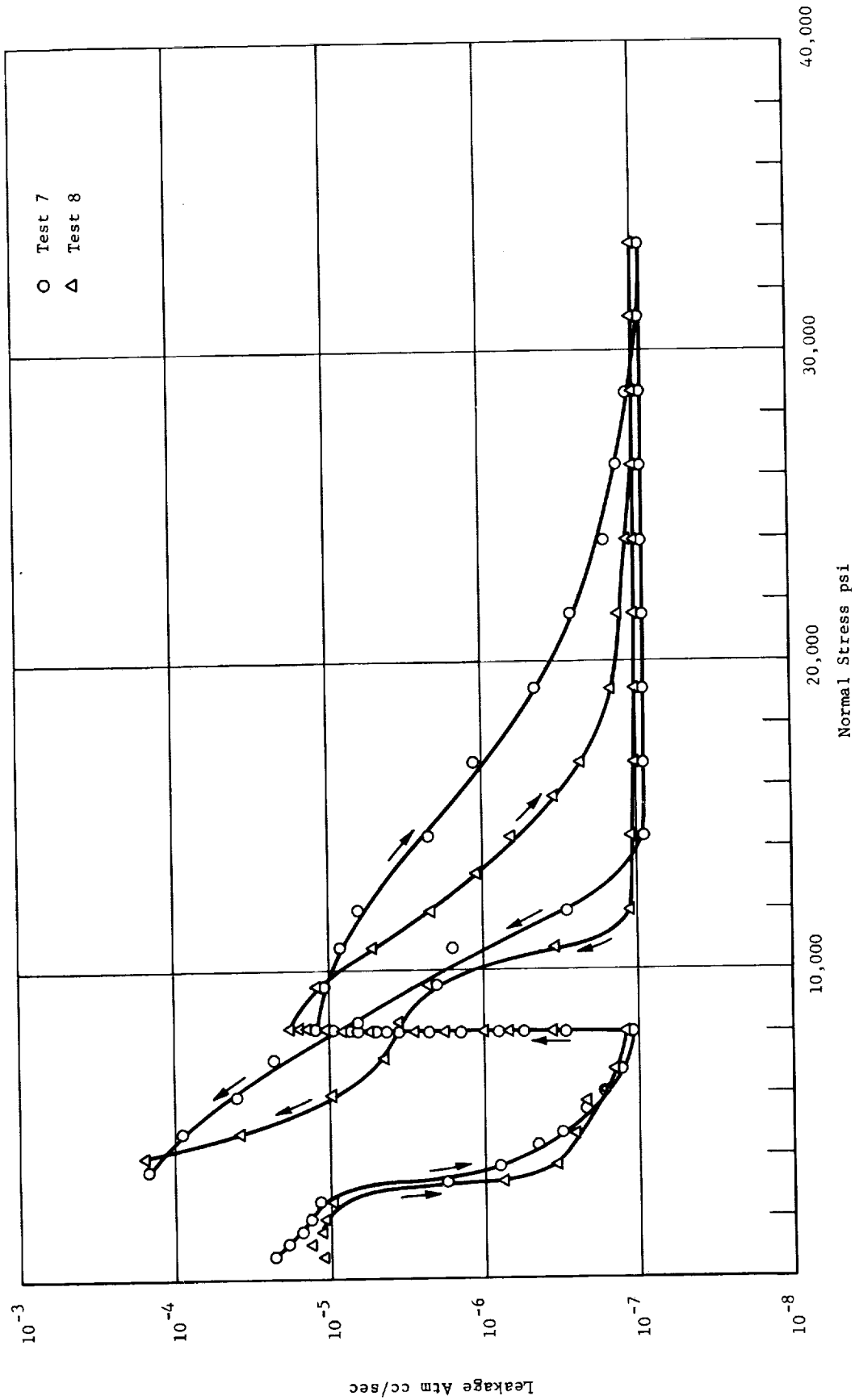
Figure 2.64. Leakage-Normal Stress Response for 347 Stainless Steel-Silver Plated Combination
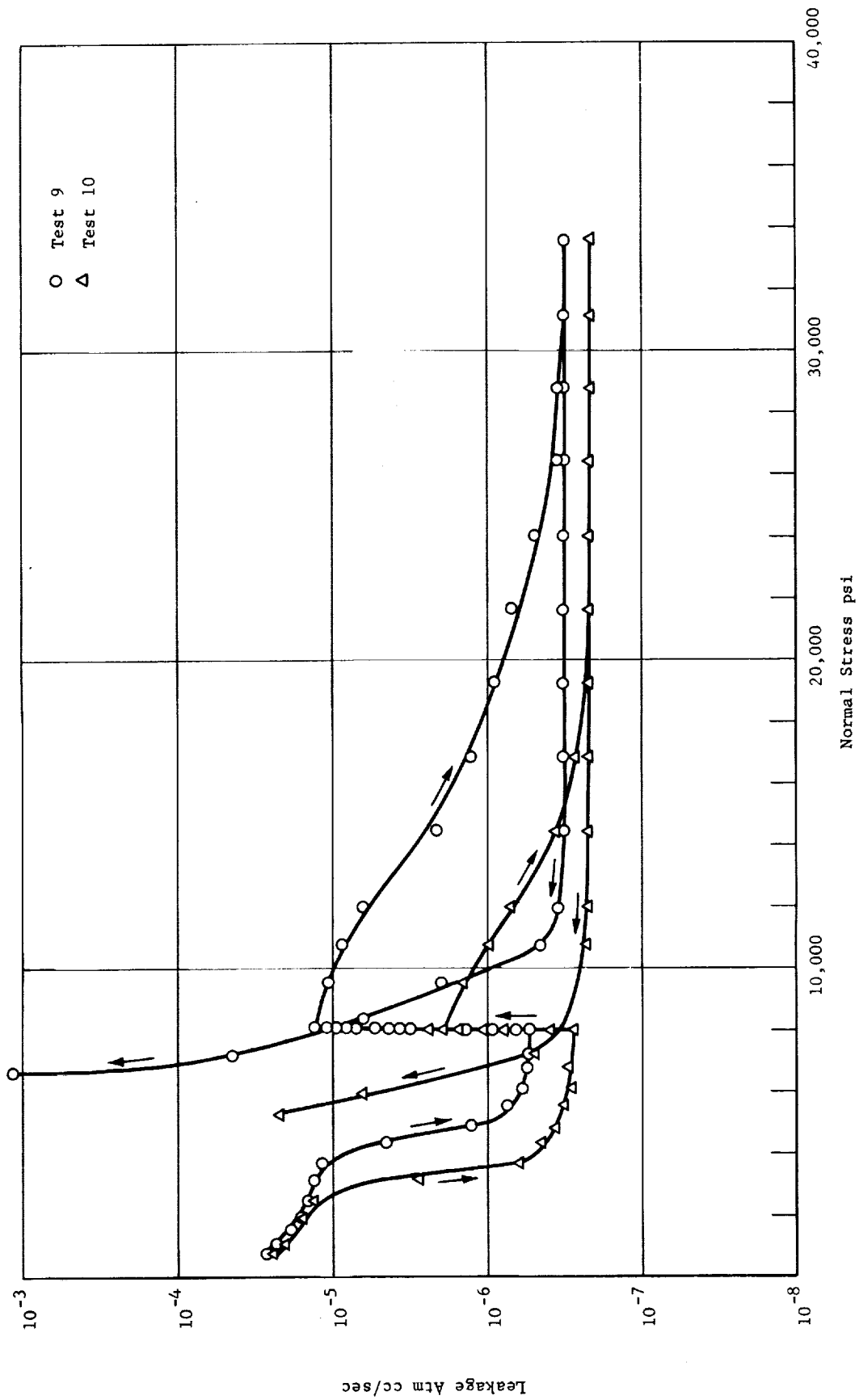
Figure 2. 65. Leakage-Normal Stress Response for 347 Stainless Steel-Silver Plated Combination
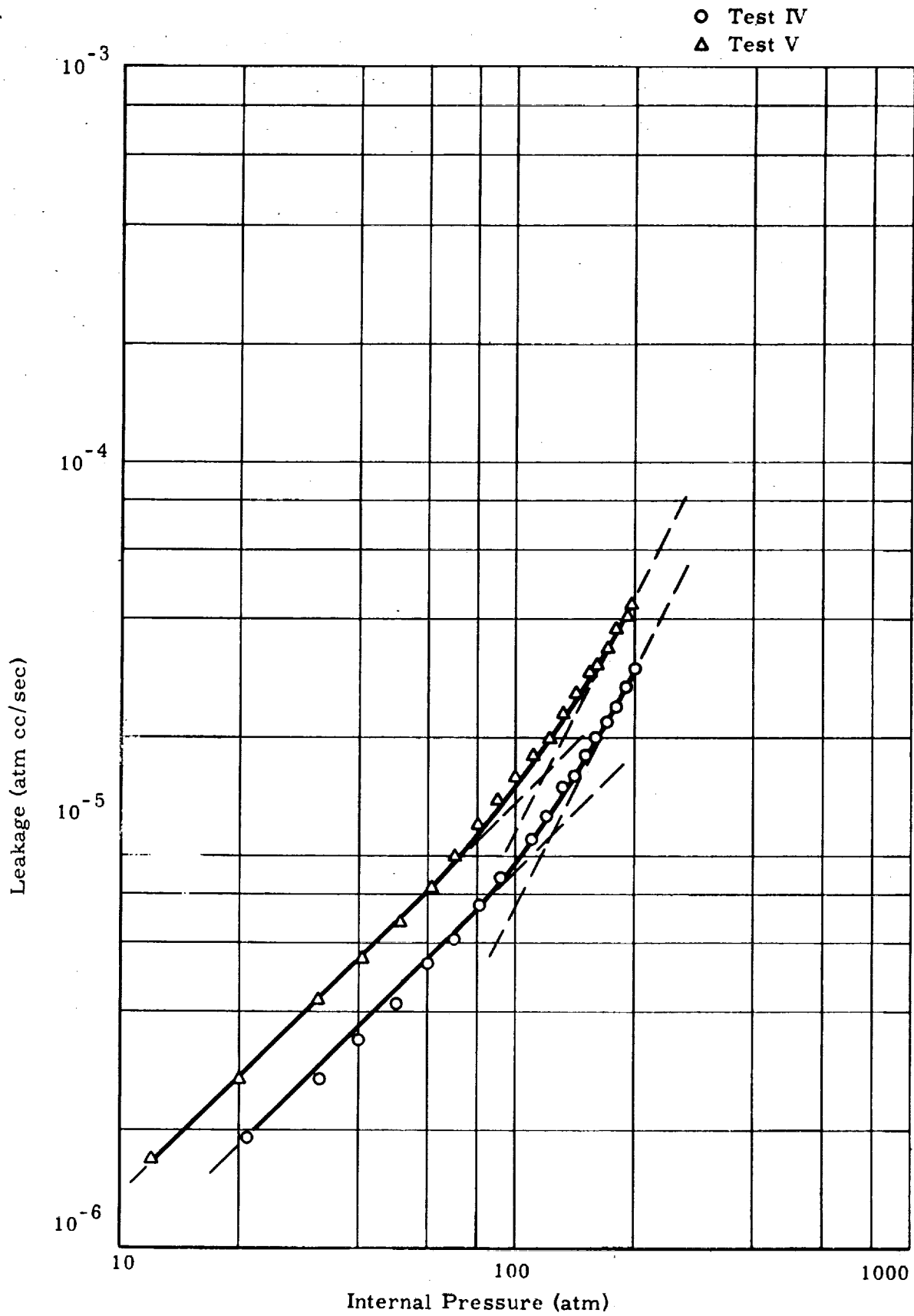
Figure 2.66. Leakage as a Function of Internal Pressure, Phase II of Experiment - Yatabe Stainless Steel (First Set).
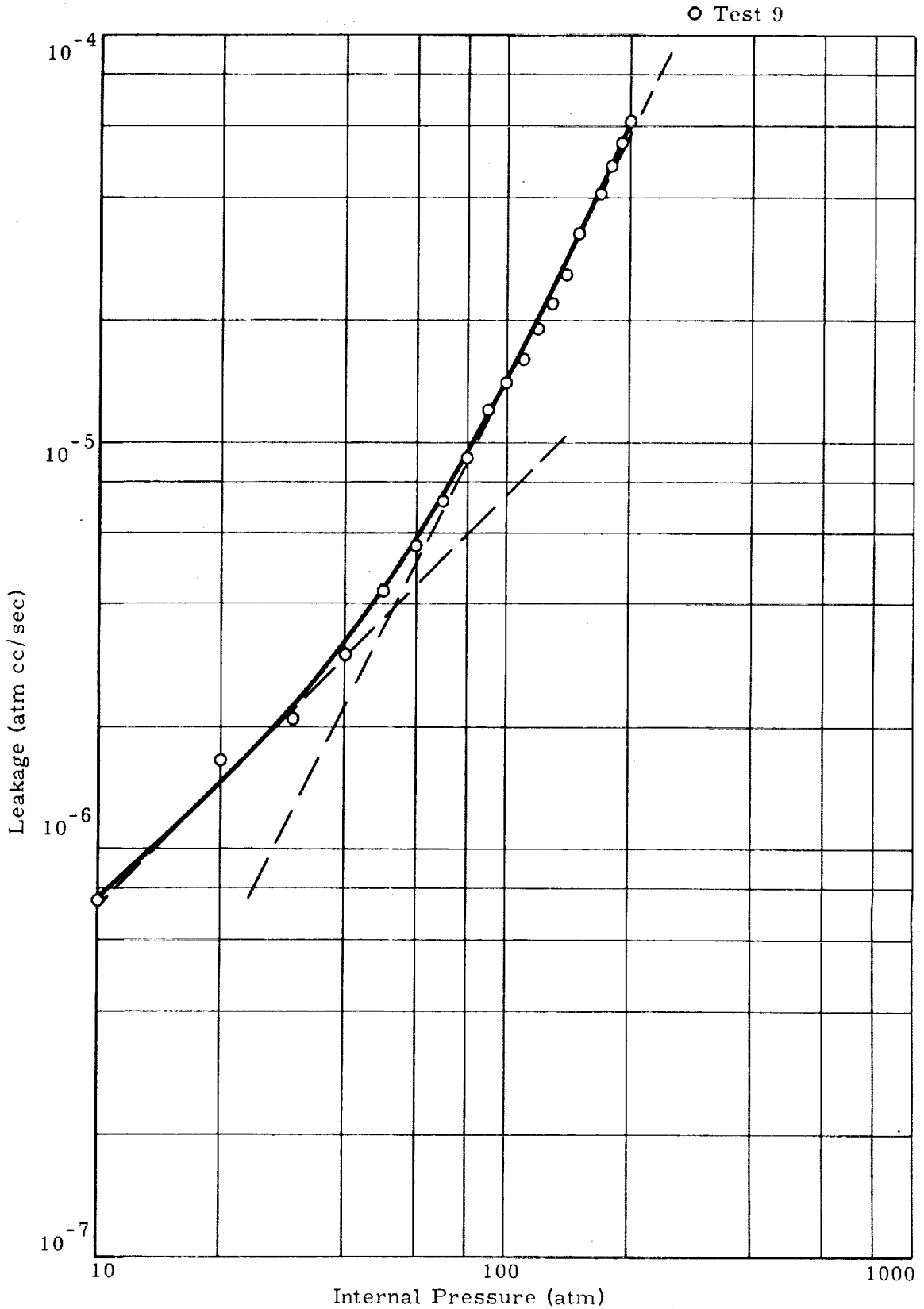
Figure 2.67.   Leakage as a Function of Internal Pressure, Phase II of
Experiment - Yatabe Stainless Steel (First Set).
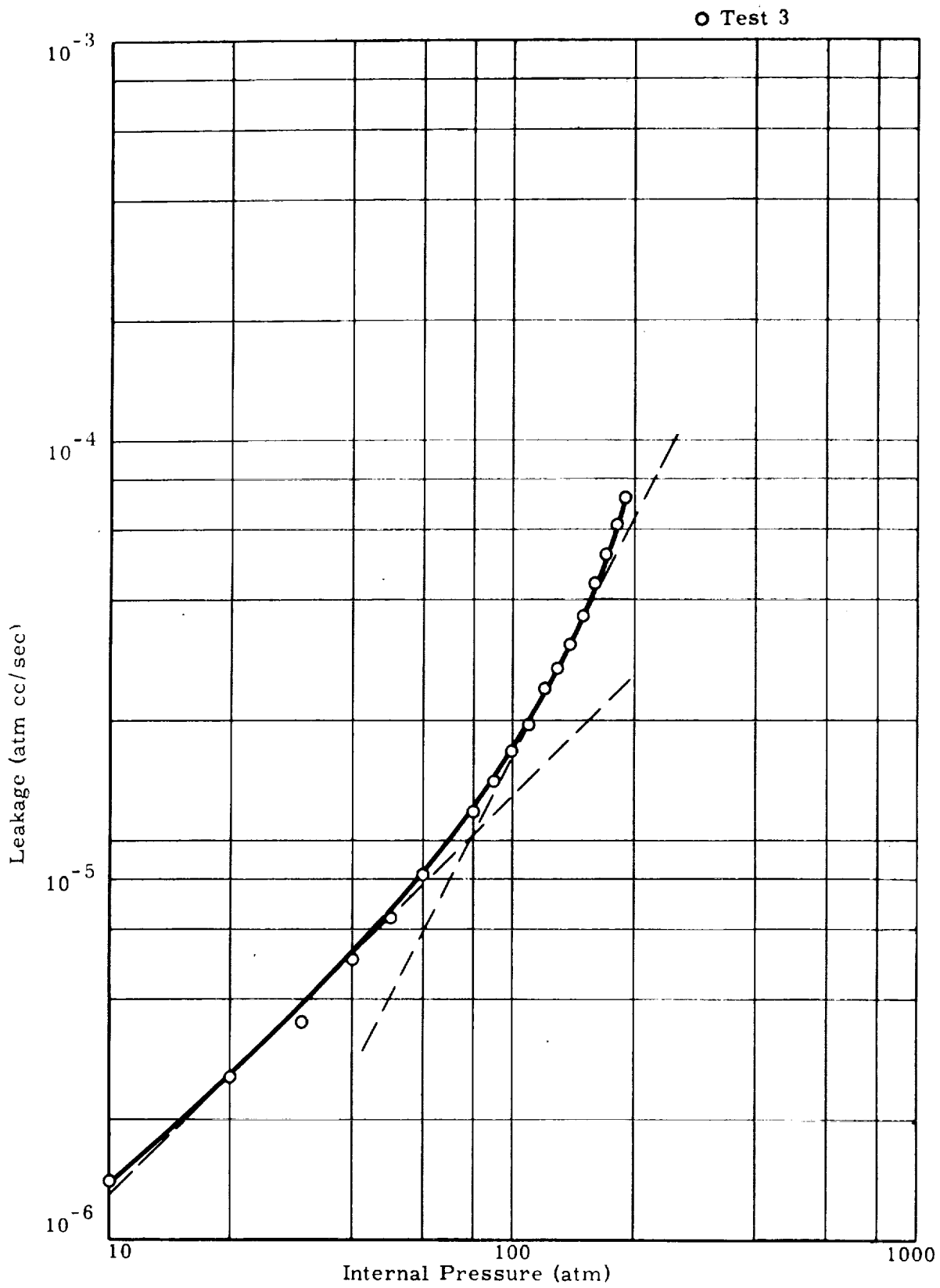
Figure 2.68. Leakage as a Function of Internal Pressure, Phase II of Experiment - Yatabe Stainless Steel (Second Set)
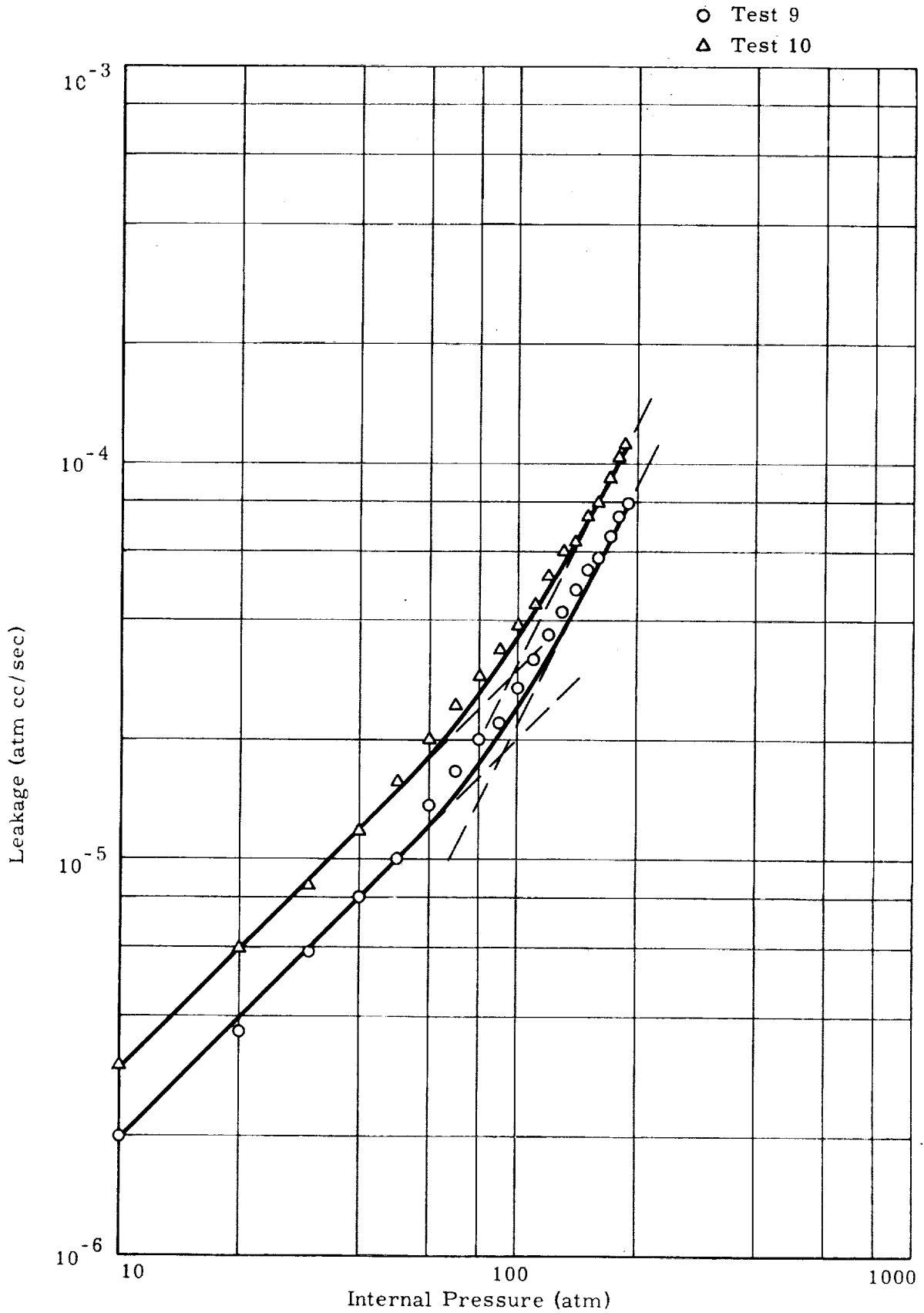
Figure 2.69. Leakage as a Function of Internal Pressure, Phase II of Experiment - Yatabe Stainless Steel (Second Set).
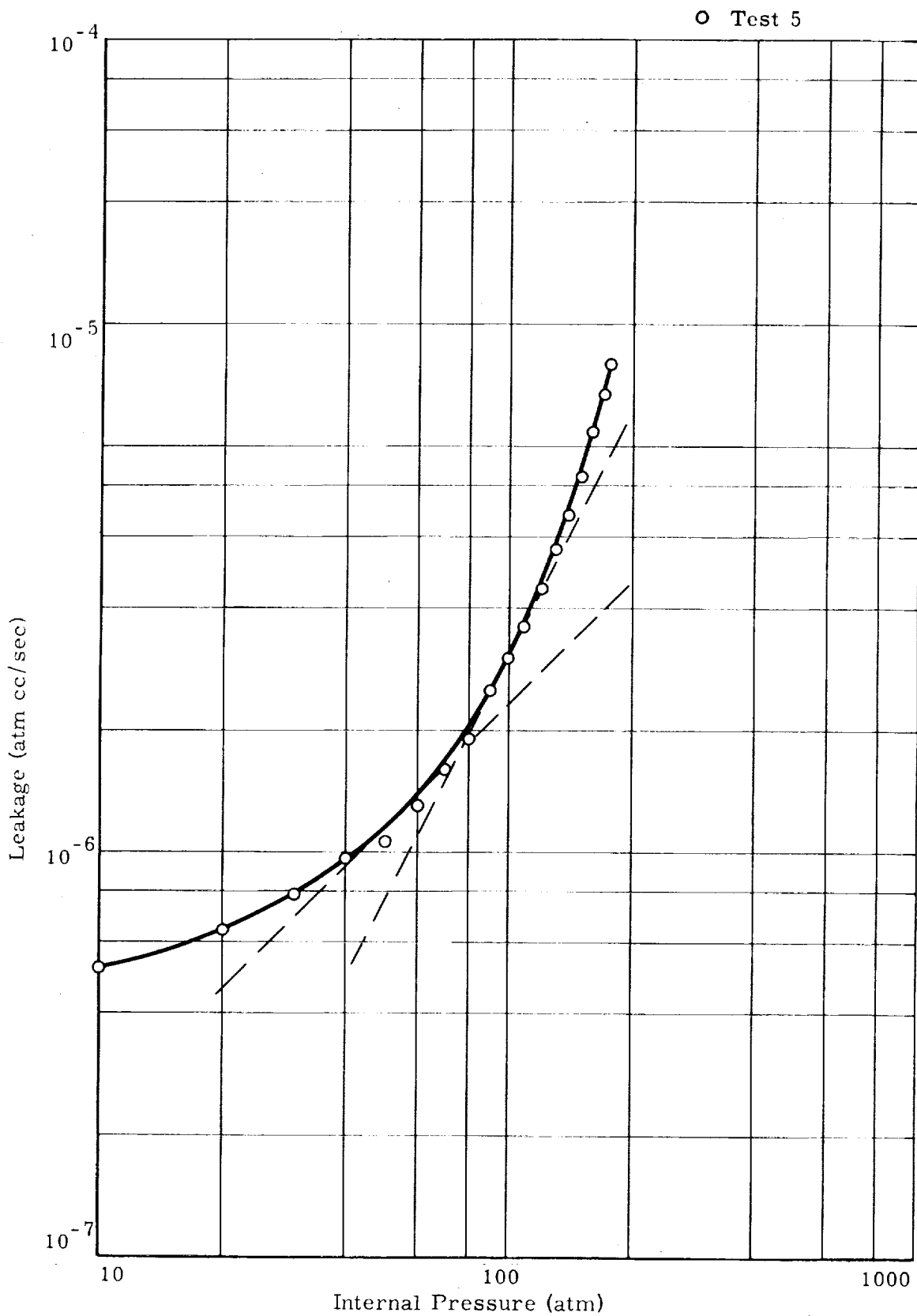
Figure 2.70. Leakage as a Function of Internal Pressure, Phase II of Experiment - Jones Optical Stainless Steel
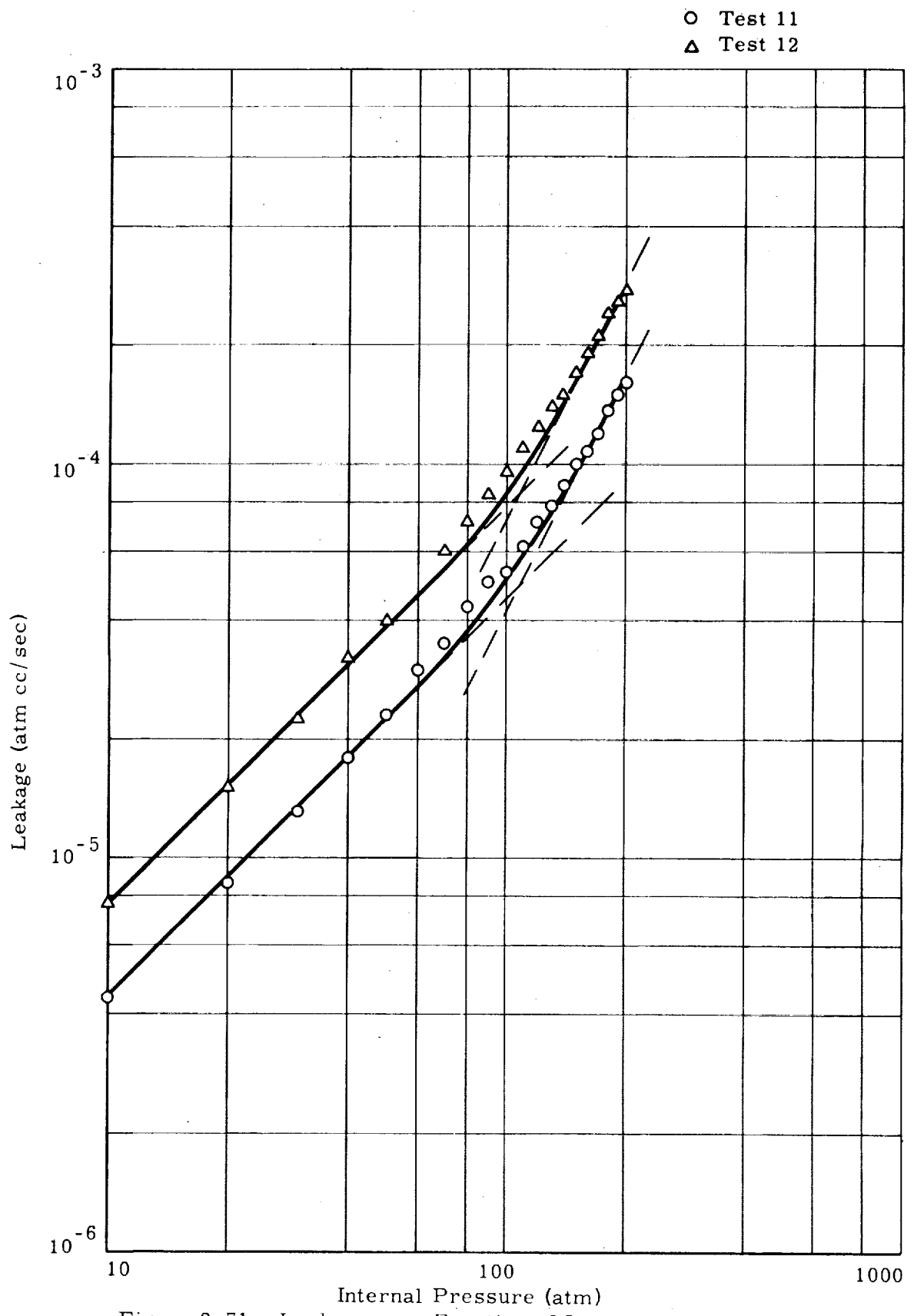
Figure 2.71. Leakage as a Function of Internal Pressure, Phase II of Experiment - Jones Optical Stainless Steel.
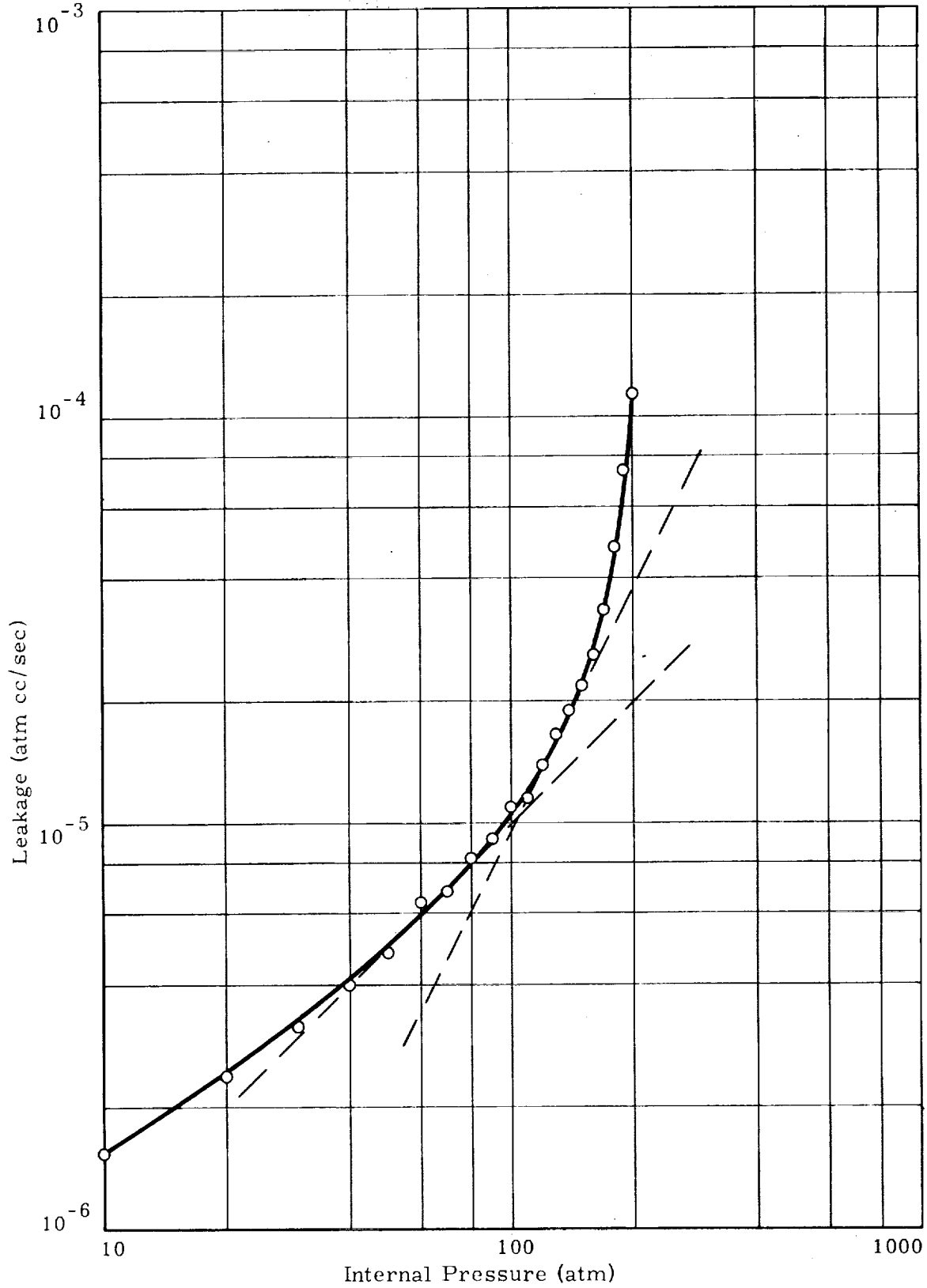
Figure 2.72. Leakage as a Function of Internal Pressure, Phase II of
Experiment - Jones Optical KANIGEN Aluminum

2-81
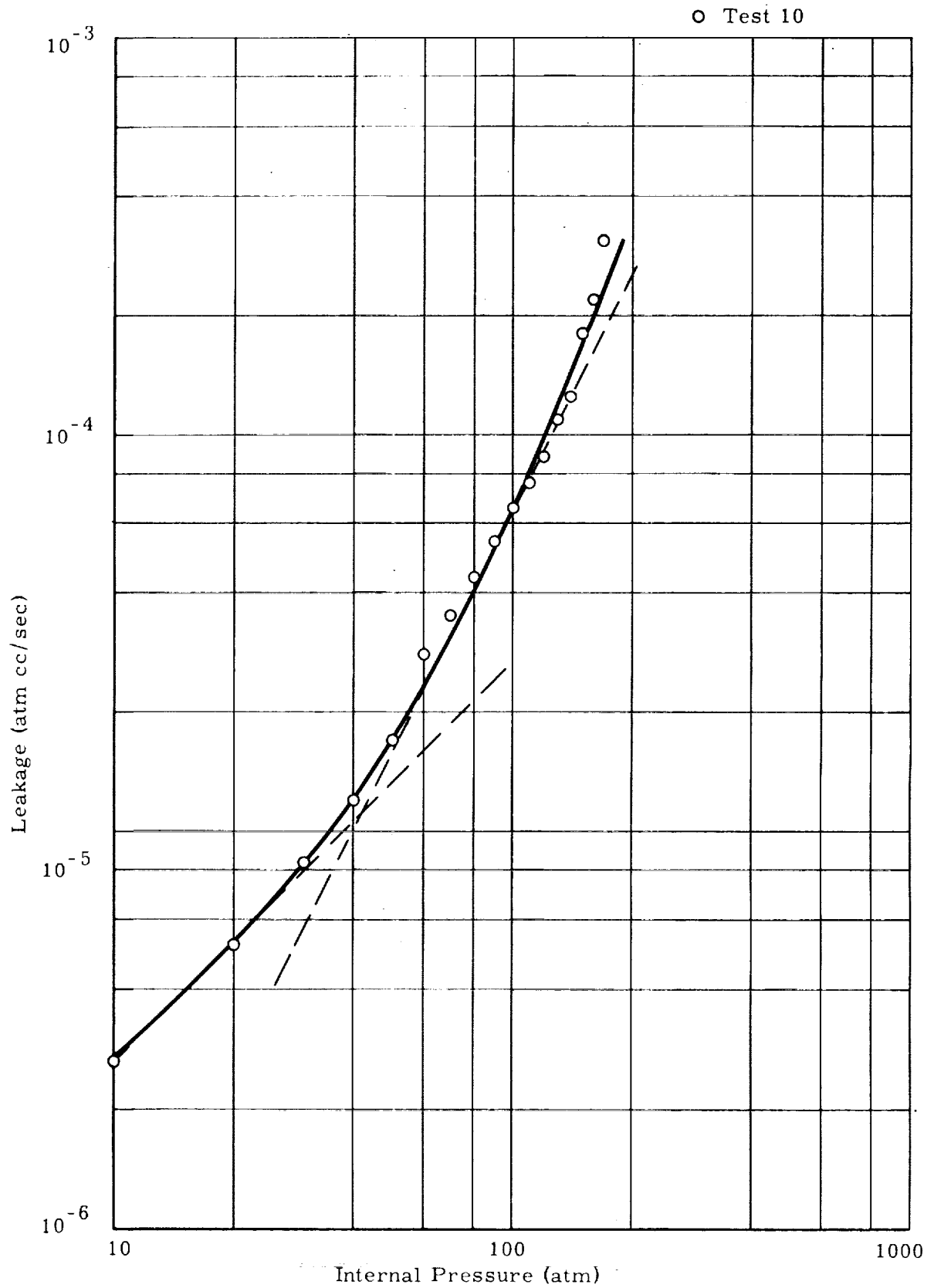
Figure 2.73. Leakage as a Function of Internal Pressure, Phase II of Experiment - Jones Optical KANIGEN aluminum.
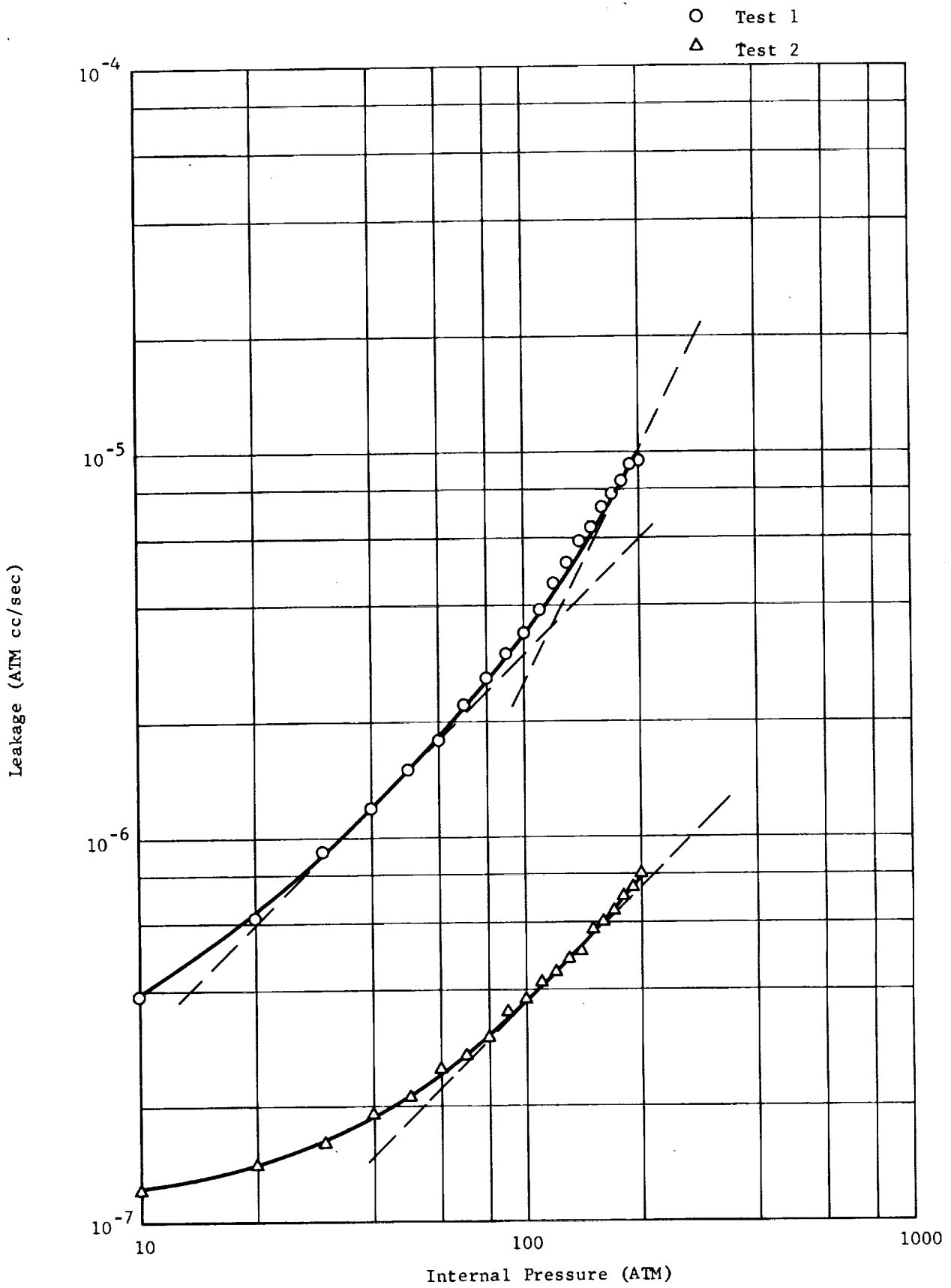
Figure 2. 74.   Leakage as a Function of Internal Pressure, Phase II
of Experiment - Stainless Steel-Silver Tests

2-83
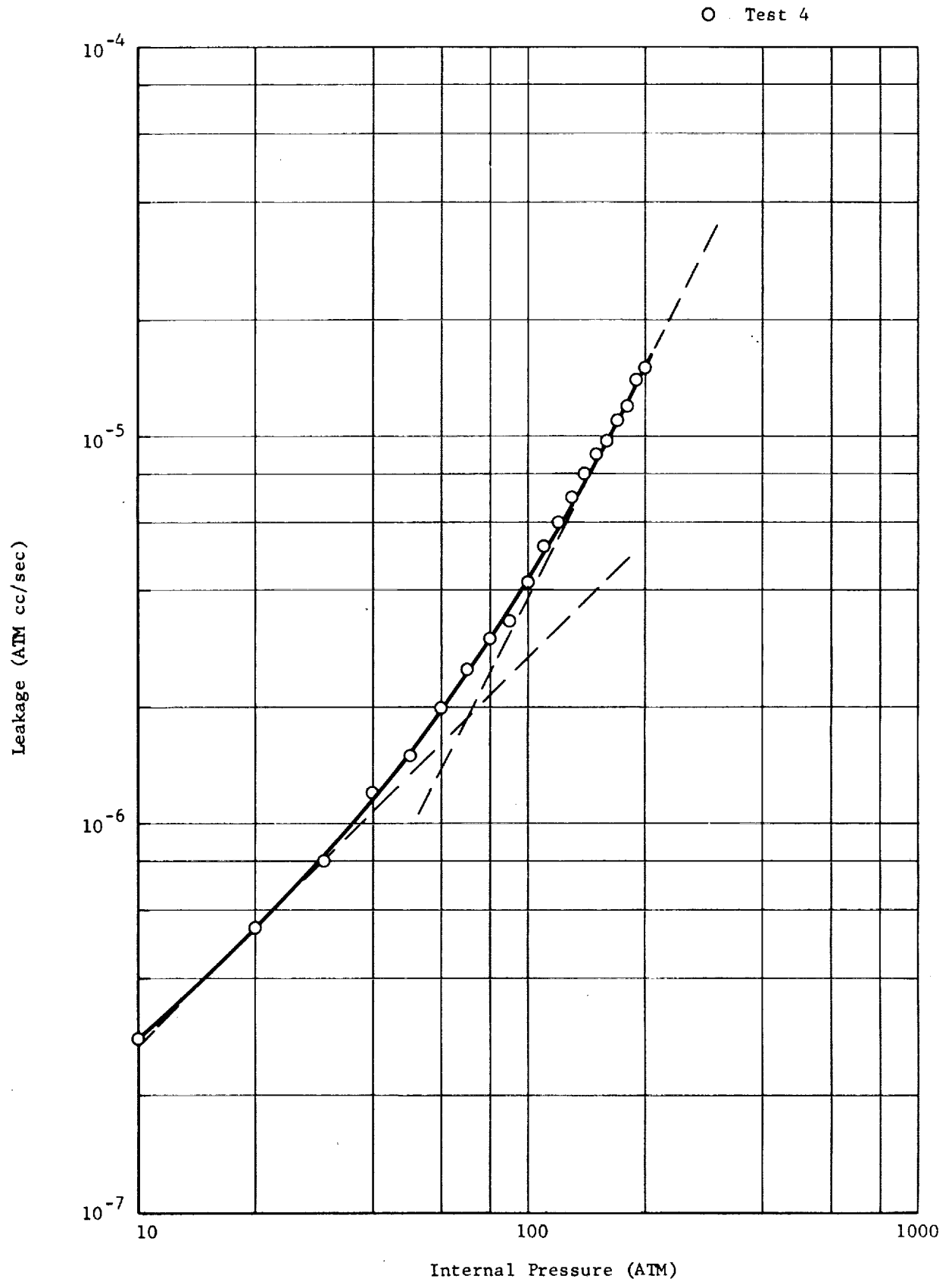
Figure 2.75.   Leakage as a Function of Internal Pressure, Phase II
of Experiment - Stainless Steel-Silver Tests
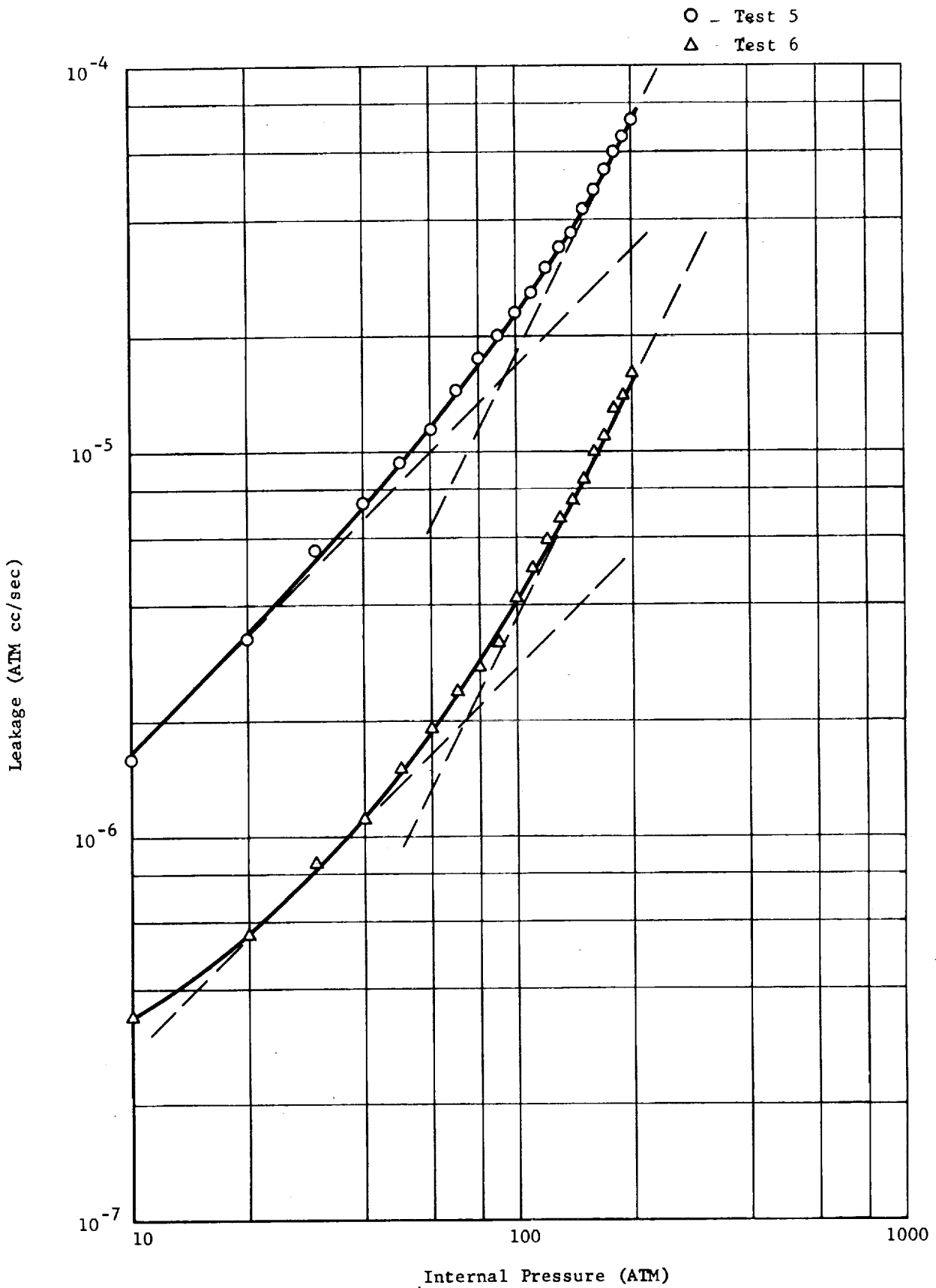
Figure 2. 76.   Leakage as a Function of Internal Pressure, Phase II
of Experiment - Stainless Steel-Silver Tests
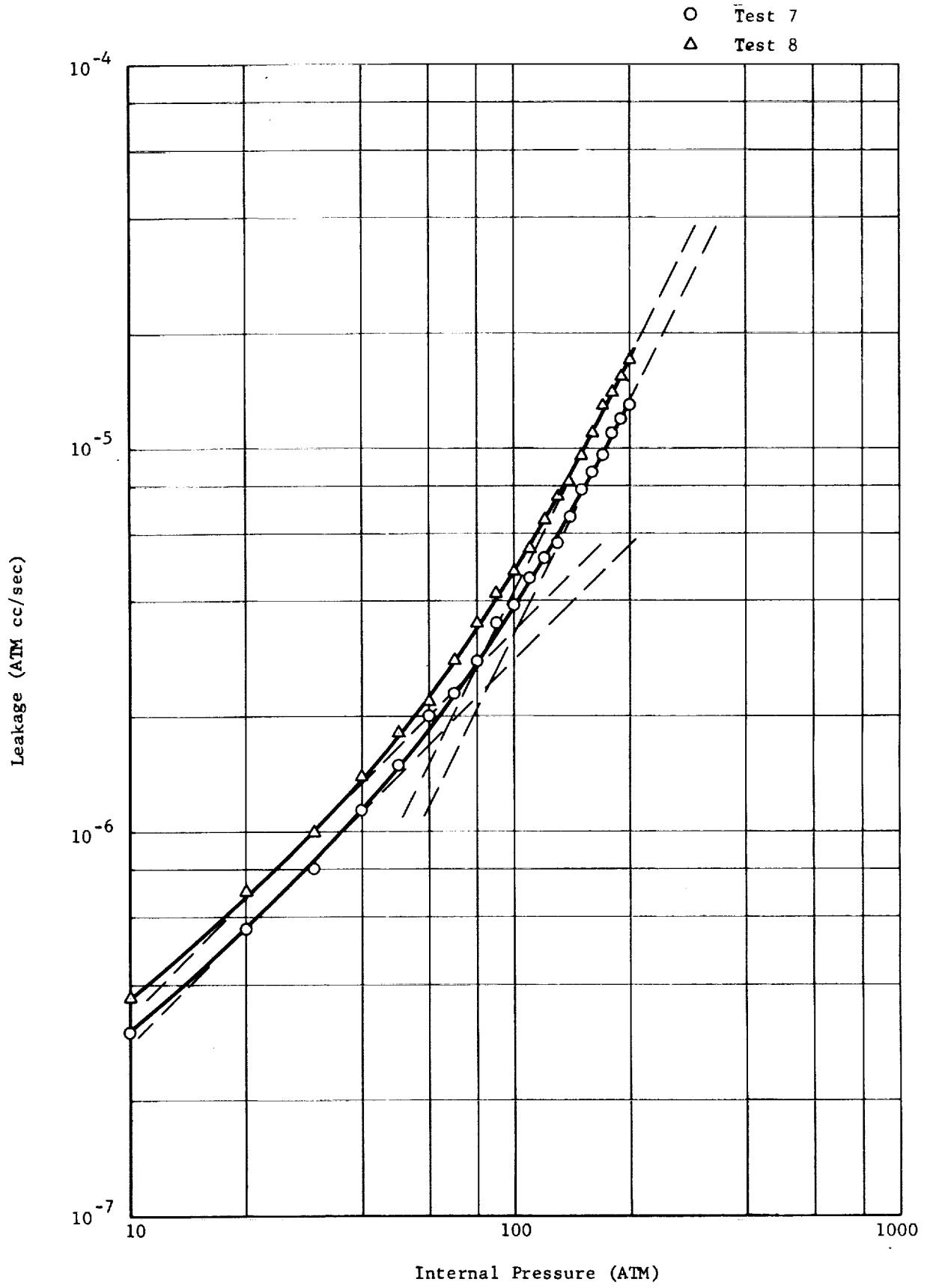
Figure 2.77. Leakage as a Function of Internal Pressure, Phase II
of Experiment - Stainless Steel-Silver Tests

2-86
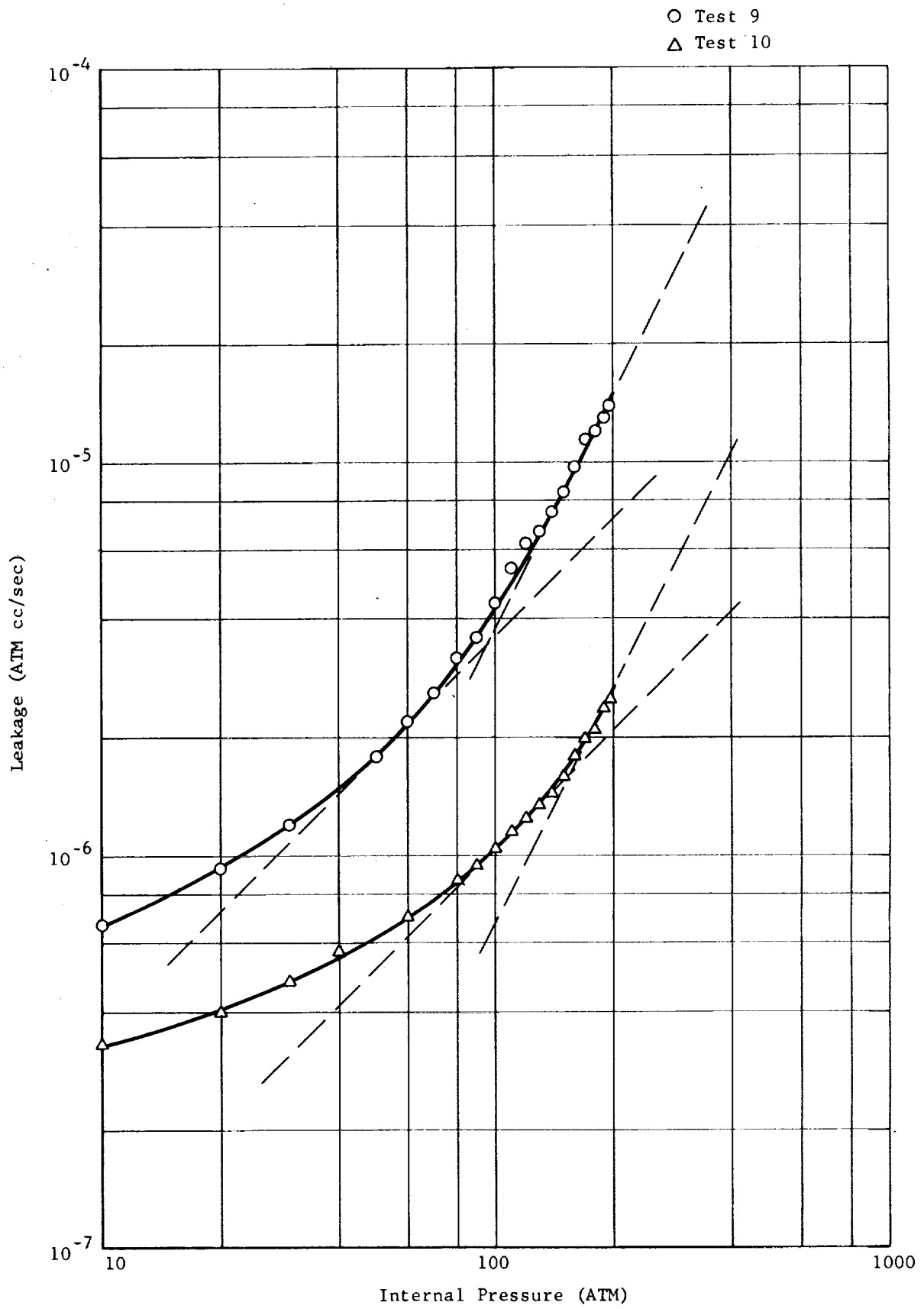
Figure 2.78. Leakage as a Function of Internal Pressure, Phase II
of Experiment - Stainless Steel-Silver Tests

2-87
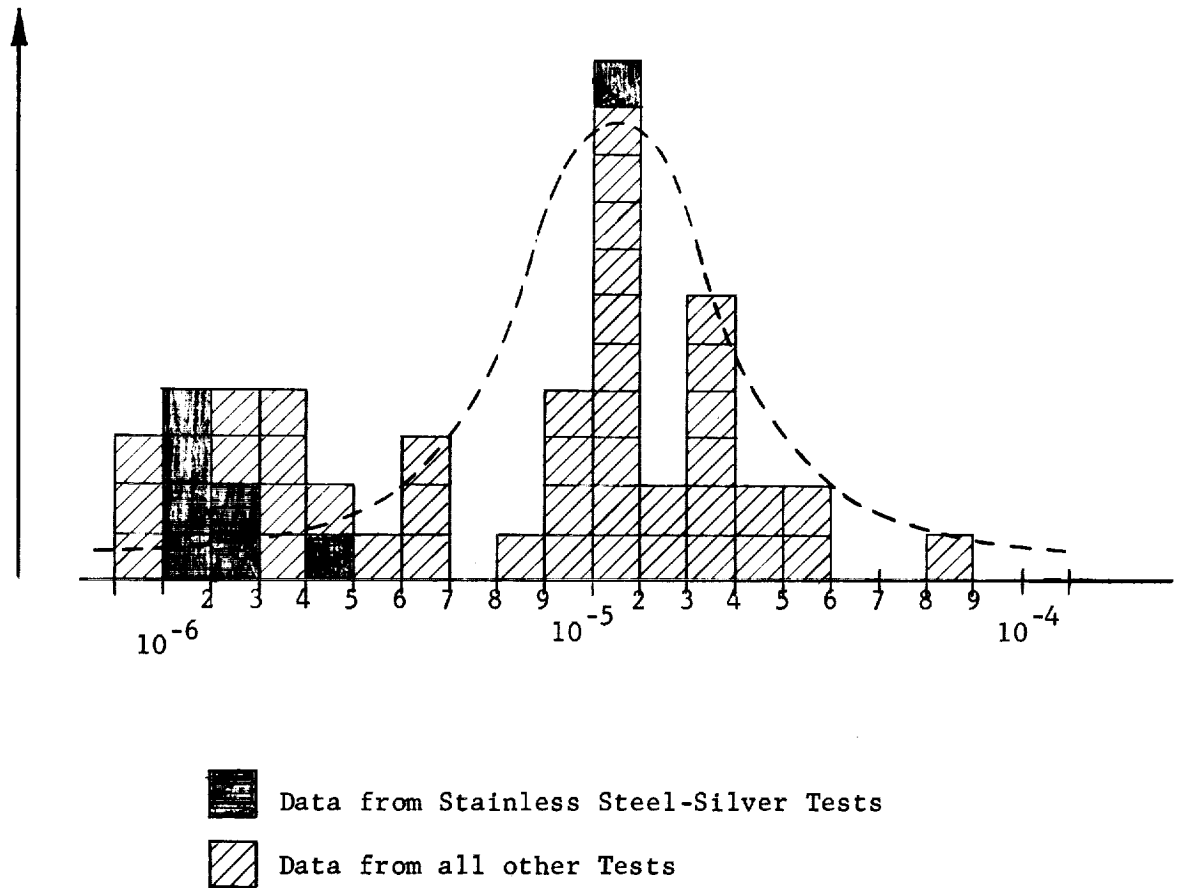
FIGURE 2.79. Histogram of Transition "Points" between Molecular
and Viscous Flow.
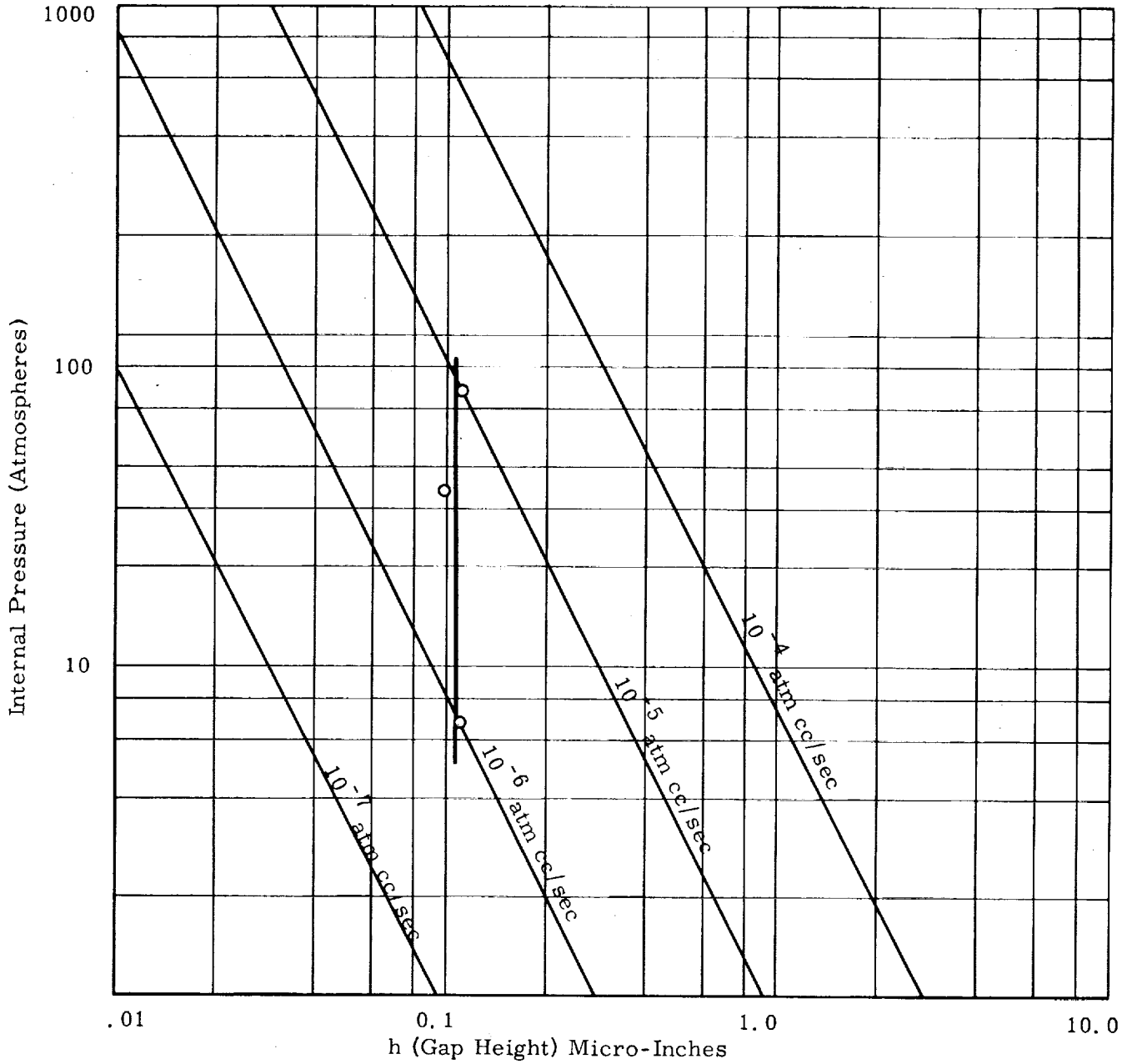
Figure 2.80. Leakage Rate for Helium at 20°C for an Annular
Passage Equal to Experimental Nominal Dimensions, with 0 psi
External Pressure. Comparison Experimental Superfinished
Surface Results.
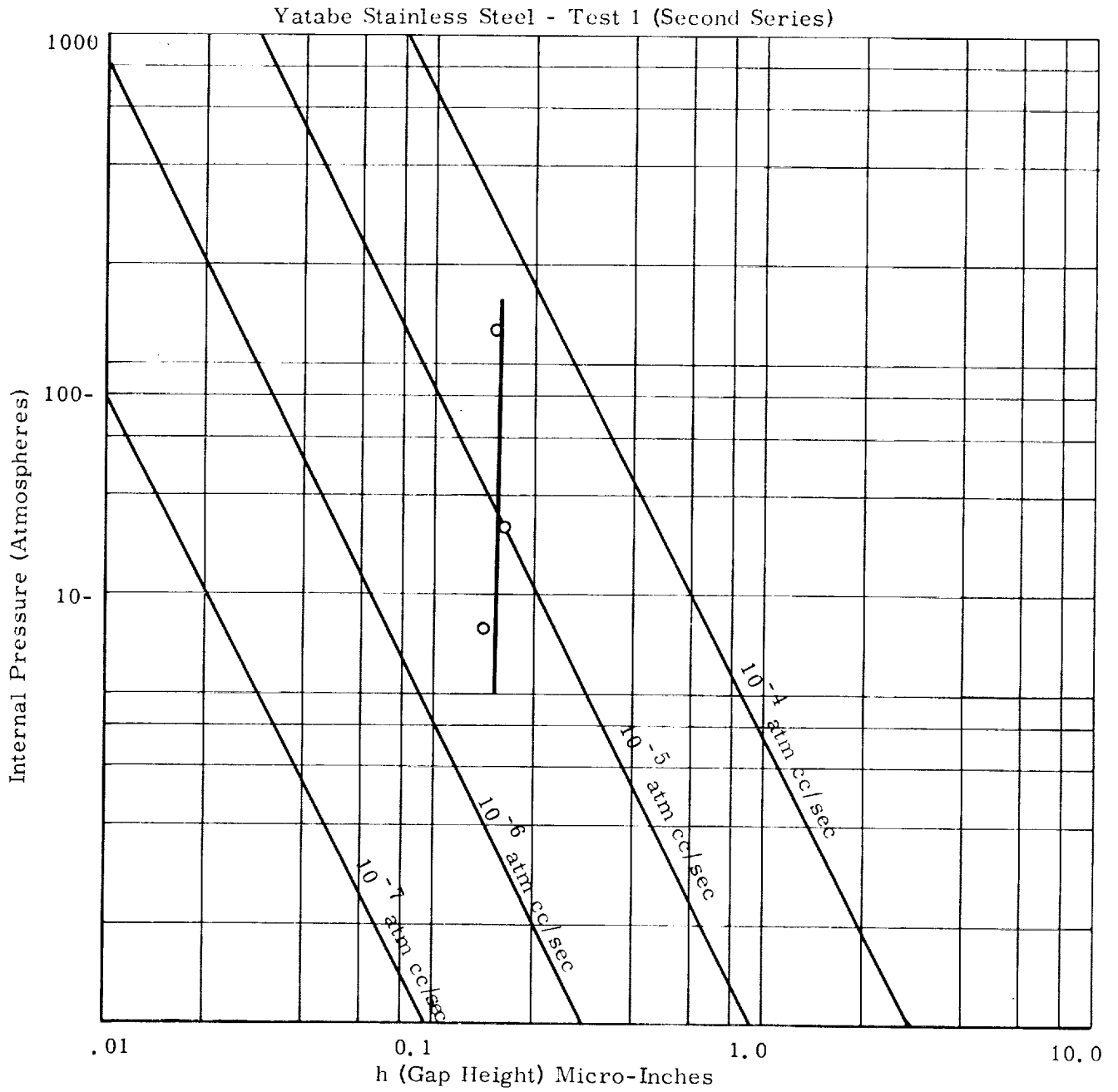
Figure 2.81. Leakage Rate for Helium at 20°C for an Annular Passage Equal to Experimental Nominal Dimensions, with 0 psi External Pressure. Comparison with Experimental Superfinished Surface Results.
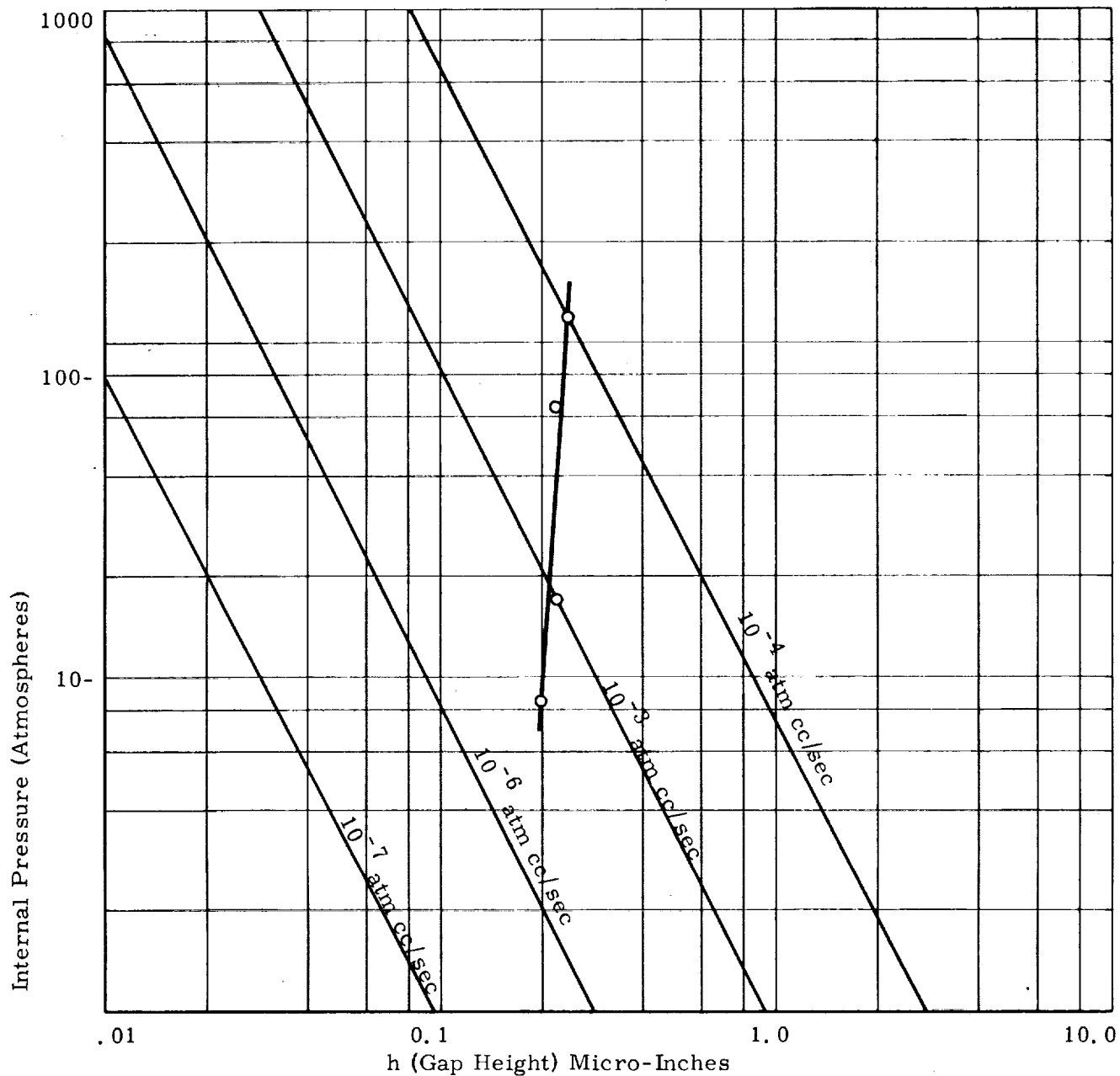
Figure 2.82. Leakage Rate for Helium at 20°C for an Annular Passage Equal to Experimental Nominal Dimensions, with 0 psi External Pressure. Comparison with Experimental Superfinished Surface Results.
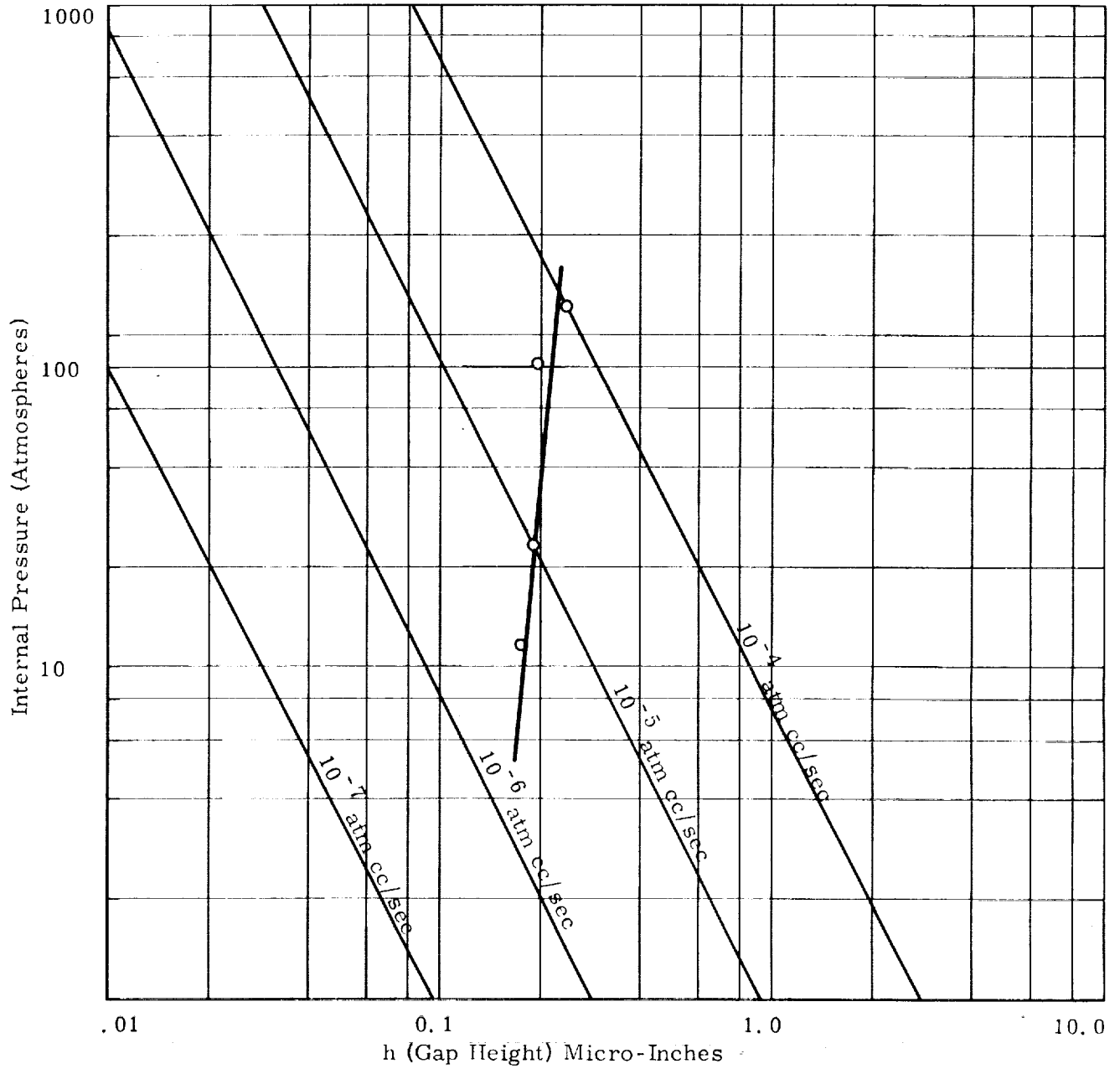
Figure 2.83. Leakage Rate for Helium at 20°C for an Annular Passage Equal to Experimental Nominal Dimensions, with 0 psi External Pressure. Comparison with Experimental Superfinished Surface Results.

Internal Pressure (Atmospheres)

1000

100

10

.01   0.1   1.0   10.0

h (Gap Height) Micro-Inches

10^{-7} atm cc/sec

10^{-6} atm cc/sec

10^{-5} atm cc/sec

10^{-4} atm cc/sec

Figure 2.84. Leakage Rate for Helium at $20^{\circ}C$ for an Annular
Passage Equal to Experimental Nominal Dimensions, with 0 psi
External Pressure. Comparison with Diamond Burnished Experi-
mental Superfinished Surface Results.

Jones Optical Stainless Steel - Test 13
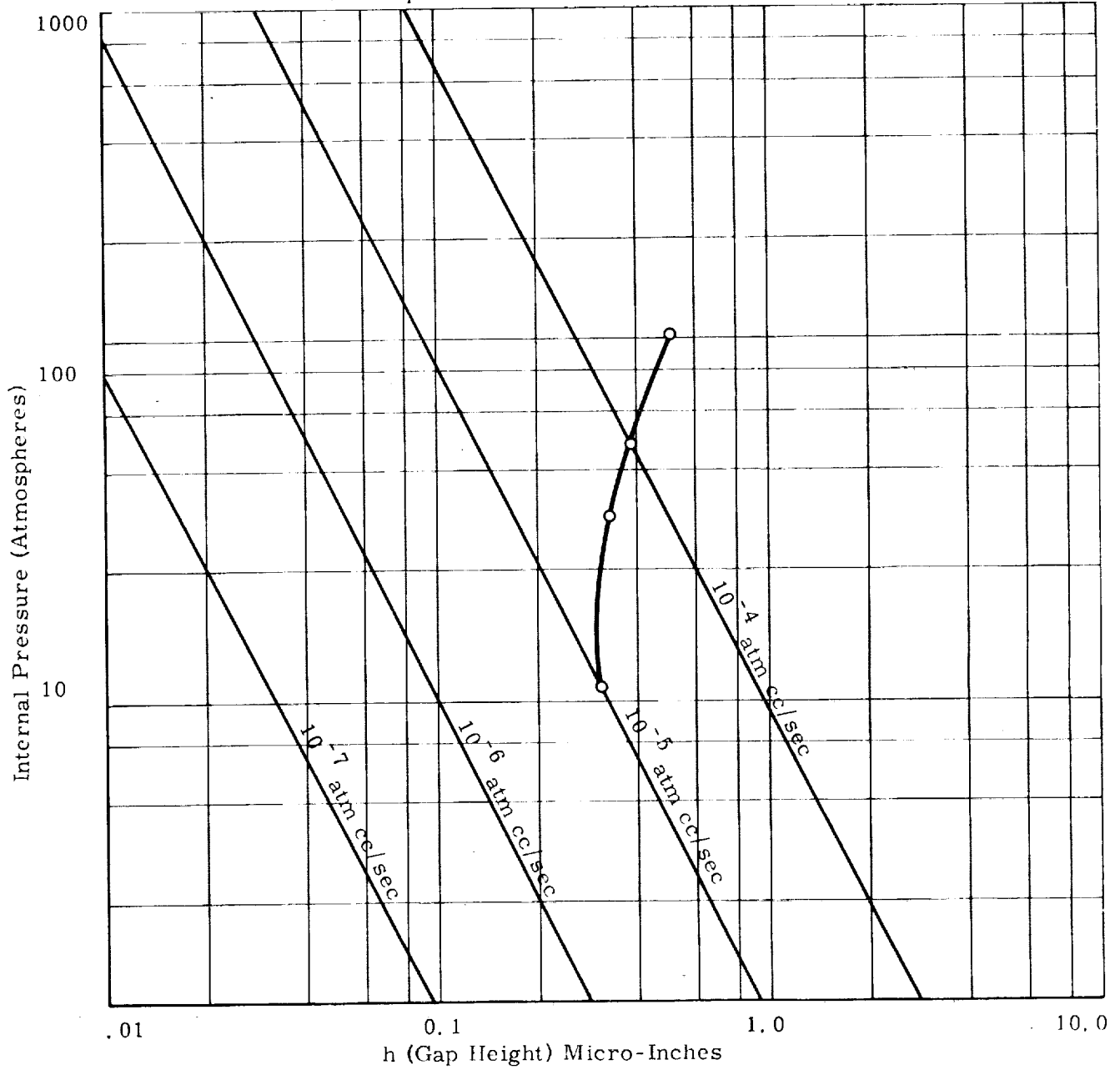
Figure 2.85. Leakage Rate for Helium at 20°C for an Annular
Passage Equal to Experimental Nominal Dimensions, with 0 psi
External Pressure. Comparison with Diamond Burnished Experi-
mental Superfinished Surface Results.

2-94

Jones Optical - Kanigen Plate - Test 6
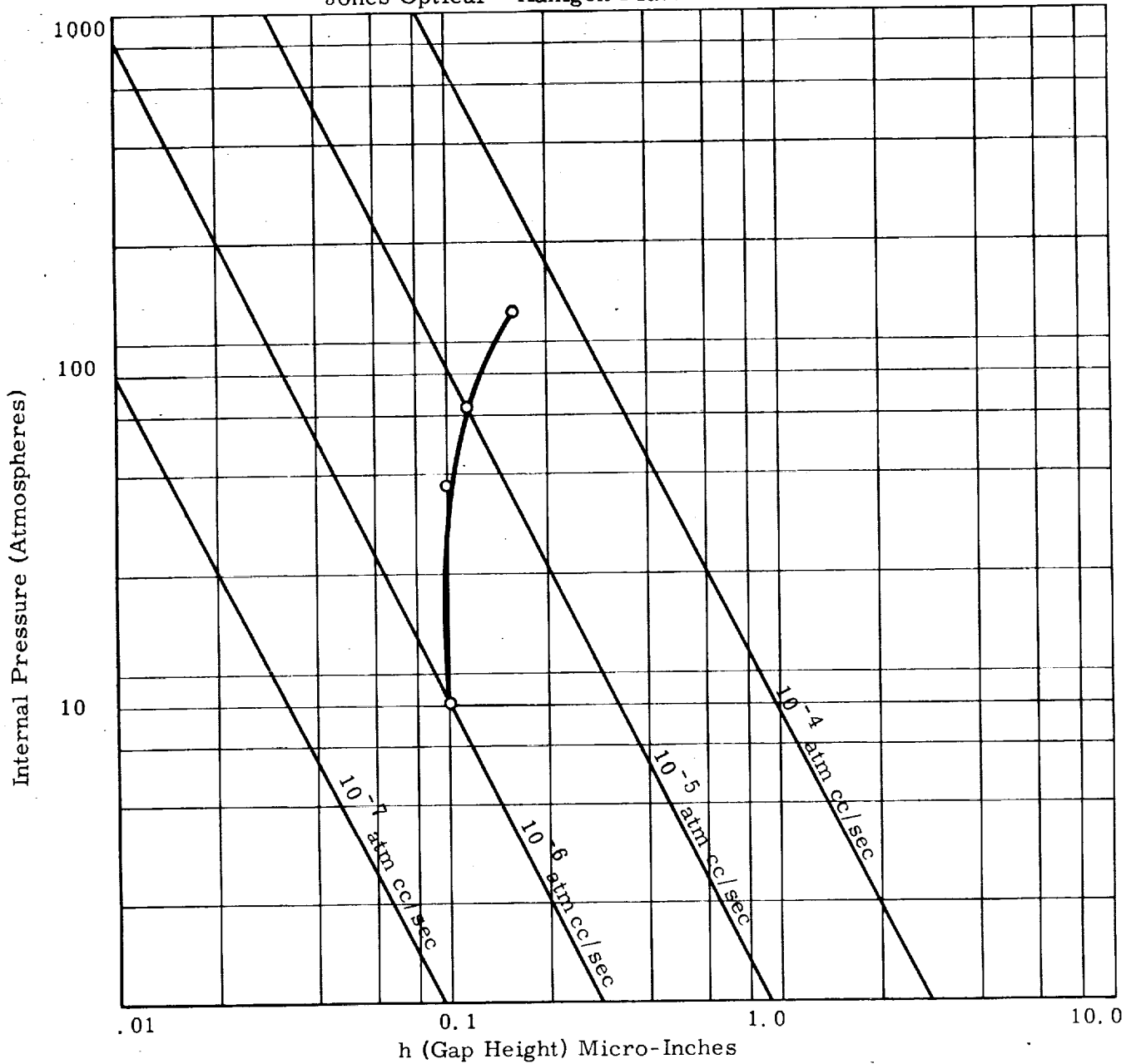
Figure 2.86. Leakage Rate for Helium at 20°C for an Annular Passage Equal to Experimental Nominal Dimensions, with 0 psi External Pressure. Comparison with Diamond Burnished Experimental Superfinished Surface Results.

UNION

A

B   C

D → M → E

n
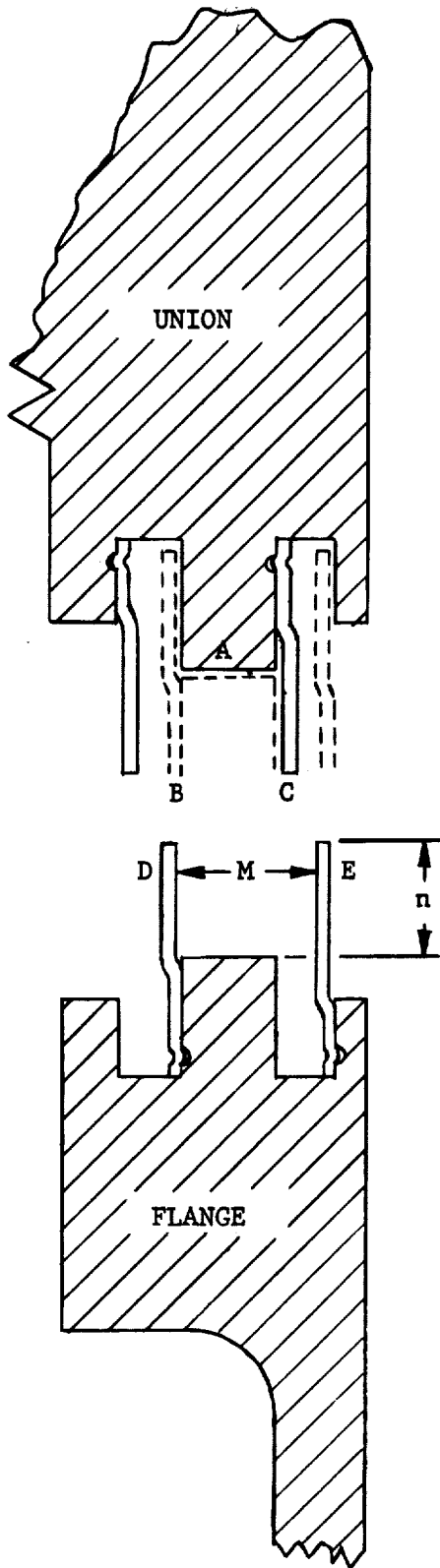
FLANGE

Surfaces A-
    superfinished mating surfaces.
    B,C,D,E - sheet metal split
    rings - snapped into recesses
    in factory.

Dimensions
    M, n adjusted to allow fit of
    flange and union and to insure
    protection of surfaces A.

Dotted lines
    show components in field
    assembled position.

FIGURE 2.87

A METHOD OF PROTECTING FINE FINISHED CONNECTOR COMPONENTS

3.0 Analysis of Leakage Probability

3.1 Problem Statement

In the design of most static fluid-seals, leakage is prevented (or held to very low levels such as 10^{-6} standard cubic centimeters per second) by causing two mating surfaces, of some initial roughness, to conform to each other. A force is needed to cause the surfaces to conform and, as a rough rule of thumb, if both surfaces are metal and the force is normal to the surfaces, the force needed is of the order of two to three times the compressive yield stress of the softer of the two materials multiplied by the nominal face area of the seal. Now, for any given application there is but little that can be done to change the seal perimeter, but the seal width is at the designer's discretion and can be reduced to reduce nominal seal area. One may draw the conclusion that reducing the seal width would reduce the force needed to make a leak-tight seal, and reduced force would permit a lighter weight connector to be designed.

In what has been stated so far there is no inherent limit to how narrow a seal could be made. The limit is found by considering a new factor, namely RELIABILITY. What is the chance that the seal will leak more than the permissible amount? There are imperfections or roughness of the original surfaces where perfect conformity does not occur. In a wider seal such imperfections can be tolerated since there is opportunity for redundancy of sealing. In a narrower seal the opportunity for redundancy of sealing is diminished. Thus, we find we are trading seal width and weight of the connector for reliability. It may well be suspected that an "optimum width" exists which would result in the minimum weight connector to just meet the reliability requirement. For the present it is not pertinent whether one should design to just meet the reliability requirement of whether factors not yet discussed would lead to a more conservative, albeit somewhat heavier, design. What is important is to gain an appreciation of the fact that reducing seal width does reduce reliability, and to also gain some quantitative understanding of the relationship so an intelligent balance of countervailing objectives can be obtained.

The importance of the work described can be appreciated by comparing the problem of designing a connector to a three-legged stool. For the connector design the "legs" are our three requirements of 1)light-weight, 2) leak-tight, and 3) reliable. It must be emphasized that there is currently no way of estimating the reliability, and thus no way of knowing the degree to which the design is conservative, or perhaps underdesigned.

While the discussion above is presumed to be for a metal-to-metal seal with loading normal to the surface, is is expected that with slight modification to allow for the rheological properties, non-metals could be included as well.

3.2 Approach to Solution

Since there are many connectors in a missile and the unreliability permissible must be kept reasonably low, the reliability of a single connector must be quite high - the chance that it would perform as intended

being perhaps 0.999. To determine reliability on an experimental basis could involve many tests and considerable expense, particularly if one wished to explore the effect of varying one or more design parameters. Also, if we assume that tests were thoughtfully planned and conducted, there may be little cause for questioning the results, but the results would probably be essentially worthless to a designer faced with a situation that was not included in the tests conducted, including of course reasonable interpolations and extrapolations of test results.

If one approaches the problem analytically and establishes a mathematical model of the interface, then the problem of exploring the effects of varying parameters may be considerably reduced. Also, once a general model has been developed and checked against experiments to a sufficient degree to establish confidence in its validity, it can be applied to new situations or even to providing some information not originally required but, nevertheless contained within the model.

The greatest part of the problem in the analytic approach is establishing a mathematical model which is simultaneously simple enough to be solvable and yet accurate enough to be meaningful. This is illustrated by noting that one may assume a very simple model of a seal, as was done in work previously reported in the final report for Phase I of this project (Ref. 1). It was soon appreciated, however, that while solution of this model was quite simple, the results were inaccurate and could not be extended to explore the effect of such important parameters as seal width. On the other extreme, a specific approach to solving a more accurate model was conceived. It is believed it could have handled very general problems and could have yielded accurate statistical results. Some rough estimates, however, indicated that the cost per solution, using a large digital computer, would exceed 10^{20}, (i.e., $100,000,000,000,000,000,000) thus leaving no doubt as to the impracticality of that approach.

Before leaving the general discussion of approach to the problem and discussing specific approaches, two more things should be noted. First, the only meaningful final result for the analysis of any given seal design is an estimate of the total sealing force required to make sufficiently high the probability that the seal will not leak more than is permissible when operated under the specified environment, or environmental cycle, for the required life. Second, it should be recognized that the problem can be subdivided into two independent problems by introducing, as an intermediate parameter, the gap distribution, or gap statistics. Specifically we can:

1. Estimate the gap statistics which will result, given a description of the original surfaces, time and environment, or environmental cycle, to which the sealing surfaces have been subjected. In the simplest case the environment may be a stated force applied normal to the surfaces.

2. For the estimated gap statistics and the fluid pressures specified, estimate the probability of leakage exceeding a stated value.

3.3 Gap Statistics

Before discussing work done on estimating gap statistics or work done on using gap statistics to estimate leakage probability, it is in order to discuss characteristics of gap statistics.

In general, the gap statistics result from the surface contours of the mated surfaces and in general can be represented by a three-dimensional or topographic map. Consider for the moment two surfaces which have been brought together to the point where the highest asperities have just made contact. The gap topography is simply the sum of the topographies of the two initial surfaces. Without any loss of generality, one can next assume an equivalent pair of surfaces, the first of which is perfectly flat and the second of which has all the necessary contours to produce the same gap topography. This substitution of an equivalent pair of surfaces is suggested to simplify the discussion, since one can then discuss a single surface. (Whether one can in fact manufacture the equivalent surface which combines the contours of the two actual surfaces is not important to its use in an analytic model).

In general, a surface may contain any or all of the components of topography which can be described as:

     1. Random function in the j direction
     2. Random function in the k direction
     3. Periodic functions in the j direction
     4. Periodic functions in the k direction
     5. Type 2 random functions in the m direction

In these descriptions j and k are assumed to be two orthogonal directions and may (but are not restricted to) correspond to directions respectively perpendicular and parallel to the direction of seal width. It is assumed, further, that for analytical purposes all seals may be assumed to be straight with length J and width K, even though in fact all seals must close upon themselves, and most are circular.

The j and k periodic functions noted would, in general, be dependent on the type of machining used and represent the tool marks. The j and k random components represent the balance of surface roughness not described by the periodic components or by Type 2 random functions. The Type 2 random functions are intended to represent an overlay of imperfections on a surface of given character and include primarily scratches. They are indicated as being in the m direction to denote that they are not necessarily oriented relative to j and k. It is difficult to conceive of a practical surface which does not have components 1 and 2 to some extent. The last three components are essentially, if not entirely, absent in some surfaces such as are produced by diamond burnishing, lapping, honing, electropolishing, vapor blasting and some forms of casting. Because of the relative magnitudes of the first two or random components, some forms of grinding produce surfaces which have primarily only one random component, and in a sense are the simplest surfaces to analyze.

3.4 Analysis of Seal Surfaces

The discussion that follows will start with consideration of the simplest surface, then add components and cover more complex surfaces.

3.4.1 Random in j, No Other Components, (No Variations in k Direction)

Such a surface is characterized by radial tool or grinding marks. It is not a surface one would normally encounter on a seal. It is of interest solely as the simplest case that could be analyzed, and with some qualifications, it can be produced for experimental verification. Rotary grinding of a disc, using a cup wheel, is the closest approach to generating this type surface. A single point fly-cutter used in place of the cup wheel would produce similar results.

If such a surface were mated with a much smoother surface, such as a diamond burnished surface, the topography of the resulting gaps between the surfaces would closely approach that under consideration. During Phase I of this contract an analysis of this case was completed and reported on. (See Ref. 1) This analysis resulted in a derived relationship between applied load and leak rate. It was checked initially using two radially ground surfaces. Agreement between test and analysis was poor and it was concluded that the grinding marks on the two surfaces were not in truth true radial and were not parallel on the two surfaces. A second test noted in the final report for Phase II (See Ref. 2) was made using one radial ground surface and one diamond burnished surface. Better agreement was obtained, but the analysis still indicated higher leakage than found by experiment. Having gone further into the more complex cases and having gained more experimental data, as explained in later sections of this report, we now appreciate that the discrepancies noted are probably explained by our having used too wide a seal and the assumption of no variations in the k direction is likely to be violated. As noted at the beginning of this section, 3.4.1, this case is not likely to be found on a seal, since it is conducive to leaking, and is primarily of interest as the simplest case one can consider.

3.4.2 Random in j and Random in k, No Other Components

The second least complex surface, and one that is of practical interest is one with random components only, but in both j and k directions.

For purposes of being able to describe and discuss a surface, consider the seal area to have superimposed on it a grid system with squares of a size consistent with the approximation that height can be considered to be uniform over the area of each square. Figure 1.1 shows such a grid where the seal is assumed to be 5 grid squares in width and some undefined length. Some squares are white, designating contact or zero gap. Other squares are cross-hatched, designating a finite non-zero gap, and possible leakage, though as indicated not all gaps result in actual leaks.

What we wish to know is the probability that a leak path will exist. The first analytic attempt followed the method used in Ref. 1. Let it be assumed that there is a probability P of a square being represented by a

non-zero gap. The probability that a flow path, as indicated on Figure 3.1 by the cross-hatched boxes (6,1), (6,2), ... (6,5), actually exists can be calculated and is P^5.
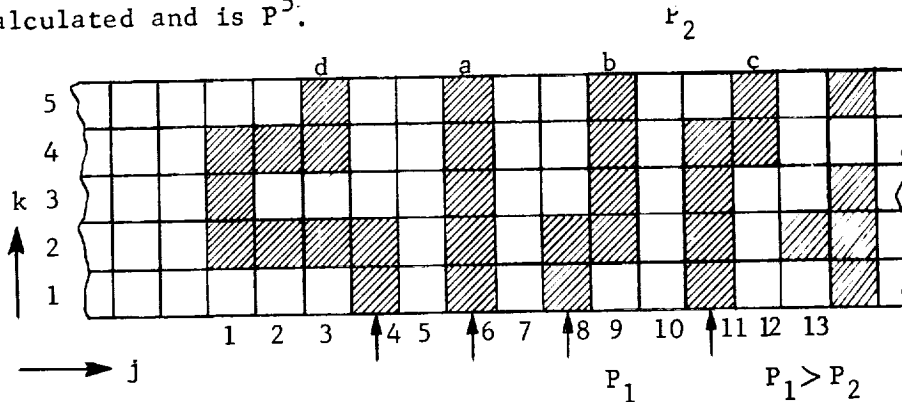
Figure 3.1. Grid Showing Possible Leak Paths

The chance for all other paths, a few of which are indicated, could presumably also be calculated. One quickly finds, however, that such an analysis would be worthless since, by the mere act of selecting a smaller grid size, one can show that the total probability of leakage can be made as small as one wishes! This is too convenient to fit physical reality and denotes a faulty analysis. A bit of thought brings to light the fact that the probability density function of the gap is not sufficent information to describe the surface. The autocorrelation function for the surfce is also needed since the probability of a given gap height (including zero) for any given square is only given by the probability density function for gap height when no specific information exists on the height of other squares. As soon as it is known or assumed that one or more squares have specific heights, the probability for all other squares is influenced. There is one exception, not to this statement, but to the consequence of it. The case where there is no variation of height in the k direction just discussed in section 3.4.1, may be viewed as a special case of this section with an autocorrelation of unity in the k direction. The autocorrelation function in the j direction then turns out to be immaterial to the leakage predicted. Hence, the fact that autocorrelation was not included in the analysis of Reference 1 does not effect its validity.

3.4.2.1 Distribution and Autocorrelation on a Random Surface

To assure that the assumptions involved in any analysis would be reasonable, Talysurf measurements were made on a surface and the recording was analyzed for answers to the following questions:

1. What size grid square should be used in order not to lose important surface detail?
2. What representation of surface height distribution would be reasonably accurate and could be used in an analysis?
3. How does the correlation of heights vary as a function of distance between points?

A relatively rough lapped surface with about 30 microinches CLA (center line average) roughness was selected for this purpose since it should be quite the same in both the j and k directions, perhaps simplifying analysis, and since the distortions of data due to the finite radius on the stylus of the measuring instrument would be negligible.

The distribution of surface heights was obtained by noting the height of 100 equally spaced points. To avoid errors of interpolating, profile chart readings were assigned to a band designated by the chart lines above and below the band and the value for the center of the band was assigned to all points in each band. The results are plotted on probability paper, which is arranged with a non-linear verticle scale such that the cumulative probability, or probability integral, for a Gaussian distribution plots a straight line. The result is shown in Figure 3.2 and shows that the distribution is quite distorted from a normal or Gaussian distribution. The abscissa is in original chart divisions, with each chart division equal to 10 microinches.

Other plots revealed that the left-hand portion of the curve was closely approximated by a simple exponential function. This information and other factors related to the physical problem led to the belief that an extreme value distribution (Ref. 3) may fit the experimental data.

The functions for the relative probability density, p, and the probability integral, P, for the extreme value distribution are generally given as,

$$p = \frac{1}{\beta} e^{-\frac{1}{\beta}(X-U) - e^{-\frac{1}{\beta}(X-U)}}$$

and

$$P = 1 - e^{-e^{-\frac{1}{\beta}(X-U)}}$$

where by rough analogy the parameter U is somewhat analogous to the mean value in a Gaussian distribution in locating the position of the distribution along the horizontal scale. The parameter β is somewhat analogous to the standard deviation in a Gaussian distribution in that it determines the horizontal scale magnification.

In its usual form the probability density functions has a short left-hand tail and a long right-hand tail. Since for surfaces one tends to think in terms of height above a datum plane, and since scratches are more prevalent than sharp, high ridges, the height density distribution is a mirror image of that given above. It is appropriate, therefore, that we make a coordinate transformation such that the equations become,

$$p = \frac{1}{\beta} e^{\left(\frac{h-h_o}{\beta}\right) - e^{\left(\frac{h-h_o}{\beta}\right)}}$$

and

$$P = 1 - e^{-e^{\left(\frac{h-h_o}{\beta}\right)}}$$
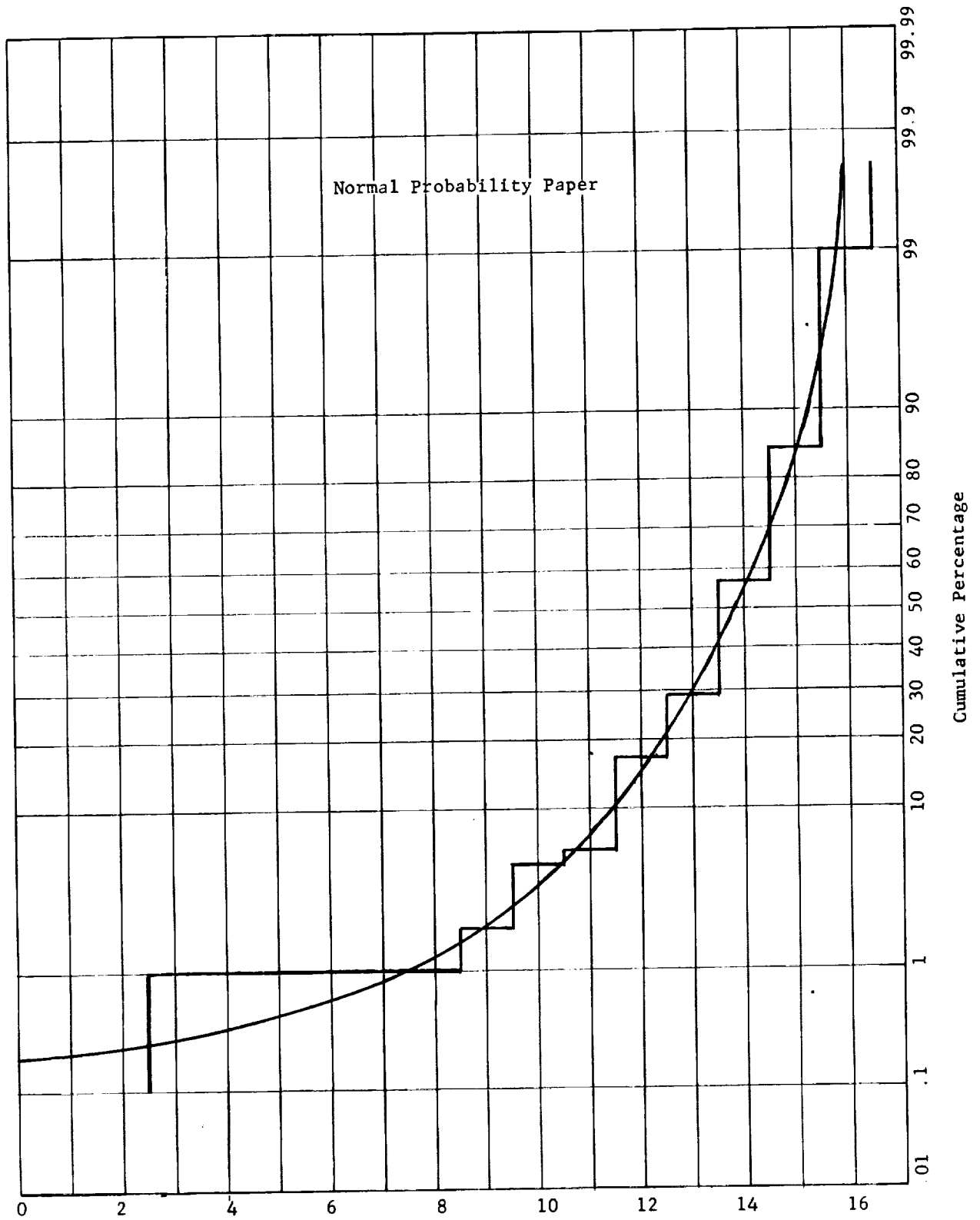
Figure 3.1. Profilometer Chart Reading

where   h = height above a datum plane

and   H = height above the datum plane that coincides with the
               greatest probability density.

Just as, for Normal or Gaussian distribution, paper can be designed
with a non-linear ordinate so probability integrals of Normal distributions
plot as straight lines, paper can be designed so extreme value distributions
plot as a straight line. Figure 3.3 shows the same date as Figure 3.2,
except plotted on extreme value paper. The "best fit" to the stair-step
data is indeed very well given by the straight line drawn.

Next, information is needed on the behavior of the autocorrelation
function for a random surface. It can be obtained from the same Talysurf
recording used to determine the probability integral function above. One
measures and tabulates a column of h_0 readings. To avoid biasing the
result these are taken at some arbitrary but convenient distance apart.
One also must measure and tabulate corresponding h_1 readings where each h_1
is measured a distance X_1 to the right of the corresponding h_0.

The autocorrelation of heights h_0 to heights h_1 can be written in
numerous ways, but one that is particularly convenient to use with a desk
calculator and which minimizes round off errors is:

$$\rho_{ol} = \frac{n \cdot \sum_1^n (h_0 \cdot h_1) - \sum_1^n h_0 \cdot \sum_1^n h_1}{\left\{ n \sum_1^n (h_0)^2 - \left[\sum_1^n h_0 \right]^2 \right\}^{\frac{1}{2}} \cdot \left\{ n \sum_1^n (h_1)^2 - \left[\sum_1^n h_1 \right]^2 \right\}^{\frac{1}{2}}}$$

If the sample size is sufficiently large, since h_0 and h_1 readings are
taken from the same surface, the two square root expressions in the
denominator will approach the same value and one could (with slight loss
of accuracy) calculate only one expression and drop taking its square root.
This should not be done until one has checked to determine the degree of
inaccuracy introduced.

The autocorrelation can be calculated for various distances x and
the values calculated can be plotted versus x to give the autocorrelation
function. This has been done for data obtained from the Talysurf of a
lapped surface (random components only) of 30 microinches CLA. It was
found that the autocorrelation function was given quite accurately by
$$\rho = e^{-680x}$$
where X is in inches. It is believed, but has not been checked, that for
any surface the autocorrelation function of the <u>random component only</u> of
surface roughness can be given by the form
$$\rho = e^{-bx}$$
where b is inversely proportional to the CLA surface roughness of the
random component. It is, of course, well known that if the raw data used
to calculate the autocorrelation function contain periodic functions as
well as random variations, the autocorrelation function will also exhibit
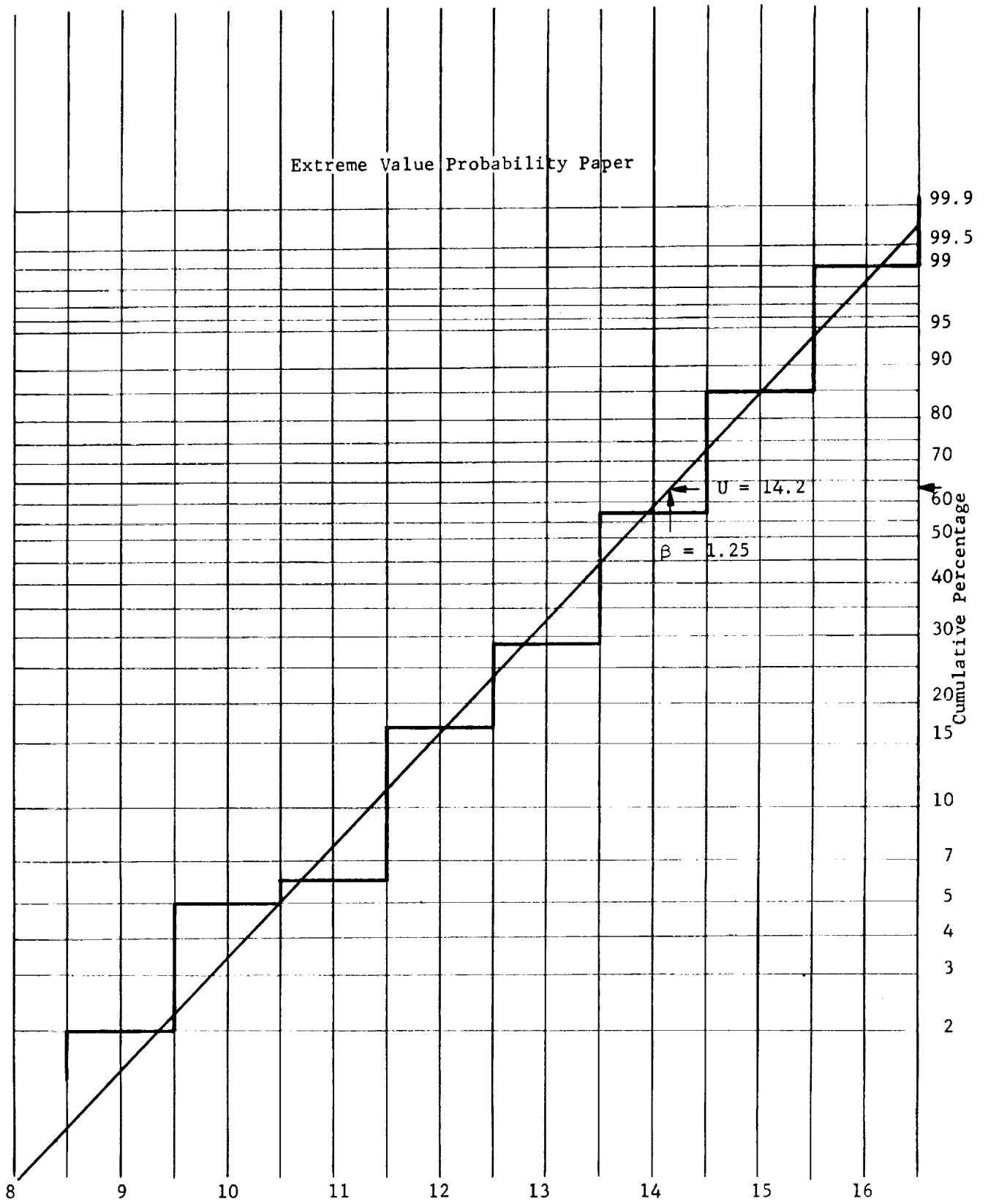
Figure 3.3.   Profilometer Chart Reading

periodic functions.

3.4.2.2   Selection of Grid Size

The problem of selecting a grid size will be taken up next. On the
one hand we do not wish to choose it too small, for that would greatly in-
crease the amount of calculations. On the other hand, we must not select
the size so large that important features of the surface are lost in the
mathematical model.

It appears reasonable that the grid size permissible should bear some
relationship to the random roughness of the surface we wish to represent.
The conclusion has been reached, based on two independent lines of reason-
ing that a grid size equal to 3 CLA roughness is as large as one can afford
to go. This is of course quite small physically, being of the order of
one ten-thousandth of an inch for a 30 microinch CLA surface. Thus,
practical seal surfaces will be hundreds to thousands of grid squares wide
and tens of thousands of grid squares long (i.e. in perimeter).

The first basis for selecting a grid 3·CLA is based on the auto-
correlation function. Across the width of a square of 0.0001 inch, which
is just slightly over 3·CLA, the autocorrelation function for the 30
microinch surface discussed in 1.4.2.1 would be

$$\rho = e^{- 680 \times 0.0001} = e^{-0.068} = 0.934$$

This indicates that the probability is reasonably high that the area
within a square is essentially all near the same height, in accord with
the assumption we make when we use a grid system and assign a height to
each square.

The second basis for concluding that 3·CLA is the approximate upper
limit for grid size is based on a determination of the average width of
"valleys". The average width of valleys through which leakage could
propogate was determined as follows. In a length of Talysurf trace the
number of times a given ordinate was crossed was noted, and from this
the average distance between valleys, S, was found for various heights.
The probability integral, P, was known and gave the fraction of time the
surface would be below each selected level. The products of P·S give
the average width of valleys present at each elevation. The tabulated
results are given in Figure 3.4, from which it may be seen that if the·
deeper valleys are not to be lost a grid size (for this particular case)
of not much over 100 microinches should be used. This is approximately
3·CLA reading. Quite obviously the tabulation of P·S in Figure 3.4 must
be a monotonically decreasing function. The fact that some values show
an increase is attributed to experimental error and the fact that a
larger sample of surface was not used.

3.4.2.3 Direct Calculation and Extrapolation

If one were confronted with calculating the probability of leakage
across a quite small grid, such as 2x2, a direct solution could be ob-
tained with no approximations introduced by the mathematics and with
relatively little work. For somewhat larger grids, such as 5x50, one
quickly realizes that simplifying approximations are needed. For grids

Height, μ"	Pounds	$S = \dfrac{.400,000}{\text{Pounds}}, \mu$"	P	P·S, μ"
170(highest peak)	0	∞	1.00	∞
160	17	23,500	0.998	23,450
150	87	4,600	0.85	3,910
140	206	1,940	0.57	1,100
130	229	1,750	0.30	520
120	175	2,290	0.14	320
110	146	2,750	0.070	190
100	95	4,200	0.039	160
90	59	6,800	0.021	140
80	32	12,500	0.013	160
70	16	25,000	0.0083	210
60	14	28,500	0.0061	170
50	10	40,000	0.0048	190
40	6	66,667	0.0037	250
30	6	66,667	0.0030	200
20	3	133,333	- - -	- -
10	2	200,000	- - -	- -
0	2	200,000	- - -	- -

Figure 3.4

Statistics Indicating Width of Valleys

of the size that would be needed to represent practical seals it appears
totally impractical to perform a direct calculation. Consequently it was
planned to estimate leakage probability by extrapolating techniques. An
algebraic and a numerical technique were investigated for determining
leakage probability. Both methods ran into the same impasse. They are,
nevertheless, reported briefly here for the sake of completeness in re-
porting work performed, and with the chance that someone may someday find
a way around the difficulty.

3.4.2.3.1 Algebraic Analysis

3.4.2.3.1.1. Acknowledgment

In discussions with Dr. T. P. Goodman concerning extension of the
simple analysis of the seal problem which he conducted on the first phase
of the contract he expressed the belief that an algebraic solution of more
complex situations may be possible. Thus, when the current phase of work
was authorized, Dr. Goodman was asked to work on the problem using his
approach. This he did until his untimely death in May 1964; that which
is reported here is, therefore, our understanding of his efforts. The
analysis is again limited, for the present, to consideration of random
variations in the j or k directions with correlation between points
included. This limitation is not theoretical in nature, and is imposed
purely for the purpose of simplifying an initial solution.

3.4.2.3.1.2 Problem Formulation

Assume that a grid system has been superimposed on a seal. Assume
that the gap between surfaces is continuously variable and that the gap
assigned to each square of the grid is the average gap over that square.
Assume further that gaps will follow a Normal probability density function.
This assumption is necessitated by the desire to use the considerable
volume of mathematics developed for Normal probability distribution and
that fact that no comparable theory has been developed for other distri-
butions. (Note that while in a previous section it was shown that heights
on a single surface differ appreciably from a Normal distribution, the
same data show that if two surfaces of the same roughness were used, the
distribution of gaps would be much more nearly normal.)

It may be shown that the probability of leakage across a very narrow
seal, only one grid square wide, is equal to the area under the tail of
the curve as shown in Figure 3.5

FIGURE 3.5

Probability of
Leakage
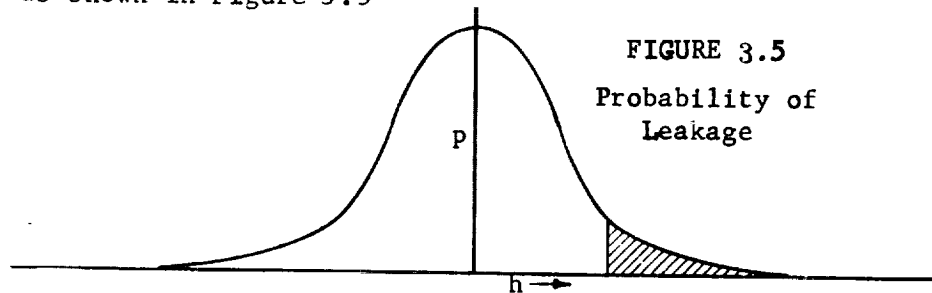
where the cross-hatched area represents that portion of the height proba-
bility density curve where the gap is still positive.

If our seal were wider and were two grid squares wide we would have to determine the probability that two squares in line with each other had a gap. This can be shown graphically as a two-dimensional "cloud" with h_1 and h_2 the heights in each square and the density of the cloud representing the probability of that combination occurring. This is shown in Figure 3.6.
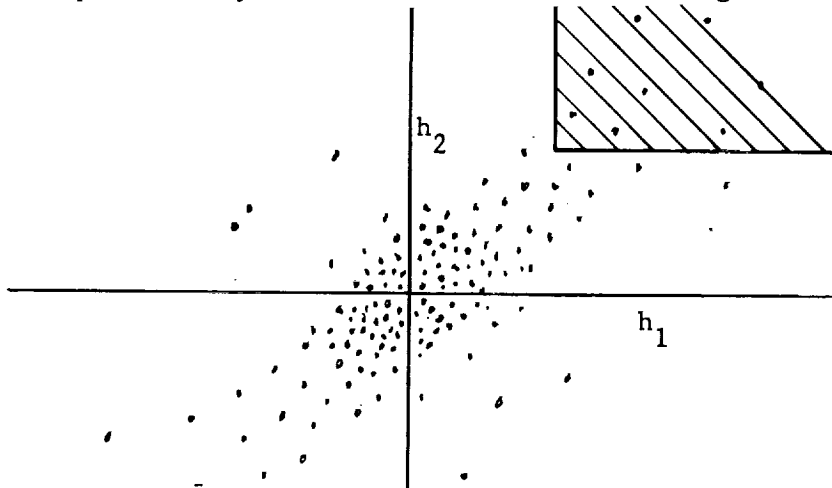
FIGURE 3.6

Probability of Combined Occurrences

The probability of both squares leaking is represented by the integral of cloud density within the cross-hatched box. Were there no correlation between h_1 and h_2, the pattern would be circular. Were there 100 percent correlation the cloud would "condense" to a line at 45° with density along the line in accord with the Normal distribution.

While one can visualize extending the above type of plot to the three-dimensional case with three variables, it is necessary to extend it to many more variables to be useful. What we need is a means of integrating the probability of residing in a given region of an n-dimensional volume of Normally distributed variables which are correlated.

This problem has been handled by M. G. Kendall (Ref. 4), who shows that the integral desired is given by a sum of terms involving Hermite polynomials. Specifically, given a general multivariant normal distribution with probability density dF given by

$$dF = \frac{1}{(2\pi)^{n/2} R^{1/2}} \exp\left[-\frac{1}{2R} \quad R_{jj}X_j^2 + 2 \quad R_{jk}X_jX_k \quad dX_1 \quad dX_n \right]$$

where

$$R = \begin{vmatrix} 1 & \rho_{12} \text{------} \rho_{1n} \\ \rho_{12} & 1 \text{-------} \rho_{2n} \\ \rho_{1n} & \rho_{2n} \text{------} 1 \end{vmatrix}$$

and R_{jk} is the minor of the jth row and k^{th} column, then it develops that for $n = 3$

$$d = \int_{h_1}^{\infty} \int_{h_2}^{\infty} \int_{h_3}^{\infty} dF = \frac{\rho_{12}^{j} \quad \rho_{23}^{k} \quad \rho_{13}^{1}}{j! \quad k! \quad 1!} \left[H_{j+k-1} (h_1) \ f(h_1) \ H_{j+1-1} (h_2) \bullet \right.$$

$$\left. f(h_2) \ H_{k+1-1} (h_3) \ f(h_3) \right]$$

In the above quotation H_r (X) is the rth Hermite polynomial and is given by (Ref. 5).

$$H_r(X) = X^r - \frac{r^2}{2 \cdot 1!} X^{r-2} + \frac{r^4}{2^2 \cdot 2!} X^{r-4} - \frac{r^6}{2^3 3!} X^{r-6} + \ldots$$

from which it is found that

H_0 = 1
H_1 = X
H_2 = $X^2 - 1$
H_3 = $X^3 - 3X$
H_4 = $X^4 - 6X^2 + 3$
etc.

Kendall also gives (Ref. 4) the technique for developing the terms to be summed for cases involving more than three variables, but, as may be appreciated, the complexity is appreciable.

It should be noted that the problem of evaluating the summation becomes impractical for hand calculations if the correlation coefficients are close to unity. A start has been made to work out a computer program for making the evaluations, but this work was dropped when more basic problems were discovered.

The more basic problems are two in number. First, for even a quite small grid there are many possible leak paths that must be considered, and we cannot treat them independently. As we compute the probability of a particular leak path, we must in some way keep track of the possibility of other leak paths. The second difficulty arises from the fact that ultimately we wish to know something about the magnitude of a leak, and not be restricted to differentiating only between "leak" and "no leak". Particularly in the light of complex paths existing, no means has been conceived for gaining this information.

3.4.2.3.2. Numerical Solution

The calculations of probabilities of heights existing which constitute a leak can be performed numerically rather than algebraically. The numerical approach has the advantage that it is not limited to assuming a Normal distribution. It has a disadvantage of involving much computation, but this can be readily programmed on a computer and involves essentially a modified form of matrix multiplication.

To work in digital form requires data to be quantized, and while it is desired to make the quanta as small as possible for accuracy's sake, it is recognized that the computations will grow out of reasonable proportions if too small a quantum is selected. Thus, we have quantized heights into 10 values, and we may now proceed to calculate the probability of a path, such as path "a" in Figure 3.1, being a leak path.

The probability of there being a height of h in the square in the first row may be represented as,

$$P_h = \begin{vmatrix} P_1 \\ P_2 \\ P_3 \\ \hline P_4 \\ \ \ \ \diagdown \\ \ \ \ \ \diagdown \\ \ \ \ \ \ \diagdown \\ P_{10} \end{vmatrix}$$

where P_1, P_2 etc. are determined by the probability density function for the surface. We can draw a line, as between P_3 and P_4, to denote that through h_3 a leak can occur, above h_3 a leak is stopped.

We can express the <u>conditional</u> probabilities of heights existing in the second row square, given the height in the first row, in matrix form as

	h_1	h_2	h_3 $\cdot$ $\cdot$ $\cdot$ $\cdot$ $\cdot$ $\cdot$		h_{10}
h_1	P_{11}	P_{12}	P_{13}		
h_2	P_{21}	P_{22}	P_{23}		
$\cdot$	P_{31}				
$\cdot$					
$\cdot$					
$\cdot$					
$\cdot$					
h_{10}					$P_{10,10}$

(h 1st row ⟶, h 2nd row ↓)

where the quantity P_{ji} represents the probability that the height in the second row square will be h_j, given that the height in the first row square is h_i.

The net probability of h_j in the second square is

$$P_j = P_i \cdot P_{j1} + P_2 \cdot P_{j2} + \cdots \cdot P_{10} \cdot P_{j10}$$

In general, probability of each height in the second row square is given by matrix multiplication and is,

$$
\begin{array}{ccc}
\underline{\text{Second Row}} & \underline{\text{First Row}} & \underline{\text{Conditional Probabilities}} \\
\downarrow & \downarrow & \downarrow \\
\begin{bmatrix} P_1 \\ P_2 \\ P_3 \\ P_4 \\ | \\ | \\ | \\ | \\ | \\ P_{10} \end{bmatrix} = \begin{bmatrix} P_1 \\ P_2 \\ P_3 \\ | \\ | \\ | \\ | \\ | \\ | \\ P_{10} \end{bmatrix} \cdot & \begin{bmatrix} P_{11} & P_{12} & - & - & - & - \\ P_{21} & P_{22} & - & - & - & - \\ P_{31} & - & - & - & - \\ | & & & & \\ | & & & & \\ | & & & & \\ | & & & & \\ | & & & & \\ P_{10,1} & & & & & P_{10,10} \end{bmatrix}
\end{array}
$$

If we again assume leakage exists for h only up to h_3, the probability that both the first and second rows leak can be found by a modified matrix multiplication wherein the summing of terms in matrix multiplying is divided into two sums. The first sum contains all terms for which neither i nor j >3. The second sum contains all other terms. In the matrix equation above, heavy lines have been added to indicate where this shift would take place. By the omission of all of the matrix for the first row below h_3 and all of the conditional matrix beyond the third row and third column, the sums appearing in the product will automatically be those pertinent to the probability of a leak across both rows.

To extend the system to the third row and beyond is practical only provided certain approximate methods are used, and this was described in more detail in the quarterly reports, particularly Quarterly Progress Report #7, June 10, 1964. In effect, what was done was to make approximations on the correlations of heights and neglect or simplify certain terms. However, the discussion will not be repeated in detail since this numerical method runs into the same impasse as described under the algebraic solution, section 3.4.2.3.1.

3.4.2.4 Random-Sample Method

It was noted in 3.4.2.3. that the use of a direct calculation of probability ran into insurmountable difficulties in not being able to keep account of the many possible leak paths. This suggests that a basically different approach may be needed and should be considered.

Just as there are many grains of sand on a beach, each of a different size, so there are many surface contour maps possible for a random surface of given roughness. To get the statistical distribution for size of the

grains of sand, we would take a sample rather than attempt to measure each and every grain. Likewise, we can analyze a sampling of surfaces, rather than all possible ones. The precaution must be observed that the sample used is representative of the total population of surfaces and is not biased. This requires a reasonably large number of samples, with each sample "picked" at random from among all possible samples.

Using the random sampling approach to estimating the probability of leakage, there are three important steps to the problem. They are:

1. Generation of random-sample surfaces,
2. Determination of leakage for each sample, and
3. Determination of force for each sample.

These steps are considered in the following sections.

3.4.2.4.1 Generation of Random-Sample Surfaces

It can be readily appreciated that we will be dealing with large grid systems. A typical case may be a seal of 32 microinches CLA roughness, 1/8 inch wide and 5 inches long. A grid size of 10^{-4} inches would be suitable, giving rise to a grid 1250 elements wide by 50,000 elements long. If each element can assume any of ten heights, then the total number of grid height combinations in the entire "family" would be $10^{62,500,000}$. Given such an astronomically large family that we wish to study, it is valid to draw statistical conclusions based on studying a sample drawn at random from the population. Or, to be more precise, we need means for "developing" a sample surface that would be representative of a random selection from the population. For the present we will assume a surface that is random and has no periodic functions in either direction of the grid. Further assume we have information on the cumulative probability distribution of heights of asperities and on the autocorrelation function.

One technique for surface development is as follows. Let us enter a plot of cumulative probability versus quantized gap height; at any specific probability between 0 and 1, inclusive, there will be a corresponding gap height. Further, if our entry point is selected purely at random, the gap height obtained will be representative of the gap height in the (1, 1) grid element of a randomly selected sample surface. Designations such as (1, 1) will be used to indicate the row and column numbers, respectively, of a grid square. If the process were repeated a number of times, the heights assigned to the (1, 1) elements should, statistically, have the same frequency of occurrence as would the heights of corresponding elements of randomly selected surfaces taken from the same family.

The assignment of height to the (2,1) element cannot be made in quite the same manner since the prior knowledge of the specific height assigned to element (1,1) biases the probability. Likewise after (1,1) and (2,1) have both been assigned, the probability of any height occurring at (3,1) is biased by knowledge of (1,1) and (2,1).

Several methods of assigning heights to elements (2,1), (3,1), etc. have been considered from two viewpoints. First is the reasonableness of the assigned heights, as compared to those found by measurements on comparable seal surfaces. Second is the suitability of the method for computer solution. Since the operation of assigning height must be repeated many times, computer time can be an important consideration in deciding between two methods that produce comparable results.

One method attempted is that of using linear extrapolation coupled with a distribution or "uncertainty" function. If we assign a number (h, i, j) to an element to designate that the height of the element in the ith row and j^{th} column is h, and a specific first element is given by (6, 1, 1), then since there is a reasonably high correlation function between (h, 1, 1) and (h, 2, 1) there will be a high probability of (h, 2, 1) being (6, 2, 1), a somewhat lower probability of (5, 2, 1) and (7, 2, 1), etc. Likewise had the first point been (2, 1, 1) there would be a high probability of (2,2,1), a somewhat lower probability of (1,2,1) and (3,2,1), and a very low probability of (10,2,1). In general, given a specific (h, 1, 1), to get (h, 2, 1) we can make a random selection from an appropriate distribution, and there will be needed as many distributions as there are values of h; i.e. ten if there are ten heights.

Having selected and assigned values (h,1,1) and (h,2,1) we can assign (h,3,1). Using a specific illustration to explain the process, assume we have assigned (4,1,1) and(5,2,1). Then by linear extrapolation we conclude (6,3,1) will be a very probable value, but certainly (5,3,1) and (7,3,1) have a significant probability also, and, in general, there will be a complete distribution curve. It is true that to utilize <u>all</u> data previously assigned we should select from one of 100 distribution curves, and later for element (h,4,1) should select from one of 1000 distributions. However, such is neither practical nor deemed necessary. Preliminary work indicates that the loss of accuracy will be unimportant if we select from the same ten distributions used to select (h,2,1). Reducing from the larger numbers of distribution curves that are theoretically needed is essentially equivalent to setting equal to zero the autocorrelations for more distant known points. Some data are neglected and some accuracy is lost in the interest of simplifying calculations.

Using the method just described we can obtain (h,3,1) and all other h's in the first row beyond the second column. Likewise the procedure can be used to assign heights to all elements (h,1,2), (h,1,3), etc., in the first column.

The assignment of the remaining heights in the grid requires a slight modification of the procedure in that we need do linear extrapolation over a surface, rather than along a line, to determine which of the ten distributions will be used for making the random selection. For example, given (6,1,1), (5,2,,1) and (5,1,2), these three points determine a plane which if extrapolated to element (2,2) gives a height at (2,2) of h =4. Using the distribution associated with h =4 we may make a random selection and assign a value to h in square (2,2).

Having assigned (h,2,2) we can in turn assign (h,3,2), (h,4,2), etc., and also (h,2,3,), (h,2,4,) etc., and by like procedure assign a height to all remaining grid elements. In this manner a surface will have been developed which we intend to be representative of a sample surface selected at random from the whole population. We must, of course, check the results obtained to determine whether in fact the method described will produce sample surfaces which are representative of ones selected at random from the type surface we wish to represent. However, before one can even apply the method, more needs to be said concerning the distribution functions to be used in conjunction with the extrapolated values, and it is in order to describe the computer program and print-outs since they will be referred to in future discussions.

The computer program developed is written in FORTRAN IV language and is currently being run on an IBM 7094 computer. It may be noted that for the work done to date smaller computers could be used. We have concluded, however, that because of the computer needs of the program as subsequent steps are developed it would be unwise to gear the program to a smaller computer since we would later have to rewrite it for the larger computer. Further, our original estimate seems to be borne out that the larger computer has enough of a speed advantage to make its net cost lower. Whether this conclusion is correct or not is a somewhat trivial concern, even during our present work when a smaller computer could be used, since in fact all computer runs to date have been completed within 0.01 hours. This is the minimum increment of time sold on the computer, and computer charges are, therefore, small.

It is important to one's understanding of the computer print-outs that the notations used be explained. By way of explaining the notation, Figure 3.7 shows a histogram of asperity heights representing an assumed typical "random surface", such as may be produced by lapping. Note that for this particular case 14 quanta of heights have been used and that they do not include equal size bands on a continuous scale. The notation T is used for 10, letters A,B,C. . . . are used for higher numbers.

Figure 3.8 shows the input information provided to the computer in the form of distribution functions. It is printed just prior to the computed information for the record's sake, along with other records not pertinent to the calculation but needed for administrative purposes. In Figure 3.8 the first line is the probability integral associated with a predicted value in the highest numbered band, which in this case is the fourteenth band. To avoid decimals an arbitrary multiplier of 10,000 has been used so the highest integral is 10,000 rather than 1.0000. To avoid computer problems, -1 is used instead of 0. The number in the first or left-hand column is the integral through the first band, that in the second column the integral through the second band, etc. The next thirteen rows printed are for the distributions associated with the remaining "expected values", in descending order. The last line is the integral associated with the distribution for the surface as a whole, which information is used only for the first selection made. While the example given uses 14 bands, the program is written to accept any number selected, up to 20 bands. In any event the bands are designated

RELATIVE PROBABILITY

D = .56%

C = 2.44%

B = 11.9%

A = 15.9%

T = 12.1%

9 = 14.1%

8 = 15.3%

7 = 13.5%

6 = 9%

5 = 4.1%

4 = .99%

3 = .106%

2 = .004%

1 = NIL

MICROINCHES ABOVE AN ARBITRARY
REFERENCE PLANE
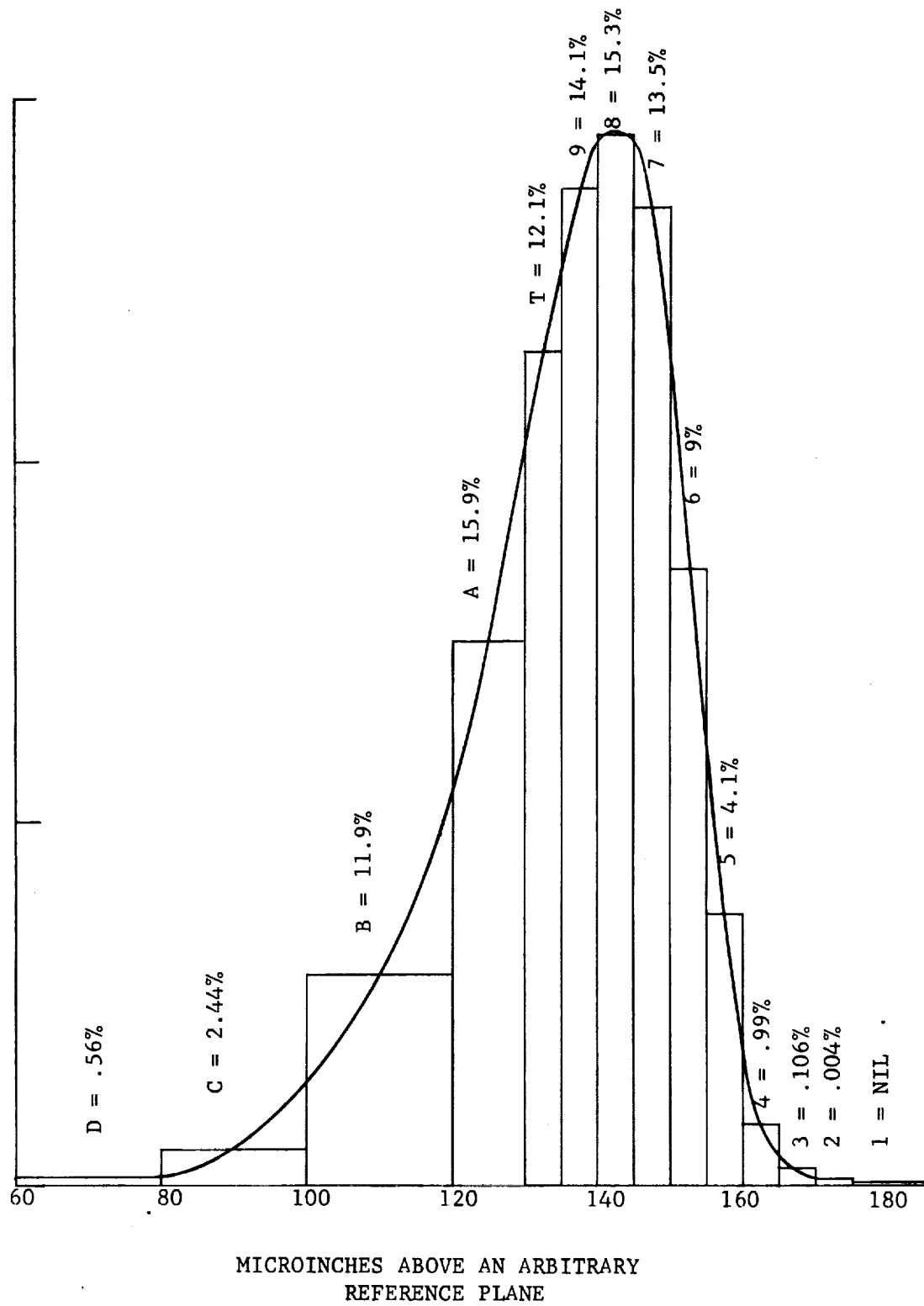
Figure 3.7. Distribution of Asperity Heights for a Lapped Surface

```
TIME  22.61          DATE 11/17/64
          $JOB
          $EXECUTE    IBJOB
IBJOB VERSION 3
$*        H.W.MOORE BLDG 37-523 SCHENECTADY 002-36395 94P 657
$IBJOB    NOSOURCE                          11/12/64
          START EXECUTION
TIME  22.63          DATE 11/17/64
```

-1	-1	1	1	3	7	20	50	130	520	3600	8150	10000	0
-1	-1	2	7	19	53	140	300	620	2000	6900	9690	10000	0
-1	2	17	50	140	310	680	1300	2200	4800	9200	9979	10000	0
2	26	80	210	500	1000	1850	3000	4500	7400	9850	9999	10000	0
5	59	170	400	880	1700	2850	4350	5900	8450	9954	10000	10000	10000
9	99	270	640	1310	2350	3720	5300	6800	9000	9980	10000	10000	10000
17	56	400	950	1820	3100	4620	6200	7650	9400	9993	10000	10000	10000
32	100	680	1440	2570	4050	5700	7250	8450	9670	9997	10000	10000	10000
63	190	1050	2080	3470	5100	6750	8050	9050	9830	9999	10000	10000	10000
110	310	1570	2850	4400	6100	7620	8750	9440	9930	10000	10000	10000	10000
190	500	2220	3720	5500	7130	8430	9250	9700	9970	10000	10000	10000	10000
300	770	3050	4800	6510	8000	9000	9600	9870	9990	10000	10000	10000	10000
520	1230	4050	5850	7510	8720	9450	9810	9945	9997	10000	10000	10000	10000
2300	4000	7700	8900	9580	9870	9968	9993	9999	10000	10000	10000	10000	10000
500	1000	2400	3900	5000	6000	6700	7500	8000	8850	9650	9900	10000	

```
50  100
```

Figure 3.8.   Input Parameters

3-21

as 1, 2, 3, ..., 8, 9, T, A, B, ... through as many numbers (or numbers and letters) as are required. In all cases, 1 represents the band of highest asperities, and higher numbers and letters represent lower asperities and valleys in the surface contour map.

Figure 3.9 shows the surface map developed by the computer for a 50 x 100 element sample surface and the input data shown in Figure 3.8. While the surface shown is 50 x 100 elements, it can be programmed to be any smaller size desired, with some saving in computer time. The rows and columns are numbered, and this information is printed also for convenience in reading data. Note that the first row is programmed to read all K's, which signifies a depth greater than will ever be called for and thus is equivalent to specifying a plenum chamber. The seal surface starts with row 2 and extends through row 51. The necessity for programming in a plenum chamber is associated with the maze threader, which is explained later.

While not shown in any figure, the computer also prints out information for plotting a histogram of each row and for the sum of all 50 rows, and also data needed to plot the cumulative distribution for the surface developed so it may be compared with that desired.

In this process for generating surfaces, we make use of random selection in entering the distributions assigned. An important consideration for computer programming is the technique used to make a random selection. We desire to avoid systems that may repeat in a manner which would cast any doubt on the complete independence of even the last sample developed from all preceding samples. Also, the system should be statistically free of any periodicity and of "runs" and should satisfy all other tests for randomness. The system we have chosen for making a selection is one developed by the General Electric Company's Apollo Support Department, for the National Aeronautics and Space Administration. It is described in Reference 6. The method satisfies our criteria and will not repeat until after approximately 10^{33} selections or more, depending on how it is used.

3.4.2.4.2 Distribution Functions

As noted in 3.4.2.4.1 the input data to the computer for a specific run consist of tabulated data on distribution functions. To develop distribution functions, comparison has been made between the extrapolated value of height along a straight line and the actual value for a number of positions along a Talysurf trace of a random (lapped) surface. The extrapolations made were based only on the heights of the two points immediately preceding the point of "unknown" height. Points were taken equally spaced at a spacing equivalent to 0.0001 inch, or about 3·CLA, since the center line average was about 30. The actual values, found for any specific expected value, plotted as very nearly Normal distributions. The mean values of the plots varied as a function of the height and differed from the expected value in the direction of the mode of the entire Talysurf trace, with a difference between expected value and mean value varying roughly linearly as the distance from the mode of the Talysurf trace. The standard deviations of the distributions for various

Figure 3.9. Surface Map for 50 x 100 Grid, Uncompressed

3-23

expected values plotted against expected value indicated that one could readily assume a constant standard deviation, or if he wished to use a straight line best-fit to the data a standard deviation which was varied slightly, being greater for valleys and lower for scale expected values.

In that the information used as an input to generating the surface is obtained on an entirely empirical basis, it is well to determine whether any criteria exist for selecting the input data, and also to investigate the sensitivity to small perturbations in the results produced. This has been done.

In general, it has been found that varying the standard deviation of the distribution functions in a systematic way produces little effect on the distribution plot of heights for the surfaces generated. (Probably the autocorrelation function is altered, but this has not been specifically checked.) Changing the mean values of the distribution in a systematic way has an appreciable effect on the mode and breadth of the distribution for the surface generated.

While it is convenient to use empirical data to get distribution functions that come reasonably close to generating surfaces such as we desire, we can make modifications to our input data to alter the results and by an iterative process produce surfaces that come progressively closer to having the characteristics we desire.

One of the characteristics of a random surface we should reproduce with reasonable fidelity is its non-directionality. Assume that one analyzed a single row (or column) of squares on a generated surface. This would be equivalent to obtaining a Talysurf trace on an actual surface. If in analyzing the row of data from left to right we found a probability P_i of going from h_a to h_b, and if the amount of data analyzed were sufficient to draw reasonably accurate statistical inferences, then we should also expect to find a probability P_i of going from h_b to h_a. This type statement would not hold at all for a surface with a saw-tooth profile, but such a surface is not a random one. Now, the net probability of finding a transition from h_a to h_b is equal to the product of the probability, P_a, of h_a existing times the conditional probability of next finding h_b given that the first point is at h_a. The probability of h_a existing is given by the distribution for the surface as a whole. The conditional probability of going from h_a to h_b is P_{a-b} and is indicated by the distribution function for h_a. It is one line of the input matrix data. For example, referring to Figure 3.8, and letting our two heights be h_a =8 and h_b =9, then we find:

$$P_8 \quad = 6700 - 6000 = 700$$

$$P_9 \quad = 7500 - 6700 = 800$$

$$P_{8-9} \quad = 6200 - 4620 = 1580$$

$$P_{9-8} \quad = 5300 - 3720 = 1580$$

Our statement above, expressed in equation form, implies that if the

data are fully self-consistent we should find

$$P_8 \cdot P_{8-9} = P_9 \cdot P_{9-8}$$

Without even performing the multiplication we can see that the criterion is only approximately satisfied. However, before becoming too concerned it should be recognized that the last line in Figure 3.8 is a distribution sought, and is not necessarily that which the computer produced. Using the input in Figure 3.8, the surface in Figure 3.9 was generated and it has an actual count of 436 eights and 525 nines out of 50,000 squares, which, including the 10^4 factor, gives

$$h_8 = \frac{436}{50,000} \times 10^4 = 872$$

$$h_9 = \frac{525}{50,000} \times 10^4 = 1050$$

The error is still present and it is apparent that some directional characteristic exists so the surface in Figure 3.9 is not true random. The error could be corrected by using a different input matrix. Figure 3.10 is a somewhat smaller and simpler input matrix which has much the same distribution, but satisfies the criterion for non-directionality. The numbers shown in Figure 3.10 are probability density, rather than probability integral x 10^4 as in Figure 3.8, to facilitate demonstrating adherence to the criterion; otherwise the format of Figure 3.10 is the same as Figure 3.8. Again, it should be noted that the distribution applicable to surfaces developed may not be precisely that desired and given by the last line in Figure 3.10. The reasons for this are covered later. Thus, some "error" may yet be introduced. No method of developing a theoretically perfect input matrix has yet been developed.

3.4.2.4.3 Analysis of Surfaces Generated

In the previous section, 3.4.2.4.2, a criterion for an appropriate computer input matrix was discussed, and even though no theoretically perfect input matrix has yet been developed, one may recognize that through a trial and error and adjusting process, the degree of perfection achieved could be increased to whatever degree one desired. However, the criterion discussed is only one of many that must be satisfied, or at least approximately satisfied. It is appropriate, therefore, that we turn attention to other criteria for suitability of the surface generated.

It has been noted that if the input matrix used to generate a surface is based on empirical data obtained from a random surface, then the distribution function for each extrapolated height will be Normal and the distribution function for the overall surface will be an extreme value function. It has been found that using this input matrix and the extrapolation routine discussed in 3.4.2.4.1, the surface generated has a distribution function that is very nearly extreme value,

	1	2	3	4	5	6	7	8	9	10
10	0	0	0	0	0	0	0	0	.09	.91
9	0	0	0	0	0	0	.03	.09	.87	.01
8	0	0	0	0	0	.02	.10	.85	.03	0
7	0	0	0	0	.02	.14	.73	.10	.01	0
6	0	0	0	.05	.15	.56	.21	.03	0	0
5	0	0	.02	.15	.47	.30	.06	0	0	0
4	0	.02	.14	.39	.27	.18	0	0	0	0
3	.02	.17	.37	.35	.09	0	0	0	0	0
2	.19	.37	.34	.10	0	0	0	0	0	0
1	.77	.19	.04	0	0	0	0	0	0	0
Surface	.01	.01	.02	.05	.09	.18	.27	.27	.09	.01

Figure 3.10

Probability Density

but with a somewhat narrower distribution than expected. Altering the standard deviation of the distributions in the matrix (in a systematic manner) produced little effect on the distribution of the surface generated, although it probably changed the autocorrelation function. The latter point was not specifically checked. Alteration, in a systematic manner, of the mean value of the distributions in the input matrix was able to produce a significant change in the width of the distribution for the surface generated, in the location of the mode, and to a lesser extent to the shape of the distribution. It has therefore been concluded that the criteria of the shape of the distribution and the location of the mode could be satisfied to any degree by a trial and error adjustment of the input matrix.

Another criterion for suitability of surfaces generated, and hence of the method of generating them, is the absence of patterns of any sort. This matter is best left for discussion until two other aspects of the surface generation program are discussed. These are compressed surface maps and the maze threader.

3.4.2.4.4. Compressed Surface Maps

Assume that a surface with random roughness is brought toward a perfectly smooth surface and that at some point the gaps at all points are represented by a plot such as is illustrated in Figure 3.9. As the surfaces continue toward each other and eventually make contact, the gaps, measured in numbers of bands, will be equal to one less than the numbers shown. That is, all 1's in Figure 3.9 would be in contact and have 0 bands gap, all 6's would have five bands of gap, etc. If we pressed harder till the next band also touched, and if we made the same assumptions that are used in the Abbott's bearing analysis, all original numbers would be lowered by two. Zero and negative numbers would represent contact. Figure 3.11 is obtained by depressing the surface a total of ten bands. To emphasize the contact areas a blank is left in the print-out wherever there would be a zero or negative number. The question arises as to whether or not a flow path still exists. If it does we must be interested, as a next step in the total analysis, in determining the flow resistance. If, however, for a particular surface and state of compression there is no flow path, then this next and rather sizable computation (in terms of estimated computer time) can be bypassed, for we already know the resistance is infinite. The message "flow path" or "no path" appears in the lower left corner of each compressed surface gap map to let us know whether or not flow resistance need be computed. This information is provided by the maze threader, which is explained next.

3.4.2.4.5. Maze Threader

The purpose of a maze threader and its potential value in reducing the number of flow impedance computations has been noted. The maze threader is also extremely useful in making visible such patterns as may exist in a generated surface map. A brief description of the operation of the maze threader is appropriate.

It has already been noted that the first row of K's represents a plenum chamber, which can never be squeezed off. The blank columns immediately to the left (and to the right) of the grid developed not only facilitate reading the map, they represent a "dam" or area in contact.

Starting in the first row first column, the computer determines whether there is a number greater than 0 in the grid element to its left (and because of the columns of zero's there never will be). It next determines if there is a number below it greater than 0, and there may or may not be. If there is a number greater than 0 the path is carried to that number and the search for a number greater than zero starts over. Each search around an element starts to the left, and proceeds in sequence to below, to the right and to above the element. When a number greater than zero is found the search around that element ends and the path moves on to the first-found new element. The sequence is repeated until finally either 1) a number is found in the last row of the surface, or 2) the path terminates in the last or right-hand K in the first row. In the first case there is <u>at least one</u> flow path, and there may be more. In the second case there is complete blockage and no flow.

3.4.2.4.6 Patterns in Surfaces Generated

In Figure 3.11 the compressed map print-out carries the notation in the lower left corner "no path". A stair-step line has been drawn indicating a line of continuous contact which blocks the leak. The fact that this line so consistently drops as one moves left causes one to suspect that there is a higher autocorrelation function on a diagonal with a positive slope than in other directions. With suspicion aroused, one can readily see that there is a diagonal pattern to the surface, and this is undesirable.

Referring to Figure 3.12 it will be seen that of all "known" information on surface heights, shown cross-hatched, to assign a height to square d we make use only of the heights of squares a, b, and c and, more specifically, do so using a linear extrapolation of a surface to get an extrapolated value for d, which we then use to determine which distribution a random selection shall be made from. In equation form the height of d in terms of the height of a, b, and c is

$$d = a + b + c$$

The existence of the diagonal pattern noted indicates that too much weight is being given to a relative to b and c. A general form for the extrapolation equation given above is

$$d = K_a \cdot a + K_b \cdot b + K_c \cdot c$$

where in the specific form given above

$$K_a = -1$$
$$K_b = +1$$
$$K_c = +1$$
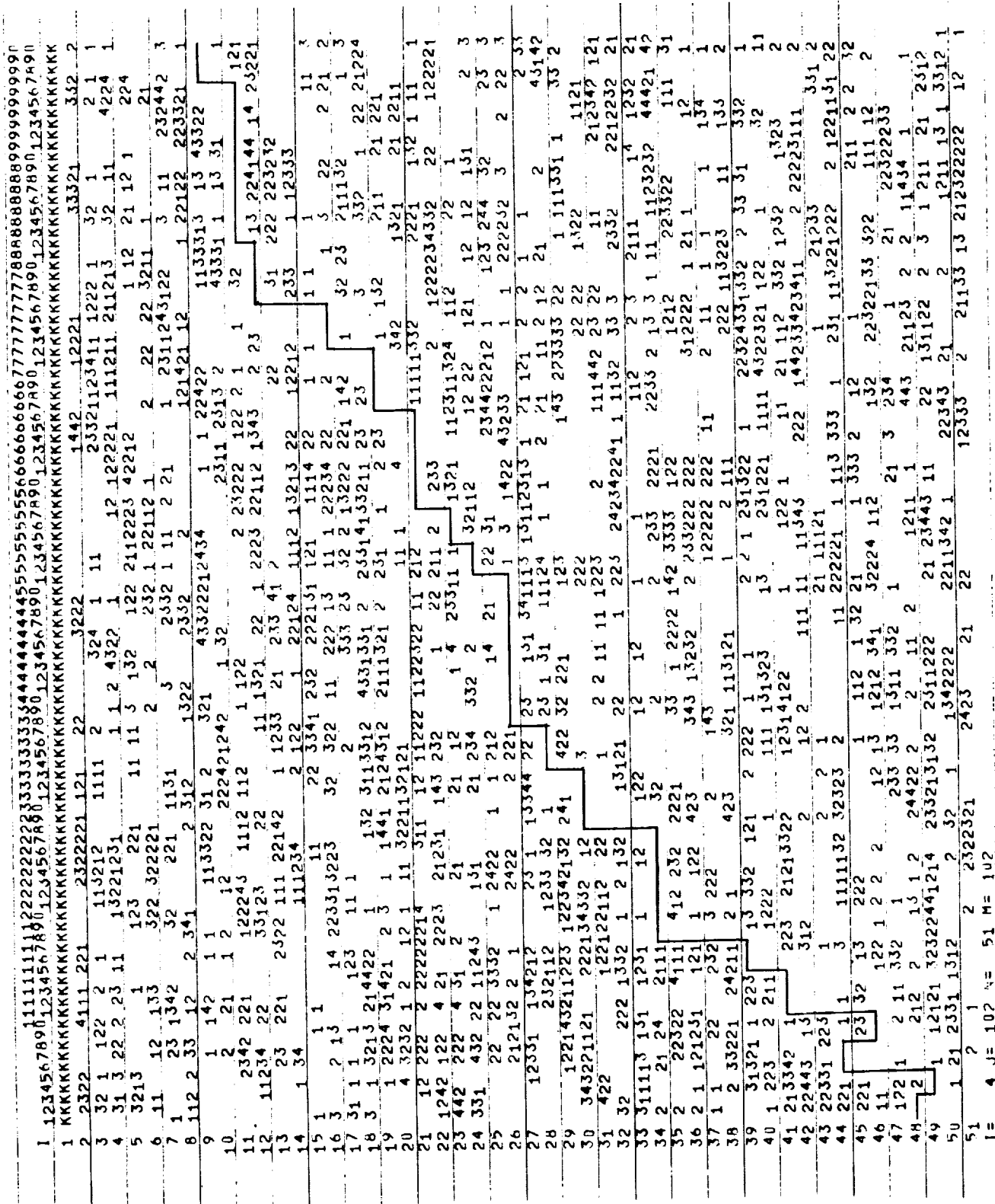
Figure 3.11. Surface Map for 50 x 100 Grid, Compressed Showing
Barrier to Flow and Diagonal Pattern

Since b and c are symmetrically disposed in Figure 3.12, clearly, to avoid patterns we should make K_b and K_c equal, which condition is satisfied above. It remains to be shown that there is also a relationship between K_a and K_b.
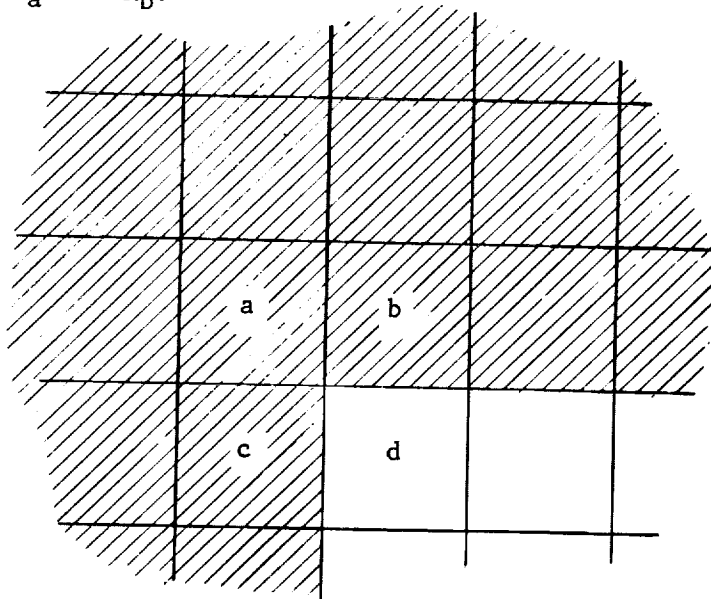
CROSS-HATCHED = AREA PREVIOUSLY DEVELOPED

BLANK = UNDEVELOPED AREA

Figure 3.12. Development of Grid Values

Assuming that one were to redesignate all heights by designating them one band higher, we would require that the extrapolated value of d also be one band number higher. Thus,

$$(d+1) = K_a (a+1) + K_b (b+1) + K_c (c+1)$$

Subtracting the original equation, one finds

$$1 = K_a + K_b + K_c$$
$$\text{or } K_a = 1 - 2K_b \quad \text{since } K_b = K_c$$

There is some theoretical justification for feeling that the weight given a should be reduced relative to that given b and c. Point a is at a greater distance from point d and would have a lower correlation. Since it has been found that correlation decreases exponentially, and since the exponential function for small arguments is nearly linear, we may assume that the ratio of K_a to K_b should be about $\sqrt{2}$. It is interesting to note that one surface was generated in which K_a was set equal to zero. As expected, there was a strong diagonal pattern with a negative slope.

Surfaces have been generated using the extrapolation equation

$$d = -.7a + .85 (b+c)$$

Two different input matrices were used, each having ten quanta of height. Further, each input matrix was designed so that if the intended surface distribution were in fact obtained, then there would be equal net probability of going between any two levels in either direction, which property is necessary to avoid directionality in the surface. The two input matrices are shown in Figures 3.13 and 3.14. Figure 3.13 assumes a surface with extreme value distribution and equal increments in gap height between quanta. One has considerable difficulty in adjusting the input matrix to satisfy all criteria.

The matrix of Figure 3.14 assumes the same surface distribution but _unequal_ increments of gap height such that 10 percent of the total surface would fall in each band. This makes it considerably easier to develop the matrix, since the first ten lines are identical to each other except for a shift and except for truncation effects at the end of the line.

It was found on examining surfaces produced using the matrix of Figure 3.13 that a diagonal pattern still existed of the same type shown in Figure 3.11. However, using the matrix of Figure 3.14, no diagonal pattern was discernible to the eye, but, as shown later, there is still a diagonal pattern. The correct ratio of K_a to K_b to avoid diagonal patterns may be a function of the matrix used, or it may be that some input matrices are more sensitive to errors in the selection of K_a and K_b.

Figure 3.15 shows the surface developed using the matrix of Figure 3.14. Figure 3.16 is the same surface depressed to bring out any patterns that may exist. (The fact that in a vertical direction there are six rows of numbers to the inch, and that in the horizontal direction there are ten columns to the inch must be taken into account when studying Figure 3.16 for patterns.)

The most convincing test for the absence or existence of patterns is of course to compute the autocorrelation function for the generated surface as a function of distance between points and direction of the vector displacement. Ideally the function should be independent of the angle of the vector representing displacement, i.e. have circular symmetry, and, according to the empirical data discussed in section 3.4.2.1, it should decay exponentially. Assuming that the correlation function decays exponentially in a given direction, we can determine the value b in the equation

$$\rho = e^{-bN}$$

where N is distance in grid squares.

Actual analysis of the surface in Figure 3.15 showed that, within the error in calculating with a given sample size, the correlation

```
                    0
  ⁻1     ⁻1     ⁻1     ⁻1     ⁻1     ⁻1     ⁻1    400  2400₁0000
  ⁻1     ⁻1     ⁻1     ⁻1     ⁻1     ⁻1    500  3700  8000₁0000
  ⁻1     ⁻1     ⁻1     ⁻1     ⁻1    900  4400  8200  9800₁0000
  ⁻1     ⁻1     ⁻1     ⁻1   1800  5400  8500  9900₁0000₁0000
  ⁻1     ⁻1     ⁻1    600  3600  7800  9800₁0000₁0000₁0000
  ⁻1     ⁻1    300  2400  8000  9500₁0000₁0000₁0000₁0000
  ⁻1    100  1100  8400  9800₁0000₁0000₁0000₁0000₁0000
  ⁻1    300  8300  9800₁0000₁0000₁0000₁0000₁0000₁0000
 100  8900  9700₁0000₁0000₁0000₁0000₁0000₁0000₁0000
9100₁0000₁0000₁0000₁0000₁0000₁0000₁0000₁0000₁0000
 100  1000  3700  6400  8200  9100  9600  9800  9900₁0000
```

Figure 3.13. Probability Integral

```
-1    -1    -1    -1    -1    -1    -1    100  2500 10000
-1    -1    -1    -1    -1    -1    100  2200  7800 10000
-1    -1    -1    -1    -1    100  2200  7800  9900 10000
-1    -1    -1    -1    100  2200  7800  9900 10000 10000
-1    -1    -1    100  2200  7800  9900 10000 10000 10000
-1    -1    100  2200  7800  9900 10000 10000 10000 10000
-1    100  2200  7800  9900 10000 10000 10000 10000 10000
100  2200  7800  9900 10000 10000 10000 10000 10000 10000
2200  7800  9900 10000 10000 10000 10000 10000 10000 10000
7700  9900 10000 10000 10000 10000 10000 10000 10000 10000
1000  2000  3000  4000  5000  6000  7000  8000  9000 10000
```

Figure 3. 13. Probability Integral.

Figure 3-16. Compressed Surface Map for 50 x 100 Grid.

Figure 3.15. Surface Map for 50 x 100 Grid.

function was close to exponential. The results of the analysis are best shown by Figure 3.17, which is a polar plot of the b values for different directions. Because of the technique of surface generation, one should expect symmetry about the diagonal with negative slope. Since the calculation of autocorrelation for each vector displacement involves two sets of data and there is no differentiation made as to which set is which, it follows that there is reflective symmetry through the origin; that is, any two values 180° apart must be equal.

It is clear from Figure 3.17 that there is still a slight diagonal pattern in the same direction shown in Figure 3.11, since the lower b value in the 45 degree direction indicates higher correlation at any distance as compared to the correlation at the same distance in the 135 degree direction. This error can no doubt be removed by using a somewhat lower value of K_a. In fact that conclusion, reached earlier in this section to the effect $K_a/K_b = \sqrt{2}$ would suggest that $K_a = -.56$ and $K_b = +.78$ are better values to use. (These values can easily be inserted in the computer program, but this has not yet been done.)

Perhaps more important than the error in diagonal autocorrelation is the tendency for the polar plot of b to be square rather than circular. This pattern suggests that the contact areas in Figure 3.16 should tend to be squares, since there is a tendency toward longer runs of the same number in a vertical and horizontal direction than in any other direction because of lower value of b in the horizontal and vertical directions.

The existence of the last pattern noted is believed to be due to the inclusion in our extrapolation method of information from only three squares. The inclusion of information from more squares in the cross-hatched area of Figure 3.12 would probably be necessary to eliminate this pattern. As noted in an earlier section, however, our concern is not to attain perfect generation of surfaces regardless of the work involved, but rather to generate reasonable surfaces without encountering undue difficulties. The square pattern noted is most noticeable (after being point out) on the surface maps depressed, either very little or considerably, and is least noticeable in the range of transition from flow to no flow. It is therefore concluded that this defect is tolerable and need not be eliminated.

The pattern introduced by error in the K_a/K_b ratio and that introduced by inconsistencies between the input matrix and the distribution for the surfaces generated can be reduced, as noted previously, by a trial and error process. Thus it is concluded that the method as developed should be suitable for producing random surfaces up to 50 x 100 elements. It is theoretically possible to program the computer to develop yet larger ones, but this is not recommended. The generated surface is of little value in itself. One must analyze it to have it of any use, and the analysis of larger surfaces could become prohibitive. Instead, it is proposed that conclusions concerning leakage probability based on grids of 50 x 100 and smaller be extrapolated to predict results on larger grids.
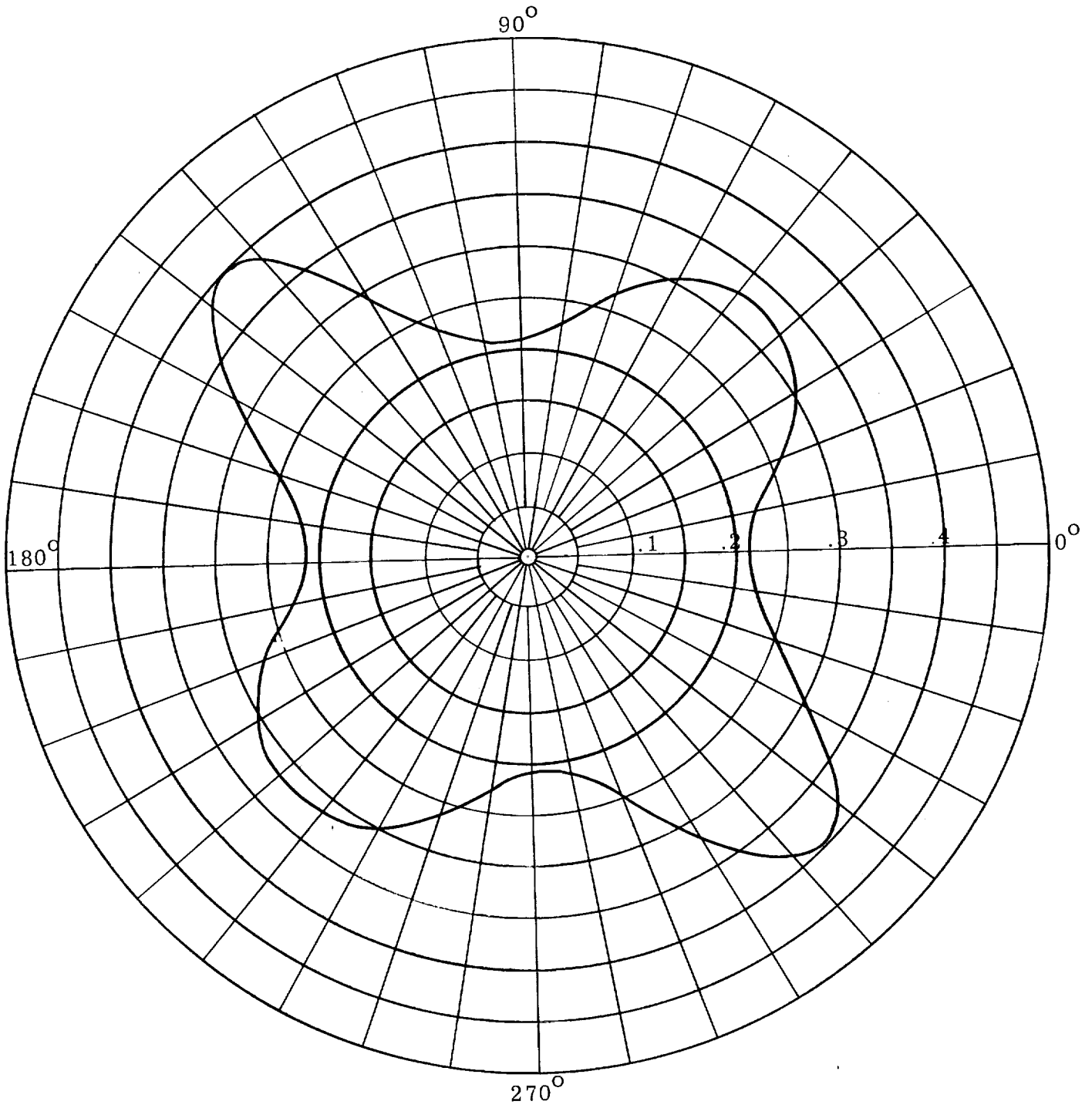
Figure 3.17. Polar Plot of Autocorrelation Decrement

3.4.3 Random Plus Other Components

Maps for machined surfaces, in general, can be generated using a combination of periodic functions and maps for random surfaces with proper coordinate transformation. For example, a lathe-turned surface may be represented by a periodic function in the direction of the seal width plus a random variation. The periodic function is to represent the shape of the tool and the feed per revolution and in general would have a fundamental frequency and harmonies. The random component represents the tendency of the tool to tear metal rather than cut it smoothly to the tool profile. One may use a mapping function in the superposition of the random and periodic components to "stretch" the random surface in the direction of tool travel. This would be equivalent to saying that the random roughness is oriented relative to the tool travel and that the hollows and hills tend to be longer and to have a higher autocorrelation function in the direction of tool travel.

The representation of a circular ground seal surface may be made in the same manner as described for a lathe-turned surface, but without the need for adding the periodic components.

Full consideration has not yet been given to the most expeditious way to use coordinate transformation and superposition of surface patterns, both random and periodic, to represent such complex surfaces as blanchard ground, end milled and the like.

3.5 Calculation of Leakage

Assuming that one has generated a reasonably large number of "randomly selected" samples of gap maps using the methods described in section 3.4, and that these represent portions of the seal interface we wish to study, we must have a way of determining the leak rate across each sample seal.

This step in the analysis has been considered purely from the viewpoint of the feasibility of its accomplishment. We have concluded that it is possible to solve the problem by introducing special techniques for extrapolating results obtained on a moderately large sized computer. The approach is explained as follows.

Let us assume we have a seal area divided into a grid so the seal is m elements in width and n elements in length or circumference. Assume further that we have quantized gap height so there are H heights possible, one of which will be zero. Then for each height there is a corresponding resistance to flow R. We can represent the resistance to flow by a network of resistances m x n in size, as illustrated in Figure 3.18.
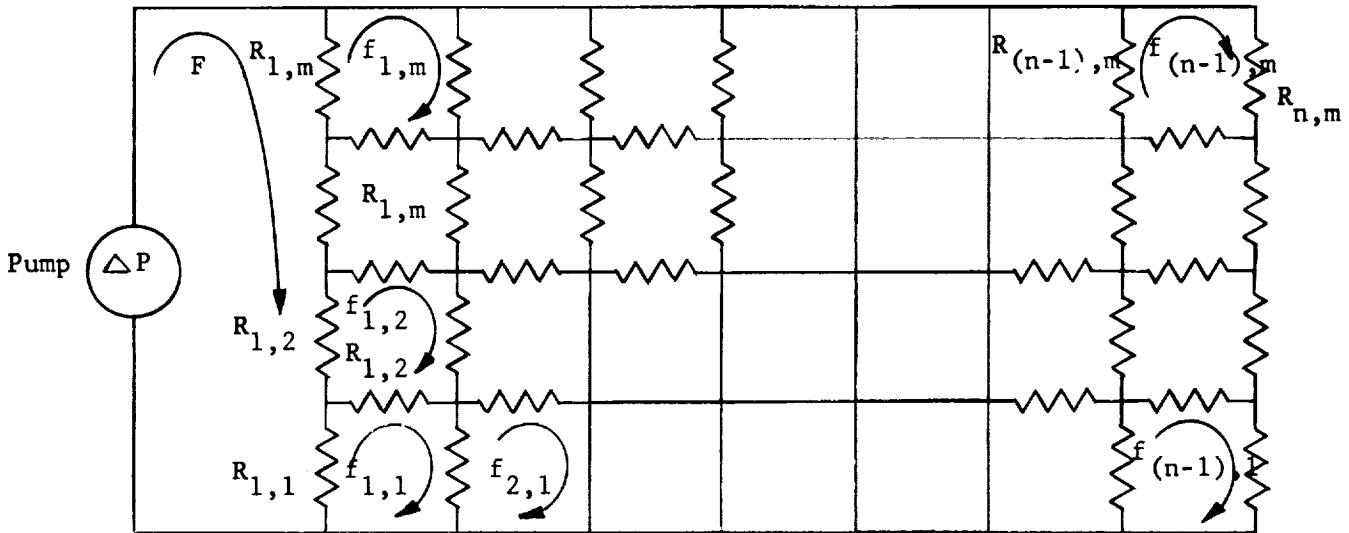
FIGURE 3.18 Flow Resistance Network

In truth the flow through each element of our grid may be molecular, laminar or turbulent and for each situation a different formula applies, further complicated by the fact that there are transition regions. Being practical, any time flow is turbulent we need not know its value - it will in all cases be termed "excessive", and presumably the probability of occurence will be nil. It has been shown experimentally that for leak rates less than about 10^{-6} atm cc/sec, flow is molecular. For leak rates above 10^{-5} std. cc/sec, it is most likely to be laminar. The location and breadth of the transition region depends on many factors, including the physical dimensions of the seal. For the present let us consider the equations with either laminar flow or molecular flow.

For molecular flow in all elements the equations can be written as:

1) $(P_m - P_o) = (F-f_{1,1}) \cdot R_{1,1} + (F-f_{1,2}) \cdot R_{1,2} + \cdots + (F-f_{1,m}) \cdot R_{1,m}$

2) $0 = (f_{1,1} - F) \cdot R_{1,1} + (f_{1,1}-f_{2,1}) \cdot R_{2,1} + (f_{1,1}-f_{1,2}) \cdot R_{1,2}$

3) $0 = (f_{(n-1),1} - f_{(n-2),1}) \cdot R_{(n-1),1} + f_{(n-1),1} \cdot R_{n,1} + (f_{(n-1),1} - f_{(n-1),2}) \cdot$

   $R_{(n-1)2}$

4) $0 = (f_{1,m} - F) \cdot R_{1,m} + (f_{1,m} - f_{1,(m-1)}) \cdot R_{1,m} + (f_{1,m} - f_{2,m}) \cdot R_{2,m}$

5) $0 = (f_{(n-1),m} - f_{(n-2),m}) \cdot R_{(n-1),m} + (f_{(n-1),m} - f_{(n-1),(m-1)}) \cdot R_{(n-1)m} +$

   $f_{(n-1),m} \cdot R_{n,m}$

6) $0 = (f_{i,1} - f_{(i-1),1}) \cdot R_{i,1} + (f_{i,1} - f_{(i+1),1}) \cdot R_{(i+1),1} + (f_{i,1} - f_{i,2}) \cdot R_{1,2}$

7) $0 = (f_{i,m} - f_{(i-1),m}) \cdot R_{i,m} + (f_{i,m} - f_{i,(m-1)}) \cdot R_{i,m} + (f_{i,m} - f_{(i+1),m}) \cdot$

$R_{(i+1),m}$

8) $0 = (f_{1,j} - F) \cdot R_{1,j} + (f_{1,j} - f_{1,(j-1)}) \cdot R_{1,j} + (f_{1,j} - f_{2,j}) \cdot R_{2,j} +$

$(f_{1,j} - f_{1,(j+1)}) \cdot R_{1,(j+1)}$

9) $0 = (f_{(n-1),j} - f_{(n-2),j}) \cdot R_{(n-1),j} + (f_{(n-1),j} - f_{(n-1),(j-1)}) \cdot R_{(n-1),j} +$

$f_{(n-1),j} \cdot R_{n,j} + (f_{(n-1),j} - f_{(n-1),(j+1)}) \cdot R_{(n-1),(j+1)}$

10) $0 = (f_{ij} - f_{(i-1),j}) \cdot R_{ij} + (f_{ij} - f_{i,(j-1)}) \cdot R_{ij} + (f_{ij} - f_{(i+1)j}) \cdot R_{(i+1)j} +$

$(f_{ij} - f_{i,(j+1)}) \cdot R_{i,(j+1)}$

In equations 6 through 10, i and j take on any value from i = 2 to i = n-2, and j =2 to j = m-2. There are, therefore, a total of (m·n-m+1) equations in (m·n-m+1) unknowns. Hence, we can solve for F.

For laminar flow in all elements, the values of the R's are different than for molecular flow, but the equations are identical to 1) through 10) except for replacing left-hand side of equation 1) with $(P_m^2 - P_o^2)$.

The case of molecular flow in some elements and laminar flow in others is too complex to consider, and we will simply assume that when the overall flow is expected to be laminar we can use equations 1) through 10) with equation 1) arranged for laminar flow, and when the overall flow is expected to be molecular we can use equations 1) through 10) with equation 1) arranged for molecular flow. It should be noted that if gap height is quantized into 10 heights, there are only 10 values of R to compute for molecular flow and 10 for laminar flow.

To determine the flow through a particular grid requires estimation of whether flow will be laminar or molecular, followed by the solution of a number of simultaneous equations to determine flow. The assumption as to type flow can then be verified. If the overall flow is found (or thought) to be in a transition region, an estimate proposed for transition flow that has been suggested is (Ref. 7)

11) $F = F_{laminar} + \epsilon F_{molecular}$

Alternatively, one may write network equations in which flow through each element is described by a symbol, and equations are written for pressure drops and for the summations of flow at junction

points. This system produces a significantly larger number of equations which are of somewhat simpler form for use in a computer. There may be merit in using this system of equations, but this point has yet to be decided.

Finally, not to be overlooked (and yet to be considered from overall suitability and merit), one could set up an electrical analog network of resistors rather than solve simultaneous equations on a large digital computer.

Regardless of whether one works with a digital or an analog solution of the flow problem, it is going to be wise to utilize techniques which permit solving smaller size problems and extrapolating the results. If the solution is analog, the amount of hardware cost could otherwise become prohibitive. If a digital solution is used, the number of simultaneous equations to be solved may otherwise be too large. The problem has been considered, assuming a digital solution, with the following conclusions.

To reduce the number of equations, and also the problem of generating the heights for sample surfaces, recognize that as n becomes large the flow per unit of seal length will approach a constant. To put flow into still more general terms, let us define q_m as the flow per element of seal length per pound pressure difference, assuming molecular flow. Also, define Q_m as the limit of q_m as $n \to \infty$. Thus,

$$12) \quad q_M = \left[\frac{F_{Mol.}}{(P_1 - P_2) \cdot n} \right] \quad \text{and} \quad Q_M = \lim_{n \to \infty} q_M$$

and, similarly define for laminar flow

$$13) \quad q_L = \left[\frac{F_{Lam.}}{(P_1^2 - P_2^2) n} \right] \quad \text{and} \quad Q_L = \lim_{n \to \infty} q_L$$

It may be practical to obtain a limiting value of q_M or q_L by selecting a large enough value of n and making the computation once. If this is not possible, the computation must be made for the largest reasonable value of n, and then repeated with the same pattern of grid heights except for truncating n to a smaller value. The procedure must be repeated for a sufficient number of randomly selected surfaces and a sufficient number of n values that the cumulative probability of q_M (and/or q_L) may be plotted with reasonable accuracy for each value of n used, and so the trend of the cumulative probability may be observed at each flow and extrapolated to obtain Q_M (and/or Q_L).

Q_M and Q_L, as defined, are functions of m, but it is expected that for any given value of m, the limit of flow as n increases can be estimated with sufficient accuracy by not going beyond n = 2m. Thus, since there are computer solutions for sparse matrix equations which can handle several thousand unknowns, it is not unreasonable to consider going to values of m as large as 50. Even this, however, is not enough for most cases, so means for extrapolating to larger values are again

needed. It is reasonable to assume that as m becomes large, Q_M will become inversely proportional to m. Assuming this to be so, we need compute Q_M only once. If the relationship is questioned, or our interest is in the range of m where the relationship does not hold true, we can repeat the entire procedure for various values of m and obtain a family of cumulative probability curves of Q_M for various m values and interpolate or extrapolate to desired m values.

3.6   Relation of Gap Statistics to Load

Thus far in this report, we have dealt with the generation of asperity distributions to duplicate real surfaces, the gap distribution which exists when two such surfaces are brought together in increments of distance, and the probability of leakage through the resultant gaps. We have not yet dealt with the problem of loads or stresses necessary to deform the surfaces and reduce the gaps.

During Phase I of the contract, an attempt was made to relate force normal on the seal faces to leakage flow in a three step problem. First, the flow path area was related to deformation; secondly, deformation was related to applied load; and thirdly, the flow through the leak path was calculated. This work, described in Reference 1, was limited by the assumption that the asperities varied in the tangential direction only, thus resulting in leak flow paths which were purely radial (in an annular seal). The portion of the work significant to estimating gap statistics is located primarily in sections 33.3 and 33.4 of Reference 1 and is based heavily on the experimental work published by I. Finne and M.C. Shaw (Reference 8).

While the gap distribution variations as a function of decreasing distance between reference lines lying immediately beneath the surface finishes can be analytically considered if statistics are called upon, the problem of the load applied over the apparent area of contact required to effect this decrease in distance can not, at this tame, be handled analytically. The original surface finishes existing on each surface (including their relative directions and location of individual asperities with respect to one another), the yield strengths of the materials mated, the strain hardenability of the materials, the elastic strength properties, and the size and configuration of material supporting the surfaces all bear heavily on the relationship between load and "degree of mating".

It would be somewhat simplifying if only area of contact could be considered as a function of applied load in that this parameter has been of interest to many investigators for several years. Electrical contact problems, thermal contact problems, and to a certain extent even bearing stress problems have been investigated experimentally by relating true area of contact to load. Unfortunately, it has been shown experimentally (Reference 1) that leakage cannot be described satisfactorily where area of contact is considered as a sole definitive parameter. Several examples of varying contact areas for different surface finishes and for identical surface finishes oriented differently under approximately equal stresses are shown in Reference 9. Each of the examples, while yielding vastly different degrees of true area of contact, resulted in leakage rates less than 10^{-6} atm cc/sec. Even though area of contact is not sufficient in describing the phenomena of mating, however, because so much work in this area has been done, and because it is certainly related to the degree of mating to cause leak tightness, it is worthwhile to review the literature concerning such studies.

A great number of investigations into the basic problem of increase in area of contact as a function of applied stress have involved great sophistication, although most of the results are limited to a particular combination of surface finish and regime of loading. For a goal such as the one at hand, wherein area of contact itself is not a meaningful parameter, while the load-vertical displacement relationship is, already accomplished area of contact investigations are quite helpful in increasing the level of understanding. References 10 through 24 deal with the load-area of contact in general. Reference 24, in particular, presents a summary of most of the results accomplished to date in the Soviet Union up to 1964.

The problem of area of contact with increasing strength involves both elastic and plastic deformations. When a model for the elastic contact stress problem is formulated, the increase in area of the function of load varies as the load to the two-thirds power if a single contact is envisioned. When plastic deformation is considered, the area of contact generally is considered to increase linearly with load. Should multiple contacts be considered, as several authors have pointed out, even the elastic area of contact increase varies with the load linearly. The problem of elastic bodies in contact is discussed in references 28 through 30.

Several authors have approached the problem of decreasing distance between reference lines in surfaces as load is applied normally to the surfaces. Reference 31, a recent paper by Japanese authors, presents a technique for calculation of the decrease in distance as a function of load. This paper has recently been reviewed by ATL investigators; the paper, review, and author's closure will be published in September 1965 in the Journal of Basic Engineering, ASME. References 32 through 39 deal with this same subject.

The actual distribution of asperities, which is being studied at ATL by computer technology, has been approached both experimentally and analytically by F.F. Ling and is reported in References 4 and 41.

The actual problem at hand, that of leakage through metal-to-metal seals, has also been studied previously, for various regimes of leakage flow and asperity distributions. References 42 through 46 deal with this problem. References 43 through 46 present a very sophisticated experimental program with some theoretical work on the subject. That work, accomplished in France, has been discussed with the authors during a visit of one of the authors to the Advanced Technology Laboratories in Schenectady.

The exact manner in which ATL will incorporate the load-displacement-area of contact relationship into the computer program has not been fully determined. The literature at hand has been in the process of evaluation for some time and is presently continuing. It is not intended to embark on a sophisticated experimental program within the present program in that the wealth of information available in all probability yields results which could not be attained or improved upon in a limited program. Beyond appraisal of all the published work, liaison with several experts in the field, many of whom are listed in the references, is being undertaken.

3.7 References

1. "Design Criteria for Zero-Leakage Connectors for Launch Vehicles, Vol. 3, Sealing Action at the Seal Interface," March 1963, edited by F.O. Rathbun, Jr. Final Report for Phase I of Contract NAS-8-4012.

2. "Design Criteria for Zero-Leakage Connectors," June 1, 1964, edited by F.O. Rathbun, Jr. Final Report for Second Contract Period, Contract NAS-8-4012.

3. E.J. Gumbel, "Statistics of Extremes," Columbia Univ. Press, 1958.

4. M.G. Kendall, "Proof of Relations Connected with the Tetrachoric Series and its Generalization," Biometrika, Vol. 32 (1941), pp. 196-8.

5. M.G. Kendall and A. Stuart, "The Advanced Theory of Statistics," Vol. I, p. 155.

6. A.M. Olsen, "A Statistical Examination of Pseudo-Random Number Generators Having a Uniform Frequency," 23 August 1963, R63ASD3. General Electric Company report prepared for NASA.

7. E.H. Kennard, "Kinetic Theory of Gases with an Introduction to Statistical Mechanics," McGraw-Hill, 1938.

8. I. Finne and M.C. Shaw, "The Friction Process in Metal Cutting," Trans. ASME, Vol. 78, 1956, pp. 1649-1653.

9. F.O. Rathbun, Jr., "Leakage Rate Experiments," Proceedings of the Conference on Design of Leak-Tight Separable Fluid Connection, G.S. Marshall Space Flight Center, Mar. 24-25, 1964, Vol. II.

10. F.F. Ling, "Some Factors Influencing the Area-Load Characteristics for Semismooth Contiguous Surfaces Under 'Static' Loading," Trans. ASME, July 1958, pp. 1113-1120.

11. T.N. Cetinkale and Dr. Margaret Fishenden, "Thermal Conductance of Metal Surfaces in Contact," The Inst. of Mech. Engineers, The American Soc. of Mech. Eng., Proceedings of the General Discussion on Heat Transfer, Sept. 11-13, 1951, pp. 271-275. Pub. by the Inst. of Mech. Eng., St. James, London, S.W. 1, England.

12. G.W. Cunningham and J.W. Spretnak, "A Study of the Effect of Applied Pressure on Surface Contact Area," Intl. J. of Mech. Sciences, May-June 1962, Vol. 4, 231-240. Pub. by Pergamon Press, Ltd.

13. Bowden and Tabor, "The Friction and Lubrication of Solids. , Chap. I, Area of Contact Between Solids," pp. 5-29.

14. J.F. Archard, "Single Contacts and Multiple Encounters," J. of Appl. Physics, Vol, 32, No. 8, August 1961, pp. 1420-1425.

15. Bowden and Tabor, "The Friction and Lubrication of Solids, Chap. III, Contact of Metals," pp. 29-38.

16. F.P. Bowden and D. Tabor, "Friction and Lubrication, Chap. II, The Nature of Solid Surfaces and the Area of Contact Between Them," pp. 12-18.

17. J. Dyson and W. Hirst, "The True Contact Area Between Solids," Proc. of the Phys. Soc., 67B, 1954, pp. 309-312.

18. J.F. Archard, "Contact and Rubbing of Flat Surfaces," J. of Appl. Physics, Vol. 24, No. 8, August 1953, pp. 981-988.

19. J.B.P. Williamson, "Surface Phenomena in Electrical Connectors," Mar. 23, 1964, Proc. Second BSD-STL Symposium, pp. 1-10.

20. J.A. Greenwood and J.B.P. Williamson, "The Contact of Nominally Flat Surfaces," pp. 1-9, Burndy Corp. Report.

21. G. Yoshimoto and T. Tsukizoe, "On the Mechanism of Wear Between Metal Surfaces," Wear, Vol. I, 1957/58, pp. 472-490.

22. I.V. Kragel'skii and N.B. Demkin, "Determination of the True Contact Area," Friction and Wear in Machinery, Vol. 14, 1960, ASME Translation dated 1962. pp. 30-53.

23. I.V. Kragelsky and N.B. Demkin, "Contact Area of Rough Surfaces," Wear, Vol. 3, 1960, pp. 170-187.

24. P.E. D'yachenko, N.N. Tolkacheva, G.A. Andreev, and T.M. Karpova, "The Actual Contact Area Between Touching Surfaces," Inst. of Mech. Engrg, Acad. of Sciences, Moscow, 1963, pp. 1-68.

25. R.D. Mindlin, "Compliance of Elastic Bodies in Contact," J. of Appl. Mechanics, Sept. 1949, pp. 259-268.

26. J.A. Greenwood and J.H. Tripp, "Elastic Contact of Rough Spheres," Feb. 25, 1965, Burndy Corp. Research Report No. 21, pp. 1-15.

27. K.L. Johnson, "Recent Developments in the Theory of Elastic Contact Stresses: Their Significance in the Study of Surface Breakdown," The Inst. of Mech. Engrs., Proceedings of the Conference on Lubrication and Wear, 1957, pp. 620-627.

28. J.F. Archard, "Elastic Deformation and the Laws of Friction," Proc. of Royal Society, A, Vol. 243, pp. 190-205, 1957.

29. J.F. Archard, "Elastic Deformation and the Contact of Surfaces," Nature, Nov. 1953, pp. 918-919.

30. B. Lincoln, "Elastic Deformation and the Laws of Friction," Nature, July 1953, pp. 169-170.

31. T. Tsukizoe and T. Hisakado, "On the Mechanism of Contact Between Metal Surfaces - The Penetrating Depth and the Average Clearance," J. of Basic Engrg., Trans. ASME, Paper No. 64, pp. 1-7.

32. Husain Lakhani, "Load Displacement Study of Surface Asperities," Jan. 1965, M.I.T. Thesis, Dept. Mech. Eng.

33. Akira Iwaki and Masaki Mori, "On the Distribution of Surface Roughness When Two Surfaces Are Pressed Together," Bulletin of JSME, Vol. 1, No. 4, 1958, pp. 329-337.

34. J.A. Greenwood and G.W. Rowe, "Deformation of Surface Asperities During Bulk Plastic Flow," J. of Appl. Physics, Aug. 1964, pp. 667-668.

35. Akira Iwaki and Masaki Mori, "On the Distribution of Pressed Surface Profile (1st Report) - The Relation Between the Parameters of Distribution and Pressure," Paper presented before Japan. Soc. of Mech. Engrs. April 1955.

36. Akira Iwaki and Masaki Mori, "On the Distribution of Pressed Surface Profile (2nd Report) - Contact Ration, Yielding of Points and Penetrating Depth," Paper presented before Japanese Mech. Eng. Soc., July 1955.

37. Akira Iwaki and Toshio Kuga, "On the Distribution of Pressed Surface Profiles (3rd Report) - On Numbers of Contact Points Estimated by the Distribution of Quartiles," Presented Nov. 1955 before Japan. Mech. Eng. Soc.

38. Akira Iwaki and Masamiki Mori, "On the Distribution of Present Surface Profiles (4th Report) - On Contact Between Rough Surfaces," presented at Japan. Mech. Eng. Soc., June 1956.

39. Akira Iwaki and Hajime Chinju, "On the Distribution of Pressed Surface Profiles (5th Report) - The Relative Material Index," presented at Japan. Mech. Engr. Meeting, June 1962.

40. F.F. Ling and R.C. Lucek, "On Model Studies of Metallic Surface Asperities," J. of Appl. Physics, Vol. 30, No. 10, October 1959, pp. 1559-1563.

41. F.F. Ling, "On Asperity Distributions of Metallic Surfaces," J. of Appl. Physics, Vol. 29, No. 8, August 1958, pp. 1168-1174.

42. Seishi Yoshida and Satoru Iuchi, "The Study of the Gas Tightness of the Statical Contact By Means of the Leakage Through It," Proc. of the 6th Japan. National Congress for Appl. Mech., 1956, pp. 245-248.

43. G. Armand, J. Lapujoulade and J. Paigne, "A Theoretical and Experimental Relationship Between the Leakage of Gases Through the Interface of Two Metals in Contact and Their Superficial Micro-Geometry," Vacuum, Vol. 14, pp. 53-57. Pergamon Press Ltd., Great Britain.

44. G. Armand, Y. Lejay and J. Paigne, "Joints Etuvables pour Ultravide a Base d'Alliage Or-Argent," PA-TE/RT-131, July 1964, pp. 1-23.

45. G. Armand, J. Lapujoulade and J. Paigne, "Correlations Between Leak Rate and Some Phenomena Observed in Metal to Metal Contact," 1961 Trans. of 8th Vacuum Symposium and 2nd Intl. Congress, Pergamon Press, Great Britain, 1962, pp. 1091-1099.

46. G. Armand, J. Lapujoulade and J. Paigne, "Correlation Between Deformations, Surface State and Leak Rate in Metal to Metal Contact," PA-TE/RT. 79, November 1961, pp. 1-24.